

The copyright of this thesis vests in the author. No quotation from it or information derived from it is to be published without full acknowledgement of the source. The thesis is to be used for private study or non-commercial research purposes only.

Published by the University of Cape Town (UCT) in terms of the non-exclusive license granted to UCT by the author.

**A KINETIC AND MECHANISTIC STUDY ON THE
OXIDATION OF CHROMIUM OXIDE IN PURE
CHEMICALS AND IN FERROMETALLURGICAL
SLAGS**

BY : Kriveshini Pillay

Dissertation Presented for the Degree of

MASTER OF SCIENCE IN APPLIED SCIENCE

In the Department of Chemical Engineering
University of Cape Town

June 2001



The copyright of this thesis vests in the author. No quotation from it or information derived from it is to be published without full acknowledgement of the source. The thesis is to be used for private study or non-commercial research purposes only.

Published by the University of Cape Town (UCT) in terms of the non-exclusive license granted to UCT by the author.

DEDICATION

To my parents who have celebrated fifty years of marital bliss

University of Cape Town

SYNOPSIS

Chromium can exist in a number of oxidation states but the environmentally stable forms are trivalent (Cr(III)) and hexavalent (Cr(VI)) chromium. These two forms are noted for their different degrees of toxicity and mobility. Hexavalent chromium is more toxic and mobile and has been responsible for a number of illnesses in humans (Sheehan et. al., 1991).

Elemental chromium and its compounds have a variety of uses in the industrial sector. The ferrometallurgical industry in particular makes use of chromium since this element imparts properties such as hardness and strength to stainless steel. However, this industry also produces slags that contain residual amounts of chromium oxide (Cr_2O_3) along with other constituents such as calcium oxide (CaO). Thermodynamic data from the literature, has shown that Cr_2O_3 can undergo oxidation at ambient temperature when in contact with CaO and atmospheric oxygen (Kilau and Shah, 1984; Hattori et al., 1978). Furthermore, the oxidation of Cr_2O_3 in the presence of $\text{Ca}(\text{OH})_2$ has also been observed at ambient temperature (Petersen, 1998).

Concerns that the oxidation of Cr_2O_3 can occur in wastes such as ferrometallurgical slags which have been disposed to landfill and exposed to atmospheric oxygen, have therefore been expressed. This has led to the need to investigate and identify the reactions that are likely to contribute to the oxidation of Cr_2O_3 under environmental conditions.

An experimental study, which aimed at investigating the oxidation of Cr_2O_3 , has been undertaken. This included an investigation of the oxidation of Cr_2O_3 both in laboratory chemicals and in ferrometallurgical slags. The study involved an investigation of the oxidation of Cr_2O_3 in the presence of CaO and $\text{Ca}(\text{OH})_2$ in the pure chemical systems. The latter investigation included studies on Cr_2O_3 - CaO powders, Cr_2O_3 - CaO pellets and Cr_2O_3 - $\text{Ca}(\text{OH})_2$ balls which were exposed to atmospheric oxygen. Corresponding experiments on slag powder and slag ball systems were also devised.

It has been observed that oxidation occurred in both the pure chemical systems and in ferrometallurgical slags with maximum conversions of typically 3 to 100 μg per g Cr for the pure chemicals and 1000 to 10000 μg per g Cr for the slags. Further to this observation, it has been noted that the rates of oxidation were relatively higher in Cr_2O_3 - CaO powder and pellet systems as opposed to the Cr_2O_3 - $\text{Ca}(\text{OH})_2$ ball systems. This also applied to the ball and powder systems in the slags and has been attributed to the limited oxygen access in the ball systems.

Another interesting observation was that the oxidation of Cr_2O_3 in the presence of CaO or $\text{Ca}(\text{OH})_2$ is the reaction which most likely contributes to the generation of Cr(VI) in the slags. The mechanism of such reactions seems to involve the interaction of Cr^{3+} centres with the oxygen centres of the calcium compounds which enhances the reactivity of the trivalent oxide and makes it more amenable to oxidation. Atmospheric oxygen has also been identified as the electron acceptor since no appreciable oxidation was observed in a nitrogen environment.

The key parameters that enhance the rate of oxidation of Cr_2O_3 have been identified as the proximity to CaO or $\text{Ca}(\text{OH})_2$, particle size and temperature. These, together with the mechanistic insights, have been used to propose preventative measures such as reduction in the CaO content of the slags.

Exponential kinetic models gave the best description for the oxidation in Cr_2O_3 - CaO powder and pellet systems in the pure chemical studies and for the slag powders that were exposed to air (including slag balls that completely disintegrated into fine powders). Such models predict that the oxidation of Cr_2O_3 in the presence of CaO or $\text{Ca}(\text{OH})_2$ proceeds to a limited extent under environmental conditions and the reaction rates become insignificant within the first year. A linear model has been identified for the Cr_2O_3 - $\text{Ca}(\text{OH})_2$ balls maintained at ambient temperature, but it is believed that such a model only adequately describes this system up to about 11 months. Thereafter the limited diffusion of atmospheric oxygen may cause the reaction rate to decrease thereby limiting the conversions that are attained. Parabolic models have been descriptive of the slag balls, which remained intact and of the slag balls, which did not completely disintegrate into fine powders.

Such observations have led to the conclusion that the oxidation of Cr_2O_3 does indeed occur in ferrometallurgical slags. The cause of the oxidation has been identified as the oxidation of Cr_2O_3 in the presence of CaO or $\text{Ca}(\text{OH})_2$ in silicate phases containing these oxides. However, the trends in conversion which have been experimentally observed and the predictions made by the exponential models have been used as a basis to conclude that the oxidation of Cr_2O_3 occurs to a limited extent, manifesting itself over a fairly short time-span. Removal of the product layers at the points of contact between Cr_2O_3 and CaO by leaching may still contribute to ongoing oxidation over the years but at slow reaction rates. So, preventative measures must be implemented prior to disposal. Essentially, the extent of oxidation is a function of the chemical composition and mineralogy of the slags. Oxidation can be controlled provided that these are altered accordingly. It is also of interest to see whether such observations can be made for the oxidation of $\text{Cr}(\text{OH})_3$ and hence other types of $\text{Cr}(\text{III})$ bearing wastes such as neutralisation sludges.

ACKNOWLEDGEMENTS

A heartfelt thanks is extended to the following people:

- My supervisor, Dr. Harro von Blottnitz for his excellent guidance and supervision in the last two years. Harro, I would also like to thank you for your endless patience and co-operation during the months of writing up and for being a wonderful human being. I really felt honoured and blessed to have had you as a supervisor and I hope that your future students realise how lucky they are.
- The honourable Dr. Jochen Petersen: Without the work that you initiated many years ago, there would no basis for this research so thank you for laying the foundation for my research. Thanks also for believing in me and for encouraging me to pursue this MSc. I also appreciate the fact that you always tried to be a part of this research despite having other commitments so please accept a special thanks for sacrificing your spare time to review my draft chapters.
- Professor Michael Brown from Rhodes University, for his guidelines on solid-gas kinetics
- My dear friend, Shehnaaz for proof reading the final chapters and for always being a good, caring and helpful friend
- Sue Buerger, my colleagues in the greenhouse and friends in the Bios group for your moral support and encouragement. Special thanks to Pippa Notten for transporting me home so that I could make progress with the write-up
- Helen Divey and Shireen Mjacu for conducting the elemental analyses on the slag samples, the Malvern analyses and the AA analyses on the pure chemicals.
- The National Research Foundation for funding the research in my second year of study
- My parents, friends and family in Pietermaritzburg for your support and encouragement over the last two years
- Mergan, Sharmala and Deshalin for helping me to get settled in Cape Town
- Sam, Jackie and Lu for your friendship and support over the last few months

TABLE OF CONTENTS

Synopsis	i
Acknowledgements	iii
List of Figures	xi
List of Tables	xv
CHAPTER ONE – INTRODUCTION	1
1.1. Background	1
1.2. Problem Statement	2
1.3. Thesis Objectives	3
1.4. Thesis Structure	4
CHAPTER TWO – LITERATURE REVIEW	6
2.1. An Introduction to Chromium	6
2.2. Chromium in the Industrial Sector	6
2.2.1. Chromium in the Ferrometallurgical Industry	7
2.3. The Natural Occurrence of Chromium	8
2.4. The Toxicity of Chromium	8
2.5. The Oxidation States of Chromium	10
2.6. Cr(III) Chemistry	10
2.6.1. Aqueous Cr(III) Chemistry	10
2.6.2. Solid-state Cr(III) Chemistry	13
i) The Chemistry of Chromium Oxide (Cr_2O_3)	13
ii) The Chromites and their Chemistry	13
2.7. Cr(VI) Chemistry	14
2.7.1. Aqueous Cr(VI) Chemistry	14
2.7.2. The Chromates	16

2.8 Reactions Contributing to the Oxidation of Trivalent Chromium under Environmental Conditions – Kinetics and Mechanisms	17
2.8.1. Aqueous Cr(III) Oxidation by Dissolved Oxygen	19
2.8.2. Oxidation by Manganese Oxides	19
2.8.3. The Oxidation of Chromium Oxide by Atmospheric Oxygen	20
2.9 The Oxidation of Cr(III) in Landfilled Wastes	22
2.10 The Chemistry and Mineralogy of Cr(III) Containing Slags (Stainless Steel Slags)	23
2.10.1. The Bulk Chemical Composition of Stainless Steel Slags	23
2.10.2. The Mineralogy of Stainless Steel Slags	24
2.11. Conclusion	25
CHAPTER THREE – EXPERIMENTAL APPROACH AND METHODS	27
3.1. Experimental Plan	27
3.2. Materials	28
3.2.1. Pure Chemicals	28
3.2.2. Ferrometallurgical Slags	28
3.3. Experiments Devised to Test Hypotheses	29
3.3.1. Oxidation in the presence of Calcium Oxide (CaO)	29
3.3.2. Oxidation in the presence of Calcium Hydroxide (Ca(OH) ₂)	29
3.3.3. Oxidation in Ferrometallurgical Slags	30
3.3.4. Elemental Analysis of Slags	30
3.4. Experimental Series Devised to Investigate the Key Parameters that Influence the Rate of Oxidation of Chromium Oxide	30
3.4.1. The Influence of CaO or Ca(OH) ₂ content	30
3.4.2. The Influence of Pore Moisture	30
3.4.3. The Influence of Temperature	31
3.4.4. The Influence of Particle Contact	31

3.4.5. The Influence of Particle Size and Chemical Composition on the Rate of Oxidation in Ferrometallurgical Slags	31
3.5. Verification that Atmospheric Oxygen Acts as the Electron Acceptor	31
3.6. Experimental Methods	32
3.6.1. The Pre-treatment of Chromium Oxide (Cr_2O_3)	32
3.6.2. The Preparation of Materials (Balls, Powder-Mixes and Pellets)	32
i) The Preparation of Cr_2O_3 - $\text{Ca}(\text{OH})_2$ Balls and Powdered Slag Balls	32
ii) The Preparation Cr_2O_3 - CaO Powder Mixes	33
iii) The Preparation of Cr_2O_3 - CaO Pellets	33
3.6.3. The Maintenance of the Different Reaction Conditions	34
i) The Maintenance of the Pore Moisture of the Cr_2O_3 - $\text{Ca}(\text{OH})_2$ Balls	34
ii) Exposure to Ambient Moisture	34
iii) Maintenance of the Cr_2O_3 - $\text{Ca}(\text{OH})_2$ Balls under Nitrogen	35
iv) The Maintenance of Dry Conditions	35
3.6.4. Sampling of the Balls, Powders and Pellets	35
i) Sampling of Cr_2O_3 - $\text{Ca}(\text{OH})_2$ Balls	35
ii) Sampling of the Cr_2O_3 - CaO Powders	36
iii) Sampling of the Cr_2O_3 - CaO Pellets	36
3.6.5. Analysis of Samples	37
i) Choice of Analytical Method	37
3.7. Measures Taken to Ensure the Accuracy of the Results Obtained	37
3.7.1. Repeat Experiments	37
3.7.2. Reproducibility Checks	37
3.7.3. The Effect of Drying the Cr_2O_3 - $\text{Ca}(\text{OH})_2$ Balls in the Oven	38
3.7.4. The Pre-treatment of Chromium Oxide (Cr_2O_3)	38
3.7.5. Temperature Control	38
3.7.6. The General Analytical Protocol	38
3.8. Sampling Times	39

3.9. Conclusion	39
------------------------	-----------

CHAPTER FOUR - RESULTS **40**

4.1. Results **40**

4.1.1. The Oxidation of Cr_2O_3 in the Presence of CaO 40

4.1.2. The Oxidation of Cr_2O_3 in the Presence of $\text{Ca}(\text{OH})_2$ 41

i) The Influence of CaO or $\text{Ca}(\text{OH})_2$ Content 43

ii) The Influence of Pore Moisture 43

iii) The Influence of Particle Contact 45

4.1.3. The Role of Atmospheric Oxygen as the Electron Acceptor 45

4.1.4. The Temperature Dependence of the Oxidation of Chromium Oxide (Cr_2O_3) 46

4.1.5. Oxidation in Ferrometallurgical Slags 47

i) The Influence of Particle Size 47

ii) The Influence of Pore Moisture 50

iii) Oxidation of Slag Powders Exposed to Air 54

iv) The Chemical Composition of the Slags 55

v) A Comparison of the Extents of Oxidation in Slags and in Pure Chemicals 56

4.2. The Repeatability of the Results **57**

4.3. Conclusion **58**

CHAPTER FIVE – THE MECHANISM OF THE OXIDATION OF CHROMIUM OXIDE BY ATMOSPHERIC OXIDATION **60**

5.1. The Experimental Evidence that Validates the Proposed Reactions **61**

5.1.1. The Oxidation in the Presence of CaO and $\text{Ca}(\text{OH})_2$ 60

5.1.2. The Role of Atmospheric Oxygen as the Electron Acceptor 61

5.2. The Factors that Influence the Rate of Oxidation **61**

5.2.1. The Influence of CaO and $\text{Ca}(\text{OH})_2$ Content 61

5.2.2. The Influence of Pore Moisture 62

5.2.3. The Influence of Temperature 62

5.2.4. The Influence of Particle Contact 63

5.3. Trends in the Reaction Rates	63
5.3.1. Logarithmic or Inverse Logarithmic Trends	64
5.3.2. Initial Linear Trends	64
5.4. Oxidation in Ferrometallurgical Slags	65
5.4.1. The Reactions Causing the Oxidation in the Slags	65
i) The Oxidation of Cr_2O_3 in the Presence of CaO and $\text{Ca}(\text{OH})_2$	65
ii) The Oxidation of Calcium Chromite	65
5.4.2. The Role of the Mineralogy of the Slags in Oxidation	66
5.4.3. An Application of the Mechanistic Insights to Interpret the Oxidation Patterns in the Slags	66
5.4.4. The Influence of Particle Size on the Rate of Oxidation in the Slags	67
5.4.5. The Influence of Pore Moisture on the Rate of Oxidation in the Slags	67
5.5. Preventative Measures for the Disposal of the Slags Based on Mechanistic Insights	67
5.5.1. Reduction in the CaO Content of Ferrometallurgical Slags	67
5.5.2. Increased Spinel Content or MgO Content of the Slags	68
5.5.3. Controlled Particle Size Distributions in the Slags	68
5.5.4. Competing Cations of the Atomic Centres for the Oxygen Centre of CaO	68
5.5.5. Competing ligands for the Cr^{3+} Ion	69
5.6. Conclusion	69
CHAPTER SIX – THE KINETIC INVESTIGATION	71
6.1. A Review of the Kinetic Theory for Solid-Gas Reactions	71
6.1.1. An Introduction to Solid-Gas (Tarnishing) Reactions	71
6.1.2. The Kinetics of Solid-Gas (Tarnishing) Reactions	72
6.1.3. The Parabolic Rate Law	72
6.1.4. The Linear Rate Law	73
6.1.5. The Logarithmic and Inverse Logarithmic Rate Law	74
6.2. The Role of the Product Layer in Solid-Gas Reactions	74
6.3. The Method Employed for the Kinetic Studies	76
6.4. The Kinetics of the Oxidation of Cr_2O_3 in the Presence of CaO	76

6.4.1. The Kinetic Model	76
6.4.2. Model Predictions for the Reaction	77
6.5. The Kinetics of the Oxidation of Cr₂O₃ in the Presence of Ca(OH)₂	78
6.5.1. Powder and Pellet Systems	78
i) The Kinetic Model	
ii) Model Predictions for the Reaction in the Long-Term	79
6.5.2. The Cr ₂ O ₃ -Ca(OH) ₂ Ball Systems	80
6.6. The Kinetics of the Oxidation of Cr₂O₃ in Ferrometallurgical Slags	82
6.6.1. Oxidation in Slag Powders	82
i) General Observations	82
ii) Graphical Fits of the Exponential Models	84
iii) Numerical tests on the Models	85
iv) Model Predictions for the Reaction in the Long-term	86
6.6.2. Oxidation in Slag Balls (with pore moisture evaporated)	87
i) General Observations	87
ii) Graphical Fits of the Model	89
iii) Numerical Tests on the Models	91
iii) Model Predictions for the Reactions in the long-term	92
6.7. The Long-Term Implications for Slags Disposed to Landfill	92
6.8 Conclusion	93
 CHAPTER SEVEN – CONCLUSIONS	
7.1. The Key Objectives of the Research	95
7.1.1. The Key Parameters Influencing the Rate of Oxidation of Cr ₂ O ₃	95
7.1.2. The Mechanism of the Oxidation of Cr ₂ O ₃	96
7.1.3. The Oxidation of Cr ₂ O ₃ in Ferrometallurgical Slags	97
7.1.4. The Key Reactions Contributing to the Oxidation of Cr ₂ O ₃ in Ferrometallurgical Slags	97
7.1.5. The Quantification of Reaction Rates	98
7.2. Validation of Hypotheses	99
7.2.1. The Oxidation of Cr ₂ O ₃ under Environmental Conditions	99
7.2.2. The Reactions Leading to the Oxidation of Cr ₂ O ₃ in Ferrometallurgical Slags	99

7.3. The Shortcomings of the Research	99
7.4. Recommendations for Future Work	100
7.4.1. The Influence of Pore Moisture	100
7.4.2. Kinetic Models for Cr ₂ O ₃ -Ca(OH) ₂ Balls and for Ferrometallurgical Slags	100
7.4.3. Comparisons between the Relative Rates of Oxidation in the Pure Chemicals and the Slags	100
7.5. Recommendations for Future Industrial Practices	101
7.5.1. Reduction in CaO content and Increase in MgO	101
7.5.2. Competing Cations for the Oxygen Centres of CaO and Ca(OH) ₂	101
7.5.3. Competing Ligands for Cr ³⁺	102
7.5.4. Oxidation in Other Cr(III) Bearing Wastes	102
REFERENCES	103
OVERVIEW OF APPENDICES	109

LIST OF FIGURES

Figure 2-1: The Solubility and speciation of Cr(III) as a function of pH	11
Figure 2-2: The predominant Cr(VI) species at varying pH values	15
Figure 2-3: The solubility curve of CaCrO_4	16
Figure 2-4: The generation of Cr(VI) via reactions involving Cr(III)-hydroxy species and oxygen at pH 12.2	19
Figure 2-5: Change in Gibbs Free Energy (ΔG_R) for the reaction $\text{Cr}_2\text{O}_3 + 1.5 \text{O}_2 + 2\text{CaO} \rightarrow 2\text{CaCrO}_4$ as a function of temperature	21
Figure 2-6: Cr(VI) generation in Cr_2O_3 - $\text{Ca}(\text{OH})_2$ and Cr_2O_3 -NaOH systems	22
Figure 3-1: A Schematic Outline of the Experimental Approach to studying the oxidation of Cr_2O_3	28
Figure 3-2: A Diagrammatic Illustration of the method used to prepare the Cr_2O_3 - $\text{Ca}(\text{OH})_2$ balls	33
Figure 3-3: A Diagrammatic Illustration showing how the pore moisture was maintained in the Cr_2O_3 - $\text{Ca}(\text{OH})_2$ Balls	34
Figure 3-4: A Schematic Illustration of the Sampling Procedure to which Cr_2O_3 - $\text{Ca}(\text{OH})_2$ balls were subjected	36
Figure 4-1: A comparison of the conversion-time data for Cr_2O_3 - CaO powders maintained in a dessicator and exposed to ambient moisture respectively (CaO content: 50%)	40
Figure 4-2: Conversion-time data for the oxidation of Cr_2O_3 in Cr_2O_3 - $\text{Ca}(\text{OH})_2$ balls with varying $\text{Ca}(\text{OH})_2$ content and with excess pore moisture prevailing	41
Figure 4-3: Conversion-time data for Cr_2O_3 - $\text{Ca}(\text{OH})_2$ Balls with varying $\text{Ca}(\text{OH})_2$ content in which the excess pore moisture was allowed to evaporate	42
Figure 4-4: Conversion-time data for the oxidation of Cr_2O_3 - CaO powder mixes with varying CaO content	42
Figure 4-5: A comparison of the conversions observed in Cr_2O_3 - CaO powder and pellet systems	42

LIST OF FIGURES (CONTD)

Figure 4-6: A Comparison of the conversions observed in Cr_2O_3 - $\text{Ca}(\text{OH})_2$ balls where the Pore Moisture was Maintained and Allowed to Evaporate Respectively ($\text{Ca}(\text{OH})_2$ Content: 20%)	44
Figure 4-7: A Comparison of the Extents of Oxidation in Cr_2O_3 - $\text{Ca}(\text{OH})_2$ Balls in which the Excess Pore Moisture was allowed to Prevail and Evaporate Respectively ($\text{Ca}(\text{OH})_2$ Content: 50%)	44
Figure 4-8: Conversion-time data for Cr_2O_3 – $\text{Ca}(\text{OH})_2$ Balls containing 50% $\text{Ca}(\text{OH})_2$ and maintained under nitrogen	45
Figure 4-9: The Influence of Temperature on the Oxidation of Chromium Oxide in the Presence of $\text{Ca}(\text{OH})_2$	46
Figure 4-10: The Influence of Particle Size on the Rate of Oxidation in Old Mixed Slag Balls in which the Pore Moisture was maintained	47
Figure 4-11: The Influence of Particle Size on the Rate of Oxidation in New CLU Slag Balls in which the Pore Moisture was Maintained	48
Figure 4-12: The Influence of Particle Size on the Rate of Oxidation in New EAF Slag Balls in which the Pore Moisture was maintained	48
Figure 4-13: The Influence of particle size on the rate of oxidation in old mixed slag balls where the excess pore moisture was allowed to evaporate	49
Figure 4-14: The Influence of Particle Size in New CLU Slag Balls where the excess pore moisture was allowed to evaporate	49
Figure 4-15: The influence of particle size on the rate of oxidation in New EAF slag balls where the excess pore moisture was allowed to evaporate	50
Figure 4-16: The Influence of Pore Moisture on the Rate of Oxidation in Old Mixed Slag Balls-Particle Size Class:<75 μm	51
Figure 4-17: The Influence of Pore Moisture on the Rate of Oxidation in New CLU Slag Balls-particle size class:<75 μm	51
Figure 4-18: The Influence of Pore Moisture on the Rate of Oxidation in New EAF Slag Balls-Particle Size Class:<75 μm	52
Figure 4-19: The Oxidation of Cr_2O_3 in Old Mixed Slag Powders Exposed to Air	54
Figure 4-20: The Oxidation of Cr_2O_3 in New CLU Slag Powders Exposed to Air	54

LIST OF FIGURES (CONTD)

Figure 4-21: The Oxidation of Cr_2O_3 in New EAF Slag Powders Exposed to Air	55
Figure 4-22: Results from a repeatability check on $\text{Cr}_2\text{O}_3 - \text{Ca}(\text{OH})_2$ Balls containing 50 % $\text{Ca}(\text{OH})_2$ and where the excess pore moisture was maintained	57
Figure 4-23: The Results from a Repeatability Check on $\text{Cr}_2\text{O}_3 - \text{Ca}(\text{OH})_2$ Balls (20% $\text{Ca}(\text{OH})_2$) in which the excess pore moisture was allowed to evaporate	58
Figure 4-24: The Results from a repeatability check on $\text{Cr}_2\text{O}_3 - \text{Ca}(\text{OH})_2$ Ball experiments in which the balls were maintained at eighty degrees	58
Figure 5-1: A Schematic Illustration of A) logarithmic or inverse logarithmic curves B) Initial Linear Sections followed by decline in slope	64
Figure 6-1: The relationship between rate and time in $\text{Cr}_2\text{O}_3 - \text{CaO}$ powder-mixes maintained in a dessicator	76
Figure 6-2: A rate versus time plot for the reaction: $\text{Cr}_2\text{O}_3 + 1.5 \text{O}_2 + 2\text{Ca}(\text{OH})_2 \rightarrow 2\text{CaCrO}_4 + 2\text{H}_2\text{O}$ in powder and pellet systems	78
Figure 6-3: A rate versus time plot for the reaction: $\text{Cr}_2\text{O}_3 + 1.5\text{O}_2 + 2 \text{Ca}(\text{OH})_2 \rightarrow 2\text{CaCrO}_4 + 2\text{H}_2\text{O}$ in ball systems	81
Figure 6-4: The Relationship between Reaction Rate and Time in Old Mixed Slag Powders exposed to air (particle size class: 300-1000 μm)	84
Figure 6-5: The Relationship between Reaction Rate and Time in New CLU Slag Powders Exposed to Air (Particle size class: 300 -01000 μm)	85
Figure 6-6: The Relationship between Reaction Rate and Time in New EAF Slag Powders exposed to air (Particle size class: 300-1000 μm)	85
Figure 6-7: The Relationship between Rate and Time in the Old Mixed Slag Balls with the pore moisture evaporated (particle size class: 300-1000 μm)	89
Figure 6-8: The Relationship between Reaction rate and Time in New CLU Slag Balls (pore moisture evaporated) which disintegrated after two weeks (particle size class: 300-1000 μm)	90

LIST OF FIGURES (CONTD)

Figure 6-9: The Relationship between Reaction rate and Time in New EAF Slag Balls (pore moisture evaporated) which disintegrated after two weeks (particle size class: 300-1000 μ m)

90

University of Cape Town

LIST OF TABLES

Table 2- 1: Available thermodynamic data for the oxidation of chromium oxide in the presence of CaO	21
Table 2-2: The Chemical Composition of Stainless Steel Slags Obtained from Different Manufacturers	23
Table 2-3: The Average Chemical Composition of EAF slags after the Meltdown Process	24
Table 4-1: A comparison of the Conversions from the Experiments under Nitrogen and the corresponding experiments in which $\text{Cr}_2\text{O}_3 - \text{Ca}(\text{OH})_2$ Balls were exposed to air	45
Table 4-2: The Moisture Contents of the Slag Balls in which the Excess Pore Moisture was Maintained (Size Fraction: $<75\mu\text{m}$)	53
Table 4-3: The Elemental Composition of each Type of Slag	56
Table 6-1: The Results from the Numerical Test of the Model for the Reaction: $\text{Cr}_2\text{O}_3 + 1.5 \text{O}_2 + 2 \text{CaO} \rightarrow 2\text{CaCrO}_4$	77
Table 6-2: The Results from the Numerical Fit of the Exponential Model to the Experimental Data	79
Table 6-3: The Predicted Reaction Rates and Conversions over a two-year period for the Cr_2O_3 -CaO Powder and Pellet Systems	80
Table 6-4: A Summary of the Kinetic Analysis conducted on the slag powders that were exposed to air	83
Table 6-5: The Results from a Numerical Test Conducted on the Exponential Models for Slag Powders Exposed to Air (Particle Size Class: 300 1000 μm)	86
Table 6-6: The Predicted Reaction Rates and Conversions for slag powders over A two-year period	87
Table 6-7: A Summary of the Results from a Kinetic Analysis conducted on the Slag Balls	88
Table 6-8: The Numerical Test on the Kinetic Models for each type of slag (particle size class:300-1000 μm)	91

LIST OF TABLES (CONTD)

Table 6-9: The Predicted Reaction Rates and Conversions for Slag Balls with
The pore moisture evaporated (particle size class: 300-1000 μm)

92

University of Cape Town

CHAPTER ONE

INTRODUCTION

1.1. Background

Chromium is an element, which has many industrial applications. It is used mainly in the metallurgical industry (Barnhart, 1997; Nriagu, 1988) but also has its uses in the production of fine chemicals eg. in the manufacture of pigments. Its wide use for metallurgical purposes stems from the inert nature of its trivalent oxide. The oxide forms a protective layer on metal surfaces and thereby plays an important role in corrosion prevention (Barnhart, 1997).

Chromium occurs naturally in various mineralogical forms. However, the use of chromium in the industrial sector has also resulted in the production of wastes due to technological and operational constraints. Such wastes include slags from metallurgical applications, and waste water from the fine chemical and metallurgical industries, which is converted into a waste sludge upon reduction and precipitation. The discharge of chromium bearing wastes has invariably resulted in increased chromium concentrations in the environment (Burke et. al., 1991; Calder, 1988).

The environmentally stable oxidation states of chromium are the trivalent (Cr(III)) and the hexavalent (Cr(VI)) forms. Both oxidation states differ with respect to their mobilities and toxicities. Cr(III) is relatively immobile and less toxic. Cr(VI) is highly mobile and toxic.

Due to its toxicity, hexavalent chromium has become a subject of considerable environmental interest over the years. Various illnesses and toxic effects such as lung cancer and mucosal ulceration have resulted from the exposure to hexavalent chromium (Sheehan et al., 1991). Numerous case studies of groundwater contamination by hexavalent chromium and illnesses caused by occupational exposure to hexavalent chromium compounds have been reported in the literature (Burke et al., 1991; Sheehan et al., 1991; Franchini et al., 1983; Mancuso, 1975; Mancuso and Hueper, 1951; Dixon, 1929). Calder (1988), reports a case study in Nassau County, New York where the discharge of untreated waste from an aircraft metal finishing plant into ponds resulted in a maximum hexavalent chromium concentration of 40mg/l in the groundwater. Another incident in Hudson County, New Jersey is reported by Burke et al. (1991) who state that the use of Cr(VI) contaminated residues as fill material in the construction of residential and commercial sites not only led to the death of a worker in a truck loading facility but also resulted in chromium contamination of the ventilation systems and the carpets of a local school.

Such incidents have led to the need for better waste management practices. Any hexavalent chromium in a waste must at least be reduced to the less harmful trivalent form prior to disposal, or chromium should be eliminated completely. An example of an industrial practice that aims at achieving this is the solidification or stabilisation of wastes such as wastewater from the metal finishing industry. This is achieved by

initially reducing the hexavalent chromium to trivalent chromium (ie. by adding a suitable reducing agent eg. ferrous ammonium sulfate) (Jacobs, 1992) and then solidifying the waste by adding a suitable solidifying agent such as lime ($\text{Ca}(\text{OH})_2$). An industrial strategy that aims at minimising chromium contamination by the disposal of chromium rich wastes, is the recycling of metallic chromium from slags and recently also furnace dusts (Language et al., 1999). Treatment technologies which aim at removing chromium from chromium bearing wastes and recovering chromium as useful chromates have been developed (Baturay et al., 1991). However, the disposal of solid chromium (III) bearing wastes such as ferrometallurgical slags and neutralisation sludges from the metal-finishing industry in landfill sites is still a common practice.

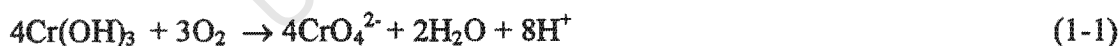
Such a practice has been viewed to be of acceptable environmental risk as the wastes contain trivalent chromium and not hexavalent chromium. However, concerns that the trivalent chromium may slowly re-oxidise to the hexavalent form upon exposure to atmospheric oxygen have been expressed. Any hexavalent chromium that is generated in the solid state can, due to its high mobility, leach out and enter ground water aquifers, where it becomes available for human consumption. Evidence for the re-oxidation of trivalent chromium in natural waters and soil environments has been reported in the literature (Fendorf and Zamoski, 1992; Milacic and Stupar, 1995; Johnson and Xyla, 1991; Eary and Rai, 1987 and Schroeder and Lee, 1975). Furthermore, it has been stated that $\text{Cr}(\text{VI})$ is the thermodynamically favoured form of chromium under oxidising conditions (Elderfield, 1970).

1.2. Problem Statement

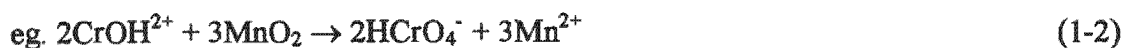
The concern for re-oxidation has motivated this investigation into the chemical reactions that could lead to the atmospheric oxidation of trivalent chromium in landfill wastes, with an emphasis on the kinetics and mechanisms of such reactions as they may occur in chromium-bearing slags.

Two reactions that have been identified and studied are:-

The Direct Oxidation of Hydroxide Forms;



Oxidation of Hydroxide Forms by Manganese Oxides;



Reaction (1-1) could result in the generation of hexavalent chromium in neutralisation sludges but has only been observed for the simple, soluble hydroxy forms in aqueous environments (Schroeder and Lee, 1975) and its potential to occur in the solid state must still be examined. Reaction (1-2) has been extensively observed in soil environments (Fendorf and Zamoski, 1992; Johnson and Xyla, 1991; Eary and Rai, 1987).

Since metallurgical slags generally contain chromium in oxide forms, the focus in the study presented here is mainly on the following reactions:



Ferrometallurgical (stainless steel) slags are known to be rich in calcium oxide, and contain the trivalent chromium oxide (Korousic et al., 2000; Kilau and Shah, 1984). So, the possibility that reaction (1-3) can give rise to the generation of Cr (VI) in slags that have been exposed to atmospheric oxygen must be investigated. Furthermore, any CaO that is present in the slags may be converted to Ca(OH)₂ upon exposure to atmospheric moisture. Hence, the likelihood that reaction (1-4) can also contribute to the oxidation of trivalent chromium in the slags must be explored.

Both reactions are known to be thermodynamically feasible and have been observed at ambient temperature (Petersen, 1998; Kilau and Shah, 1984; Hattori et al., 1978). However, the kinetics and mechanisms of reactions (1-3) and (1-4) have not been studied. Furthermore, the extent to which such reactions can occur in wastes such as ferrometallurgical slags must be properly evaluated in order to justify the concerns that have been expressed. This will depend on the chemistry of the slags.

Calcium and chromium oxides are by no means the only oxides that are present in ferrometallurgical slags. The mineralogical phases in which Cr₂O₃ exists in the slags will also determine its level of reactivity. Furthermore, it has been shown that while oxides such as CaO enhance the leachability of Cr(VI) from the slags, other oxides such as MgO hinder the leachability of Cr(VI) (Kilau and Shah, 1984). Hence, the extent to which the oxidation of trivalent chromium can occur in the slags should be evaluated and interpreted in light of the composition of the slags.

1.3. Thesis Objectives

The work presented in this study aims at achieving the following objectives:

- Identification of key parameters which are likely to influence the oxidation of trivalent chromium oxide;
- Examining the extent to which the oxidation of chromium oxide occurs in ferrometallurgical slags, and how this relates to their composition and mineralogy;
- Identification of the key reactions that contribute to the oxidation of trivalent chromium in ferrometallurgical slags;
- Use of an understanding of the mechanisms of such reactions to devise preventative measures which ultimately aim at minimising the re-oxidation of trivalent chromium in slag deposits; and
- Collection and interpretation of data which will be used to quantify the reaction rates in order to assess the long-term environmental implications.

1.4. Thesis Structure

The thesis begins with a literature review (Chapter two) in which a brief introduction to chromium, its origin, industrial uses, oxidation states and toxicity is presented. The aqueous and solid-state chemistries of trivalent and hexavalent chromium are also reviewed. A review on reactions that are likely to contribute to the oxidation of Cr(III) under environmental conditions is given. The chapter also discusses the current knowledge on the chemistry and mineralogy of ferrometallurgical slags and concludes with a brief discussion on aspects of the oxidation of chromium oxide, that have not been extensively studied.

Chapter three presents the hypotheses on the oxidation of chromium oxide that, were formulated upon reviewing the literature. An outline of the experimental methodology that was used to validate the hypotheses is also given. The experimental series that were set up to investigate those key parameters, which are likely to influence the reaction rates, are outlined. The chapter concludes with a description of the methods employed to check the reproducibility of the analytical results and to verify the accuracy of the data.

Chapter four presents the results from the experimental work conducted on Cr_2O_3 -CaO and Cr_2O_3 -Ca(OH)₂ systems in the pure chemical form as well ferrometallurgical slags. Some features of the results are discussed with a special reference to the influence of some key parameters on the rate of oxidation. Certain aspects of the results, which need to be viewed with care, are also mentioned and the chapter ends with remarks on the accuracy of the data presented.

Chapter five focuses on the experimental evidence that validates the proposed reactions, which are likely to contribute to the oxidation of Cr_2O_3 in ferrometallurgical slags. The conversion-time curves obtained experimentally are used to gain some mechanistic insights and to identify possible rate laws that the reactions obey. The key factors that influence the rates of oxidation are also discussed. The mechanistic insights are used to understand the oxidation trends observed in ferrometallurgical slags. A discussion on how the chemical composition of the slags and their mineralogy relates to the oxidation of chromium oxide is also presented. The chapter concludes with a discussion on how the mechanistic insights may be used to establish preventative measures for the oxidation of trivalent chromium in slag deposits.

Chapter six focuses largely on the kinetics of the atmospheric oxidation of the chromium oxide in the presence of CaO or Ca(OH)₂, both in pure chemicals and ferrometallurgical slags. This includes a review of the solid-gas kinetic theory, and a manipulation of selected conversion-time data sets presented in Chapter four to quantify the reaction rates. The relationship between reaction rates and time are used to identify a suitable solid-gas kinetic model, which best describes the oxidation reactions in pure chemicals and in ferrometallurgical slags. The kinetic models are numerically tested, used to identify the rate-limiting steps of the reactions and to predict trends in reaction rates and conversions in the long-term. The chapter concludes with a discussion on the overall implications for slags disposed to landfill.

Chapter seven is the concluding chapter which re-examines the key objectives of the thesis and discusses the main findings of the research together with conclusions that can be drawn. This chapter also addresses the validation of the hypotheses and examines the shortcomings of the research. Recommendations for future work and future industrial practices are made.

University of Cape Town

CHAPTER TWO

LITERATURE REVIEW

This chapter gives a brief introduction to chromium, reviews its industrial uses and environmental occurrence. The toxicity of chromium particularly its hexavalent form is also discussed. The chemistries of the trivalent and hexavalent forms are reviewed, and the reactions leading to the oxidation of the trivalent form to hexavalent form are extensively discussed. The current knowledge on the chemistry and mineralogy of ferrometallurgical slags is also discussed. The chapter concludes with a discussion on the shortcomings of the research that has been conducted on the oxidation of chromium oxide.

2.1. An Introduction to Chromium

Chromium is the 24th element on the periodic table. Its average atomic weight is 52 and it is one of the d-block elements or transition metals.

The physical properties of elemental chromium are typically those which characterise metals. It is grey-white in colour, brittle, highly polishable and has a cubic crystalline structure. It is also chemically unstable under atmospheric conditions and passivates easily with a thin oxide layer (Deltombe et al., 1966). This renders it useful in corrosion protection.

Besides corrosion protection, chromium has other industrial applications. These include wood preservation, leather tanning, metal-finishing and ferrometallurgical applications (Barnhart, 1997; Nriagu, 1988). Hence, knowledge of the role played by chromium in the industrial sector is needed.

2.2. Chromium in the Industrial Sector

The use of chromium in the industrial sector dates back to over 100 years ago when the first attempts to produce corrosion resistant materials were made (Jacobs, 1992). Nriagu (1988) indicates that 76% of the chromium produced from ore processing is used in the metallurgical industry. This is mainly in the production of stainless steel, 13% is used for the manufacture of refractory linings and 11% for other uses such as metal finishing, corrosion control, leather tanning, dyes, pigments, wood-preservation etc.

There are no suitable substitutes for chromium in these industrial sectors so the demand for this metal is quite high. Since chromium resources are abundant, little attempts to recover chromium from industrial wastes have been made. This has invariably resulted in some chromium being present in industrial wastes. Such wastes can be hazardous due to their toxicity and leaching potential (Jacobs, 1992). This has led to the concern that chromium-containing wastes may not be environmentally benign.

2.2.1. Chromium in the Ferrometallurgical Industry

About 80% of mined chromium, is used for metallurgical applications with most of this being used in the manufacture of stainless steel (Barnhart, 1997). Its extensive use in this industrial sector is due mainly to its chemical properties. According to Barnhart, it is chromium that makes stainless steel “stainless”.

The fundamental chemistry of chromium that needs to be understood in order to justify its use in the stainless steel industry is the stability of the trivalent oxide (Cr_2O_3). Chromium oxide forms a protective layer on the surface of the metal and prevents the underlying layer from corrosion upon exposure to the environment.

In fact, chromium imparts properties such as hardness, strength and high temperature resistance to stainless steel and the inert nature of Cr_2O_3 has made its use in the stainless steel industry absolutely essential. At the same time, the possibility that chromium oxide, which is a chemical constituent of stainless steel slags (Korousic et.al, 2000; Kilau and Shah, 1984) can slowly react with calcium-compounds and atmospheric oxygen to form calcium chromate, can render it an environmental concern to the stainless steel industry.

The chromium minerals are used to manufacture stainless steel, refractories and fine chemicals (Nriagu, 1988). This invariably results in the production of wastes such as slags from stainless steel and refractory production and leach residues from fine chemical production. Two types of fine chemical production need to be distinguished. These are the production of Cr(VI) fine chemicals eg $\text{K}_2\text{Cr}_2\text{O}_7$ from the roasting of chromite ore and leaching and precipitation, and the production of Cr(III) fine chemicals eg, Cr_2O_3 from the reduction of Cr(VI). The Cr(III) fine chemicals are used for applications such as leather tanning while the Cr(VI) chemicals are used for metal-plating. Both the production and use of these fine chemicals result in wastes that contain Cr(VI) eg. the metal finishing industry generates waste-waters that are rich in Cr(VI). If such wastes are inappropriately stored, leakage into the environment may occur resulting in elevated levels of chromium in the ground and surface waters. This phenomenon has been observed in some case studies detailed in Chapter one (Calder, 1988).

In other words chromium can be found in the environment in increased concentrations as a result of industrial activities. Excessive levels of chromium can result in severe pollution, which is detrimental to all forms of life.

Thus, chromium has become the subject of an industrial paradox where it has many useful industrial applications but at the same time can be extremely toxic depending on its oxidation state. So, an understanding of the occurrence of chromium in the environment, its mobility, toxicity and interconversions with respect to oxidation states is important.

2.3. The Natural Occurrence of Chromium

Chromium is widely distributed in the environment but does not occur in the free state (Mellor, 1931). It has been identified as the seventh most abundant element on earth where it is present mostly in the core and mantle (Nriagu, 1988). It is also the 21st most abundant element in the earth's crust with an average concentration of 100µg /g (Barnhart, 1997; Nriagu, 1988) and ranks fourth among the 29 elements of biological importance. Chromium is an essential nutrient at trace quantities with a recommended dietary intake of < 200µg/day (Nieboer and Jusys, 1988) but becomes lethal when consumed in large quantities.

Besides the earth's crust, chromium is also found in natural water-bodies eg. sea water (Nriagu, 1988; Elderfield, 1970) and sediments. Nearly all soils contain about 35-100mg/kg chromium but some workers have reported lower concentrations of typically 0.3-10 mg/kg (McGrath and Smith, 1991). Its concentration in natural water bodies have been reported as < 5x10⁻⁸M (median concentration) in fresh water (Richard and Bourg, 1991) and between 10⁻⁸ to 10⁻⁹M in oceans (Mayer, 1988).

Chromium occurs naturally in various mineralogical forms, which typically occur in trace quantities and are dissolved in natural waters and soils. The principal mineralogical phase of chromium is chromite (FeO.Cr₂O₃) which has a maximum chrome content of 46% (Nriagu, 1988). Gemstones such as rubies and emeralds also contain chromium. Most chromium minerals are rich in trivalent chromium, but minerals containing the hexavalent form, for example lead chromate, also exist.

2.4. The Toxicity of Chromium

Chromium is said to be an essential nutrient for plants, animals and humans due to its role in glucose metabolism but can be toxic and even lethal when consumed in large quantities (McGrath and Smith, 1991; Sheehan et al., 1991; Burke et al., 1991). The toxicity of Cr(III) is not well understood although it can inhibit soil bacterial growth in excessive quantities (Ross et al., 1981), can cause equal damage to food seedlings (McGrath and Smith, 1991) and can even harm certain forms of aquatic life (Schroeder and Lee, 1975). Cr(VI) is by far the most toxic form of chromium. Its toxic effect stems from its role as a bio-oxidant where it can enter cell membranes, oxidise organic molecules and destroy cells (Ross et al., 1981). The lethal dose of Cr(VI) is 0.1 g per kg body weight (Mertz et al in Richard and Bourg, 1991), the recommended drinking water level has been set at 0.05ppm (Sheehan et al., 1991) and a limit of 0.1mg/m³ has been set for air pollution (Proctor et al., 1997).

The toxicity of hexavalent chromium has been well documented in the literature. Its toxic effects range from dermatitis to various cancers (Sheehan et al., 1991). The US Environmental Protection Agency (EPA) has classified airborne Cr(VI) as an inhalation carcinogen (Proctor et al., 1997). The chromates in particular have been found to be extremely toxic to plants, animals and man even in trace quantities (Gemmell, 1973). The fundamental concern regarding Cr(VI) toxicity is the occupational exposure to it which can result in various illnesses. Besides, human exposure other adverse effects of Cr(VI) on the environment need to be considered. Some selected case studies, which justify such concerns, are discussed in this section.

Dixon (1929) has reported a series of eighteen incidents where employees of the chrome-plating industry suffered severe cases of nasal perforations upon exposure to chromic acid mists in poorly ventilated areas. Signs of ulceration in five workers who were working near a poorly ventilated tank for less than one month were also observed.

Further evidence of the toxic effects of Cr(VI) in occupational scenarios has been presented by other workers (Franchini et al., 1983; Royle, 1975; Mancuso, 1975; Mancuso and Hueper, 1951) who have in epidemiological studies reported an increased risk of respiratory cancer from occupational exposure to Cr(VI). It has in fact been shown that workers who are exposed to chromium concentrations of greater than 4mg/m^3 have an increased risk of lung cancer (Sheehan et al., 1991). Cr(VI) is considered to be responsible for these cancer risks and has thus been rated as a Class A human carcinogen.

The carcinogenic effects of Cr(VI) are by no means its only toxic effects. Dermal exposure to hexavalent chromium (chromates) has resulted in kidney damage and severe skin lacerations (Sheehan et al., 1991; Calder, 1988). Calcium chromate has also been identified as a compound that causes tumour formation during inhalation (Palmer and Wittbrodt, 1991). Exposure to chromic acid has also caused skin irritation in industrial workers (Adams, 1990). Cases of allergic contact dermatitis in workers of the printing, leather tanning and metal plating industries have also been extensively reported in the literature (Lee and Goh, 1988; Peltonen and Fraki, 1983; Korallus et al., 1974; Houding, 1970; Winston and Walsh, 1951).

Industrial exposure to hexavalent chromium compounds can also result in gastrointestinal symptoms and bleeding with later toxic effects resulting in liver or kidney failure. Burke et al. (1991) describe hexavalent chromium as "corrosive, allergenic and mutagenic".

In addition to the concern that Cr(VI) is a human health hazard, other concerns such as the economic implications for the industries whose wastes are disposed of in landfill sites need to be considered. Costs of the most appropriate methodology for clean-up measures or the remediation of landfill sites have been estimated as $\pm \$1$ billion (Sheehan et al., 1991) and could even exceed this amount. Furthermore the concern at large is not only for the occupational exposure but also for residential exposure i.e. the concern for the health of people living in the vicinity of landfill sites.

However, Cr(VI) is not only detrimental to the human environment but also to the plant environment. Gemmell (1973) reports incidents where wastes rich in chromates have resulted in "serious eyesores" in areas adjacent to chromate smelters and also observed that the growth of white mustard on unweathered chromate waste heaps was extensively inhibited.

Other workers support the findings of Gemmell. McGrath and Smith (1991) also report the inhibition of plant growth in chromium contaminated landfill sites. Evidence for severe river pollution in the river Croal where biota were adversely affected by run-off from a chromite ore process landfill residue has been reported by Breeze (1973).

Thus, although the environmental concern at large is mainly on the toxicity of hexavalent chromium to the human environment, its toxicity to plants and adverse impact on the environment must not be ignored. Such incidents not only depict poor waste management and poor waste disposal practices but also raise pressing questions about the origin of the hexavalent chromium. Although the wastes typically contain residual concentrations of Cr(VI), the possibility that the oxidation of trivalent chromium could be giving rise to hexavalent chromium compounds cannot be ignored. This has led to the need to review the oxidation states of chromium and their potential to inter-convert.

2.5. The Oxidation States of Chromium

Chromium can exist in a variety of oxidation states ranging from +2 to +6. However, its two environmentally stable forms are the trivalent (+3) or the hexavalent (+6) forms. The divalent state (+2) of chromium is known to exist in aqueous solution (Baes and Mesmer, 1976) but is very unstable and oxidises very easily to the trivalent state. The quadrivalent (+4) and pentavalent (+5) oxidation states can also occur as unstable reactive intermediates in chemical reactions involving Cr(III) to Cr(VI) interconversions (Eary and Rai, 1987).

The trivalent and the hexavalent forms differ significantly in their chemical and toxicological effects (Fendorf et al., 1992). The trivalent form is known to be less toxic and relatively immobile, which implies that it cannot migrate in an aqueous phase because of its tendency to precipitate as $\text{Cr}(\text{OH})_3$ in the normal pH range. The hexavalent form, on the other hand, is extremely toxic and mobile i.e. it remains in aqueous solution throughout the pH range.

Some workers believe that potential for the trivalent form to oxidise to the hexavalent form make its toxicity tantamount to that of hexavalent chromium (Fendorf et al., 1992). However, the complete oxidation of Cr(III) to Cr(VI) is yet to be observed. Hence, there is an increasing need to study the inter-conversions between Cr(III) and Cr(VI) in environmental scenarios and to gain an understanding of the chemistries of these oxidation states.

2.6. Cr(III) Chemistry

2.6.1. Aqueous Cr(III) Chemistry

The Cr(III) ion is noted for its ability to form strong complexes with water molecules (Elderfield, 1970) in aqueous solution. This is based on the fact that chromium is one of those elements in which the inner sphere co-ordination of the water molecules is kinetically permanent i.e. the complex formation is irreversible. It has been shown that the formation of the aquo Cr(III) ion $\text{Cr}(\text{H}_2\text{O})_6^{3+}$ has a reaction half-life of approximately 40 hours (Hunt and Taube, 1951). Furthermore, the Cr(III) ion has a high affinity for oxygen centres and the complex formation with water molecules is also based on the interaction between Cr(III) and the oxygen centres on water molecules.

Other workers have also supported this phenomenon although they have proposed different aquo-species. Baes and Mesmer (1976) have shown that the Cr(III) ion can hydrolyse to varying extents forming simple hydroxy-bridged species such as $\text{Cr}(\text{OH})_2^+$ and $\text{Cr}(\text{OH})_2^{2+}$. Polynuclear hydroxy-bridged species such as $\text{Cr}_3(\text{OH})_4^{5+}$ (green) have also been identified by ion exchange techniques (Finholt, 1960; Laswick and Plane, 1959). Rai et al (1987) have identified CrOH^{2+} and $\text{Cr}(\text{OH})_4^-$ as the dominant species at pH values 4-6 and 11-14 respectively. This is clearly shown in Figure 2.1. Higher order polymeric species of up to Cr_5 have been identified (Stuenzi and Marty, 1983).

Cr(III) is a Lewis acid and forms insoluble $\text{Cr}(\text{OH})_3$ (Weng et al, 1994). This renders it amphoteric in nature where it can behave both as an acid and a base. Figure 2-1 shows the various hydrolysed Cr(III) species that can exist at different pH values and also shows the pH values at which the soluble hydrolysed species exist.

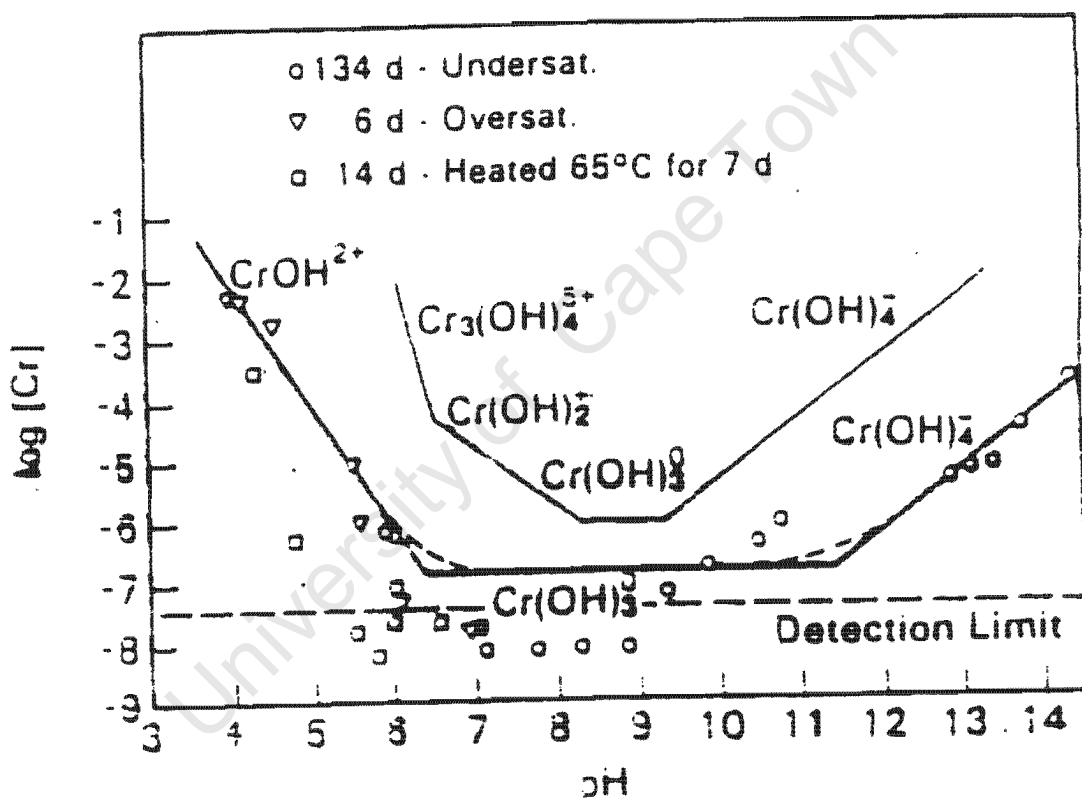


Figure 2-1: The Solubility and speciation of Cr(III) as a function of pH (from Rai et al., 1987 and Baes and Mesmer, 1976)

There are some discrepancies with respect to the actual pH ranges in which some of the species exists. Nevertheless Figure 2-1 shows that Cr(III) exists as a variety of hydrolysed species at different pH. In the pH range 6-11 Cr(III) exists primarily as the insoluble hydroxide $\text{Cr}(\text{OH})_3$. This pH range is characteristic of natural aqueous environments. Hence, in natural environments Cr(III) is most likely to predominate as the insoluble and immobile $\text{Cr}(\text{OH})_3$. This explains why it has been viewed as stable and as non-hazardous.

At lower pH values the solubility of Cr(III) increases with CrOH^{2+} predominating in the pH range 4-6 and the free Cr(III) ion (Cr^{3+}) predominating below pH 3.8 but Figure 2-1 also shows that some soluble species of Cr(III) viz. $\text{Cr}(\text{OH})_4^-$ can exist at high pH. Cr(III) can even exist as anionic species (chromite ions) in alkaline solution eg. the CrO_2^- and the CrO_3^{3-} anions.

Cr(III) also forms a variety of complexes with ligands such as F^- , Cl^- , Br^- , and SO_4^{2-} (Elderfield, 1970) and can even form complexes with ammonium salts, cyanides, sulphocyanides, oxalates and citrates (Deltombe et al., 1966). Cr(III) hydroxo-complexes are expected to be the predominant species of Cr(III) in natural waters (Rai et al., 1987). The complex formation is dependent on the stabilisation of the d^3 ion which, affects ligand displacement. Hartford (1979) has indicated that the complexes of Cr(III) are metastable and ligand exchange is usually very slow. Nakayama (1981) showed that when Cr(III) is complexed with citrate even MnO_2 cannot oxidise it. Thus, the reactivity of Cr(III) can be considered to be dependent on the rate of ligand exchange.

The ability of Cr(III) to form complexes with organic ligands has been supported by James and Bartlett (1983a) who have identified fulvic acid as another potential organic ligand in soil environments. In fact, these workers have also shown that the release of Cr(III) from a citric complex reduces its reactivity (James and Bartlett, 1983b). Complexes with such ligands also render the Cr(III) ion more soluble and mobile at pH values as high as 7. Other organic complexes of Cr(III) are also known but are less common. High molecular weight organics immobilize Cr(III) and thus have an opposing effect on its mobility. Cr(III) forms very stable complexes with proteins and this forms the basis of its use in the leather tanning industry (Nriagu, 1988).

The high affinity that the Cr(III) ion has for oxygen centres also enables it to form strong complexes with oxides ions (O^{2-}). Furthermore its affinity for oxygen centres enables it to adsorb onto surfaces such as Fe-oxides (Bartlett and Kimble, 1976) and on natural solid surfaces such as sand, bentonite, $\text{Fe}(\text{OH})_3$ and MnO_2 (Schroeder and Lee, 1975). This adsorption behaviour becomes more prominent at higher pH (Richard and Bourg, 1991). The hydroxy-complex of Cr(III), CrOH^{2+} , also adsorbs fairly readily to such surfaces (James and Healy in Van der Weijden and Reith, 1982) and the adsorbed Cr(III) species are said to be stable with desorption rates being slow especially in the absence of competing metal cations.

Thus the chemistry of Cr(III) is somewhat complex but nevertheless crucial in understanding its behaviour and interconversions in the environment. However, in order to understand its behaviour in solid landfilled wastes its solid-state chemistry namely the chemistry of its oxide (Cr_2O_3) and its major mineralogical phases, the chromites also needs to be understood.

2.6.2. Solid-State Cr(III) Chemistry

i) The Chemistry of Chromium Oxide (Cr₂O₃)

An important chemical characteristic of Cr₂O₃ is its insolubility in water. It can dissolve slowly in acids at low temperatures (Traube in Mellor, 1931). It is also soluble in alkaline solutions. Its dissolution rates are higher in alkaline media (Reartes et al., 1991). An important dissolution property is its redox dissolution where Cr(III) in the oxide may be reduced to Cr(II) or oxidised to Cr(VI) and is thus converted into a more soluble form. (Reartes et al., 1991).

Chromium oxide is known to oxidise to chromic acid. The oxidation was observed electrochemically in the presence of pure water but has not been observed under environmental conditions (Saxon in Mellor, 1931). The addition of manganese dioxide to chromium oxide also increases the yield of chromic acid and a much more rapid oxidation occurs in the presence Ca(OH)₂ or KOH or both (Mellor, 1931). Chromium oxide has been described as the most environmentally stable form of Cr(III) (Barnhart, 1997). It must, however be noted that other stable forms of Cr(III) occur naturally. These include chromite and picochromite (Nriagu, 1988; Kilau and Shah, 1984).

Barnhart also describes Cr₂O₃ as a chemical that has a low solubility, low reactivity, low mobility and low toxicity to living organisms and states that: " Even when put in environments where it is not thermodynamically stable, chromium oxide is very slow to react". However, Petersen (1998) has presented experimental evidence that chromium oxide undergoes oxidation in the presence of calcium hydroxide (Ca(OH)₂) at ambient temperatures. So, despite its slow reactivity the possibility that Cr₂O₃ can slowly transform it into a hazardous compound must not be overlooked.

ii) The Chromites and their Chemistry

As stated earlier the major mineralogical phase of chromium under environmental conditions is chromite. The term chromite usually refers to FeCr₂O₄ but it is also used to refer to any mineral containing a significant amount chromium and having a crystal structure similar to that of the mineral spinel MgAl₂O₃. Small amounts of manganese, titanium, nickel and vanadium may also be present in these chromites.

Various types of chromite exist but those of fundamental interest particularly in the context of ferrometallurgical slags are calcium and magnesium chromite. When calcium chromite is heated in oxygen calcium chromate forms and this reaction was found to begin below 100^oC in air (Dufau in Mellor, 1931). This chromite can be attacked by halogens namely fluorine or chlorine and even by hydrogen chloride and fluoride when heated (Mellor, 1931) but it is not easily attacked by the corresponding acids namely hydrochloric acid and hydrofluoric acid or even by sulfuric and nitric acid.

Magnesium chromite (picotite) has become known as picochromite due to the bitter taste of the magnesium salts (members of the spinel chromite series with the chemical formula $Mg(CrO_2)_2$). Its crystals are of the spinel type (Huggins in Mellor, 1931).

Picochromite does not undergo any change when strongly heated (Dufau in Mellor, 1931). It can be oxidised by oxygen with some difficulty upon heating (Mellor, 1931) and is not attacked by chlorine or bromine. It is attacked by hydrochloric and hydrofluoric acids with some difficulty (Ebelmann in Mellor, 1931). It is also easily attacked by hot, concentrated sulfuric acid (Dufau in Mellor, 1931) and is insoluble in alkali.

Picochromite is slowly oxidised to magnesium chromate in the presence of sodium carbonate and potassium nitrate (Nichols, in Mellor, 1931). It is also oxidised by calcining at red heat (Viard in Mellor, 1931). This reaction has not been observed under environmental conditions and the conditions that are required for this oxidation to occur rule out the possibility that the oxidation of picochromite can lead to Cr(VI) generation in wastes such as ferrometallurgical slags.

Magnesium chromate ($MgCrO_4$) is very unstable and can only form at high oxygen pressures (Bayer and Wiedemann, 1977). This supports the findings of Kilau and Shah (1984) who observed that the addition of magnesium oxide to stainless steel slags resulted in the formation of picochromite ($MgO.Cr_2O_3$) which was very stable towards oxidation and was also resistant to chromium leachability.

Thus, the chemistries of magnesium chromite and calcium chromite are different despite the fact that that magnesium and calcium are in the same group on the periodic table. So while the calcium content of slags is a concern the magnesium content is important in terms of acting as a stabiliser with respect to oxidation.

2.7. Cr(VI) Chemistry

2.7.1. Aqueous Cr(VI) Chemistry

As stated earlier, hexavalent chromium (Cr(VI)), is the other environmentally stable oxidation state of chromium. Like Cr(III), Cr(VI) is also hydrolysed in water giving rise to neutral and anionic species (Baes and Mesmer, 1976) but exists only as the oxoanion. Such oxoanions include $HCrO_4^-$, CrO_4^{2-} and $Cr_2O_7^{2-}$ (dichromate). Chromic acid (H_2CrO_4) is also known to exist at very low pH ($pH < 0.6$). The solid form of chromic acid CrO_3 , the anhydride, undergoes hydrolysis upon contact with water to form chromic acid. Based on the speciation of Cr(VI), three equilibria are important namely:-

The hydrolysis of the anhydride



The first dissociation of chromic acid which is a very strong acid.



The second dissociation of chromic acid



When Cr(VI) concentrations exceed 0.01M at low pH, the hydrogen chromate dimerizes to the di-chromate and this is shown below:



In alkaline media, the only significant species is CrO_4^{2-} . H_2CrO_4 predominates in acidic media. Figure 2-2 shows the predominant Cr(VI) species at various pH values.

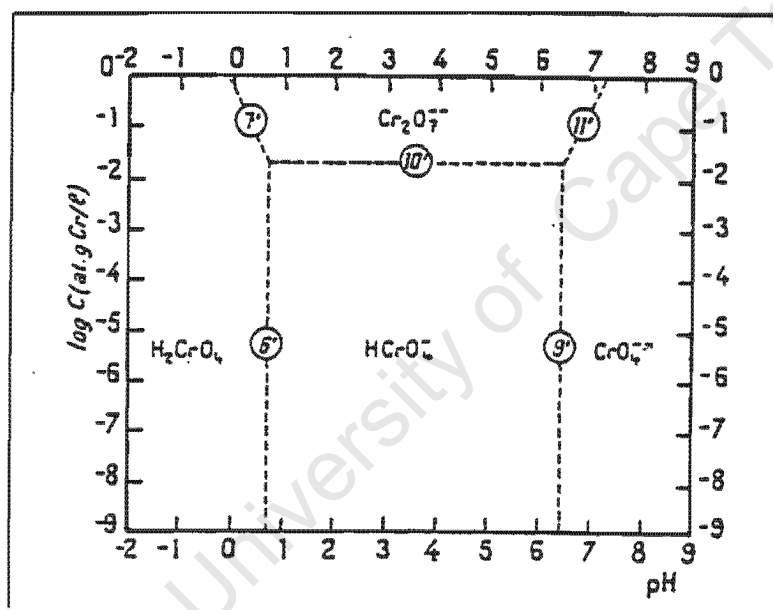


Figure 2-2: The predominant Cr(VI) species at varying pH values (Based on information from Deltombe et al., 1966 and Rai et al., 1987)

Figure 2-2 shows that Cr(VI) remains soluble throughout the pH range hence it is considered to be a mobile species and unlike Cr(III), forms very few stable complexes. Its only known stable complex is that of chromylchloride (Cl_2CrO_2) where a strong Cr-O bond forms and the inner co-ordination is fixed such that the ligands cannot be replaced. However, upon examining the equilibria in equations (2-1), (2-2) and (2-3), it may also be argued that chromic acid can be a stable complex of Cr(VI).

2.7.2. The Chromates

The chromates are regarded as salts of chromic acid (Mellor, 1931). The chromate of fundamental interest in solid wastes is calcium chromate as this is the hexavalent chromium compound that is believed to form when calcium chromite is exposed to air (Kilau and Shah, 1984).

Calcium chromate does not decompose at temperatures below 1000°C. A saturated aqueous solution of calcium chromate is very stable. The percentage solubility of calcium chromate and is given in Figure 2-3.

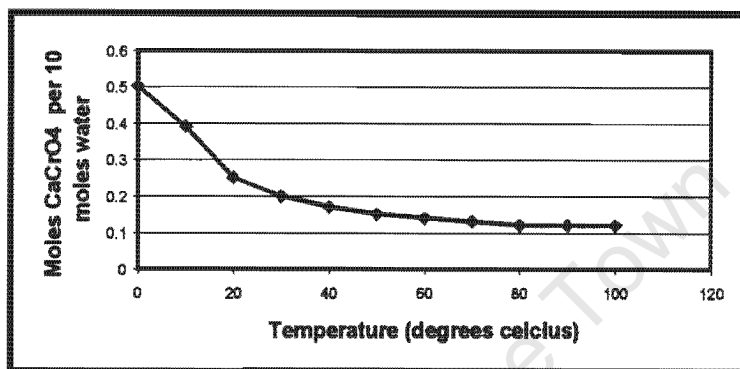


Figure 2-3: The solubility curve of CaCrO_4 (adapted from Mellor, 1931)

Clearly, at higher temperatures the solubility of CaCrO_4 in water becomes lower and eventually attains a constant value. Its solubility increases at lower temperatures. From Figure 2-3, it can be discerned that at ambient temperature ($\pm 22^\circ\text{C}$) about 0.22 moles CaCrO_4 dissolves in 100 moles of water. This translates into a solubility of 6.35 mg Cr of hexavalent chromium in one litre of water, which is quite high.

An aspect of the chromates is their different degrees of solubility. Basically, the metal chromates can be grouped into three categories of solubility (Nieboer and Jusys, 1988). Such categories include the highly soluble chromates eg. sodium and potassium chromates which have a solubility of $> 1\text{M}$, the intermediately soluble chromates eg. calcium chromate which has a solubility of between 0.1 and 1M and the sparingly soluble chromates eg. barium chromate which has a solubility of $< 0.01\text{M}$.

Other chromates like lead chromate are known to be totally insoluble. So, care must be taken when referring to hexavalent chromium as a mobile species. Clearly the form

in which hexavalent chromium exists and its degree of solubility will also determine its level of mobility.

In the presence of lime (CaO) chromium oxide reacts to produce calcium chromate and calcium chromite (Gemmell, 1973). The calcium chromate or chromite complexes are insoluble in water but soluble in acid. This is contradictory to the solubility data from Mellor (1931) which showed that the solubility of CaCrO_4 in water is quite high at ambient temperatures.

The chromates are strong oxidising agents and are good oxidisers of organics. This explains the rapid removal of Cr(VI) from most soil environments where any Cr(VI) that may be generated is reduced to the trivalent form upon oxidising organic molecules.

2.8. Reactions Contributing to the Oxidation of Trivalent Chromium

under Environmental Conditions – Kinetics and Mechanisms

The concern that trivalent chromium can slowly oxidise to the hexavalent form in landfill sites is a legitimate concern in light of the environmental catastrophies that have resulted upon exposure to hexavalent chromium. It has therefore become essential to study reactions that could lead to the generation of hexavalent chromium in natural environments. Three reactions have been identified and studied to date. These include:

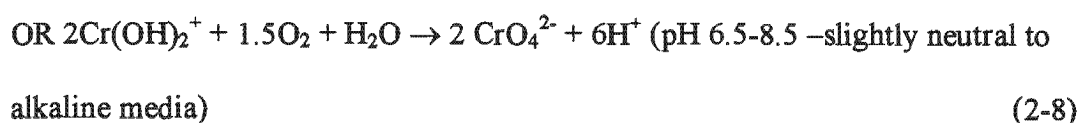
- the aqueous oxidation of Cr(III) by dissolved oxygen
- oxidation by manganese oxides
- the oxidation of chromium oxide by atmospheric oxygen.

2.8.1. Aqueous Cr(III) Oxidation by Dissolved Oxygen

This has been identified as a reaction that is most likely to occur in natural water systems such as oceans and lakes. Several workers have attempted studying this reaction (Petersen, 1998; Saleh et al., 1989; Van der Weijden and Reith, 1982; Nakayama et. al. 1981; Schroeder and Lee, 1975; Nyholm, 1947; Wood and Black, 1916).

The ability of this reaction to occur under environmental conditions has been dismissed as thermodynamically feasible but kinetically too slow. Three likely reactions that have been identified are listed below:-





Schroeder and Lee (1975) are the only workers who have successfully deduced the kinetics of the reaction (2-8). They observed this reaction at room temperature and at higher temperatures (35°C and 45°C) and calculated a high activation energy of 92kJmol⁻¹. The extent of conversion observed by them was typically a 3% conversion at room temperature over a 50 day period which suggests that the reaction although very slow can occur at ambient temperatures. Nevertheless, they also state that the rate of this reaction is slow enough to warrant the participation of Cr(III) in other reactions before any appreciable oxidation occurs.

Van der Weijden and Reith (1982), on the other hand, were unable to observe this reaction at room temperature and were also unable to observe any appreciable oxidation even at higher temperatures. They have, however, established a speculative first order rate law, which is based on assumptions and an order of magnitude estimation of their experimental data. From this speculative data, they estimated a rate constant of 0.35/year and a half-life of 1.75 years. Their findings are in agreement with those of Nakayama et al. (1981).

Saleh et al. (1989) observed that dissolved oxygen did not oxidise Cr(III) to any appreciable extent even after 128 days. These workers only observed slow oxidation in one of the natural water and sediment environments that they have studied and established half-lives of 2 to 9 years. This data is based on first order kinetics.

Petersen (1998) also studied this reaction using an 80mg/l Cr(III) solution at the pH values of 2.7-12.2 and observed an increase in Cr(VI) formation with increasing pH. The formation of Cr(VI) was therefore most prominent at pH 12.2 where a “clear first order type development” in the reaction was observed. This suggested that the reactions which occur under alkaline conditions are favoured over the reaction which is known to occur under acidic conditions. Figure 2-4 depicts the results obtained at pH 12.2.

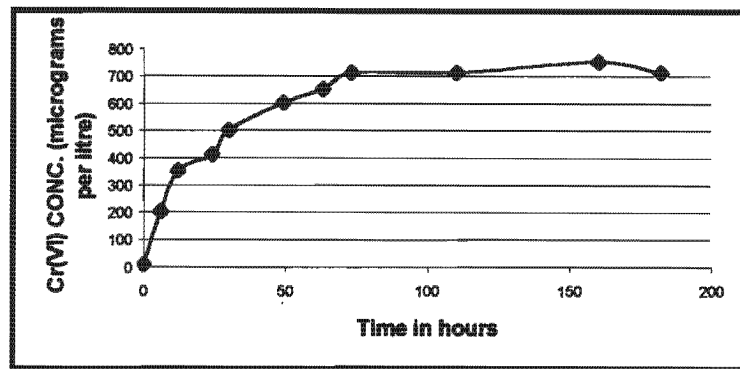


Figure 2-4: The generation of Cr(VI) via reactions involving Cr(III)-hydroxy species and oxygen at pH 12.2 (adapted from Petersen, 1998)

The results clearly show that although a reaction does occur thereby resulting in the generation of Cr(VI), the extent of oxidation is limited as is evident from the eventual levelling off of the data points. Petersen states that more data points are essential in establishing the reality of this trend. Another valid point raised by this researcher is that oxidation is not necessarily limited to aqueous Cr(III) but may also involve a solid form namely Cr(OH)₃. Petersen also investigated the influence of varying initial concentrations of Cr(III) (concentration range 10-500 mg/l) on this reaction and found that these did not have any significant influence on the extent of the reaction.

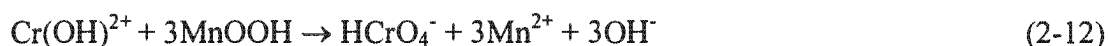
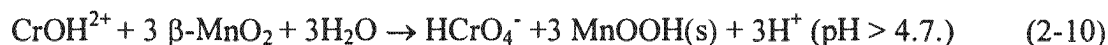
Another important observation was that the addition of MnO₂ to a 50mg/l Cr(III) resulted in rapid Cr(VI) formation but this attained a slower rate after a day. Petersen accounts for this in terms of limited reactive sites on MnO₂ and attributes marginal increases in the Cr(VI) concentrations after a day to the direct oxidation by oxygen. However, the experimental data presented by Petersen has been described as “insufficient to quantify the oxidation reaction in terms of a kinetic model.”

Thus, although some workers have observed oxidation, it seems to be a rather slow reaction, which may present a long-term environmental hazard. Half-lives of anywhere between 1-9 years have been quoted thereby suggesting that Cr(III) may oxidise to Cr(VI) over a 10 year period at least to some extent in natural water environments. The question of whether the solid phase oxidation of Cr(OH)₃ is likely to contribute to any Cr(VI) generation in solid landfilled wastes particularly neutralisation sludges, which are known to contain Cr(OH)₃ must still be addressed. It is beyond the scope of this thesis to address this question but a recommendation for future work is presented in Chapter seven.

2.8.2. Oxidation by Manganese Oxides

Much emphasis has been placed on this reaction as the manganese oxides have been considered as the only naturally occurring oxidants of Cr(III), particularly in soil environments (Eary and Rai, 1987). Oxidation by three types of manganese oxides

have been studied. These include pyrolusite (β - MnO_2) (Eary and Rai, 1987), birnessite (δ - MnO_2) (Fendorf and Zasoski, 1992) and manganite (γ - MnOOH) (Johnson and Xyla, 1991). The equations for these reactions are shown below.



Oxidations by unspecified manganese oxides have also been studied (Saleh et al., 1989; Van der Weijden and Reith, 1982; Nakayama, 1981b; Schroeder and Lee, 1975).

Such reactions have been studied only in soil and water environments. The question of whether these reactions can proceed in the pure solid state in landfill wastes has already been addressed. Petersen (1998) found that 1% manganese dioxide in pure Cr_2O_3 - $\text{Ca}(\text{OH})_2$ systems did not appreciably enhance the rate of oxidation.

2.8.3. The Oxidation of Chromium Oxide by Atmospheric Oxygen

This reaction has not received a lot of attention largely because chromium oxide is known to react very slowly under environmental conditions (Barnhart, 1997). However, two reactions which are of fundamental interest are:-

1. The oxidation of chromium oxide in the presence of CaO



2. The oxidation of chromium oxide in the presence of $\text{Ca}(\text{OH})_2$



Reaction (2-13) is known to be thermodynamically feasible at ambient temperature (Kilau and Shah, 1984; Hattori et al., 1978) despite the slow reactivity of Cr_2O_3 . Table 2-1 shows the thermodynamic data for the reactants and products of this reaction.

Table 2- 1: Available thermodynamic data for the oxidation of chromium oxide in the presence of CaO (Adapted from Hattori et al, 1978)

Material	Enthalpy of formation (kJmol ⁻¹) at 298,15K	Entropy of formation at 298,15 K (JK ⁻¹ mol ⁻¹)	Heat Capacity (298.15-1300K) (JK ⁻¹ mol ⁻¹)
Cr ₂ O ₃	-1141	81.1	119.4 + 9,20X 10 ⁻³ T-15.65 X 10 ⁵ T ⁻²
CaO	-635.1	39.7	49.63 + 4.52 X 10 ⁻³ T - 6.95 X10 ⁻⁵ T ²
CaCrO ₄	-1379	134	160.96 + 9.333 x 10 ⁻³ T- 2.80 X10 ⁻⁶ T ²
O ₂	0	205	25.46 + 15.192 X 10 ⁻³ T -0.715 X10 ⁻⁵ T ²

Such data may be used to calculate the change in Gibbs Free Energy for the reaction at specified temperatures. Figure 2-5 shows the change in Gibbs free energy of the reaction as a function of temperature.

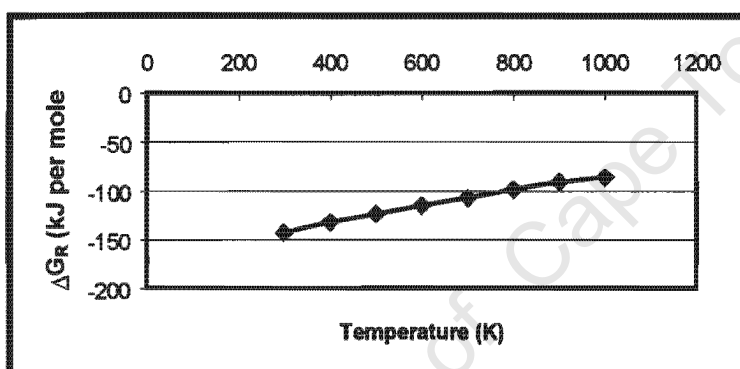


Figure 2-5: Change in Gibbs Free Energy (ΔG_R) for the reaction $Cr_2O_3 + 1.5 O_2 + 2CaO \rightarrow 2CaCrO_4$ as a function of temperature (Based on data from Hattori et al., 1978)

This figure shows that the reaction is thermodynamically feasible over the temperature range 298.15-1000K. Most noteworthy is the Gibbs free energy of -143.3 kJ mol⁻¹ that was calculated at 298K. There is a discrepancy between this value and that of -299.6 kJ calculated by Kilau and Shah (1984) who do not indicate how they calculated this value or what thermodynamic tables they used. Nevertheless, the negative values obtained for the Gibbs Free energies clearly show the thermodynamic feasibility of this reaction at environmental temperatures.

The reaction in the presence of CaO has not been studied or even observed under environmental conditions. At elevated temperatures however, the reaction is well known and has been studied extensively (Mellor, 1931).

Bayer and Wiedemann (1977) studied the reaction in the presence of Ca(OH)₂ at higher temperatures using the technique of thermal analysis. Petersen (1998) observed this reaction at ambient temperature in pure Cr₂O₃-Ca(OH)₂ balls and also

conducted some studies on pure Cr_2O_3 balls containing NaOH as a pore solution. In both cases the balls were maintained under moist conditions.

The results of Petersen are depicted in the Figure 2-6.

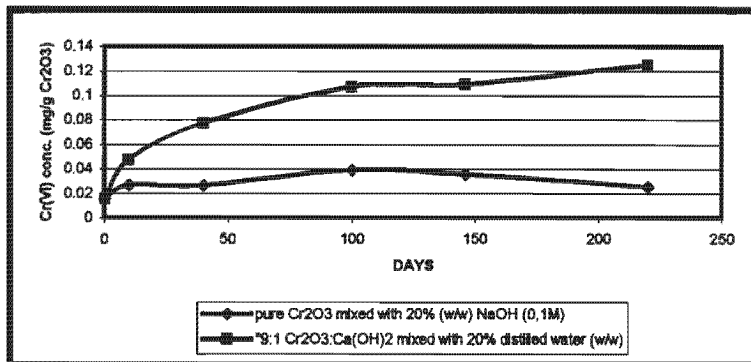


Figure 2-6: Cr(VI) generation in Cr_2O_3 - $\text{Ca}(\text{OH})_2$ and Cr_2O_3 -NaOH systems (Adapted from the data of Petersen (1998))

Petersen's rationale in devising these experiments was to establish whether oxidation proceeds faster when alkalinity is introduced as an aqueous phase (NaOH solution) or as a solid phase (solid $\text{Ca}(\text{OH})_2$). Since the results showed that the oxidation proceeds much faster in the presence of $\text{Ca}(\text{OH})_2$ it was concluded that the oxidation of trivalent chromium was more likely to be a solid-phase oxidation rather than an aqueous oxidation.

Petersen also reports a first order rate constant of $6.3 \times 10^{-7} \text{ day}^{-1}$ which was calculated by plotting the conversion as a fraction of the total chromium present in each ball. This is several orders of magnitude lower than the rate constant reported by Schroeder and Lee (1975) for the aqueous oxidation and would suggest that a solid phase oxidation is significantly slower than the aqueous oxidation. However, the reaction is fundamentally a solid-gas reaction, so the solid-gas rate laws need to be considered when studying the kinetics. These are reviewed in Chapter six.

Studies on real landfilled waste systems are also crucial in establishing the extent to which such reactions can occur in real waste systems.

2.9. The Oxidation of Cr(III) in Landfilled Wastes

Few attempts have, again, been reported by researchers to study the potential for Cr(III) oxidation to occur in industrial wastes. The soil science community has focussed on the potential oxidation of Cr(III) in soils that have been amended with wastes rich in trivalent chromium (Milacic and Stupar, 1995).

Although the reactions discussed in Section 2.8., are likely to contribute to the generation of Cr(VI) in real waste systems, the form in which the reactants are present also need to be understood in order ascertain whether these reactions can indeed occur

in landfilled wastes. For example, the potential for Cr(III) oxidation to occur in ferrometallurgical slags can be established by examining the potential for calcium chromite to undergo oxidation to calcium chromate under environmental conditions. Very little is known about whether this reaction can proceed under environmental conditions. Kilau and Shah (1984) have provided experimental evidence that CaO does indeed play a role in Cr(VI) generation by showing that chromium leachability is enhanced by a CaO/SiO₂ ratio of 2.0, but also state that the question of whether calcium chromite can undergo any appreciable oxidation upon exposure to summer heat, acid precipitation and atmospheric oxygen must still be answered. These workers have also failed to establish the thermodynamic feasibility of this reaction.

Petersen (1998) has presented experimental evidence for the generation of Cr(VI) in slags. The most significant findings of Petersen were that increasing amounts of Cr(VI) leached out over time from slag columns sprayed with acid rain. This presented strong evidence that oxidation had occurred in the slags.

Additionally, Petersen noted that the Cr(VI) levels of the leachates increased between various repeat runs while the Na and K concentrations decreased. Petersen accounts for this in terms Na and K being washed out from the bed until they attain zero concentrations and in terms of Cr(VI) being generated continuously from oxidation in the slag beds.

Thus, although the kinetics and mechanisms of reactions leading to the generation of Cr(VI) in slags are not properly understood, sufficient evidence that hexavalent chromium compounds can form in such wastes exists in the literature. However, the reactions contributing to the oxidation must also be studied in light of the composition of the slags.

2.10. The Chemistry and Mineralogy of Cr(III)-Containing Slags

(Stainless Steel Slags)

2.10.1. The Bulk Chemical Composition of Stainless Steel Slags

Stainless steel slags consist mainly of key elements such as chromium, calcium, magnesium and aluminium. Kilau and Shah (1984) determined the elemental composition of stainless slags obtained from four manufacturers. The results from their findings are shown in Table 2-2.

Table 2-2: The Chemical Composition of Stainless Steel Slags Obtained from Different Manufacturers (from Kilau and Shah, 1984)

Slag	Chemical Composition (weight %)							
	Chromium	CaO	SiO ₂	MgO	Al ₂ O ₃	Fluorine	Mn	Fe
A	0.9	60.4	22.7	8.1	3.5	1.8	0.5	0.4
B	0.7	54.0	32.8	4.7	2.4	2.4	1.0	0.2
C	4.8	29.7	24.2	19.7	6.6	2.3	4.4	1.9
D	8.1	18.0	31.6	11.9	9.4	3.3	8.4	1.9

Although these workers report the chromium content of the slag as the element it must be noted that chromium is actually present as chromium oxide (Cr_2O_3). This oxide originates from the oxidation of elemental chromium during the formation of the slags. In the production of Electric Arc Furnace (EAF) slags, oxygen which is injected into the arc furnace to aid the melting of steel scrap results in the oxidation of elemental chromium (Korousic et al., 2000).

Lime (CaO) and MgO are added to the slags during the melting period to promote slag formation and to eliminate sulfur and phosphorus. Al is added to the slag in an attempt to minimize Si and Cr oxidation. Korousic et al. (2000) have in fact observed that when Al concentrations exceed 0.04%, the oxidation of silicon, manganese and chromium is minimised.

Manganese, iron and nickel originate from the melting of stainless steel. However, it must be stated that in C-steelmaking FeO is formed as a major oxidation product of the oxygen blow and can therefore be a major constituent of EAF slags (Pretorius and Nunnington, 2000). Table 2-3 shows the chemical composition of EAF slags after the meltdown process, which was conducted at different temperatures.

Table 2-3: The Average Chemical Composition of EAF slags after the Meltdown Process (Adapted from Korousic et al., 2000)

Cr_2O_3	CaO	MgO	SiO_2	Al_2O_3	MnO	FeO
Wt %	Wt %	Wt %	Wt %	Wt %	Wt %	Wt %
15.8	42.2	8.3	12.1	7.0	2.0	6.9

Upon comparing the data in Tables 2-2 and 2-3, it is clear that chemical compositions of the slags differ depending on the type of slag and on how the slags are produced. However, Cr_2O_3 , SiO_2 , MgO , CaO and Al_2O_3 are oxides that are common to all of the slags that have been studied. Another common feature that is evident from Tables 2-2 and 2-3 is that the amount of Cr_2O_3 relative to CaO is small. The amount of MgO relative to CaO is also small. Thus, there is ample CaO present to participate in the oxidation of Cr_2O_3 and to result in the formation of CaCrO_4 . However, the extent to which this reaction can occur in the slags is also dependent on the mineralogical phases in which Cr_2O_3 exists. It is therefore important to gain an understanding of the mineralogy of the slags.

2.10.2. The Mineralogy of Stainless Steel Slags

Very little is known about the mineralogical phases of Cr_2O_3 that are likely to undergo oxidation in slag deposits. Kilau and Shah (1984) have postulated that the oxidation of Cr(III) in the slags is due to the oxidation calcium chromite ($\text{CaO} \cdot \text{Cr}_2\text{O}_3$) which is converted to acid-soluble calcium chromate. They have further postulated that the addition of MgO to the slags in the furnace resulted in the formation of picochromite

($\text{MgO} \cdot \text{Cr}_2\text{O}_3$) which is resistant to chemical attack and is therefore stable to oxidation. However, these workers have not conducted mineralogical analyses, which explicitly identify the chromites as the major mineralogical phases of chromium and as stated earlier have failed to establish the thermodynamic feasibility for the oxidation of calcium chromite due to the lack of available thermodynamic data.

Pretorius and Nunnington (2000) have also stated that Cr_2O_3 can exist as solid spinel phases eg. MgCr_2O_4 and CaCr_2O_4 even in the liquid portions of the slag. Based on Kilau and Shah's observations and the different chemistries of calcium chromite and magnesium chromite, it may be argued that slags rich in MgCr_2O_4 will undergo little or no oxidation while slags rich in CaCr_2O_4 will undergo an appreciable amount of oxidation. Thus, the mineralogy of a slag must be determined in order to understand the oxidation trends.

2.11. Conclusion

Sufficient evidence that occupational exposure to hexavalent chromium has resulted in numerous illnesses and toxic effects in humans, have been reported in the literature. Evidence that hexavalent chromium can also have detrimental effects on plants and adverse impacts on the natural environment has also been documented in the literature. Furthermore, some studies have presented evidence that Cr(VI) can indeed be generated in waste materials, such as slags.

However, the reactions that contribute to generation of Cr(VI) in such wastes have not been extensively studied under environmental conditions. The kinetics of such reactions, particularly the solid-gas reactions involving atmospheric oxygen as an electron acceptor have not been deduced and the mechanisms of such reactions are not understood.

The potential of Cr_2O_3 to react under environmental conditions and to undergo any oxidation when in contact with atmospheric oxygen and other reactants has been ignored, as its reactivity has been considered to be too low to warrant any significant environmental concern. However, experimental evidence which shows that the slow reactivity of Cr_2O_3 can render it a long term environmental hazard has been presented by Petersen (1998), whilst other workers have indicated that the reaction between Cr_2O_3 , CaO and O_2 is thermodynamically feasible at ambient temperature (Kilau and Shah, 1984 ; Hattori et al., 1978).

Studies on slag chemistries have shown that Cr_2O_3 and CaO are key chemical components of stainless steel (ferrometallurgical) slags. It is thus likely that the oxidation of Cr_2O_3 in the presence of CaO can lead to Cr(VI) formation in such slags. However, this also depends on the mineralogical phases in which Cr_2O_3 exists.

Thus, it is concluded that the following issues concerning the reactions that lead to the oxidation of Cr_2O_3 need to be examined:

- the physical and chemical parameters that promote and inhibit the rates of these reactions ;
- the kinetics of such reactions ;

- the mechanism of the reactions both in the presence of CaO and Ca(OH)₂ ; and
- the extent to which the reaction can occur in ferrometallurgical slags and how this relates to the chemical composition and the mineralogy of the slags.

Chapter three presents the hypotheses that have been formulated to address these issues and the experimental methodology.

University of Cape Town

CHAPTER THREE

EXPERIMENTAL APPROACH AND METHODS

Based on the literature survey presented in Chapter two, it is hypothesised that:-

- As indicated by other workers, significant oxidation can, indeed be observed under environmental conditions, in solid Cr(III) bearing wastes.
- The oxidation of Cr_2O_3 in the presence of CaO or $\text{Ca}(\text{OH})_2$ is the key reaction which contributes to the generation of Cr(VI) in ferrometallurgical slags.

This chapter presents an overview of the experimental plan and the experimental methods that were employed to test these hypotheses. The experimental series that were devised in order to investigate the key parameters, which influence the rate of the oxidation of chromium oxide by atmospheric oxygen both in pure chemical systems and in ferrometallurgical slags, are also discussed. Details of the experimental approach, which is based extensively on the experimental procedure employed by Petersen (1998) in his studies on Cr_2O_3 - $\text{Ca}(\text{OH})_2$ balls are provided. The chapter concludes with a discussion on the various measures that were taken to verify the accuracy of the data.

3.1. Experimental Plan

In each part of the experimental plan discussed, sets of balls or powder mixes and pellets were prepared and allowed to rest for different periods of time, sufficient so that a reaction could occur. This period of time ranged from 1 to 56 weeks. At specified intervals, the balls or powders were analysed for their Cr(VI) content in order to quantify the conversion of Cr(III) to Cr(VI) as a function of time. In addition to these oxidation studies, the elemental composition of the slags was determined. The experimental approach to studying the oxidation of Cr_2O_3 is schematically outlined in Figure 3-1.

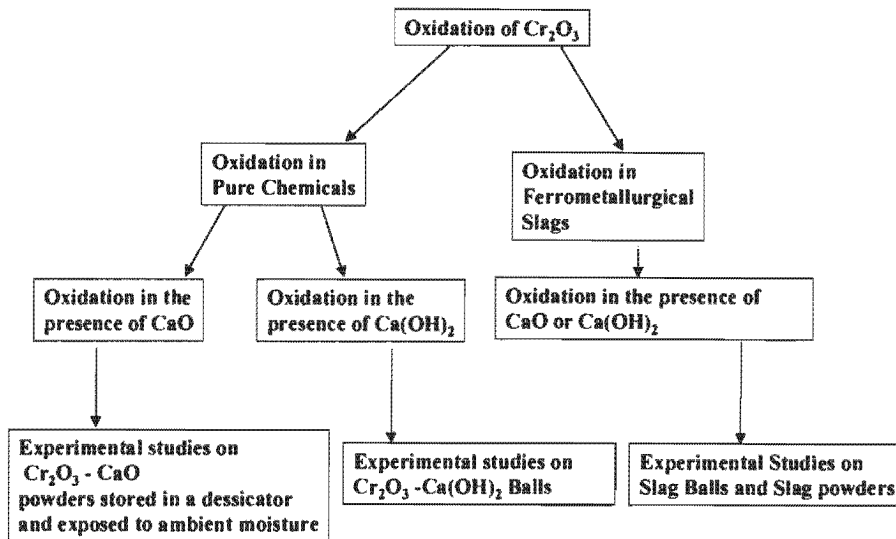


Figure 3-1: A Schematic Outline of the Experimental Approach to studying the oxidation of Cr_2O_3

3.2. Materials

In this study, experiments were conducted both on pure chemicals and on ferrometallurgical slags. These materials are described below:

3.2.1. Pure Chemicals

The pure chemicals used in the experiments were analytical grade chromium oxide (Cr_2O_3) and calcium oxide (CaO) powders. The Cr_2O_3 powder was pre-washed in 2M NaOH and distilled water. The washing procedure is described in more detail in Section 3.6. The particle size distributions of these powders were also determined with the aid of a Malvern Mastersizer and are shown in Appendices B1 and B2.

3.2.2. Ferrometallurgical Slags

Three types of ferrometallurgical slags were supplied by a local stainless steel smelter. These included:

- A slag formed in a CLU converter and supplied fresh from production (New CLU Slag)
- A slag prepared by a meltdown process in an electric arc furnace and supplied fresh from production (New EAF slag)
- An aged slag sampled directly from the disposal site (Old Mixed slag)

All three types of slags were supplied in the powder form and in three different particle size classes namely, $< 75\mu\text{m}$, $75\text{-}300\mu\text{m}$ and $300\text{-}1000\mu\text{m}$. Basically the slags were crushed by the supplier and sieved into their respective size classes. The coarse fraction of the CLU slag, had to be pulverised into a powder form prior to use in the

experiments. This was in order to ensure that the material was sufficiently fine to be rolled into balls. The actual particle size distributions of the slags were determined with the aid of a Malvern Mastersizer. This is shown in Appendix B3.

3.3.Experiments¹ Devised to Test Hypotheses

In order to test the hypotheses presented earlier on in this chapter, the following reactions need to be investigated:

- Oxidation of Cr_2O_3 in the presence of CaO
- Oxidation of Cr_2O_3 in the presence of $\text{Ca}(\text{OH})_2$
- Oxidation of Cr_2O_3 in ferrometallurgical slags (containing calcium compounds) both in the presence of CaO and $\text{Ca}(\text{OH})_2$.

The experiments devised to study these reactions are described below. In addition, the elemental composition of the slags was also determined by an elemental analysis in order to verify that chromium and calcium are present in the slags and to test the hypothesis that the key reaction contributing to oxidation in the slags is the oxidation of Cr_2O_3 in the presence of CaO or $\text{Ca}(\text{OH})_2$. The experiments devised also aimed at gathering conversion-time data, which could be used to quantify the reaction rates as a function of time so that the kinetic models, which best describe the reactions could be identified.

3.3.1. Oxidation in the Presence of Calcium Oxide (CaO)

In order to investigate this reaction, analytical grade Cr_2O_3 and CaO powders were mixed together thoroughly in the dry powder form and stored in a dessicator. The reason for storage in a dessicator was to prevent the CaO from reacting with atmospheric moisture to form $\text{Ca}(\text{OH})_2$ and hence to obtain a pure Cr_2O_3 - CaO system. This reaction was also investigated by mixing the Cr_2O_3 and CaO powders together and storing these on a shelf where some exposure to ambient moisture was achieved. Pressed pellets containing Cr_2O_3 and CaO were also prepared and stored under similar conditions.

3.3.2.Oxidation in the Presence of Calcium Hydroxide ($\text{Ca}(\text{OH})_2$)

The experimental plan devised to investigate this reaction involved preparing powder mixes consisting of Cr_2O_3 and CaO . Sufficient water was added to these powder mixes to convert the CaO to $\text{Ca}(\text{OH})_2$ and to form a paste so that the grains of Cr_2O_3 and $\text{Ca}(\text{OH})_2$ would be in close proximity for a reaction to occur. A sample calculation showing the relative amounts of CaO and water that were added are presented in Appendix A4. Such experiments also aimed at examining the influence of pore moisture on the rate of oxidation. The experimental series devised for this purpose are detailed in section 3.4.

¹ Unless otherwise stated, all experiments were conducted at ambient temperature ($\pm 22^\circ\text{C}$).

3.3.3. Oxidation in Ferrometallurgical Slags

The oxidation of Cr_2O_3 in ferrometallurgical slags was investigated by preparing balls out of the powdered slag samples in the same manner in which the Cr_2O_3 - $\text{Ca}(\text{OH})_2$ balls were prepared and exposing these to air over extended periods of time. These experiments aimed at investigating the oxidation of Cr_2O_3 in the presence of $\text{Ca}(\text{OH})_2$ in the slags. A variation of this method also involved exposing the slag powders to air without adding any water. This aimed at investigating the oxidation of Cr_2O_3 in the presence of CaO . Such experiments were also devised to establish whether there may be an uptake of atmospheric moisture by the slags which can convert CaO to $\text{Ca}(\text{OH})_2$ thereby leading to the oxidation of Cr_2O_3 in the presence of $\text{Ca}(\text{OH})_2$.

3.3.4. Elemental Analysis of Slags

In order to determine the chemical composition of the slags, the powdered slag samples were digested in a hydrofluoric acid/perchloric acid mixture and each digested sample was then analysed for selected elements by Atomic Absorption Spectroscopy (AAS). The elements that were analysed for included Cr, Ca, Mg, Mn and Fe.

3.4. Experimental Series Devised to Investigate Key Parameters that Influence the Rate of the Oxidation of Cr_2O_3

3.4.1. The Influence of CaO or $\text{Ca}(\text{OH})_2$ Content

In order to investigate the influence of CaO or $\text{Ca}(\text{OH})_2$ content and the roles played by these compounds in the oxidation of Cr_2O_3 , the following experiments were set up:

- Three experiments in which Cr_2O_3 - $\text{Ca}(\text{OH})_2$ balls were prepared by adding water to a Cr_2O_3 - CaO powder mix and varying the amount of CaO added at 5%, 20% and 50% respectively in order to achieve a varied $\text{Ca}(\text{OH})_2$ content. These balls were maintained under conditions where the excess pore moisture (water that did not react with the CaO) was maintained
- Two experimental series in which the Cr_2O_3 - $\text{Ca}(\text{OH})_2$ balls were maintained under conditions where the excess moisture (pore moisture) was allowed to evaporate and the $\text{Ca}(\text{OH})_2$ content was varied at 20% and 50% respectively.
- Two experimental series in which the Cr_2O_3 and CaO powders were mixed together without the addition of water and allowed to react for a specified time with the CaO content being varied at 20% and 50% respectively. It must again be noted that the powders were exposed to ambient moisture.

3.4.2. The Influence of Pore Moisture

By comparing the first two experimental series described in Section 3.4.1, it would also be possible to deduce the effect of pore moisture. Corresponding experiments were set up for the slags where the slags balls prepared from the supplied powdered slags were maintained under conditions where the pore moisture was retained and allowed to evaporate respectively.

3.4.3. The Influence of Temperature

The influence of temperature on the rate of the oxidation of Cr_2O_3 (in the presence of $\text{Ca}(\text{OH})_2$) was also investigated by setting up the following experiments:

- Cr_2O_3 - $\text{Ca}(\text{OH})_2$ Balls maintained at 50°C
- Cr_2O_3 - $\text{Ca}(\text{OH})_2$ Balls maintained at 80°C .

In each case the balls contained 20% $\text{Ca}(\text{OH})_2$.

These experiments were also set up in order to investigate the possibility of an Arrhenius rate law being obeyed by the reaction and to gain some insight as to whether the reaction can proceed via a solid-state diffusion of Cr^{3+} centres or Cr^{3+} ions towards the oxygen centres of $\text{Ca}(\text{OH})_2$.

3.4.4. The Influence of Particle Contact

The following experiment was devised in order to investigate the influence of particle contact on the rate of oxidation of Cr_2O_3 in the presence of CaO :

- An experimental series in which the Cr_2O_3 and CaO powders were mixed together and pressed into pellets to achieve intimate contact between Cr_2O_3 and CaO . The pellets contained 50% CaO and were exposed to ambient moisture.

Another purpose for devising this experiment was to gain some insight on the implications for the rate of oxidation if Cr_2O_3 and CaO are found in the same mineralogical phase in slags where they are in intimate contact.

3.4.5. The Influence of Particle Size and Chemical Composition on the Rate of Oxidation in Ferrometallurgical Slags

As discussed earlier all the powdered slags were supplied in three particle size classes ranging from fine ($<75\mu\text{m}$) to coarse ($300\text{-}1000\mu\text{m}$) each of which had varying chemical composition. Experiments on both slag balls and slag powders were set up for each particle size class in order to investigate the influence of particle size and varying chemical composition on the rate of oxidation in the slags.

3.5. Verification that Atmospheric Oxygen acts as the Electron Acceptor

To verify that atmospheric oxygen is the electron acceptor for the oxidation reactions of Cr_2O_3 , an experimental series in which Cr_2O_3 - $\text{Ca}(\text{OH})_2$ balls were maintained under nitrogen was set up. A control experiment in which Cr_2O_3 - $\text{Ca}(\text{OH})_2$ balls were exposed to air was also conducted at 2, 4 and 7 week intervals for comparative purposes. These balls contained 50% $\text{Ca}(\text{OH})_2$ and were maintained under conditions where the excess pore moisture was allowed to evaporate. It is argued that if no appreciable oxidation occurs under nitrogen, this would prove that atmospheric oxygen is the only electron acceptor. However, if a significant amount of oxidation is observed under nitrogen then another electron acceptor has to be identified.

3.6. Experimental Methods

The experimental methodology that was employed to set up the various experiments and to conduct the sampling and analysis of the balls, powders and pellets included the following steps:

- The pre-treatment of chromium oxide (Cr_2O_3)
- The preparation of materials (balls, powder- mixes and pellets)
- The maintenance of the different reaction conditions
- The sampling of the balls, powder-mixes and pellets
- The analysis of samples for their Cr(VI) content.

3.6.1. The Pre-treatment of Chromium Oxide (Cr_2O_3)

Although commercial chromium oxide powder is supplied as analytical grade, it was found to contain residual concentrations of Cr(VI). Therefore a pre-treatment step in which the chromium oxide powder was washed to remove all the residual hexavalent chromium was conducted. This pre-treatment step involved washing the chromium oxide first in a 2M NaOH solution and then three times in distilled water. The washing was conducted by placing the chromium oxide powder in contact with the wash solution in a two litre glass bottle and rotating the bottles ends over for two hours. After each wash the solid was filtered through a pressure filter. After the final wash the filter cake was collected and dried in oven before being used to prepare the balls, powder-mixes and pellets. The period of drying was typically 4-5 hours (long enough to ensure that all the wash liquid had dried but short enough to avoid any re-oxidation of the chromium oxide powder).

3.6.2. The Preparation of Materials (Balls, Powder-Mixes and Pellets)

i) The Preparation of the Cr_2O_3 - $\text{Ca}(\text{OH})_2$ Balls and the Powdered Slag

Balls

The relative proportions of the Cr_2O_3 and CaO powders were weighed out. For example, if balls containing 50% Cr_2O_3 and 50% CaO were to be prepared, 50% Cr_2O_3 and 50% CaO by mass were weighed out. Typically 250g batches consisting of both powders were weighed out. The powders were mixed thoroughly in the dry powder form to initiate contact between the Cr_2O_3 and CaO powders.

Sufficient distilled water was added to ensure that all the CaO added was converted to $\text{Ca}(\text{OH})_2$ and to form a workable paste that could be rolled into balls. The amount of water added varied for each experimental series and this is shown in Appendix A4. The paste was then rolled into balls of approximately 25g each which were stored under the appropriate conditions.

The slag balls were prepared in a similar manner by weighing out 250g of slag powder and adding distilled water to this. Figure 3-2 shows an illustration of how the Cr_2O_3 - $\text{Ca}(\text{OH})_2$ balls were prepared.

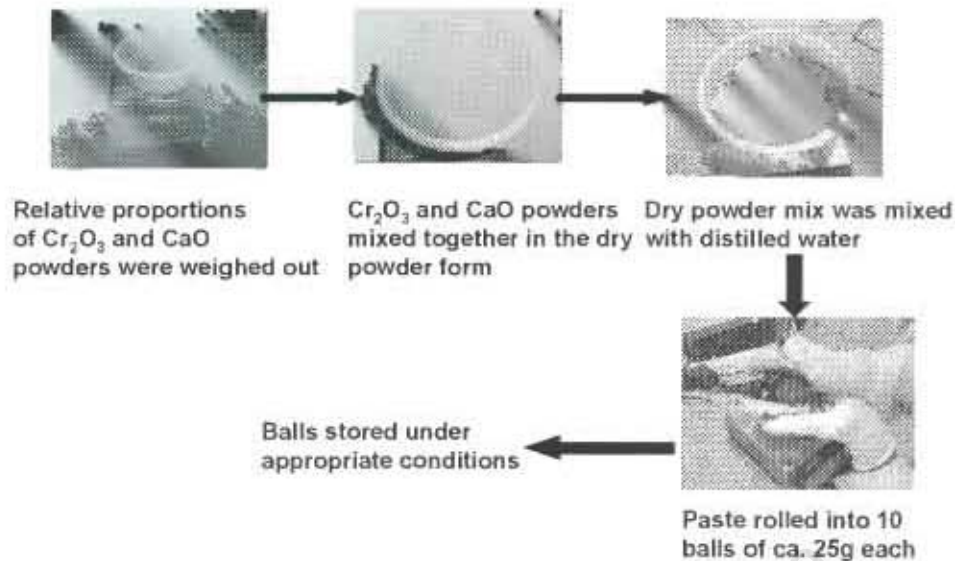


Figure 3-2 : A Diagrammatic Illustration of the method used to prepare the Cr_2O_3 - Ca(OH)_2 balls

ii) The Preparation of Cr_2O_3 - CaO Powder Mixes

The relative proportions of Cr_2O_3 and CaO powders were weighed out and mixed together thoroughly to achieve significant contact between Cr_2O_3 and CaO . The dry powder mix was then divided into 25g portions, which were placed into weighing boats and stored under the appropriate conditions. In the case of the powdered slags, 25g of the slag powder was simply weighed out into weighing boats and exposed to ambient conditions.

iii) Preparation of Cr_2O_3 - CaO Pellets

Again, the relative proportions of the Cr_2O_3 and CaO powders were weighed out and mixed together. The dry powder mix was divided into 20g portions, which were placed into moulds and pressed into cylindrical pellets at 10 bar on a pellet-presser. In order to obtain a pure Cr_2O_3 - CaO system a binder was not added to the powders. The pellets were stored on a shelf where sufficient exposure to atmospheric oxygen from both sides of the pellet could be achieved.

3.6.3. Maintenance of the Different Reaction Conditions

i) Maintenance of the Pore Moisture of the $\text{Cr}_2\text{O}_3\text{-Ca(OH)}_2$ Balls

To ensure that the excess pore moisture (the water added that does not react with the CaO) prevails in the $\text{Cr}_2\text{O}_3\text{-Ca(OH)}_2$ balls and the slag balls, the balls were stored in close contact with a moist piece of cotton wool. However, since the cotton wool dries out rather quickly, this had to be re-moistened regularly, first on a weekly basis and eventually on a daily basis. The balls were also enclosed in plastic bags to maintain the moist environment. To ensure that sufficient oxygen was present in the plastic bags, a wire was placed into each plastic bag. This helped to keep the bags inflated. This method of maintaining the pore moisture is shown in Figure 3-3.

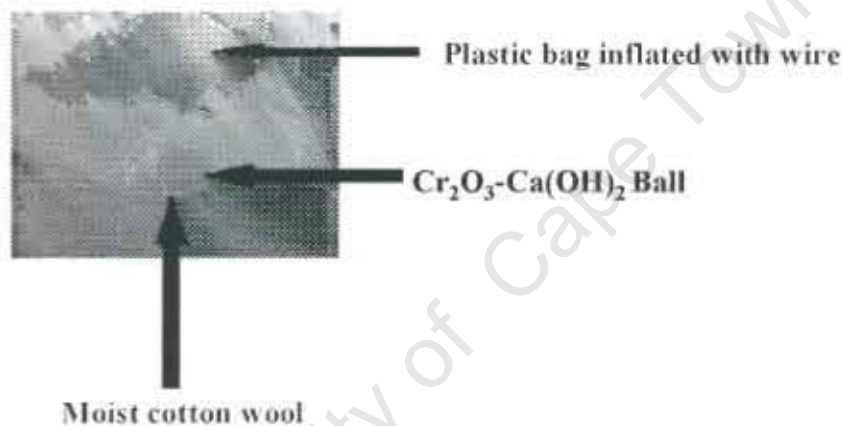


Figure 3-3: A Diagrammatic Illustration showing how the pore moisture was maintained in the $\text{Cr}_2\text{O}_3\text{-Ca(OH)}_2$ Balls

ii) Exposure to Ambient Moisture

To maintain conditions under which the pore moisture evaporates in both the $\text{Cr}_2\text{O}_3\text{-Ca(OH)}_2$ balls and the slag balls, the balls were prepared and simply stored on a shelf where they were left to dry out. The $\text{Cr}_2\text{O}_3\text{-CaO}$ powder mixes and pellets as well as the slag powders were also stored under the same conditions except that these were not prepared moist and did not contain pore moisture but were simply in contact with ambient moisture.

iii) Maintenance of the $\text{Cr}_2\text{O}_3\text{-Ca(OH)}_2$ Balls under Nitrogen

The $\text{Cr}_2\text{O}_3\text{-Ca(OH)}_2$ balls were prepared and stored in a closed container which was purged with nitrogen and sealed to prevent any oxygen from entering. The excess pore moisture of the balls also evaporated during storage in the container. The container was opened for the sampling of the balls, re-sealed and purged with nitrogen for an hour.

iv) The Maintenance of Dry Conditions

As discussed earlier, in order to ensure that a reaction between Cr_2O_3 , CaO and atmospheric oxygen could be observed without any uptake of atmospheric moisture (which can convert CaO to Ca(OH)_2), $\text{Cr}_2\text{O}_3\text{-CaO}$ powder mixes were prepared and stored in a dessicator.

3.6.4. Sampling of the Balls, Powders and Pellets

i) Sampling of $\text{Cr}_2\text{O}_3\text{-Ca(OH)}_2$ Balls

After being exposed to air for a specified period of time, the $\text{Cr}_2\text{O}_3\text{-Ca(OH)}_2$ balls were sampled and analysed for their Cr(VI) content. The sampling of the moist balls (balls in which the pore moisture was maintained) was conducted by weighing the balls moist, drying them in an oven maintained at 80°C for 4-5 hours and weighing them dry. The time span in the oven was selected such that no appreciable oxidation could occur upon exposure to the higher temperature. This is discussed further in the section on precautionary measures (section 3.7). The dried balls were crushed into a fine powder using an agate pestle and mortar. The fine powder was leached in a 1M NaOH solution for one hour by agitating a two litre bottle end over. The leach suspension was filtered through a Millipore filter. The filtrates were collected, stored refrigerated and analysed for their Cr(VI) content. The dry balls were sampled in the same manner except that they were not weighed moist or dried in the oven but were simply weighed dry, ground and leached in 1M NaOH. The slag balls were also sampled in the same manner. This sampling procedure is shown in Figure 3-4.

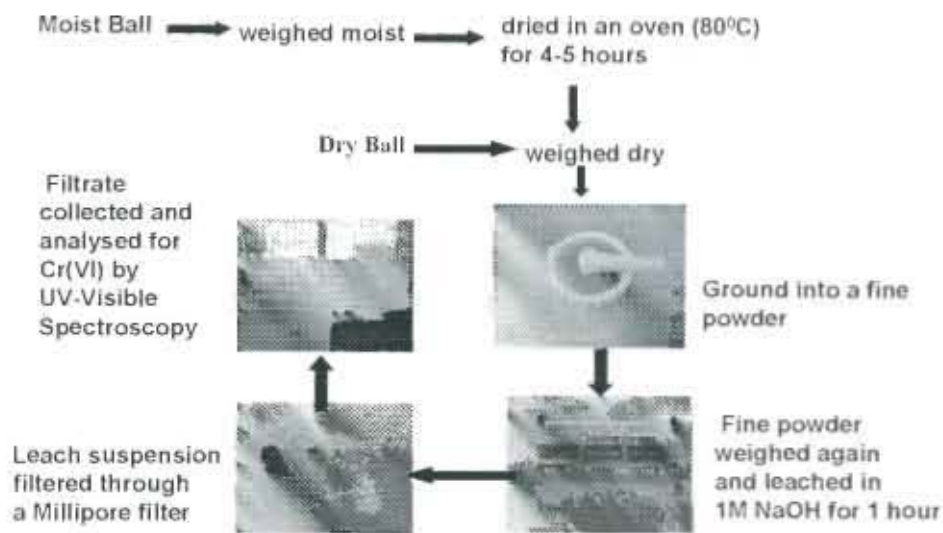


Figure 3-4: A Schematic Illustration of the Sampling Procedure to which $\text{Cr}_2\text{O}_3\text{-Ca(OH)}_2$ balls were subjected

ii) Sampling of $\text{Cr}_2\text{O}_3\text{-CaO}$ Powders

The $\text{Cr}_2\text{O}_3\text{-CaO}$ powder mixes which were pre-weighed when the experiments were set up, were weighed again upon sampling to establish whether there was any uptake of moisture from the atmosphere which might have converted the CaO to Ca(OH)_2 . The powders were also leached in 1M NaOH for one hour with the leach suspensions being filtered through a Millipore filter to collect filtrates that could be analysed for their Cr(VI) content. The slag powders were subjected to the same sampling procedure.

iii) Sampling of the $\text{Cr}_2\text{O}_3\text{-CaO}$ Pellets

The pellets were subjected to the same sampling procedure as the powders except that they were weighed in the pellet form first, crushed into a fine powder using an agate pestle and mortar and then leached in 1M NaOH for one hour.

In all of the above cases the analysis samples were derived from leaching in 1M NaOH. The reasoning behind this technique was that since the product calcium chromate is very soluble in alkali solutions, all or most of it that forms should leach out in a sodium hydroxide solution in one hour. This is also based on the sampling protocol of Petersen (1998) who used a strong NaOH solution to minimise the re-adsorption of chromate onto the mineral matrix.

3.6.3. Analysis of Samples

i) Choice of Analytical Method

Upon reviewing the literature, it was noted that the most commonly used analytical method for the analysis of Cr(VI) is UV-Visible Spectroscopy. This is due mainly to high sensitivity and high level of reproducibility. The Mohr titration, which involves the addition of Mohr's salt solution (ferrous ammonium sulfate in 1N H₂SO₄) to the sample and the titration of the excess iron with a KMnO₄ solution has been used (Hattori et al., 1978). Other instrumental analytical methods such as reverse phase HPLC (High Performance Liquid Chromatography) have been tested and used for Cr(VI) analysis (Milacic et al., 1992) but only for samples extracted from soil. However, the reactions under investigation were expected to proceed at slow rates due to the slow reactivity of Cr₂O₃. Thus, low concentrations of Cr(VI) were expected to be present in the samples collected after the first few weeks. This brought about the need for an analytical method that has low limits of detection and hence a high sensitivity to low concentrations. For this purpose, UV-Visible Spectroscopy was selected as the analytical method for the Cr(VI) analyses. The analytical protocol followed is based on a method employed Sandell (1950) which was modified by Petersen (1998). A description of this method is included in Appendix C for reference.

3.7. Measures Taken to Ensure the Accuracy of the Results Obtained

3.7.1. Repeat Experiments

Repeat experiments (particularly for the pure chemicals) were set up in order to check the repeatability of the results. The repeat experiments were set up on different days and the values obtained for the Cr(III) to Cr(VI) conversions were compared. The repeatability of the results is discussed in Chapter four (see Section 4.2).

3.7.2. Reproducibility checks

Since the data for the Cr(VI) measurements was obtained by analysis using only one analytical method, the absorbance readings obtained for each sample were checked for reproducibility by repeating the analysis on a batch of samples on different days and comparing the absorbance readings. Samples were reanalysed at least twice for this purpose. All datapoints found to unreliable due to the use of contaminated equipment was discarded and is not reported for any of the experiments conducted. The statistical analysis on the absorbance readings obtained on each sample from a given experimental series is presented and briefly discussed in Appendix C.

7.3. The Effect of Drying the Cr₂O₃-Ca(OH)₂ Balls in the Oven

As discussed earlier, all Cr₂O₃-Ca(OH)₂ balls in which the pore moisture was maintained were dried in an oven set at 80⁰C. Care was taken to select the drying period so that this would not result in any additional oxidation. Typically, the balls were dried for 4-5 hours, which allowed for a sufficient period of time for the moisture to evaporate. To verify that this drying does not cause any additional oxidation, two balls containing 50% Ca(OH)₂ were prepared and their pore moisture was maintained. One of the balls was dried in the oven for the 4-5 hour period and the other was dried in a pure nitrogen atmosphere. A slag ball was also prepared and subjected to the same test. The results from these tests are shown in Appendix D. Since both the balls that were oven-dried and dried under nitrogen had essentially the same conversions, it was concluded that drying the balls in the oven for 4-5 hours does not contribute to any additional oxidation.

3.7.4. Pre-treatment of Chromium Oxide (Cr₂O₃)

As discussed earlier, commercial chromium oxide may contain residual (or already auto-oxidised) concentrations of Cr(VI), so this had to be washed before any experiments were set up to remove all the residual Cr(VI). Any trace Cr(VI) that does not wash off is noted by taking a zero sample and recording the background Cr(VI) concentration.

In addition, other reagents used such as calcium oxide and sodium hydroxide were also analysed for background Cr(VI) concentrations or for other impurities such as manganese and silver which are known to be oxidisers of Cr(III). These results are shown in Appendix E.

3.7.5. Temperature Control

To ensure that a constant environmental temperature was maintained between 20 and 25⁰C, all experiments that were set up and maintained at ambient temperature were stored in an enclosed area where the temperature was maintained reasonably constant. A heater was also switched on cold days to ensure that the temperature did not appreciably decrease. On hot days the heater was switched off. The temperature of the "experimental" area was recorded on a daily basis in the morning, at noon and in the afternoon. These average day time temperatures are recorded in Appendix F.

3.7.6. General Analytical Protocol

Besides the general measures taken to ensure the accuracy of the analytical data, extreme care was exercised at all times to avoid contamination of the glassware and the samples. Clean, dry glassware was always used. Imprecise analytical data due to contamination was declared unreliable and was discarded.

Other equipment, such as the pipettes used for dispensing fixed volumes of reagents, was also calibrated on a regular basis to ensure that accurate volumes of reagents were dispensed and that reliable analytical data could be obtained.

3.8. Sampling Times

All samples were stored for specified periods of time before being subjected to sampling and analysis. Typically the sampling was conducted at first at weekly intervals and eventually at monthly intervals. This was in order to ensure that a sufficient amount of time was allowed for reaction to occur since the reactivity of chromium oxide is known to be slow.

3.9. Conclusion

This chapter has presented the experimental approach that was used to test the hypotheses regarding the oxidation of chromium oxide, both in pure chemicals and in ferrometallurgical slags. The rationale applied in devising the experiments has also been discussed. Great care has been taken to ensure the accuracy of the experimental data. Subsequently, all experimental work has led to the collection of conversion-time data. This data is presented in Chapter four.

CHAPTER FOUR

RESULTS

This chapter presents the results obtained from all the experimental work that was carried out to test the hypotheses presented in Chapter three. In all cases the data is reported as conversion-time data and is graphically depicted. Selected results are presented in tabular form but the fully tabulated results are given in appendix A4. The chapter also discusses the influence of selected parameters on the oxidation reactions under investigation, examines the accuracy of the data presented and, concludes with a brief introduction on how the data is interpreted in Chapters five and six.

4.1. Results

4.1.1. The Oxidation of Cr_2O_3 in the Presence of CaO

In Chapter three, experiments that were devised to study the oxidation of Cr_2O_3 in the presence of CaO were described. The results from these experiments are shown in Figure 4-1.

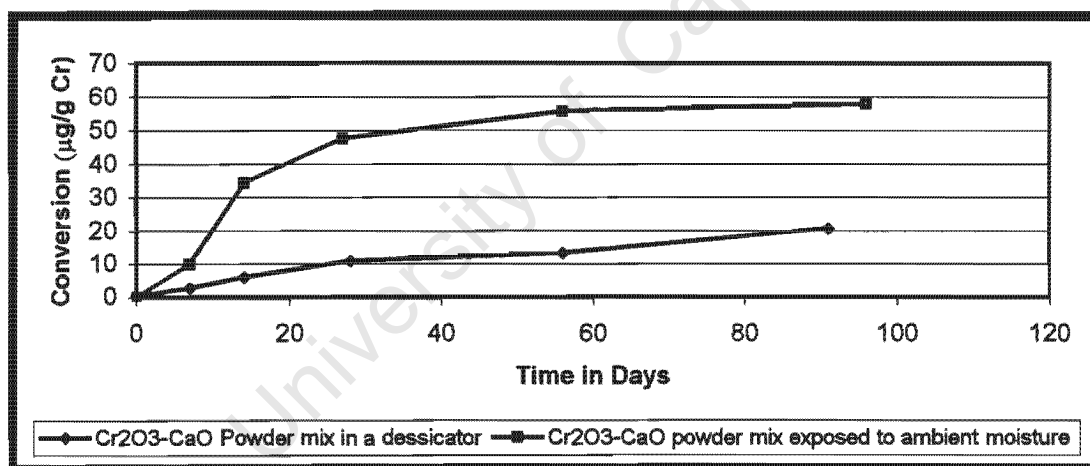


Figure 4-1: A comparison of the conversion-time data for Cr_2O_3 - CaO powders maintained in a dessicator and exposed to ambient moisture respectively (CaO content: 50%)

A comparison of the mass of the sample initially weighed out and the mass analysed (shown in Table A40-appendix A4) show clearly that there was no uptake of atmospheric moisture by the samples stored in the dessicator. It may thus be safely stated, that the CaO added to the powder mix was not converted into $\text{Ca}(\text{OH})_2$ even though there was

some exposure to ambient moisture when the dessicator was opened for sampling purposes.

It is also interesting to note that the conversions achieved in the experiments where the Cr_2O_3 -CaO powders were exposed to ambient moisture are about three times higher than those achieved for the experiment where the corresponding powders were stored in a dessicator. Table A45 in appendix A4 clearly shows that there was an uptake of atmospheric moisture by the samples (except for the zero samples). This is evident from the increase in the mass of the samples over the sampling period. Clearly, atmospheric moisture plays an important role in promoting oxidation. This phenomenon together with the mechanistic implications is discussed in more detail in Chapter five.

4.1.2. The Oxidation of Cr_2O_3 in the Presence of $\text{Ca}(\text{OH})_2$ ¹

All results from the experiments devised to investigate this reaction are shown in Figures 4-2 to 4-5. It must be noted that although CaO was added to prepare the balls, the oxidation still proceeds in the presence of $\text{Ca}(\text{OH})_2$. Water was also added to the powder-mixes and this would have converted all of the CaO to $\text{Ca}(\text{OH})_2$ (see sample calculation in Appendix A4)

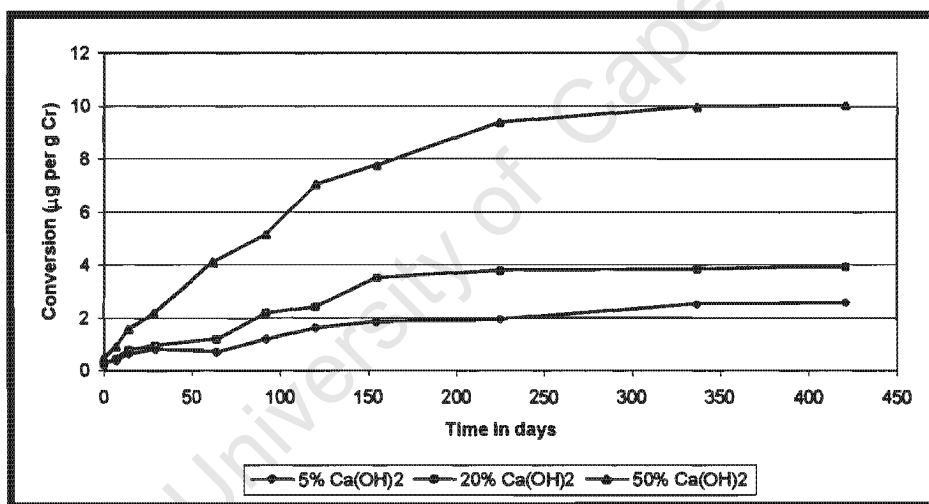


Figure 4-2: Conversion-time data for the oxidation of Cr_2O_3 in Cr_2O_3 - $\text{Ca}(\text{OH})_2$ balls with varying $\text{Ca}(\text{OH})_2$ content and with excess pore moisture prevailing

¹ All Cr_2O_3 - $\text{Ca}(\text{OH})_2$ ball experiments were set up in duplicate and the average results of the original and duplicate runs are reported here.

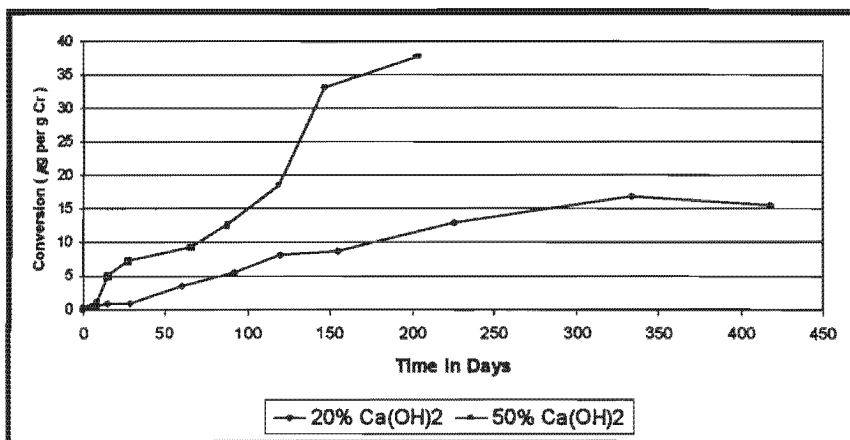


Figure 4-3: Conversion-time data for $\text{Cr}_2\text{O}_3\text{-Ca(OH)}_2$ Balls with varying Ca(OH)_2 content in which the excess pore moisture was allowed to evaporate

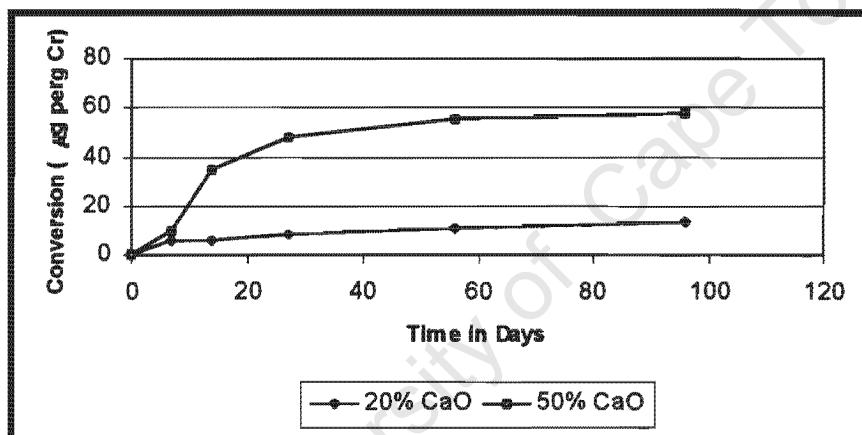


Figure 4-4: Conversion-time data for the oxidation of $\text{Cr}_2\text{O}_3\text{-CaO}$ powder mixes with varying CaO content

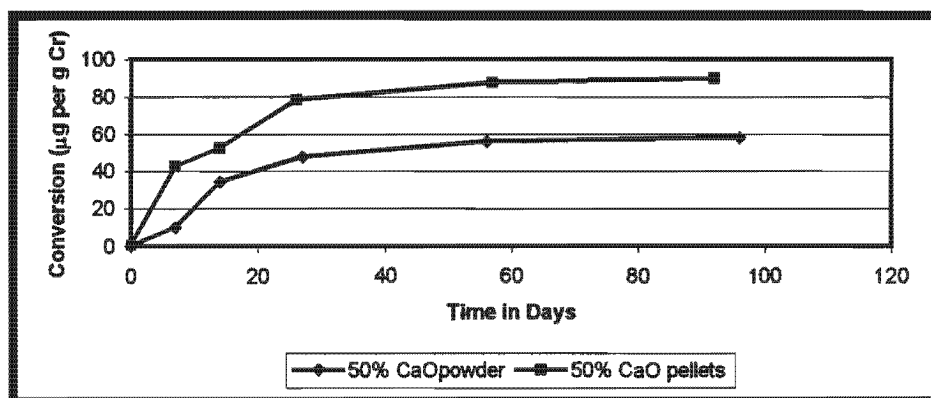


Figure 4-5: A comparison of the conversions observed in $\text{Cr}_2\text{O}_3\text{-CaO}$ powder and pellet systems

It must be noted at the outset that there was an uptake of atmospheric moisture in all of the powder and pellet samples (except for the zero samples). This is clearly shown in Tables A45 to A46 (see appendix A4). The increase in weights range typically from 5-27%. The relative number of moles of CaO and atmospheric moisture (shown in Tables A44 to A46) indicate that these compounds are present mostly in stoichiometric quantities so there is clearly enough uptake of atmospheric moisture for the CaO added to be converted to $\text{Ca}(\text{OH})_2$. Likewise, the sample calculation in appendix A4 shows that sufficient water was added to convert CaO into $\text{Ca}(\text{OH})_2$ when preparing the Cr_2O_3 - $\text{Ca}(\text{OH})_2$ balls.

It is also of interest to note that the oxidation rates are faster in the powder and pellet systems than in the ball systems. This may be due to free oxygen access in the powders and pellets as opposed to the balls where atmospheric oxygen has to diffuse through the surface of the balls. However, there is more inter-particle contact between Cr_2O_3 and $\text{Ca}(\text{OH})_2$ in the Cr_2O_3 - $\text{Ca}(\text{OH})_2$ balls than there is in the powder-mixes. Another point to take note of is that the CaO powder used for the powder mix and pellet experiments had a finer particle distribution than that used for the ball experiments. The supporting Malvern particle size distribution data is shown in Appendix B2. So care must be exercised when making comparisons between the data sets.

The results reveal that the oxidation of Cr_2O_3 is dependent on three key factors, namely CaO or $\text{Ca}(\text{OH})_2$ content, pore moisture and particle contact.

i) The Influence of CaO or $\text{Ca}(\text{OH})_2$ Content

Figures 4-2 to 4-4 show that the rate of oxidation of Cr_2O_3 increases as the amount of CaO or $\text{Ca}(\text{OH})_2$ added increases. This is regardless of the reaction conditions employed. Thus, the roles played by CaO and $\text{Ca}(\text{OH})_2$ in the oxidation reaction seem to be important. The mechanistic insights that can be gained from this are discussed in Chapter five.

ii) The Influence of Pore Moisture

A comparison of Figures 4-2 and 4-3, shows that the oxidation of Cr_2O_3 proceeds faster in the absence of pore moisture. This point is perhaps best illustrated by plotting the data sets for both conditions on the same set axes. This is shown in Figures 4-6 and 4-7.

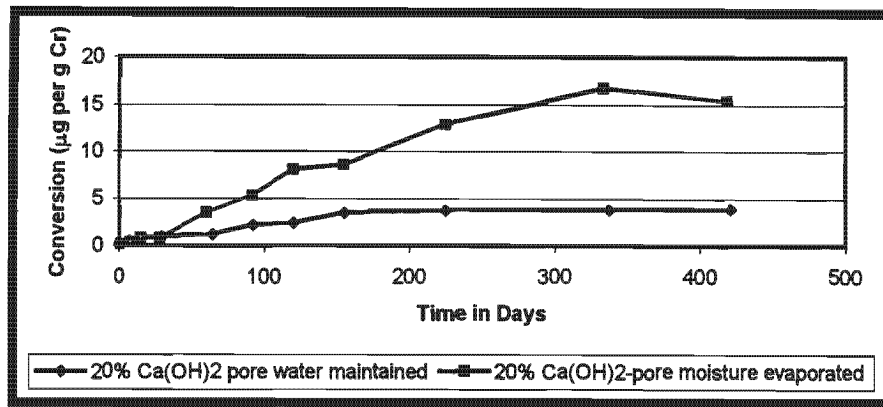


Figure 4-6: A Comparison of the conversions observed in $\text{Cr}_2\text{O}_3\text{-Ca(OH)}_2$ balls where the Pore Moisture was Maintained and Allowed to Evaporate Respectively (Ca(OH)_2 Content: 20%)

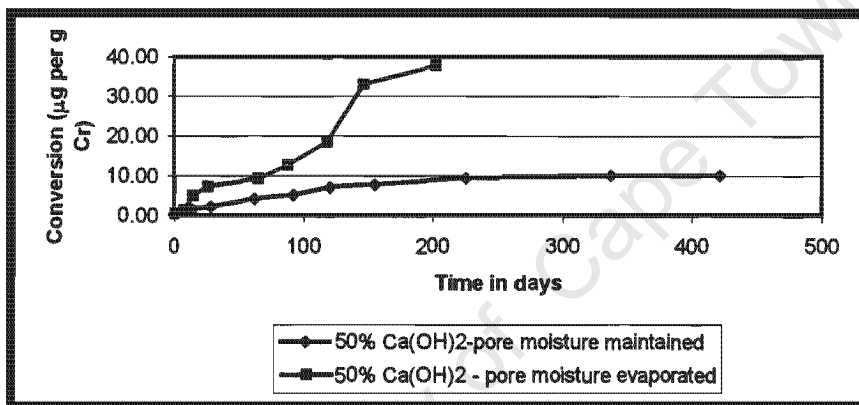


Figure 4-7: A Comparison of the Extents of Oxidation in $\text{Cr}_2\text{O}_3\text{-Ca(OH)}_2$ Balls in which the Excess Pore Moisture was allowed to Prevail and Evaporate Respectively (Ca(OH)_2 Content: 50%)

Care must again be exercised when analysing the first few data points in these figures. These seem to suggest that initially the conversions are similar under both conditions. This could be misleading as the first few data points are well below the lower analytical limit. As time progresses, and as the analytical range is approached the difference in conversions becomes more pronounced. This strongly suggests that pore moisture has an inhibitory effect on the oxidation of Cr_2O_3 . Such an effect needs to be understood in the context of the mechanism of the reaction. This phenomenon is therefore re-examined in Chapter five.

iii) The Influence of Particle Contact

Figure 4-5 reveals that the oxidation proceeds faster in Cr_2O_3 -CaO pellets than in Cr_2O_3 -CaO powders. This implies that intimate contact between Cr_2O_3 and CaO promotes oxidation. The implications for the mechanism of the oxidation reaction are discussed in Chapter five.

4.1.3. The Role of Atmospheric Oxygen as the Electron Acceptor

In Chapter three, an experiment in which Cr_2O_3 -Ca(OH)₂ balls (50% Ca(OH)₂) were maintained under nitrogen has been described. The purpose of this experiment was to verify the assertion that atmospheric oxygen acts the electron acceptor in the oxidation of Cr_2O_3 . The result of this experiment is shown in Figure 4-8. For comparative purposes, the results from a control experiment in which the balls were exposed to air were sampled at 2, 4 and 7 week intervals respectively are shown in Table 4-1 together with the corresponding results from the nitrogen experiments.

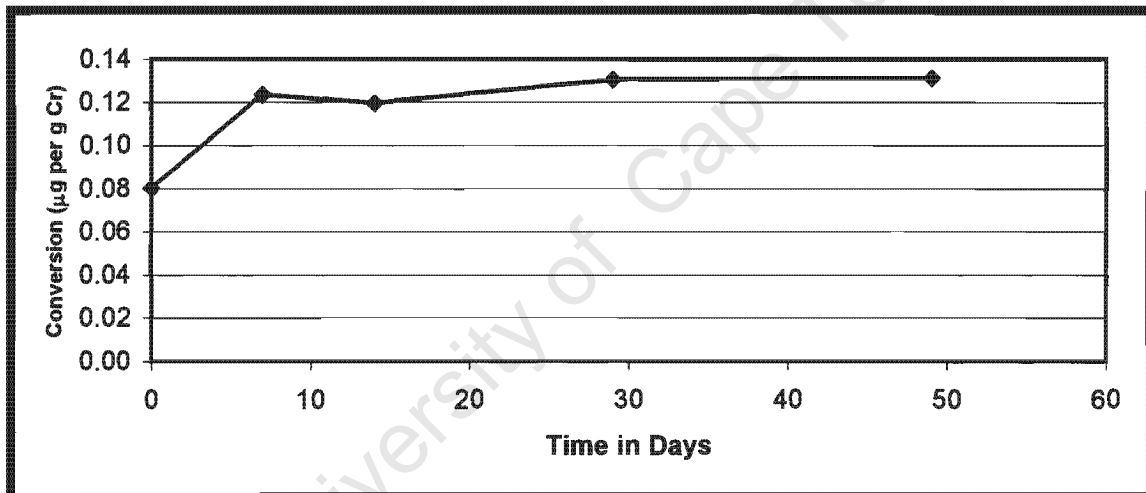


Figure 4-8: Conversion-time data for Cr_2O_3 -Ca(OH)₂ Balls containing 50% Ca(OH)₂ and maintained under nitrogen

Table 4-1: A comparison of the Conversions from the Experiments under Nitrogen and the corresponding experiments in which Cr_2O_3 -Ca(OH)₂ Balls were exposed to air

Experimental Series	Conversions (µg per g Cr)	Time in Days
Cr_2O_3 - Ca(OH) ₂ Balls maintained under nitrogen	0.12	14
	0.13	29
	0.13	49
Cr_2O_3 - Ca(OH) ₂ Balls exposed to air	0.21	14
	5.30	29
	6.36	49

exercised when viewing results below the analytical range so any initial oxidation that is observed under nitrogen must be treated with care.

The results show clearly that no significant oxidation occurs under nitrogen and that oxidation is more pronounced in the balls that were exposed to air.

4.1.4. The Temperature Dependence of the Oxidation of Chromium Oxide (Cr_2O_3)

The temperature dependence of the oxidation of chromium oxide, namely the oxidation in the presence of calcium hydroxide has also been investigated. Chapter three has described two experimental series in which Cr_2O_3 - $\text{Ca}(\text{OH})_2$ balls were maintained at 50°C and 80°C respectively. All balls contained 20% $\text{Ca}(\text{OH})_2$. The results from these experiments are shown in Figure 4-9. For comparative purposes, the results from the experiment in which the Cr_2O_3 - $\text{Ca}(\text{OH})_2$ balls (containing 20% $\text{Ca}(\text{OH})_2$) were maintained at ambient temperature ($\pm 22^\circ\text{C}$) are also shown in this figure.

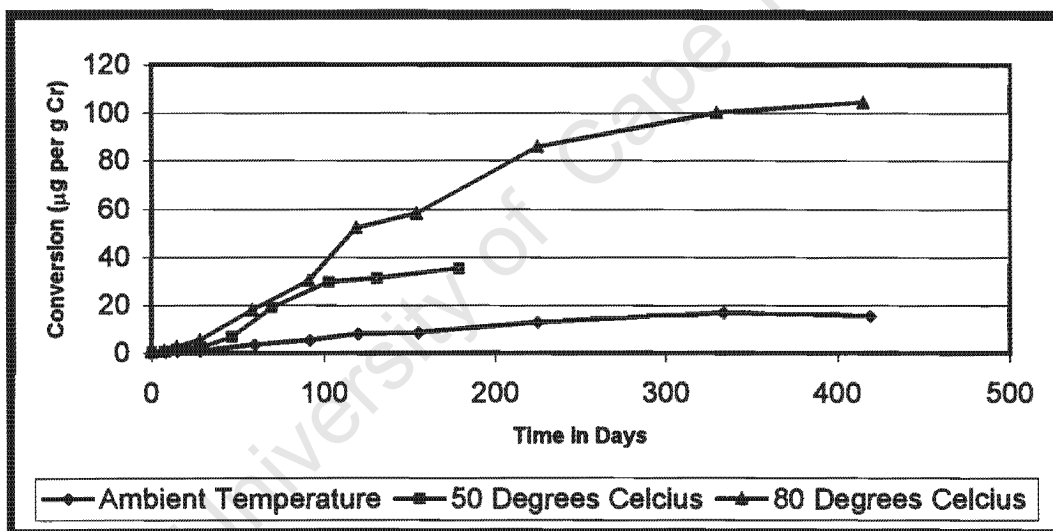


Figure 4-9: The Influence of Temperature on the Oxidation of Chromium Oxide in the Presence of $\text{Ca}(\text{OH})_2$

Although the sampling times are not equivalent for each of the data series, it can be clearly seen that the rate of oxidation of Cr_2O_3 increases with an increase in temperature. There is therefore a temperature dependence of the reaction rate, and it will need to be tested whether a rate law with an Arrhenius type rate constant can describe this reaction. This phenomenon is discussed in Chapter six where the kinetics of the reaction is investigated. The implications for the mechanism of the reaction are also discussed in Chapter five.

1.5. Oxidation in Ferrometallurgical Slags

In Chapter three, the experimental series that were devised to test the hypothesis that oxidation of Cr_2O_3 occurs in ferrometallurgical slags were described. The results from these experiments are shown in Figures 4-10 to 4-21. Some key parameters, which are likely to influence the rate of oxidation in the slags are also discussed. These include particle size, pore moisture and the chemical composition of the slags. This section concludes with a brief comparison of the rates of oxidation in the slags and the pure chemical systems.

i) The Influence of Particle Size

Figures 4-10 to 4-15 show the conversions that have been observed for three types of slags, which were supplied in three particle size classes namely, $<75\mu\text{m}$, $75\text{-}300\mu\text{m}$ and $300\text{-}1000\mu\text{m}$. This includes the data from the experiments in which the excess pore moisture of the slag balls was maintained and allowed to evaporate respectively.

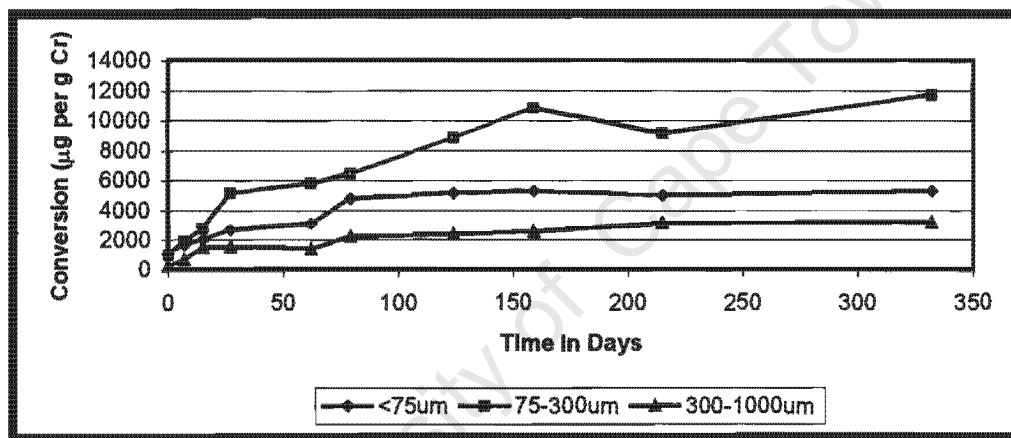


Figure 4-10: The Influence of Particle Size on the Rate of Oxidation in Old Mixed Slag Balls in which the Pore Moisture was maintained

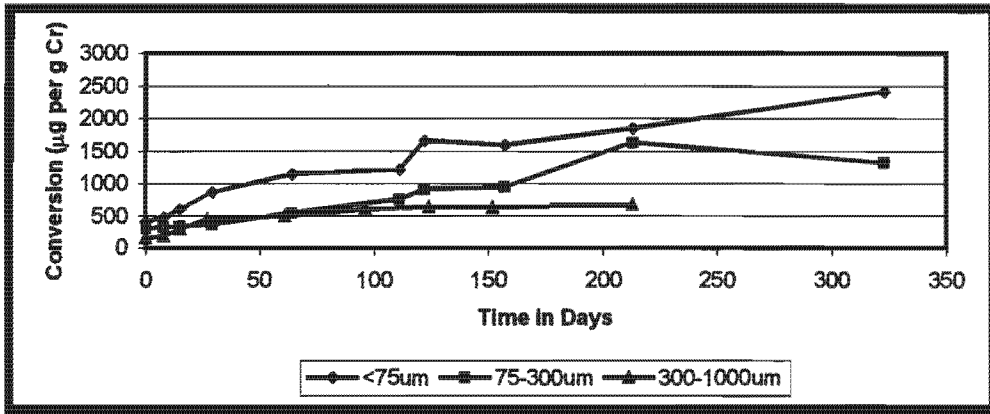


Figure 4-11: The Influence of Particle Size on the Rate of Oxidation in New CLU Slag Balls in which the Pore Moisture was Maintained

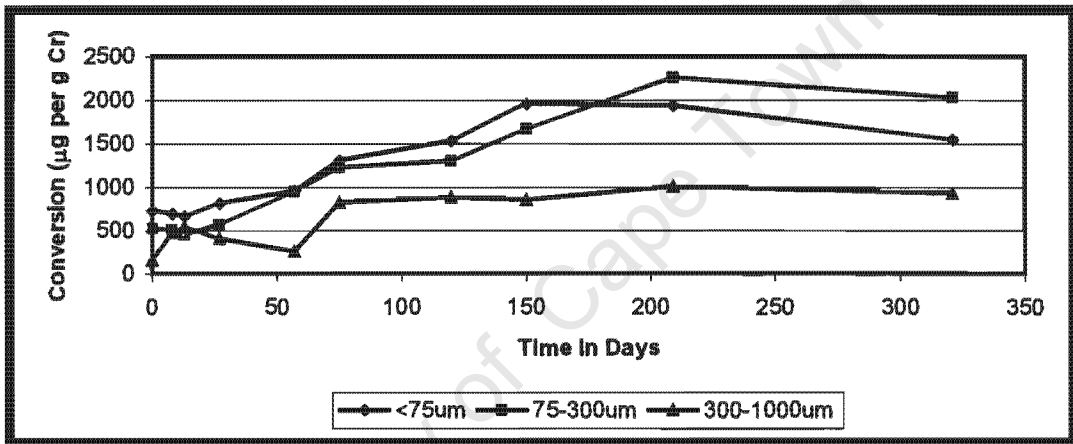


Figure 4-12: The Influence of Particle Size on the Rate of Oxidation in New EAF Slag Balls in which the Pore Moisture was maintained

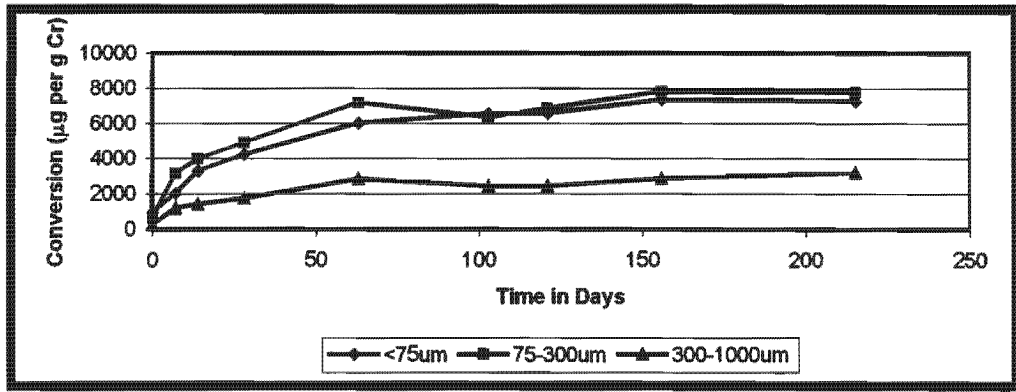


Figure 4-13: The Influence of particle size on the rate of oxidation in old mixed slag balls where the excess pore moisture was allowed to evaporate

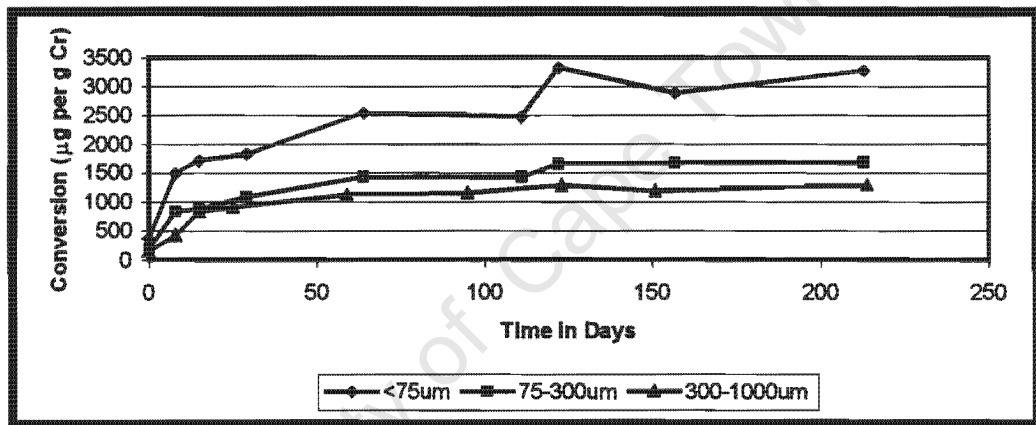


Figure 4-14: The Influence of Particle Size in New CLU Slag Balls where the excess pore moisture was allowed to evaporate

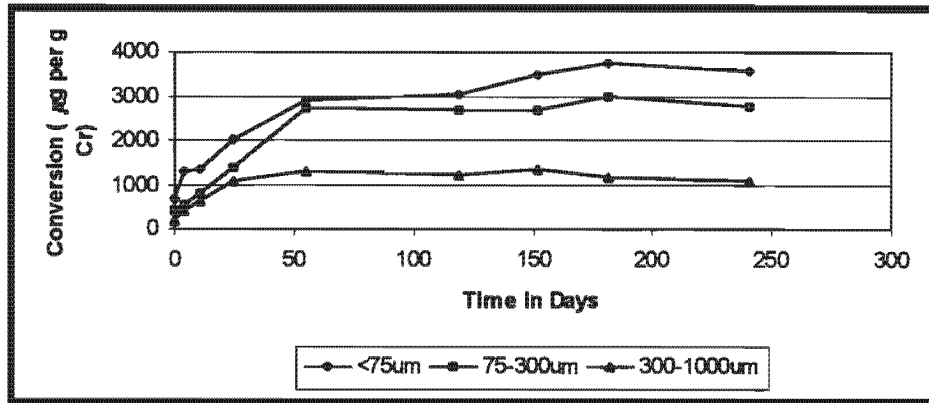


Figure 4-15: The influence of particle size on the rate of oxidation in New EAF slag balls where the excess pore moisture was allowed to evaporate

The results depicted in Figures 4-10 to 4-15 show that the conversions vary for each particle size class. The general trend observed is that the rate of oxidation increases with a decrease in particle size. This has been observed regardless of whether the excess pore moisture was maintained or not. An exception is noted for the old mixed slag where the middle fraction undergoes a highest rate of oxidation than the smallest fraction.

There is a fair amount of scatter in the data points especially for the CLU and the EAF slags. This may be due to inhomogeneity in the slags. Thus, it must be noted that any conclusions pertaining to the trends observed must be based on the entire data series and not on a single data point.

It must also be noted that with the exception of the old mixed slag balls, all slags in which the pore moisture evaporated, disintegrated into a powder after two weeks. However, some of the balls did not completely disintegrate into powders but contained a fair amount of agglomerates. This included the fine fractions of the CLU and EAF slags respectively.

ii) The Influence of Pore Moisture

The results from the experiments in which the excess pore moisture of the slag balls was maintained and allowed to evaporate respectively can be compared in order to examine the influence of pore moisture on the rates of oxidation. Such comparisons are made in Figures 4-16 to 4-18. Only the results obtained for the smallest particle size fractions of each type of slag are shown since in most cases (with the exception of the old slag) these showed the highest rates of oxidation. Table 4-2 also shows the moisture contents of the slag balls in which the excess pore moisture was maintained.

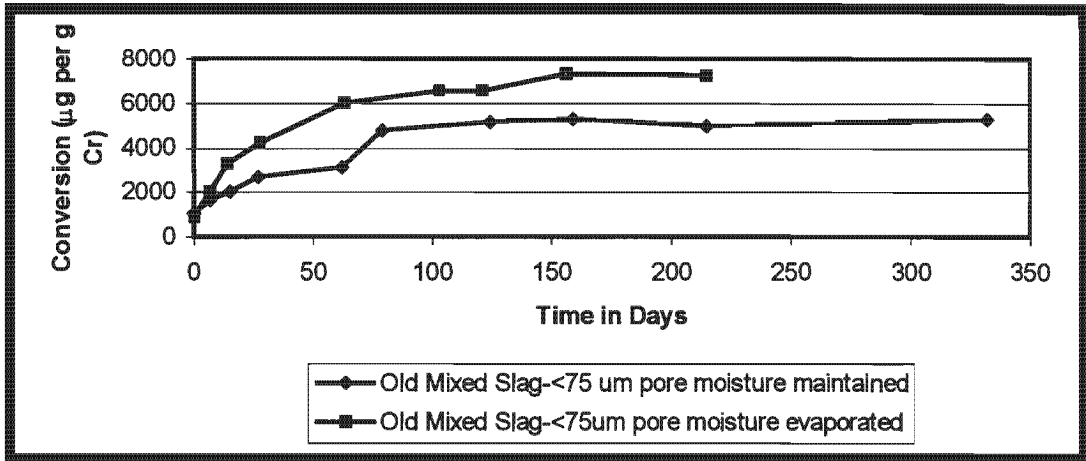


Figure 4-16: The Influence of Pore Moisture on the Rate of Oxidation in Old Mixed Slag Balls-Particle Size Class:<75µm

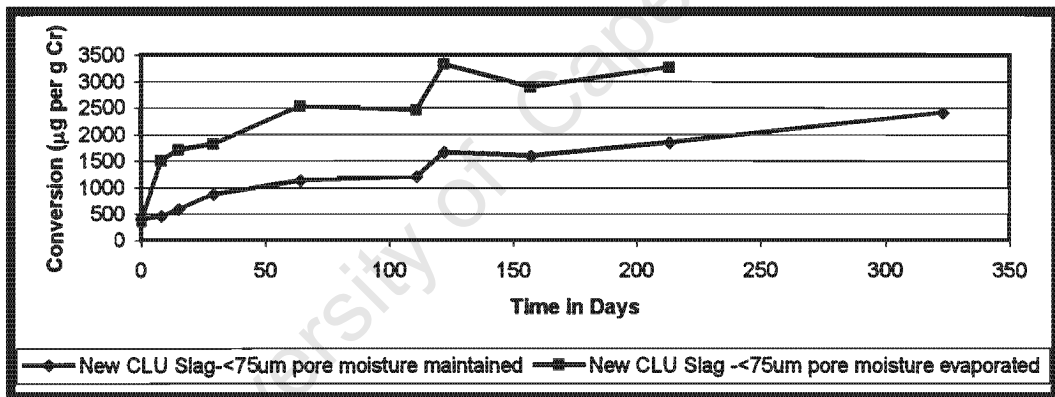


Figure 4-17: The Influence of Pore Moisture on the Rate of Oxidation in New CLU Slag Balls-particle size class:<75µm

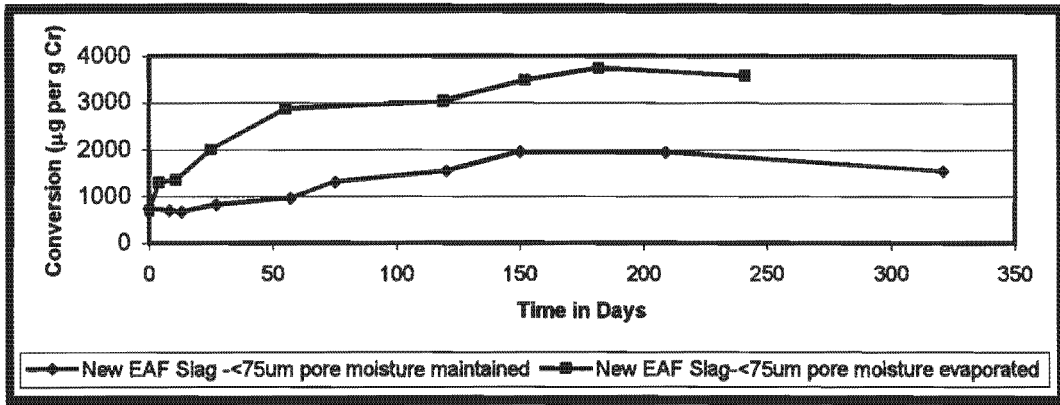


Figure 4-18: The Influence of Pore Moisture on the Rate of Oxidation in New EAF Slag Balls-Particle Size Class:<75µm

University of Cape Town

Table 4-2: The Moisture Contents of the Slag Balls in which the Excess Pore Moisture was Maintained (Size Fraction: <75 μ m)

Type of Slag	Moisture Content (%)	Days
Old Mixed	40.31	0
	37.61	7
	33.72	15
	25.98	27
	0.86	62
	30.66	79
	24.71	124
	32.38	159
	21.94	215
	23.36	332
New CLU	35.11	0
	35.54	8
	35.68	15
	37.48	29
	28.28	64
	20.11	111
	34.07	122
	34.43	157
	33.70	213
40.04	323	
New EAF	29.42	0
	29.68	8
	11.82	13
	22.00	27
	30.27	57
	32.41	75
	26.50	120
	31.50	150
	35.37	209
	37.52	321

Figures 4-16 to 4-18 show clearly that oxidation proceeds faster in the absence of pore moisture. This is consistent with the observations made for the $\text{Cr}_2\text{O}_3\text{-Ca(OH)}_2$ balls (See section 4.1.2.ii)). However, the relative extents to which pore moisture inhibits oxidation in pure chemicals and in slags need to be critically considered. Section 4.1.5.v) evaluates this subject.

Table 4-2 shows that the moisture contents of the slag balls in which the pore moisture was maintained has typically stayed constant between 11 and 40%. An exception is noted for the old slag where the moisture content drops significantly after 62 days. This is due to the cotton wool not being adequately moistened and the data point in question must be treated with care.

iii) Oxidation of Slag Powders Exposed to Air

In Chapter three, experiments in which slag powders were exposed to air were discussed. The results from these experiments are shown in Figures 4-19 to 4-21.

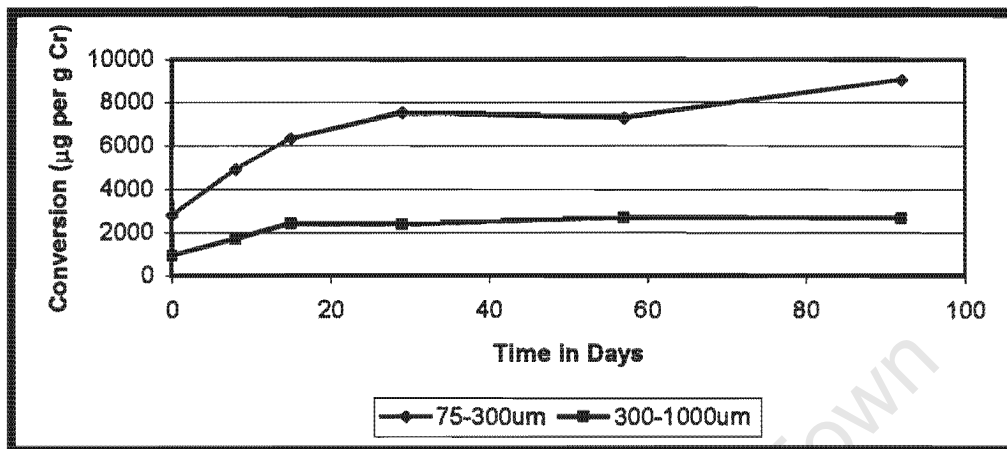


Figure 4-19: The Oxidation of Cr_2O_3 in Old Mixed Slag Powders Exposed to Air

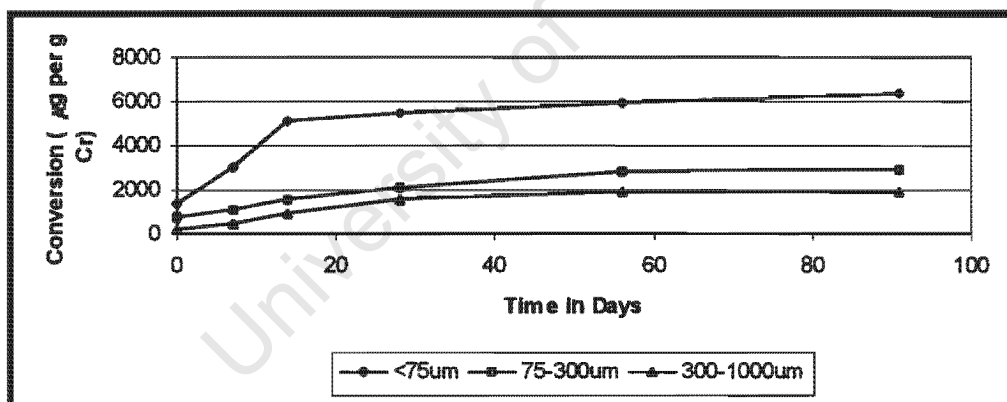


Figure 4-20: The Oxidation of Cr_2O_3 in New CLU Slag Powders Exposed to Air

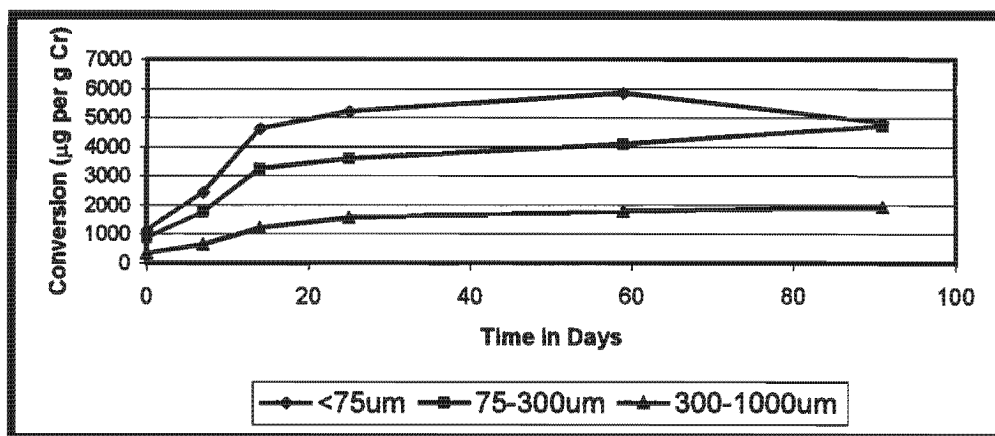


Figure 4-21: The Oxidation of Cr_2O_3 in New EAF Slag Powders Exposed to Air

It is again of interest to note the faster oxidation rates in the slag powders relative to the slag balls. This is consistent with the observation made for the pure chemicals but care must be exercised when attributing this to greater oxygen access in the powders. Most of slag balls (in which the excess pore moisture evaporated) disintegrated into a powder after 2 weeks although some still contained agglomerates. This excluded the old slag.

Tables A62 to A64 (in Appendix A4) shows that the moisture content of the slag powders varies typically from 0.1 to 15%. So, there is clearly some uptake of atmospheric moisture which can convert CaO in the slags to $Ca(OH)_2$. However, the calcium contents of the individual samples were not determined. This would have been useful in establishing whether or not CaO and atmospheric moisture were present in stoichiometric quantities. It is therefore difficult to state whether oxidation in the presence of $Ca(OH)_2$ predominates in the slag powders as in the case of the powders and pellets in the pure chemicals.

The trends regarding the extent of oxidation relative to the particle sizes is consistent with those observed for the slag balls. In the case of the old slag, the experiments were only set up for the middle and the largest fractions. This was due to the limited availability of the smallest fraction of this slag.

Some scatter in the data points is again noted, especially for the old and the EAF slags. The trends observed are therefore based on the entire data series and not on single data points.

iv) The Chemical Composition of the Slags

When examining the oxidation of Cr_2O_3 in ferrometallurgical slags, it is also important to examine the chemical composition of the slags as this would provide some insight as to which reactions are contributing to the oxidation of Cr_2O_3 in the slags. The elemental composition of each type of slag was therefore determined. The experimental methods used for the elemental analysis have been described in Chapter three. The results from this analysis are presented in Table 4-3.

Table 4-3: The Elemental Composition of each Type of Slag

TYPE OF SLAG	PARTICLE SIZE CLASS (µm)	Chemical Composition				
		%Mg	% Cr	% Ca	% Mn	% Fe
Old Mixed	< 75	5.52	0.8	34.8	0.9	0.7
	75-300	ND	0.9	31.2	1.0	1.4
	300-1000	6.13	2.4	24.9	1.2	6.6
New CLU	< 75	5.13	0.7	41.6	0.7	0.6
	75-300	ND	1.4	32.5	1.3	1.1
	300-1000	5.14	2.2	29.0	1.3	2.0
New EAF	< 75	5.39	0.6	38.2	0.6	1.3
	75-300	ND	0.8	36.6	0.8	1.7
	300-1000	4.45	2.0	31.5	1.0	3.6

(ND indicates not determined)

It must be noted that only the key elements or rather the elements most likely to have an impact on oxidation in the slags were analysed for. The results show that the chromium content of the slags varies for each particle size class. An interesting observation that is made upon examining Table 4-3 is that for each type of slag the largest fraction has the highest chromium content. Another noteworthy observation is the relative proportions of calcium and chromium in the slags. A higher calcium content relative to the chromium content is noted. The question of whether the results from oxidation of the slags can be compared to the results of the pure chemicals has therefore arisen. This issue is discussed in Section v) where attempts to compare these data sets are made.

It is also interesting to note that the magnesium content of the slags is lower than the calcium content. The Mn content is low so it is unlikely that this would contribute to any oxidation in the slags and the Fe content is also low enough not to warrant any reduction of CaCrO_4 , which forms in the slags.

v) A Comparison of the Extents of Oxidation in Slags and Pure

Chemicals

A further examination of the results shown in Figures 4-1 to 4-21 show that the oxidation of Cr_2O_3 proceeds about a hundred times faster in the slags than in the pure chemicals. This is true for both the powders and balls. Furthermore, the influence of pore moisture seems to be more pronounced in the pure chemicals. Before any attempts are made to explain this observation the question of whether these systems are directly comparable must be addressed.

Firstly, although similar experimental conditions were employed when devising the experiments, it must be noted that the chemical compositions of the slags and the pure chemicals differ. In particular the chromium to calcium ratios differ. For the slags, a

$\text{Cr}_2\text{O}_3:\text{CaO}$ ratio of around 1:40 (w/w)¹ is observed while in the pure chemical runs the $\text{Cr}_2\text{O}_3:\text{CaO}$ ratio was 4:1, 1:1 and 15:1(w/w) respectively. Since the $\text{Cr}_2\text{O}_3:\text{CaO}$ ratios in the slags and pure chemicals differ it is argued the two systems are not directly comparable. Nevertheless, the possibility that a reaction between Cr_2O_3 and CaO or $\text{Ca}(\text{OH})_2$ results in oxidation in the slags is still explored in Chapter five .

4.2. The Repeatability of the Results

The data presented thus far has been presented with much confidence in the accuracy. Chapter three has described the measures that have been taken to verify the accuracy. Much emphasis has been placed on the reproducibility and the repeatability of the results. As discussed in Chapter three, selected experiments were set up in duplicate in order to check the repeatability of the results. This was conducted mainly for the $\text{Cr}_2\text{O}_3\text{-Ca}(\text{OH})_2$ ball experiments. The findings of the verification measures for the repeatability of the results are presented in Figures 4-22 to 4-24. Appendix C shows the findings with respect to the reproducibility of the analytical data.

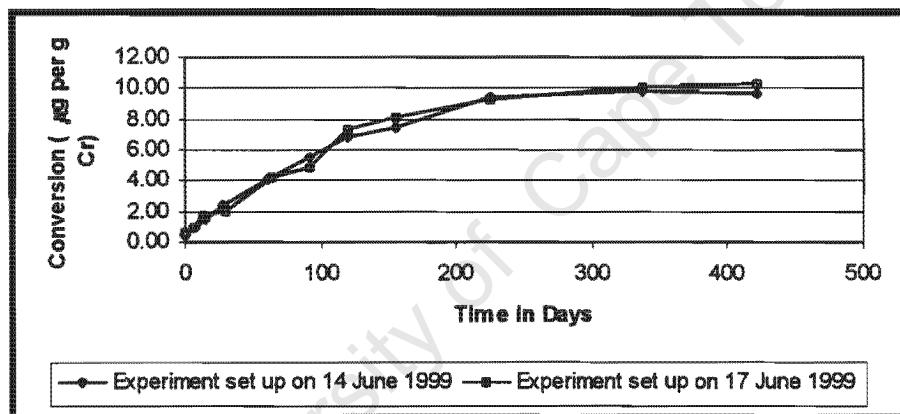


Figure 4-22: Results from a repeatability check on $\text{Cr}_2\text{O}_3 - \text{Ca}(\text{OH})_2$ Balls containing 50 % $\text{Ca}(\text{OH})_2$ and where the excess pore moisture was maintained

¹ Assuming that all Cr in the slag is present as Cr_2O_3 and all Ca is present as CaO .

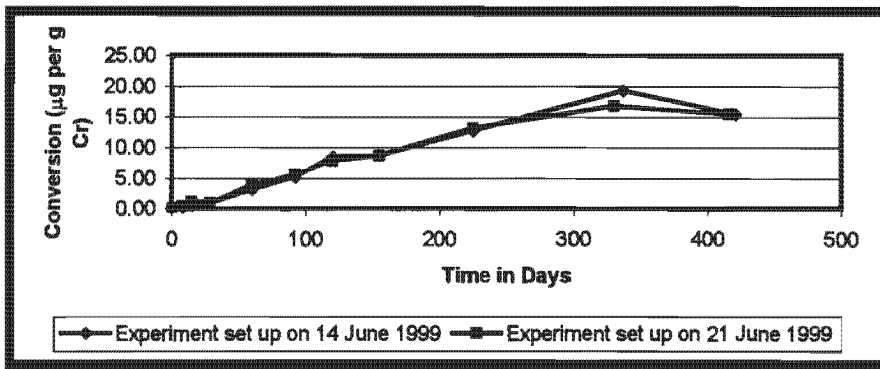


Figure 4-23: The Results from a Repeatability Check on $\text{Cr}_2\text{O}_3\text{-Ca(OH)}_2$ Balls (20% Ca(OH)_2) in which the excess pore moisture was allowed to evaporate

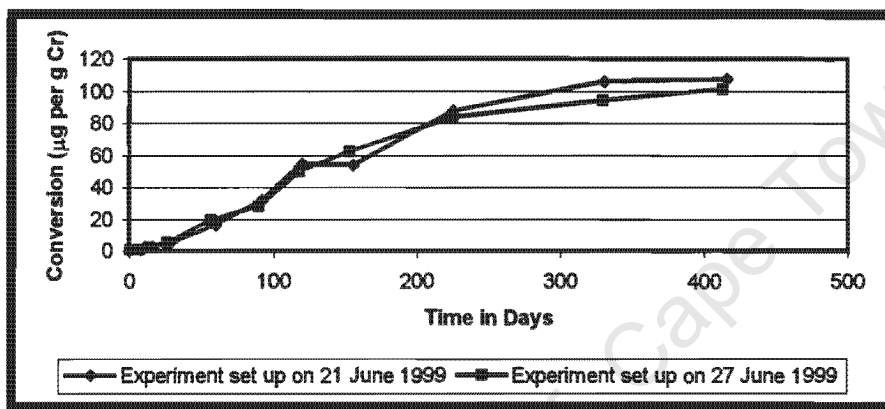


Figure 4-24: The Results from a repeatability check on $\text{Cr}_2\text{O}_3\text{-Ca(OH)}_2$ Ball experiments in which the balls were maintained at eighty degrees

Figures 4-22 to 4-24 show that a good level of repeatability was achieved in the $\text{Cr}_2\text{O}_3\text{-Ca(OH)}_2$ ball experiments. This is regardless of the experimental conditions employed and the time span between the original and the repeat experiments. An outlier (data point at 334 days) is noted in the original experiment for the $\text{Cr}_2\text{O}_3\text{-Ca(OH)}_2$ balls (20% Ca(OH)_2) where the pore moisture was allowed to evaporate. Despite this outlier, the results from the repeat experiments are in generally good agreement with those of the original experiments. So, it may be concluded that the data is sufficiently accurate to be used for interpretative purposes.

4.3. Conclusion

This chapter has presented the results obtained as conversion-time data. Although some aspects of the results, eg, the lower limits of the analytical data, need to be viewed with care, it may be asserted that the data presented is sufficiently accurate to be used for interpretative purposes. The interpretations presented are both of a qualitative and a quantitative nature. Chapter five presents the qualitative interpretations where the conversion-time data is used to gain some insights on the

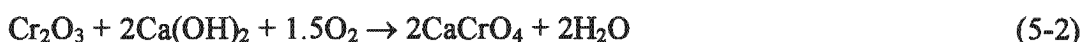
mechanisms of the reactions studied. Chapter six follows this, with quantitative interpretations of the conversion–time data in order to conduct a kinetic investigation.

University of Cape Town

CHAPTER FIVE

THE MECHANISM OF THE OXIDATION OF CHROMIUM OXIDE BY ATMOSPHERIC OXYGEN

In this chapter, the results from Chapter four are interpreted in order to elucidate the mechanisms of the reactions that contribute to the oxidation of chromium oxide. As discussed, in Chapter two, two reactions, which result in the oxidation of chromium oxide are known. These are the oxidation of Cr_2O_3 in the presence of CaO and $\text{Ca}(\text{OH})_2$ respectively.



The experimental evidence that proves that these reactions can occur under environmental conditions is summarised and used to gain some insight regarding the roles played by the calcium compounds in the oxidation reactions. The conversion-time data in Chapter four is also used to establish the key factors that influence the rates of oxidation that have been observed. The conversion-time curves are interpreted in order to identify rate laws that the reactions obey are likely to obey. The chemical composition and information on the mineralogy of the slags is then examined in order to establish the key reactions that contribute to the generation of $\text{Cr}(\text{VI})$ in these slags. The chapter concludes with a discussion on how the mechanistic insights may be used to establish preventative measures for the oxidation reactions during waste disposal.

5.1. Experimental Evidence that Validates the Proposed Reactions

5.1.1. The Oxidation of Cr_2O_3 in the Presence of CaO and $\text{Ca}(\text{OH})_2$

Figures 4-1 to 4-5 have shown that the oxidation of Cr_2O_3 occurs both in the presence of CaO and $\text{Ca}(\text{OH})_2$. Furthermore it is clearly evident from Figures 4-2 to 4-4 that the rate of oxidation is enhanced with higher CaO and $\text{Ca}(\text{OH})_2$ contents. These calcium compounds therefore play an important role in the oxidation of Cr_2O_3 . It is postulated that this is related to the high affinity, which Cr^{3+} has for oxygen centres (see Chapter two). Both CaO and $\text{Ca}(\text{OH})_2$ contain oxygen centres. So, clearly a higher CaO and $\text{Ca}(\text{OH})_2$ content will result in more oxygen centres for the Cr^{3+} centres on Cr_2O_3 . This may lead to some interaction of the Cr^{3+} centres with the oxygen centres of CaO and $\text{Ca}(\text{OH})_2$ which in some way weakens the covalent Cr-O bonds in the oxide, thereby enhancing its reactivity.

Upon examining Figure 4-1 it is noted that the rate of oxidation of Cr_2O_3 is enhanced when the Cr_2O_3 - CaO powders are exposed to ambient moisture. In Chapter four, it

was noted that enough atmospheric moisture has been taken up by the powders to convert CaO to Ca(OH)₂. Thus, the results in Figure 4-1 indicate that the oxidation of Cr₂O₃ occurs faster in the presence of Ca(OH)₂ than in the presence of CaO. This observation can again be explained in terms of the high affinity of Cr³⁺ for oxygen centres. Clearly, Ca(OH)₂ has twice as many oxygen centres as CaO so the reactivity of Cr₂O₃ is enhanced in the presence of an additional oxygen centre.

5.1.2. The Role of Atmospheric Oxygen as the Electron Acceptor

Figure 4-8 and Table 4-1 have shown that oxidation proceeds much faster under normal atmospheric conditions than in a pure nitrogen environment. It was stated in Chapter four that any oxidation that is observed in a nitrogen environment must be viewed with care. This is due to the initial data point being out of range with respect to the lower analytical limit. Overall, it may be stated that no appreciable oxidation occurs under nitrogen and this proves that atmospheric oxygen is the electron acceptor.

The electron transfer mechanism that leads to the oxidation of Cr³⁺ is presently not understood. At this stage all that the experimental results have revealed is that the reactivity of the Cr³⁺ centres in Cr₂O₃ is somehow enhanced in the presence of compounds that contain oxygen centres viz. CaO and Ca(OH)₂. It is thus postulated that the reactivity of the oxide is related to the affinity of Cr³⁺ for oxygen centres. It must be noted that one and a half atmospheric oxygen molecules can supply three oxygen centres possibly by the dissociation of oxygen molecules. The Cr³⁺ centres on the oxide can thus sacrifice their electrons whilst taking up oxygen centres from atmospheric oxygen. The calcium compounds supply the fourth oxygen centre that is needed for a chromate compound to form.

A more rigorous experimental study which specifically aims at identifying the reactive intermediates of the reaction, which in turn will provide clues as to how the electron transfer occurs, needs to be initiated.

5.2. The Factors that Influence the Rate of Oxidation

In Chapter four, it was noted that some important parameters influence the rate of oxidation. These are the CaO and Ca(OH)₂ content, pore moisture, temperature and particle contact. The effect of these parameters and the mechanistic insights, which can be gained from this are discussed below.

5.2.1. The Influence of CaO and Ca(OH)₂ Content

Figures 4-2 to 4-4 have shown a clear trend towards enhanced rates of oxidation with an increase in CaO and Ca(OH)₂ content. This has already been accounted for in terms of increased quantities of these compounds supplying additional oxygen centres for the Cr³⁺ centres, in some way weakening the covalent Cr-O bonds in the oxide and promoting its reactivity.

5.2.2. The Influence of Pore Moisture

Figures 4-6 and 4-7 have shown that the rate of oxidation in Cr_2O_3 – $\text{Ca}(\text{OH})_2$ balls is lower in the presence of pore moisture. This may be due to some inhibitory mechanism where the pore water molecules serve as competing sources of oxygen centres for Cr^{3+} centres. It is known from literature that Cr^{3+} can form hydroxy complexes in aqueous solution (see Chapter two). Thus, there may be a mechanism whereby Cr^{3+} ions released from oxide, are possibly forming complexes with excess pore water molecules and are therefore unable to undergo any oxidation in the presence of $\text{Ca}(\text{OH})_2$.

However this is purely speculative and the experimental approach that was devised to maintain the pore moisture must be critically considered. As discussed in Chapter three, the Cr_2O_3 – $\text{Ca}(\text{OH})_2$ balls were stored in close contact with a moist piece of cotton wool in order to maintain the pore moisture of the balls. The possibility that some of the $\text{Cr}(\text{VI})$ that is generated can, due to its high mobility, leach out into the moisture and diffuse onto the cotton wool must not be discounted. The rates of oxidation that have been observed under these conditions may thus be underrated.

Experimental evidence to test this assertion must be obtained before any definite conclusions are drawn. Chapter seven presents a proposed experimental approach that may be useful in verifying this assertion.

5.2.3. The Influence of Temperature

Figure 4-9 has shown that the rate of oxidation increases with an increase in temperature. Experimental evidence to show that the calcium compounds (in this case $\text{Ca}(\text{OH})_2$) play an important role in the oxidation reaction has already been discussed so there is clearly an interaction between the two solid reactants which promotes the reactivity of the trivalent oxide and makes it more amenable to oxidation. It is known from literature that two solids usually react by a solid–state diffusion of one of the reactants (Hannay, 1976). An Arrhenius type relation for the temperature dependence of the diffusion coefficient of a point defect (i) in the solid state has been experimentally observed and reported in the literature for solid state reactions (Schmalzried, 1981). This expression is shown below:

$D_i = D_i^0 \exp (-Q/RT)$ where D_i is the product of the concentration of the point defect (where the point defect can be a diffusing particle or ion) and its diffusion coefficient, R is the gas constant, Q is the lattice energy and T is temperature.

From this relation it is seen that the rate at which a particle or ion diffuses has an exponential dependence on the reciprocal of temperature. Thus, a higher temperature increases the mobilities and diffusivities of the diffusing particles or ions.

In the context of the reaction studied, it may therefore be argued that Cr^{3+} ions diffuse to the $\text{Ca}(\text{OH})_2$ particles where these in some way interact with the oxygen centres of $\text{Ca}(\text{OH})_2$. The higher temperatures would therefore increase the diffusivity and mobilities of the Cr^{3+} ions. These ions therefore come into contact with the $\text{Ca}(\text{OH})_2$ at a faster rate and the overall reaction rate increases.

5.2.4. The Influence of Particle Contact

Figure 4-5 has shown that intimate contact between CaO and Cr₂O₃ enhances the rate of oxidation in Cr₂O₃-CaO pellets. This can be explained in terms of the intimate contact between CaO and Cr₂O₃ resulting in a larger number of the Cr³⁺ centres and the oxygen centres on CaO being in close proximity. This facilitates the interaction of these centres with the oxygen centres of CaO and the reactivity of the oxide is enhanced.

However, upon further examination of Figure 4-5 it is noted that the extent to which the rate of oxidation is increased is not appreciable. This therefore suggests that some rate-limiting factor is controlling the rate of oxidation even when Cr₂O₃ and CaO are in close proximity to each other.

5.3. Trends in the Reaction Rates

Upon examination of figures 4-1 to 4-5 and figure 4-9 it is interesting to note the different shapes of the conversion-time graphs. Such graphs may be used to identify two basic trends in reaction rates. These are

- Logarithmic or Inverse Logarithmic Trends
- Initial Linear or sections followed by a decline in the slope

These trends are schematically illustrated in Figure 5-1.

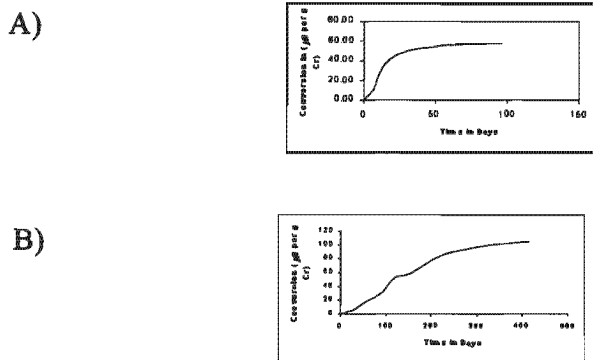


Figure 5-1: A Schematic Illustration of A) logarithmic or inverse logarithmic curves B) Initial Linear Sections followed by a decline in slope

A classification of these experimental results and the implications thereof are discussed below; the kinetic theory of solid-gas reactions is discussed in Chapter six.

5.3.1. Logarithmic or Inverse Logarithmic Trends

Figures 4-1, 4-4 and 4-5 show steep initial upward slopes of the conversion-time curve followed by an approach towards an asymptote. This suggests that the reaction may have attained equilibrium where both the rates of the forward and reverse reactions are equal. However, the possibility that the reaction is kinetically controlled is also explored in Chapter six.

Figure 4-2 also shows this trend for the $\text{Cr}_2\text{O}_3\text{-Ca(OH)}_2$ balls in which the pore moisture was maintained. While the asymptotic decline may again be due to the reaction attaining equilibrium, it must also be noted that this could be due to an inhibitory mechanism eg. the formation of complexes between Cr^{3+} and excess pore water molecules. However, it must again be emphasised that these trends in the reaction rate that have been observed may be false as some of the Cr(VI) that formed might have leached out into the pore moisture and diffused onto the cotton wool with which the balls were kept in contact.

5.3.2. Initial Linear Trends

This trend is characteristic of the dry $\text{Cr}_2\text{O}_3\text{-Ca(OH)}_2$ Balls (Figures 4-3, 4-6, 4-7 and 4-9). There seems to be a decrease in the reaction rates in most cases due to some rate-limiting step in the reaction. The pronounced initial linear sections observed in these, curves (in comparison to the logarithmic, or inverse logarithmic curves) suggests that the reactions could be obeying different rate laws in the ball and powder or pellet systems and under different reaction conditions. This observation is therefore re-examined in Chapter six.

5.4. Oxidation in Ferrometallurgical Slags

5.4.1. The Reactions Causing Oxidation in the Slags

Figures 4-10 to 4-21 have shown that oxidation has occurred in the slags regardless of the conditions employed. The question of which reaction contributes to the oxidation in the slags needs to be firstly addressed. The following reactions have to be considered when establishing which reactions contribute to the generation of Cr(VI) in the slags:

- The Oxidation of Cr_2O_3 in the Presence of CaO and $\text{Ca}(\text{OH})_2$
- The Oxidation of Calcium-Chromite ($\text{Cr}_2\text{O}_3 \cdot \text{CaO}$)

i) The Oxidation of Cr_2O_3 in the Presence of CaO and $\text{Ca}(\text{OH})_2$

The results from the elemental analysis shown in Table 4-3 have indicated that chromium and calcium are elemental constituents of ferrometallurgical slags. Furthermore, there is evidence from the literature that elemental chromium is oxidised to chromium oxide during slag formation and that lime (CaO) is added to slags to promote the slag viscosity (see Chapter two). Thus, Cr_2O_3 and CaO are present in ferrometallurgical slags and there is therefore a strong possibility that the oxidation of Cr_2O_3 in the presence of CaO contributes to Cr(VI) generation in the slags.

However, it must be noted that oxidation has also taken place in the slag balls. Since water was added to prepare the balls it can be argued the CaO present in the slags was converted to $\text{Ca}(\text{OH})_2$. Thus, the possibility that oxidation of Cr_2O_3 in the presence of $\text{Ca}(\text{OH})_2$ also contributes to the generation of Cr(VI) in the slags must not be ruled out. The likelihood of this reaction occurring in a landfill site is however dependent on the water content of the slags and the landfill conditions. If humid conditions prevail it is also likely that atmospheric moisture will react with the CaO in the slag thereby giving rise to $\text{Ca}(\text{OH})_2$. This is supported by the fact there is an uptake of atmospheric moisture by the slag powders, which were exposed to ambient moisture (see Table A62 to A64 in appendix A4 for moisture contents).

ii) The Oxidation of Calcium Chromite ($\text{Cr}_2\text{O}_3 \cdot \text{CaO}$)

Calcium chromite is a mineralogical phase of calcium and chromium oxide, which forms when CaO and Cr_2O_3 are fused together at high temperatures. According to Kilau and Shah (1984) there is an uncertainty as to whether calcium chromite can oxidise to calcium chromate under environmental conditions. Nevertheless, these workers have proposed that this reaction can occur upon exposure to atmospheric oxygen.

Such a reaction is only likely to occur in the slags containing calcium chromite. However, a mineralogical analysis conducted on the slags by an external source did not identify any calcium chromite in the slags (see Section 5.4.2). This therefore rules

out the possibility the oxidation of calcium chromite is contributing to the generation of Cr(VI) in the slags.

Thus, it may be argued the major reactions contributing to the generation of Cr(VI) in the slags is the oxidation of Cr_2O_3 in the presence of CaO or $\text{Ca}(\text{OH})_2$.

5.4.2. The Role of the Mineralogy of the Slags in Oxidation

The mineralogy of the slags has to be considered when interpreting the oxidation trends observed for the slags. A mineralogical analysis of the slags studied here has revealed that chromium exists in different mineralogical phases. The bulk is associated with magnesium in spinel phases but a sizeable fraction of the trivalent chromium is found in solid solutions in silicate phases which also contain virtually all of the calcium (Nell and Mostert, 1999).

The oxidation that has been observed in the slags is therefore due mainly to the intimate contact between Cr_2O_3 and CaO in the silicate phases. The fact that most of the Cr_2O_3 is locked away in spinel phases where it is in intimate contact with MgO probably is one of the reasons for the limited rates of oxidation in the slags. Clearly, a reaction between MgO and Cr_2O_3 is unlikely to proceed under environmental conditions. This is due to the high oxygen pressures that are required for the formation of MgCrO_4 , the product of the reaction between Cr_2O_3 , MgO and oxygen (Bayer and Wiedemann, 1977). So Cr_2O_3 in the spinel phases is not reactive and is unable to undergo any oxidation.

5.4.3. An Application of the Mechanistic Insights to Interpret the Oxidation Patterns in the Slags

The relative rates of oxidation in the slags are higher than those observed for the pure Cr_2O_3 -CaO and Cr_2O_3 - $\text{Ca}(\text{OH})_2$ systems. As stated in Chapter four, care must be exercised when making a comparison. The Cr_2O_3 :CaO ratios are lower in the slags than in the pure chemical systems.

However, in terms of the mechanistic insights discussed in Section 5.1., where it was inferred that the reactivity the oxide is driven by the presence of oxygen centres on CaO and $\text{Ca}(\text{OH})_2$ respectively, it may be argued that the excess calcium or rather CaO present in the slags results in excess oxygen centres that are available to the Cr^{3+} centres on the oxide. So, the reactivity of the trivalent oxide that is in contact with CaO in the silicate phases is to some extent enhanced.

As in the case of some the pure chemical experiments the curves level off. This again suggests that the extent of oxidation is limited or the reaction rates decrease. As discussed in Section 5.4.2. this may also be due to the limited amount of Cr_2O_3 that exists in silicate phases which are rich in calcium. However, this may also be due to some rate-limiting step in the reaction.

5.4.4. The Influence of Particle Size on the Rate of Oxidation in the Slags

In Chapter four, it was noted that the rate of oxidation in the slags increased with decreasing particle size (see Figures 4-10 to 4-15). This excludes the old slag where the middle fraction underwent the highest extent of oxidation. Such an observation may be accounted for in terms of the smaller particles providing a larger surface area, which promotes the diffusion of atmospheric oxygen and electron transfer. Table 4-3 also reveals that the smaller fractions have the highest calcium content (CaO content). Thus, the higher CaO content is promoting the reactivity of Cr_2O_3 , which is found in the silicate phases in these fractions.

5.4.5. The Influence of Pore Moisture on the Rate of Oxidation in the Slags

Figures 4-16 to 4-18 have shown that the rate of oxidation in all the types of slags seems inhibited in the presence of pore moisture. This may again be due to a mechanism involving the release of Cr^{3+} ions from the oxide and some complex formation between these ions and the excess water molecules.

The extent of inhibition in the slags is not as pronounced as in the case of the pure chemicals. However, such observations must be treated with care. The possibility that some of the Cr(VI) that forms leaches out into the excess pore moisture and diffuses onto the moist cotton wool that is used to maintain the pore moisture of the slag balls must again be considered. If this does indeed occur, the reaction rates are underestimated. Thus, this possibility must be investigated further.

5.5. Preventative Strategies for Waste Disposal Based on Mechanistic Insights

The purpose of studying the reactions that contribute to the oxidation of chromium oxide under environmental conditions was to identify the reactants that are likely to promote such reactions and hence to identify the chemical constituents of the slags that may be contributing to such oxidation reactions. Such insights may thus be used to control the chemical compositions and to a certain extent the physical characteristics of the slags so that preventative measures for the oxidation reactions may be established. Some suggestions for preventative measures are discussed in this section. The most obvious step is to reduce or eliminate chromium in the slags. Beyond this, a number of strategies can be applied.

5.5.1. Reduction in the CaO Content of Ferrometallurgical Slags

The discussion in Section 5.1, has focussed on the experimental evidence that validates the reactions contributing to the oxidation of Cr_2O_3 . From this, it was seen that the oxidation of Cr_2O_3 proceeds to an appreciable extent in the presence of increasing quantities of CaO and $\text{Ca}(\text{OH})_2$. Thus, it is clear that the CaO content of the slags should be reduced.

Also, experimental evidence, which proves that intimate contact between Cr_2O_3 and CaO enhances oxidation rates, was presented in Figure 4-5. So, any intimate contact between Cr_2O_3 and CaO should be avoided. In other words, Cr_2O_3 should not exist in the same mineralogical phase as CaO .

5.5.2. Increased Spinel Content or MgO Content of the Slags

The mineralogical analysis by Nell and Mostert (1999) has revealed that most of the Cr_2O_3 exists in spinel phases where it clearly cannot undergo any oxidation due to being bonded to MgO . Nevertheless, oxidation in the slags has still been observed due to some Cr_2O_3 that exists in silicate phases where it is in contact with CaO . Thus, a strategy whereby the MgO content of the slags is increased relative to the CaO content must be devised in order to minimise the oxidation of Cr_2O_3 . The role played by CaO in this reaction was accounted for in terms of the affinity of the Cr^{3+} centres for oxygen centres. The reactivity of the trivalent oxide is enhanced when its chromium centres interact with the oxygen on CaO . Clearly MgO can act as a competing source of oxygen centres for the Cr^{3+} centres. In this case the reactivity of Cr_2O_3 is not enhanced under environmental conditions. This is supported by evidence from the literature where it was noted that the oxidation of Cr_2O_3 in the presence of MgO does not proceed under environmental conditions because of the high oxygen pressures that are required for the formation of MgCrO_4 (Bayer and Wiedemann, 1977). This phenomenon is also supported by Kilau and Shah (1984) who have shown experimentally that the addition of MgO to stainless slags resulted in minimal leachable chromium and therefore proved that oxidation had been minimised in the slags.

In this respect it is also important to note that the Mg content of the slags is much lower than the Ca content of the slags (See Table 4-3).

5.5.3. Controlled Particle Size Distributions of the Slags

The results in Chapter four have shown that in most cases the extent of oxidation is enhanced oxidation rates as with a smaller particle size distribution in the slags. In Section 5.4.4 this was explained in terms of the smaller particle sizes presenting a larger surface area to facilitate the diffusion of atmospheric oxygen so that electron transfer can occur. Thus, another preventative strategy will involve ensuring that slags have a larger distribution of coarse particles (preferably greater than $1000\mu\text{m}$) to limit oxygen diffusion and hence to lower the extent of oxidation.

5.5.4. Competing Cations or Atomic Centres for the Oxygen Centre of CaO

As discussed in Chapter two, the Cr^{3+} ion has a tendency to adsorb onto surfaces that are rich in oxygen centres at high pH. The adsorbed Cr^{3+} ion is known to be stable with very slow desorption rates (James and Healy, in Van der Weijden and Reith, 1982). However, this only occurs in the absence of competing cations. Such a phenomenon is due to the affinity of Cr^{3+} for oxygen centres. This in turn can be used

to explain the interaction between Cr_2O_3 and CaO in the oxidation reaction. It is therefore proposed that competing cations or atomic centres, for the oxygen centre on CaO could be introduced into the slags. This is another strategy that may prevent the Cr^{3+} centres from interacting with the oxygen centre of CaO . The types of cations or atomic centres that can act as competing cations or atomic centres are unknown and this requires some further research. Clearly, the ideal competing cation must have a higher affinity for oxygen centres in order to outcompete Cr^{3+} for the oxygen centre on CaO . This phenomenon is reviewed in Chapter seven where recommendations for future work are discussed.

It must however be noted that such a suggestion is based on an understanding of the aqueous chemistry of Cr(III) , so clearly an aqueous phase or a medium in which Cr_2O_3 is soluble must be present in order to promote such a phenomenon. This can be achieved by adding the competing cations to the slags in the aqueous phase or rather where there is sufficient natural alkalinity in the slag to cause soluble Cr(III) to be present. This will ensure that Cr^{3+} can be out competed by other cations.

5.5.5. Competing Ligands for the Cr^{3+} Ion

Arguably, the interaction of the Cr^{3+} centres on the trivalent with the oxygen centre of CaO is not only based on the affinity of the Cr^{3+} ion for oxygen centres but also on its ability to form complexes with oxide ions. Thus, if competing ligands are present in the slag the Cr^{3+} ion may be locked away in complexes (if released from the oxide) that will prevent it from interacting with the oxygen centre of CaO . This phenomenon has already been explored when the influence of excess pore moisture on the extent of oxidation was discussed. However, the inhibitory effect of pore moisture is presently unresolved.

The Cr^{3+} ion is known to form complexes with other ligands such chlorides (see Chapter two for detailed discussion). It has been shown experimentally that when the Cr^{3+} ion is complexed with an organic ligand such as citrate even MnO_2 cannot oxidise it (Nakayama, 1981). Thus, the addition of competing ligands for the Cr^{3+} ion such as citrate to the slags may be a good preventative strategy.

Again, it must be noted that this suggestion is based on the aqueous chemistry of Cr(III) so citrate should be added to the slags only when there is sufficient natural alkalinity in the slag to cause soluble Cr(III) to be present for complex formation with citrate.

5.6. Conclusion

This chapter has focussed on the reactions that contribute to the oxidation of chromium oxide. Experimental evidence that validates these reactions has been presented. It has been observed that the oxidation of Cr_2O_3 is appreciably enhanced in the presence of increasing quantities of CaO and Ca(OH)_2 . The role of these compounds in the oxidation of Cr_2O_3 has been accounted for in terms of such compounds supplying oxygen centres for the Cr^{3+} centres in the trivalent oxide. The actual mechanism whereby this promotes the reactivity of the oxide and its

amenability to oxidation is not completely understood but it is possible that this serves as an activation mechanism for the transfer of electrons to atmospheric oxygen. The effect of pore moisture is not yet understood and the experimental approach that has been employed must be critically considered. The information on the chemical composition and the mineralogy of the slags has also been utilised to understand the trends in the rates of oxidation in the slags. It was concluded that the oxidation that was observed in the slags was mainly due the intimate contact between CaO and Cr₂O₃ in silicate phases.

In all cases, the conversions achieved are limited. While this may be due to an exhaustion of one of the reactants, there might also be a rate-limiting step in such reactions eg. the diffusion of atmospheric oxygen, or one of the solid phase reactants

A full scale mechanism for the oxidation of Cr₂O₃ in the presence of CaO and Ca(OH)₂ cannot be proposed as an experimental study which specifically aimed at identifying the reactive intermediates was not undertaken. Nevertheless, it can be proposed that the oxidation proceeds via the following key steps namely;-

- A solid-state diffusion of Cr₂O₃ or Cr³⁺ ions
- Some interaction of the Cr³⁺ centres of the oxide with the oxygen centre of CaO eg. the adsorption of Cr³⁺ ions which may be released from the oxide onto the oxygen centre of CaO which may serve as an activation mechanism for the oxidation reaction.
- Diffusion of atmospheric oxygen and electron transfer

Different shapes in the conversion-time graphs have also been noted. This has suggested that the oxidation of Cr₂O₃ in the presence of CaO and Ca(OH)₂ could be obeying different rate laws in the ball and powder systems. A decrease in the reaction rates with time has also been observed upon examining the conversion-time graphs. Some rate-limiting factor or rate-limiting step in the reactions is therefore coming into effect after a period of time. The rate laws, which the reactions obey need to be identified before such rate-limiting steps can be deduced.

Chapter six therefore focuses on the kinetics of the oxidation of Cr₂O₃ in the pure chemicals and the slags where the rates of oxidation are quantified and suitable kinetic models are tested.

CHAPTER SIX

THE KINETIC INVESTIGATION

This chapter shows how the conversion-time data presented in Chapter four has been manipulated in order to fit suitable solid-gas kinetic models. Also the kinetic models are applied to deduce the rate-limiting steps of the reactions, to evaluate certain kinetic parameters and to make some predictions for the long-term fate of trivalent chromium oxide in the wastes (ferrometallurgical slags) studied.

The chapter begins with a review of solid-gas (tarnishing) reactions. This theory is then applied to understand the observed trends in the reaction rate for the reactions leading to the oxidation of chromium oxide. Since it was established in Chapter five that the key reactions contributing to the oxidation of Cr_2O_3 in ferrometallurgical slags are the oxidation of the trivalent oxide in the presence of CaO and $\text{Ca}(\text{OH})_2$ respectively, only the kinetics of these reactions are examined. The chapter concludes with a discussion of the extent to which such reactions may pose an environmental hazard in the long-term.

6.1. A Review of the Kinetic Theory for Solid-Gas Reactions

6.1.1. An Introduction to Solid-Gas (Tarnishing) Reactions

A tarnishing reaction is defined as one in which a solid or more specifically a metal reacts with a gas to form a solid product (Schmalzried, 1981). A general equation for such a reaction is shown below:



where X_2 is any gas eg. oxygen, sulfur, chlorine, bromine etc. The products of solid-gas reactions form by the same elementary nucleation and growth steps as that of classical solid-state reactions. The transport of the reacting species will thus occur across phase boundaries where the transport processes are determined by the chemical driving forces and the relevant transport coefficients. The transport processes are also dependent on the microstructure of the reaction product. As an example, the reacting gas will diffuse easily through a porous product layer.

Simple experimental conditions have been employed in the study of tarnishing reactions and it is generally easier to study tarnishing reactions experimentally than it is to study solid-state reactions. This is due mainly to the difficulties experienced in maintaining a solid-solid interface as opposed to a solid-gas interface. Nevertheless, Schmalzried (1981) also states that it is possible to apply the theory derived from tarnishing experiments to solid-solid reactions.

The rate laws that have been experimentally derived for tarnishing reactions depend largely on the nature of the product layer. Other parameters that influence the rate law that is obeyed for tarnishing reactions include among others temperature, partial

pressures and sample shape. The rate laws that have been derived for tarnishing reactions have been derived from a one-dimensional experimental geometry but can also be applied to reactions where a three-dimensional geometry prevails (Schmalzried, 1981).

6.1.2. The Kinetics of Solid–Gas (Tarnishing) Reactions

The oxidation of metals at elevated temperatures which results in the formation of fairly thick product layers ($\geq 10^{-4}$ cm) is often accompanied by diffusion processes through the product layer (Kauffe in Hannay, 1976). This results in a parabolic rate law, which was first observed by Tammann in 1919 and then by Pilling and Bedworth in 1923. Such a diffusion-controlled oxidation only occurs if a coherent and pore-free product layer forms.

In most cases the growing product layer has pores and grain boundaries which act as favourable diffusion paths for the reacting species. The phase boundary reactions often become rate-determining resulting in a linear rate law. However, a linear rate law does not always imply that a porous product layer has formed.

In some cases reactions may obey two different rate laws depending on the conditions. This is characteristic of reactions where volatile reaction products are formed. An example of such a reaction is the chlorination of nickel. This reaction initially obeys a complex rate law and then a linear rate law due to the rate-determining evaporation of NiCl_2 (Kauffe in Hannay, 1976).

Deviations from the classical parabolic rate law may be expected at lower temperatures. In the thin layer region (initial period of oxidation) complications arise due to the formation of whiskers, blades and platelets of a solid product. In such cases, weight increase measurements cannot reveal whether a uniform and pore-free product layer has formed.

Other rate laws besides the parabolic and linear rate laws have been experimentally observed. Such rate laws include the cubic, fourth-power, logarithmic and reciprocal logarithmic (exponential) rate laws. In all cases surface phenomena eg. the ionosorption of the reacting species on the product layer, surface reactions in connection with nucleation processes or field transport phenomena within the growing product layer (Kauffe in Hannay, 1976) may be important. It is difficult to determine which of these mechanisms may be responsible for the product layer formation, as most of the solid-gas rate laws cannot be traced back to a uniform mechanism.

6.1.3. The Parabolic Rate Law

As stated earlier, Tammann first described this rate law in 1919. This is the most common rate law that is obeyed by solid-gas reactions (Schmalzried, 1981). In terms of this rate law, the rate constant is dependent on the product layer thickness and is mathematically expressed as:

$$\Delta m_x \propto \sqrt{t} \quad (6-2)$$

$$\text{or } \frac{dm_{x_1}}{dt} \propto \frac{1}{\sqrt{t}} \quad (6-3)$$

where Δm_{x_1} is the mass of gas consumed and t is time.

This rate law applies mostly to the oxidation of metals (Kauffe in Hannay, 1976; Schmalzried, 1981) and has been derived on the same assumptions as that of classical solid-state reactions. The most important assumption is that thermodynamic equilibrium is maintained throughout the reaction at all phase boundaries. However, the assumptions need to be tested experimentally for each individual case (Schmalzried, 1981).

6.1.4. The Linear Rate Law

In the event of the parabolic rate law not being fulfilled, other rate laws may apply for solid-gas reactions (Schmalzried, 1981). For example, the reaction rate may be constant or independent of the product layer thickness. In this case, the rate may be mathematically represented as:-

$$\Delta m_{x_1} \propto t \quad (6-4)$$

$$\text{or } \frac{dm_{x_1}}{dt} = \text{const} \quad (6-5)$$

In each of the above cases, the change in the mass of the gas consumed is expressed as a function of time. As discussed earlier, the linear rate law governs if the rate-determining step is caused by a reaction at one of the interfaces. This is characteristic of porous product layers which may attain any thickness as long as the attacking gas diffuses rapidly to the reaction front due to the formation of pores. A porous product layer forms only if the molar volume of the reaction product is smaller or larger than the corresponding volume of the underlying metal or metal reactant.

With a few exceptions, the linear rate law can be applied to reactions in which very thin product layers have formed. In the context of the study presented here, the linear rate law can be applied to cases where very thin product layers form at the points of contact between Cr_2O_3 and CaO or Ca(OH)_2 for example, in the Cr_2O_3 - Ca(OH)_2 balls. The linear rate law cannot be traced back to a uniform reaction mechanism (Schmalzried, 1981). It has been nevertheless acknowledged that individual reaction steps during adsorption or chemisorption of the reacting gas can be rate-determining giving rise to the linear rate law. This is supported by Kauffe (in Hannay, 1976) who suggests that when the linear rate law is obeyed the dissociation molecular oxygen is usually the rate-determining step. In this case, the supply of gas molecules or gas atoms may become rate controlling.

When product layers are very thin and electrical space charges at the phase boundaries are negligible, a phase boundary reaction which is usually the transport of the gas at the solid-gas interface may become the rate-limiting step of the reaction (Schmalzried, 1981).

Linear rate laws have been observed for reactions involving oxides and have even been observed for the formation of spinels and silicates. An example of such a reaction is the reaction between ZnO and cristobalite to form Zn_2SiO_4 when heated at $1348^{\circ}C$ (Schmalzried, 1981).

6.1.5. The Logarithmic and the Inverse Logarithmic Rate Laws

This rate law has been observed mainly in the low-temperature region. A uniform reaction mechanism has not been traced back to this rate law and this is mathematically represented below:

$$\Delta m_{x_1} \propto \log t \text{ or } \frac{dm_{x_1}}{dt} \propto \frac{1}{t} \quad (6-6)$$

A number of logarithmic rate laws have been derived (Kauffe in Hannay, 1976). However, these are complex and depend largely on the specific reaction that is under investigation. Inverse logarithmic rate laws (exponential) rate laws have also been reported in the literature.

The logarithmic rate law has been accounted for in terms of the transport of the reacting species along grain boundaries, pores and dislocations which are accompanied by changes in the pore sizes and diffusion paths (Evans in Hannay, 1976). Another transport mechanism that explains the logarithmic rate law is the nucleation and crystal growth that varies over the solid surface in relation to defects, grain boundaries and surface orientation. Some workers have also attributed the logarithmic rate law to the transport of electrons via a tunnelling mechanism (Mott, Hauffe and Illschner and Scheuble in Hannay, 1976). In such a tunnelling mechanism, the transport of electrons out of the solid through the reaction layer and the solid-gas boundary is the rate-determining step (Schmalzried, 1981).

The initial fast oxidation that is observed when a logarithmic rate law and in particular the inverse logarithmic (or exponential rate law) is obeyed has been accounted for in terms of site exchange processes. Here adsorbed oxygen species react with surface metal atoms by means of activated interchanges between metal and oxygen species (Fehlner and Mott in Hannay, 1976).

Some uncertainty as to the nature of the product layer that forms when the logarithmic rate law is obeyed also exists.

6.2. The Role of the Product Layer in Solid–Gas Reaction Kinetics

The discussion in the previous section has shown clearly that the nature and thickness of the product layer formed can have an important bearing on the rate law describing the reaction. Before a kinetic investigation is attempted, it is necessary to investigate whether a significant product layer could have formed in any of the experiments conducted, which were characterised by very low conversions ($\pm 0.01\%$).

The conversion at which a monolayer of product forms can first be estimated as follows:

The thickness of the monolayer is assumed to be 10^{-9} m. Another assumption that is made is that the Cr_2O_3 particles are spherical in shape. The Malvern particle size distribution data in Appendix B reveals that most of the Cr_2O_3 particles have an average diameter of $5\mu\text{m}$. The surface area of a single particle may thus be calculated as follows:

$$\begin{aligned} A &= 4\pi r^2 \\ &= 4\pi(2.5 \times 10^{-6})^2 \text{ m}^2 \\ &= 7.86 \times 10^{-11} \text{ m}^2 \end{aligned}$$

If a monolayer with a thickness of 10^{-9} m forms, the volume of this layer is approximated by:

$$\begin{aligned} \text{Surface Area} \times \text{thickness of the product layer} &= 7.86 \times 10^{-11} \text{ m}^2 \times 10^{-9} \text{ m} \\ &= 7.86 \times 10^{-20} \text{ m}^3 \\ &= 7.86 \times 10^{-14} \text{ cm}^3 \end{aligned}$$

Assuming that the density of the product CaCrO_4 is 2g/cm^3 , the mass of the product layer formed may be calculated as:

$$2\text{g/cm}^3 \times 7.86 \times 10^{-14} \text{ cm}^3 = 1.57 \times 10^{-13} \text{ g} = 1.57 \times 10^{-10} \text{ mg}$$

The mass of chromium in the monolayer is therefore $(1.57 \times 10^{-10} \times 52) \div 156$
 $= 5.2 \times 10^{-11} \text{ mg}$

The mass of the spherical Cr_2O_3 particle is given by: Volume \times Density

$$\begin{aligned} &= 4/3 \pi r^3 \times 2 \\ &= 4/3 \pi (2.5 \times 10^{-6})^3 \times 2 \times 10^6 \\ &= 1.3 \times 10^{-10} \text{ g} \end{aligned}$$

The mass of Cr in a Cr_2O_3 particle = $(104 \div 152) \times 1.36 \times 10^{-10} = 9.3 \times 10^{-11} \text{ g}$
 $= 9.3 \times 10^{-8} \text{ mg}$

The conversion necessary for the formation of a monolayer is therefore

$$(5.2 \times 10^{-11} \div 9.3 \times 10^{-8}) \times 100 = 0.06\% \text{ conversion}$$

The maximum conversion achieved in the pure chemicals is for pellet experiments (see Figure 4-5) at 0.08 mg/g Cr , which is 0.008% .

Since the conversion required for a monolayer to form around a single Cr_2O_3 particle is much greater than that achieved in the experiments, it may be concluded that a single product layer has not formed around the Cr_2O_3 particles in any of the pure Cr_2O_3 -CaO or Cr_2O_3 -Ca(OH)₂ experiments. However, this does not discount the possibility that there could be diffusional resistances through product layers at the points of contact between Cr_2O_3 and CaO or Ca(OH)₂.

The kinetic analysis has been conducted firstly by using the conversion-time data presented in Chapter four to quantify the reaction rates. Since the solid-gas rate laws are based on the relationships between reaction rates and time, the reaction rates are plotted against time and the mathematical expression which best describes the relationship between the reaction rates and time is used to express the rate law of the reactions. This has been conducted by ignoring data points, which resulted in negative reaction rates or outliers, and recalculating the reaction rates accordingly.

The solid-gas rate law which is described by the appropriate mathematical expression (kinetic model) is also used to identify a possible rate-limiting step of the reaction. The rate equation is integrated in order to obtain a mathematical expression for conversions. The kinetic model is numerically tested and the results from the numerical tests are compared to the observed reaction rates and conversions in order to establish how accurately the model predicts the reaction rates and conversions. This model is then used to predict further trends in the reaction rates and conversions in the long-term, typically a two-year period. Further details of the kinetic data are given in Appendix G.

6.4. The Kinetics of the Oxidation of Cr_2O_3 in the Presence of CaO

6.4.1. The Kinetic Model

Figure 6-1 shows the results from a kinetic investigation on Cr_2O_3 - CaO powders maintained in a dessicator (refer to Figure 4-1 for the corresponding conversion-time data).

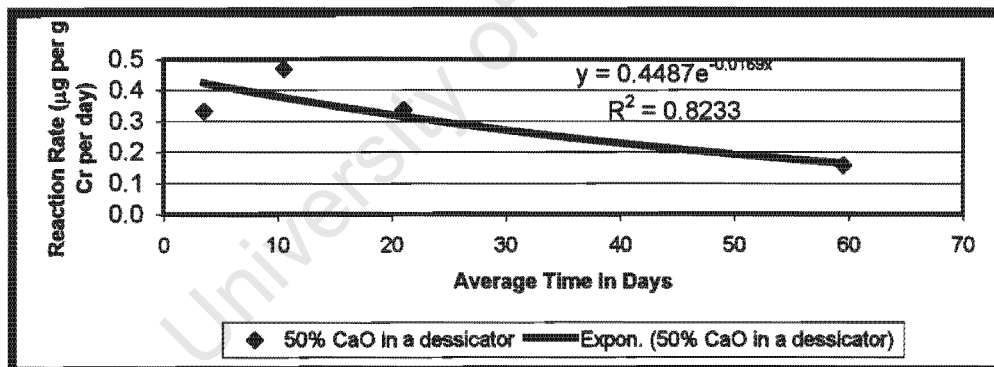


Figure 6-1: The relationship between rate and time in Cr_2O_3 - CaO powder-mixes maintained in a dessicator

Firstly, it must be noted that the data point at 56 days was treated as an outlier and ignored when fitting the kinetic model. This is consistent with the method outlined in Section 6.3. The results from the kinetic analysis therefore show that an exponential or inverse logarithmic rate law best describes this reaction. So, the rate law of the reaction may be written as:

$$\text{Rate} = k e^{-bt} \quad (6-7)$$

$$\text{or } \frac{dx}{dt} = ke^{-bt} \quad (6-8)$$

where x = conversion, k = initial reaction rate, b = the exponential decay factor,
 t = time.

Equation (6-8) can therefore be integrated to obtain an expression for the conversion x . This is shown in equation (6-9).

$$x = \frac{k}{b}(e^{-bt} - 1) \quad (6-9)$$

Equations (6-8) and (6-9) can be used to numerically test the fit of this model. The results from this numerical test are shown in Table 6-1.

Table 6-1: The Results from the Numerical Test of the Model for the Reaction:
 $\text{Cr}_2\text{O}_3 + 1.5 \text{O}_2 + 2 \text{CaO} \rightarrow 2\text{CaCrO}_4$

Average Time in Days	Observed Reaction Rates ($\mu\text{g per g Cr per day}$)	Predicted Reaction Rates ($\mu\text{g per g Cr per day}$)	Observed Conversion ($\mu\text{g per g Cr}$)	Predicted Conversion ($\mu\text{g per g Cr}$)
4	0.33	0.42	2.33	1.52
11	0.47	0.38	5.61	4.32
21	0.34	0.31	10.32	7.93
60	0.16	0.16	20.16	16.84

These results show that the values predicted for reaction rates are in good agreement with the observed reaction rates, especially at longer period of times. However, the conversions are under-predicted and this must be taken into account when making long-term predictions. Nevertheless, the model seems to be sufficiently accurate and may therefore be used to make predictions for the trends in conversions and reaction rates.

6.4.2. Model Predictions for the Reaction

Equations (6-8) and (6-9) can be used to predict the reaction rate and conversion for this reaction after one year.¹ These calculations are shown below:

$$\begin{aligned} \text{Reaction Rate after one year} &= 0.4487e^{(-0.0169 \times 315)} \\ &= 2.19 \times 10^{-3} \mu\text{g per g Cr per day} \end{aligned}$$

$$\text{Conversion after one year} = (0.4487 \div -0.0169) (e^{(-0.0169 \times 315)} - 1) = 26.42 \mu\text{g per g Cr}$$

¹ These calculations are performed by using average times

$$\begin{aligned} \text{Reaction rate after two years} &= 0.4487 e^{(-0.0169 \times 675)} = 4.99 \times 10^{-6} \mu\text{g Cr per day} \\ \text{Conversion after two years} &= (0.4487 \div -0.0169) \times (e^{(-0.0169 \times 675)} - 1) \\ &= 26.55 \mu\text{g per g Cr} \end{aligned}$$

The model therefore predicts that the reaction rate will become insignificant after the first year, with a maximum conversion of 26.55 $\mu\text{g per g Cr}$ being attained. The decline in the reaction rate may be attributed to a rate-limiting step such as the diffusion of atmospheric oxygen along grain boundaries and the solid-state diffusion of the reactants coming into effect. This could also be due to the penetration of electrons through thin product layers at the points of contact between Cr_2O_3 and CaO . The results seem to indicate that the oxidation reaction is significant as long as Cr_2O_3 and CaO are in close contact.

6.5. The Kinetics of the Oxidation of Cr_2O_3 in the Presence of $\text{Ca}(\text{OH})_2$

6.5.1. Powder and Pellet Systems

i) The Kinetic Model

Figure 6-2 shows a plot of the reaction rate against time for Cr_2O_3 - $\text{Ca}(\text{OH})_2$ powders and pellets containing 50% $\text{Ca}(\text{OH})_2$ and the kinetic models which best describe the relationships between the reaction rates and time (refer to Figure 4-5 for the corresponding conversion-time data).

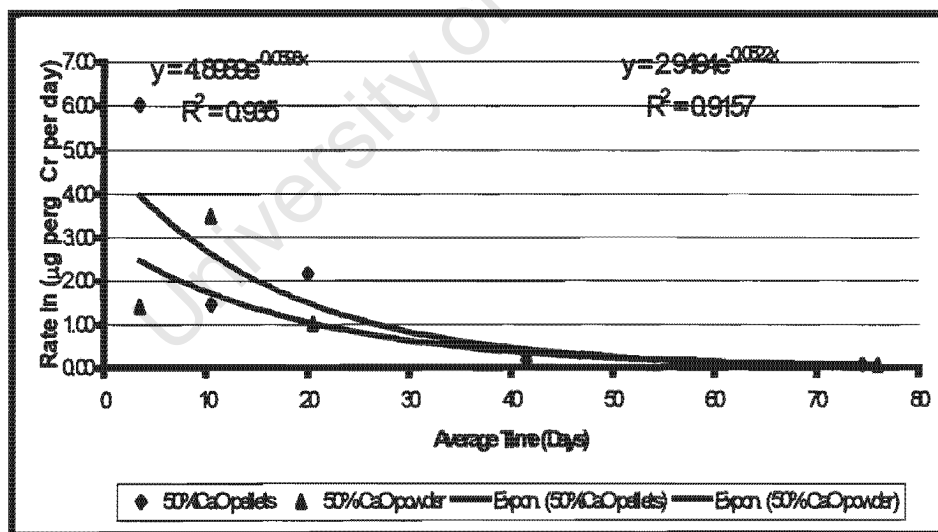


Figure 6-2: A rate versus time plot for the reaction:



From this figure it can be clearly seen that the reaction is well described by an exponential or inverse logarithmic rate law. This rate law can again to be used to explain why the

reaction rates decrease asymptotically. The rate-limiting steps of the reaction could be the penetration of electrons through thin product layers at the points of contact between Cr_2O_3 and $\text{Ca}(\text{OH})_2$. As in the case of the reaction involving CaO it is also likely that the transport of the one of the reacting species is the rate-limiting step. This could either be the solid state diffusion of Cr_2O_3 to the oxygen centres on $\text{Ca}(\text{OH})_2$ or the diffusion of atmospheric oxygen along grain boundaries of the solid reactants.

The results from the numerical test of the model using equations (6-8) and (6-9) are shown in Table 6-2.

Table 6-2: The Results from the Numerical Fit of the Exponential Model to the Experimental Data

Experimental Series	Average Time in Days	Observed conversions ($\mu\text{g per g Cr}$)	Predicted Conversions ($\mu\text{g per g Cr}$)	Observed Reaction Rates ($\mu\text{g per g Cr per day}$)	Predicted Reaction Rates ($\mu\text{g per g per day}$)
50% CaO powder systems	4	9.9	9.4	1.41	2.46
	11	34.4	23.8	3.49	1.70
	21	47.4	37.1	1.01	1.01
	42	55.5	50.0	0.28	0.34
	76	57.8	55.4	0.06	0.06
50% CaO pellets	4	42.1	15.5	6.02	3.97
	11	52.2	38.2	1.43	2.61
	20	78.0	57.1	2.16	1.48
	42	87.0	75.1	0.29	0.41
	75	89.3	81.0	0.07	0.06

There is initially some over-predictions and under-predictions in the reaction rates but as time progresses the reaction rates are quite accurately predicted. The conversions are initially under-predicted but as time progresses the difference between the predicted and the experimentally observed conversions, becomes smaller. Thus, the model does not accurately predict rates and conversions at shorter periods of times but makes reasonably accurate predictions for rates and conversions over longer periods of time and can therefore be used to make predictions for the reaction rates and conversions in the long-term.

ii) Model Predictions for the Reaction in the Long-term

Equations 6-8 and 6-9 can be used to calculate the reaction rates and conversions within one year and two years for both the powder and pellet systems, using average times. The predicted reaction rates and conversions are shown in Table 6-3.

Table 6-3: The Predicted Reaction Rates and Conversions over a two-year period for the Cr₂O₃-CaO Powder and Pellet Systems

Experiment	Average time in days	Predicted Reaction Rate($\mu\text{g per g Cr}$)	Predicted Conversion
Cr ₂ O ₃ -CaO Powders (50% CaO)	315	2.13×10^{-7}	56.50
	675	1.47×10^{-15}	56.50
Cr ₂ O ₃ -Ca(OH) ₂ Pellets (50% CaO)	315	3.23×10^{-8}	81.92
	675	1.44×10^{-17}	81.92

The results from the model prediction therefore reveal that the reaction rates are initially high but decrease more rapidly with final conversions of 56.50 and 81.92 $\mu\text{g per g Cr}$ being attained well within the first year.

Thus, in terms of this model, the reaction proceeds under environmental conditions, initially at high reaction rates but as time progresses the reaction rate decreases exponentially and the conversions are limited. The theory of Fehlner and Mott may be applied to explain the higher initial oxidation rates (see Section 6.1). This is due to site exchange processes where adsorbed oxygen species (most likely oxygen atoms) react with surface Cr³⁺ centres or ions by a series of activated electron transfers between the two species. The activation mechanism for the electron transfer process is possibly the interaction of the Cr³⁺ centres on the oxide with the oxygen centre of CaO (alluded to Chapter five). With the passage of time, either the transport of Cr³⁺ centres to the oxygen centre of CaO via a solid state diffusion or the diffusion of atmospheric oxygen become restricted by diffusional resistances. This causes the reaction rates to decrease exponentially and only a limited conversion is achieved.

The reaction is therefore kinetically controlled. Nevertheless, some oxidation has been observed under environmental conditions within the first year and is therefore certainly one that could contribute to the generation of hexavalent chromium in ferrometallurgical slags. The implications for hexavalent chromium formation in such slags are reviewed in Section 6.6.

6.5.2. Cr₂O₃-Ca(OH)₂ Ball Systems

i) The Kinetic Model

The trends in reaction rate for this reaction are shown in Figure 6-3. The data series selected for analysis included the experimental series in which Cr₂O₃-Ca(OH)₂ balls were maintained at three different temperatures namely ambient temperature, fifty degrees and eighty degrees. The corresponding conversion-time plot is shown in Figure 4-9.

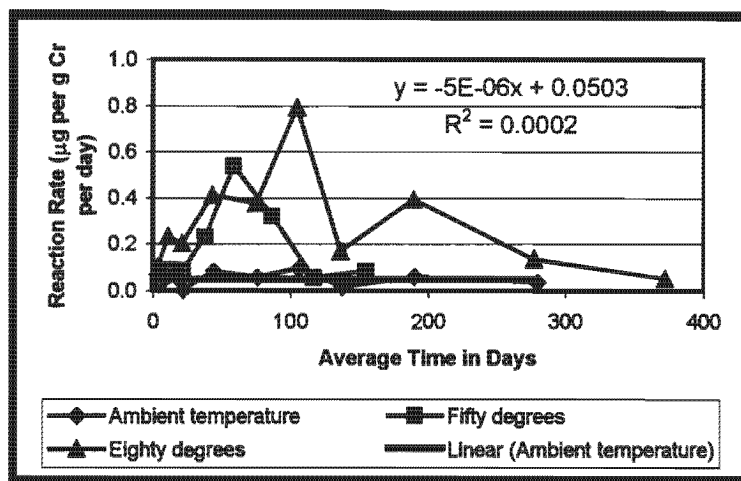


Figure 6-3: A rate versus time plot for the reaction:
 $\text{Cr}_2\text{O}_3 + 1.5\text{O}_2 + 2 \text{Ca}(\text{OH})_2 \rightarrow 2\text{CaCrO}_4 + 2\text{H}_2\text{O}$ in ball systems

In Chapter five, it was noted that the conversion-time graph for this reaction in the Cr_2O_3 - $\text{Ca}(\text{OH})_2$ ball systems (pore moisture evaporated) showed initial linear sections, which eventually tapered off. Ideally, it may be argued that the reaction should obey a linear rate law where the reaction rate is initially constant but decreases as phase boundary reactions set in causing some diffusional resistance. However, Figure 6-3 shows that while this may be true for the experiments conducted at ambient temperature, this does not necessarily apply to the experiments which were conducted at higher temperatures (80 and 50 degrees celcius) respectively. At such temperatures an initial increase in the reaction rate is noted. This is followed by a decline in the reaction rates after 59 days for the experiment at fifty degrees and after 105 days for the experiment at eighty degrees. This observation is unusual and can only be tentatively explained. A possible explanation may be due to a transition in the rate law at higher temperatures.

In Chapter five it was asserted that the reaction possibly obeys an Arrhenius rate law. However, this is unlikely to be a classical Arrhenius rate law as this rate law can only be applied to reactions that are free of diffusion (Smith,1981) and is based on initial rates only. This reaction like most classical solid-state and solid-gas reactions is a diffusion controlled reaction and it is seen quite clearly from Figure 6-3 that the reaction rate varies with time and eventually decreases. Hence, an Arrhenius rate law that is more representative of such reactions needs to be applied for example, one that takes into account diffusion coefficients and diffusivities of the reacting species and rates at specified times in the reaction.

Since a uniform kinetic model cannot be applied to the data sets from the experiments conducted at higher temperatures, it is only envisaged to attempt fitting kinetic models to the conversion-time data of the experiments conducted at ambient temperature. The trendline shown in Figure 6-3 shows that a linear rate law best describes the reaction in the ball systems up to 334 days (see Figure 4-9 for reference to the number of days). The correlation is poor due to scatter in the data points. Nevertheless, it is seen that the reaction proceeds at a constant rate of $0.0503 \mu\text{g per g Cr per day}$. The slope of -5×10^{-6} may be ignored as this is very close to zero. The rate equation for this

$$\frac{dx}{dt} = k \text{ where } x \text{ is the conversion and } k \text{ is the rate constant} \quad (6-10)$$

This equation can be integrated to equation (6-10) obtain an expression for the conversion:

$$x = kt \quad (6-11)$$

The fact that a linear rate law best describes this reaction indicates that a phase boundary reaction, in this case the diffusion of atmospheric oxygen at the solid-gas interface, is the rate-limiting step of the reaction. Some predictions for conversions can be made using equation (6-10) and (6-11) and using average times.

$$\begin{aligned} \text{Conversion after one year} &= 0.0503 \times 315 \\ &= 15.84 \mu\text{g per g Cr} \end{aligned}$$

This indicates that the reaction will continue to proceed at a constant rate thereby resulting in increasing conversions. However there is a time limitation on this i.e. this may only occur up to 334 days, after which the reaction rates will start to decrease and the conversions will then become limited. This is supported by the conversion-time plot shown in Chapter four (see Figure 4-9).

It is also interesting to note that the initial reaction rates in the balls are much slower in the balls than in the powders. This is possibly due to the slower diffusion of atmospheric oxygen in the balls as opposed to the powders. The outer surface of the balls possibly presents a thick impervious layer, which acts as a barrier to oxygen diffusion.

6.6. The Kinetics of the Oxidation of Cr₂O₃ in Ferrometallurgical Slags

6.6.1. Oxidation in Slag Powders

i) General Observations

Table 6-4 shows a summary of the kinetic models which best describe the oxidation of Cr₂O₃ in the slag powders that were exposed to air (based on the data in Figures 4-19 to 4-21).

Table 6-4: A Summary of the Kinetic Analysis conducted on the slag powders that were exposed to air

Type of Slag	Particle Size Class (μm)	Best Fit Kinetic Model	R ² Value	Value for k	Value for b
Old Mixed Slag	75-300	Exponential	0.9601	290.7	-0.0423
	300-1000	Exponential	0.9477	188.5	-0.091
New CLU Slag	<75	Power	0.8251	1494.7	-1.1325
		Exponential	0.7166	204.9	-0.0445
	75-300	Linear	0.9682	-0.8	61.339
	300-1000	Exponential	0.9067	91.6	-0.0428
New EAF Slag	<75	Exponential	0.8359	322.5	-0.0695
	75-300	Exponential	0.6899	149.4	-0.0461
	300-1000	Exponential	0.8132	64.6	-0.0387

It is firstly of interest to note in the most cases the oxidation of Cr_2O_3 has been described by exponential kinetic models. This is consistent with the observations made for the pure chemical powder and pellet systems.

However this excludes the CLU slag where the fine and middle fractions are best described by power and linear models respectively. The corresponding exponential fits for these size fractions also describe the oxidation reactions well especially in the middle fraction. It may therefore be argued that the fits obtained for the power and the linear models are possibly due to the scatter in the data and the oxidation reactions in the fine and the middle fractions are perhaps best described by exponential models. In this regard, it is also important to note that while the power model may make accurate predictions at longer periods of time, it also predicts that as time approaches zero, the reaction rates approach infinity. This is not a realistic prediction so the power model may not necessarily give the best description for oxidation in the fine fraction.

Another interesting observation (where exponential models are concerned) is the trends in the pre-exponential factors (k-values) which have been observed for each particle size class in type of slag. These seem to decrease with increasing particle sizes. This is as expected since the k-values represent the initial reaction rates. In Chapters four and five it was noted that the reaction rates decrease with increasing particle size due to the larger particle sizes resulting in smaller surface areas, which limit the diffusion of atmospheric oxygen. Quantitative evidence to support this has now been presented. An exception is again noted in the CLU where there isn't much of a difference between the k-values of the middle and coarse fractions, but this is due to the similarity in the particle size distributions (see appendix B3 for the corresponding Malvern particle size distribution data).

Upon further examination of Table 6-4, it is important to note that no definite trends in the exponential decay factor (b-values) can be deduced. This excludes the EAF slag where a decrease in the exponential decay factor with increasing particle size is made (taking absolute values into account). Such an observation suggests that the reaction rates will decrease to a greater extent with finer particle sizes and is quantitatively supported by the long-term predictions for reaction rates shown in appendix G4. It therefore seems that where fine particle sizes are concerned, the reaction rates are initially high due to greater oxygen diffusion, causing the rate-limiting steps to come into effect much quicker and resulting in a greater decline in reaction rates. However, this is based on an observation for one type of slag and therefore cannot be conclusively stated.

Since the coarse fractions underwent the lowest rates of oxidation, these are presented in more detail in order to predict the implications in the long-term when the minimum extents of oxidation occur.

ii) Graphical Fits of the Exponential Models

Figures 6-4 to 6-6 show the graphical fits of the exponential models for the coarse fraction of each type of slag.

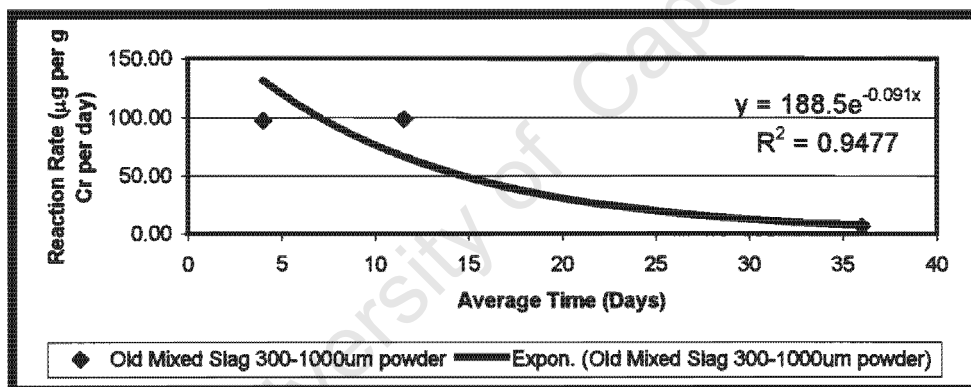


Figure 6-4: The Relationship between Reaction Rate and Time in Old Mixed Slag Powders exposed to air (particle size class: 300-1000µm)

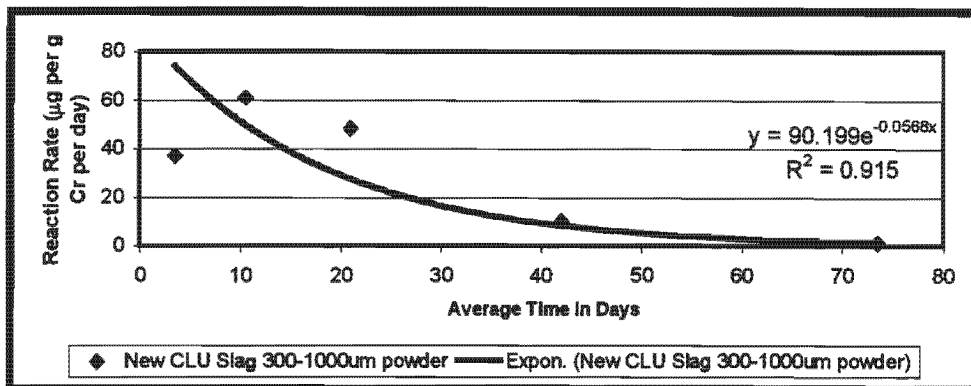


Figure 6-5: The Relationship between Reaction Rate and Time in New CLU Slag Powders Exposed to Air (Particle size class: 300 -1000µm)

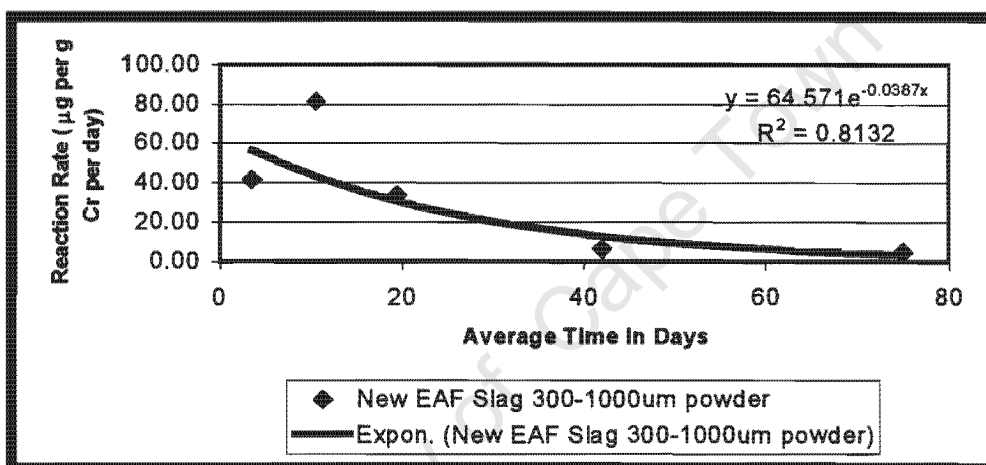


Figure 6-6: The Relationship between Reaction Rate and Time in New EAF Slag Powders exposed to air (Particle size class: 300-1000µm)

In all of the above cases it is evident that initially the graphical fits are not very good but improve as time progresses. Thus, the models are expected to give good predictions for reaction rates and conversions over extended periods of time but some under-predictions and over-predictions are expected over shorter periods of times. To verify this assertion the numerical fits of the models have been tested and are reported in Section iii).

iii) Numerical Tests on the Models

The results from the numerical tests on the models are shown in Table 6-5.

Table 6-5: The Results from a Numerical Test Conducted on the Exponential Models for Slag Powders Exposed to Air (Particle Size Class: 300 -1000 μ m)

Type of Slag	Average Time in Days	Observed Reaction Rates (μ g per g Cr)	Predicted Reaction Rates (μ g per g Cr per day)	Observed Conversions (μ g per g Cr)	Predicted Conversions (μ g per g Cr)
Old Mixed Slag	0			936	936
	4	96.84	130.99	1711	1568
	12	98.29	66.19	2399	2280
	36	6.50	7.12	2672	2929
New CLU Slag	0			222	222
	4	36.87	73.94	480	508
	11	60.76	49.68	905	935
	21	48.23	27.36	1581	1328
	42	10.13	8.30	1864	1664
New EAF Slag	0			320	320
	4	41.45	56.39	610	531
	11	81.27	43.01	1179	877
	20	33.43	30.36	1547	1204
	42	6.04	12.71	1752	1660
	75	4.84	3.54	1907	1897

From the data shown in Table 6-5 it is evident that there are no perfect matches between the predicted and observed values for reaction rates and conversions. Firstly, it is noted that for reaction rates, there is initially some significant over-predictions and under-predictions. As time progresses, the difference between the predicted and observed values becomes less pronounced. The conversions are generally well predicted where the maximum difference between the observed and the predicted conversions is about 200 to 300 units. This is acceptable when experimental error or rather scatter in the data points is taken into account. However, it must be noted that the model predictions for conversion have been adjusted in accordance with the conversions which have been experimentally observed at time = 0. Such adjustments also need to be made when making long-term predictions for conversions.

iv) Model Predictions for Oxidation in the Long – Term

As before the relevant exponential equations and exponential parameters may be used to calculate the reaction rates and conversions at specified periods of time. The calculations that have been conducted in order to predict the trends in conversion over a two-year period.

Table 6-6: The Predicted Reaction Rates and Conversions for Slag Powders over a two – year period (particle size class: 300-1000µm)

Slag	Average Time in Days	Predicted Reaction Rate (µg per g Cr)	Predicted Conversion (µg per g Cr)
Old Mixed	315	6.70×10^{-11}	3007
	675	3.97×10^{-25}	3007
New CLU	315	1.53×10^{-6}	1809
	675	2.02×10^{-15}	1810
New EAF	315	3.28×10^{-4}	1989
	675	2.92×10^{-10}	1989

The above data show that as in the case of the pure chemicals the reaction rates will continue to decrease rapidly resulting in maximum conversions of 3007, 1810 and 1989 µg per g Cr in the old, CLU and EAF slags respectively. These results therefore show clearly that the oxidation reactions will continue at decreasing reaction rates with the ultimate conversion of trivalent chromium to hexavalent chromium being attained well within the first year.

The oxidation rates are initially high but eventually decrease asymptotically due to a rate-limiting step such the slow diffusion of atmospheric oxygen setting in. So, the oxidation reactions are controlled by a rate-limiting step.

6.6.2.Oxidation in Slag Balls (with the pore moisture evaporated)

i) General Observations

Table 6-7 shows a summary of the kinetic models which best describe the oxidation reactions in the slag balls (with the pore moisture evaporated), which were exposed to ambient conditions.

Table 6-7: A Summary of the Results from a Kinetic Analysis conducted on the Slag Balls (with the pore moisture evaporated)

Type of Slag	Particle size Class (μm)	Best Fit Kinetic Model	R ² value	K value	b value
Old mixed	<75	Logarithmic	0.824	-48.1	239.19
	75-300	Parabolic	0.841	549.3	-
	300-1000	Parabolic	0.795	191.2	-
New CLU	<75	Parabolic	0.690	208.2	-
	75-300	Exponential	0.853	31.9	-0.0286
	300-1000	Exponential	0.794	31.4	-0.0307
New EAF	<75	Parabolic	0.746	172.0	-
	75-300	Exponential	0.882	58.3	-0.0256
	300-1000	Exponential	0.986	56.4	-0.0453

The first noteworthy observation from this table is that with the exception of the fine fraction, the oxidation reactions in the old mixed slag balls are described mostly by a parabolic kinetic model. Here there is a linear relationship between reaction rates and the inverse of the square root of time. These are in fact the only slag balls (with the pore moisture evaporated) which did not disintegrate into a powder. The parabolic model may be explained in terms of the outer surface of the slag balls acting as an impervious layer, which limits the diffusion of atmospheric oxygen.

It is also of interest to note that despite the fact that all of the CLU and the EAF balls disintegrated into powders, the oxidation reactions are still described by parabolic models in some cases. This is contrary to what is expected as the oxidation reactions in the slag powders were in most cases described by an exponential rate model. However, it was noted that agglomerates remained after the balls disintegrated. Thus, the parabolic models that have been observed are possibly due to a larger quantity of agglomerates in the respective size fractions which presented a thick layer, which in turn restricts oxygen diffusion. The size fractions for which exponential models have been observed did indeed contain no agglomerates but completely disintegrated into a fine powder.

Since different models have been observed, it is difficult to make direct comparisons of the k-values. It may be stated that in general where uniform kinetic models have been observed there is a decrease in the k-value with an increase in particle size class. This again provides quantitative evidence that oxidation rates decrease with an increase in particle size. Surprisingly, there isn't much of a difference between the k-values for the middle and coarse fractions of the EAF slag where exponential models have been observed. This observation is contrary to what has been observed for the EAF slag powders. The same is noted for the CLU slag but in this case, the particle sizes are quite similar (see Malvern particle size distribution results in appendix B3) so the similarity of the k-values (reaction rate at time = 0) is understood.

In this respect it is also important to note that both the middle and the coarse fractions of the EAF and the CLU slags disintegrated into fine powders and the oxidation reactions are described by exponential models in both cases. However, the k-values for the balls, which disintegrated into powders are still lower than those of the slag powders exposed to air. This indicates that oxygen access has still been restricted, possibly due to the balls disintegrating into powders in stages with intermediary agglomerates forming.

It is also noted that where exponential models have been observed, the absolute values of the exponential decay factors increase with increasing particle size. This is contrary to the observation made for the EAF slag powders in section 6.6.2 i).

The approach to reporting the results of the kinetic analysis in more detail has been one where the implications for “minimum oxidation” scenario have been reported. The kinetic observations for the coarse fractions of each type of slag are therefore reported in more detail in the following sections.

ii) Graphical Fits of the Models

Figures 6-7 to 6-9 show the graphical fits of the models for the coarse fractions of each type of slag.

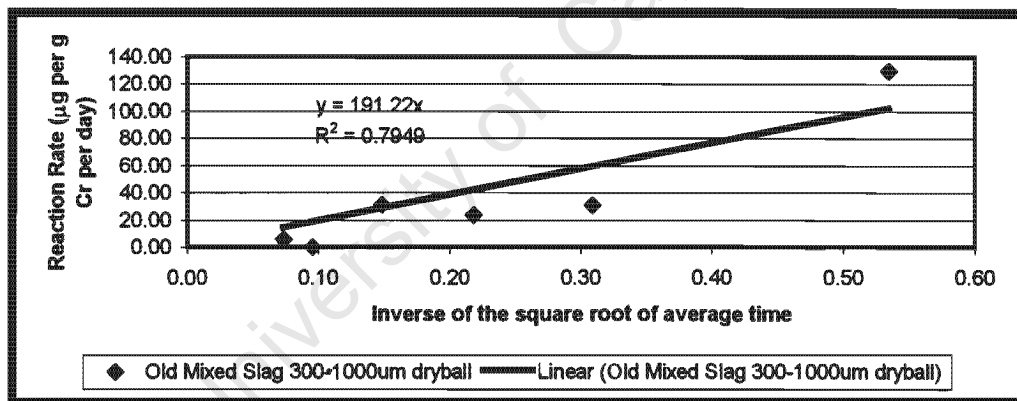


Figure 6-7: The Relationship between Rate and Time in the Old Mixed Slag Balls with the pore moisture evaporated (particle size class: 300-1000µm)

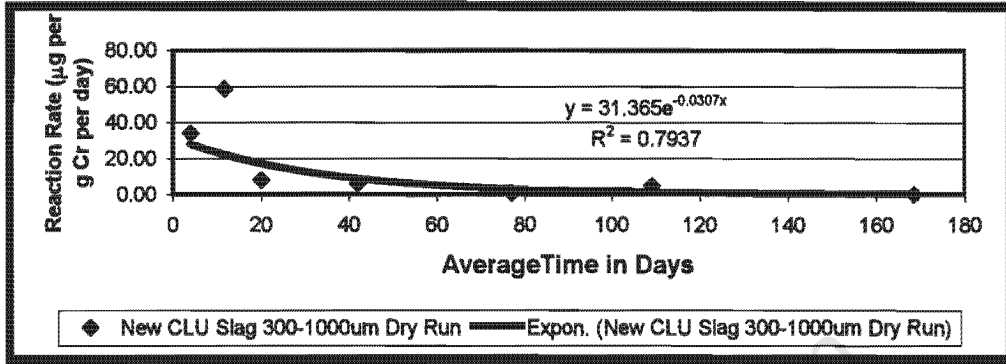


Figure 6-8: The Relationship between Reaction Rate and time in New CLU Slag Balls (pore moisture evaporated) which disintegrated after two weeks (particle size class: 300 - 1000µm)

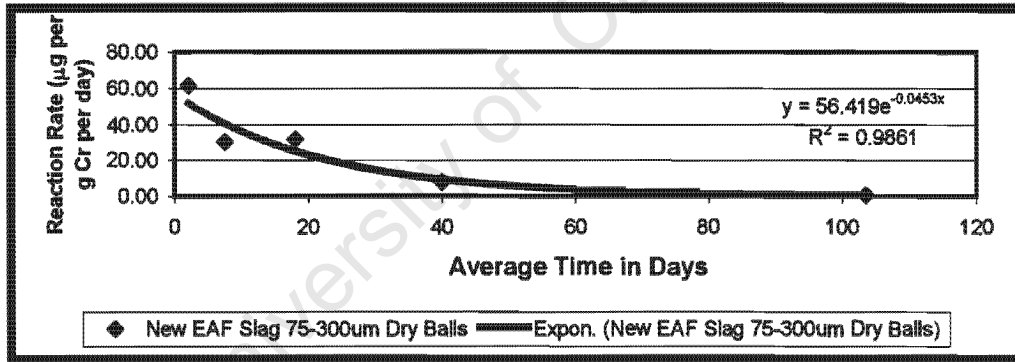


Figure 6-9: The Relationship between Reaction rate and Time in New EAF Slag Balls (pore moisture evaporated) which disintegrated after two weeks (particle size class: 300-1000µm)

As in the case of the slag powders, the graphical fits show some under-predictions and over-predictions at shorter periods of time but the graphical fits improve as time progresses. This also applies to the parabolic model but in this case it must be noted that the intercept of the trendline has been set to zero in order to avoid obtaining an equation that predicts negative reaction rates at longer periods of time.

iii) The Numerical Tests for the Models

Before tests on the numerical fits of the model are conducted, it must be noted that for the parabolic model, the rate equation is expressed as:-

$$\frac{dx}{dt} = \frac{k}{\sqrt{t}} \quad (6-12)$$

where x is the conversion and k is the reaction rate at time = 0.

This equation can be integrated to equation (6-13) in order to obtain an expression for conversion:-

$$x = 2k\sqrt{t} \quad (6-13)$$

Equations (6-12) and (6-13) have been used to calculate the predicted reaction rates and conversions for the parabolic model.

Table 6-8: The Numerical Tests on the Kinetic Models for each type of Slag (particle size class: 300 -1000 μ m)

Type of Slag	Average time in Days	Observed Reaction Rates (μ g per g Cr per day)	Predicted Reaction Rates (μ g per g Cr per day)	Observed Conversions (μ g per g Cr)	Predicted Conversions (μ g per g Cr)
Old Mixed Slag	0			263	263
	4	129.6	106.5	1171	1008
	11	30.6	61.5	1384	1554
	21	23.7	43.5	1717	2089
	46	31.2	29.5	2808	2951
	110	0.2	19.0	2825	4432
	186	5.6	14.6	3156	5690
New CLU Slag	0			149	149
	4	34.0	27.7	421	267
	12	58.4	22.0	830	453
	20	7.9	17.0	908	618
	42	6.2	8.6	1120	889
	77	0.8	3.0	1151	1075
	109	4.6	1.1	1279	1135
	169	0.1	0.2	1292	1165
New EAF Slag	0			167	167
	2	61.2	51.5	412	275
	8	30.1	40.2	623	526
	18	31.7	25.0	1067	861
	40	7.8	9.2	1302	1209
	104	0.5	0.5	1354	1401

Significant over-predictions are noted both for the reaction rates and conversions in parabolic model, for the old slag, especially at larger times. This results from setting the y-intercept of the model to zero in order to avoid negative predictions for conversions at larger times. It must therefore be noted that over-predicted conversions can be expected when making long-term predictions.

As in the case of the slag powders, the exponential models give some over-predictions and under-predictions for reaction rates and conversions initially but as time progresses there are smaller discrepancies between the predicted values and the observed values. The predicted conversions have again been adjusted according to the baseline conversion that was initially observed and this must be borne in mind when making long-term predictions.

iv) Model Predictions for Oxidation in the Long-Term

Table 6-9 shows the predictions for the trends in conversion and reaction rates over a two - year period.

Table 6-9: The Predicted Reaction Rates and Conversions for Slag Balls with the pore moisture evaporated (particle size class: 300-1000µm)

Slag	Time in Days	Predicted Reaction Rate (µg per g Cr)	Predicted Conversion (µg per g Cr)
Old Mixed	315	11.22	7335
	675	7.67	10615
New CLU	315	1.98×10^{-3}	1171
	675	3.14×10^{-8}	1171
New EAF	315	3.58×10^{-5}	1412
	675	2.96×10^{-12}	1412

Ideally, the reaction rates and conversions reported in Table 6-9 should be similar to those reported in Table 6-6 since all the slags balls disintegrated into a powder whilst the pore moisture evaporated. Instead complex trends in reaction rates and conversions have been observed. This may be due to inhomogeneity in the slag samples used for each experiment and the possibility that significant agglomerates may have remained after the some of the slag balls disintegrated.

6.7. The Long-term Implications for Slags Disposed to Landfill

The detailed kinetic analyses, which have been presented for the slags, have shown that mostly exponential and parabolic models describe the rates of oxidation in the slags. Although some discrepancies in the numerical fits to the models have been noted, the models have predicted that the oxidation rates will decrease as time progresses due to

some rate-limiting step, mainly the diffusion of atmospheric oxygen setting in. The model predictions have shown that in all cases the ultimate conversions are achieved well within the first year.

Such observations indicate that slags disposed to landfill will undergo oxidation even when the oxidation rates are reduced by larger particle sizes. The reaction rates will decrease as time progresses due to some diffusional resistances and most of the oxidation occurs within the first year with the ultimate conversion being attained within this period. Thus, the oxidation of Cr_2O_3 in the slags manifests itself over a relatively short period in the slags.

Further to the above observations it is also of interest to compare the kinetic parameters that have been observed for both the pure chemicals and the slags. Upon examining the values for the initial reaction rates and the exponential decay values in Figure 6-2 and Table 6-4 it is noted that the initial reaction rates (k-values) for the pure chemical powder systems are 2-3 orders of magnitude lower than those of the powder systems. This is consistent with the observations made in Chapter four where it was noted that the reaction rates for the pure chemical systems are slower.

However, the exponential decay factors are very similar which suggests that the extent of decay is similar in both cases. In other words, the rate-limiting steps of the reactions control the rates of the reaction to the same extent in both systems.

6.8. Conclusion

This chapter has presented the findings of a kinetic analysis on the oxidation of Cr_2O_3 in the pure chemicals and in ferrometallurgical slags. It has been observed that mostly exponential models have described the powder and pellet systems. An exception was noted for some of the slag balls (pore moisture evaporated), which disintegrated into powders. Here parabolic models have been observed. This is possibly due to agglomerates, which remained after disintegration.

Parabolic models described the oxidation rates in the old mixed slag balls, which remained intact. This has been accounted in terms of the surface of the ball presenting a barrier to oxygen diffusion. In the pure chemicals, however, oxidation in the Cr_2O_3 – $\text{Ca}(\text{OH})_2$ balls showed a complex kinetic behaviour at higher temperatures but was described by a linear model at ambient temperature. However, this linear model is not expected to indefinitely describe the oxidation rates as at some point in time the reaction rates are expected to decrease when a rate-limiting step of the reaction eg. the diffusion of atmospheric oxygen sets in.

The exponential models observed have revealed that the reaction rates will decrease rapidly within the first year and with maximum conversions of around 1000 to 3000 μg per g Cr being attained.

The parabolic model also predicts decreasing reaction rates but gives significant over-predictions for conversions. This was due to setting the intercept to zero so that negative predictions for reaction rates could be avoided.

Overall, it may be stated that oxidation will occur in ferrometallurgical slag disposed to landfill. This will continue at decreasing rates resulting in a maximum conversion being attained asymptotically. The exponential models have predicted that the ultimate conversions are achieved well within the first year. Such predictions indicate that the oxidation reactions will only present an environmental problem with the first year of disposal.

University of Cape Town

CHAPTER SEVEN

CONCLUSIONS

In this chapter, the key objectives of the research, which were presented in Chapter one are reviewed. The extent to which these objectives have been fulfilled is discussed. The hypotheses presented in Chapter three are reviewed and the validation of these hypotheses is discussed. The chapter concludes with a discussion on the shortcomings of the research and recommendations for future work on this topic.

7.1. The Key Objectives of the Research

As indicated in Chapter one, this study has aimed at achieving the following objectives:

- Identification of key parameters which are likely to influence the oxidation of trivalent chromium oxide;
- Examining the extent to which the oxidation of chromium oxide occurs in the slags and how this relates to their composition and mineralogy;
- Identification of the key reactions that contribute to the oxidation of trivalent chromium in ferrometallurgical slags;
- Use of an understanding of the mechanisms of such reactions to devise preventative measures, which ultimately aim at minimising the re-oxidation of trivalent chromium in slag deposits; and
- Collection and interpretation of data, which will be used to quantify the reaction rates in order to assess the long-term environmental implications.

The extent to which these objectives have been fulfilled is discussed below.

7.1.1. The Key Parameters Influencing the Rate of Oxidation of Cr_2O_3

Three key parameters, which influence the rate of oxidation of Cr_2O_3 have been identified. These are the proximity to CaO and $\text{Ca}(\text{OH})_2$, temperature and, where Cr_2O_3 is embedded in solid solution, particle size.

A fourth parameter, namely pore moisture has also been identified but the influence of this parameter may have been falsely represented by the experimental data. Some uncertainty as to whether some of the hexavalent chromium that formed leached out into the pore moisture and diffused onto the cotton wool (see Chapter three for a description of the experimental set-up) has been expressed in Chapter five. The influence of pore moisture is therefore unresolved.

As indicated in Chapter five, all other key parameters that influence the rate of oxidation of Cr_2O_3 resulted in enhanced oxidation rates. Intimate contact between CaO or $\text{Ca}(\text{OH})_2$ and Cr_2O_3 enhances oxidation rates by bringing the oxygen centres on the calcium

compounds in closer proximity to the Cr^{3+} centres of Cr_2O_3 . Higher temperatures promote the solid-state diffusion of the solid reactants thereby increasing the oxidation rates. Decreasing particles sizes in the slags have also resulted in higher oxidation rates by providing a larger surface area for the diffusion of atmospheric oxygen. The influence of particle size on the rates of oxidation in slags has been quantitatively proven in Chapter six where higher initial oxidation rates were observed for finer particle size fractions.

7.1.2. The Mechanism of the Oxidation of Cr_2O_3

Although the experimental study has been insufficient to elucidate a detailed mechanism for the oxidation of Cr_2O_3 , sufficient evidence has been gathered to propose some key steps in the oxidation reactions. These have been discussed in Chapter five and include:

- A solid state diffusion of the solid reactants, possibly the diffusion of Cr^{3+} centres or ions from the oxide towards the oxygen centres on CaO and $\text{Ca}(\text{OH})_2$
- The interaction of Cr^{3+} centres on the trivalent oxide with the oxygen centre of CaC or $\text{Ca}(\text{OH})_2$ which somehow promotes the reactivity of the oxide and its amenability to oxidation
- The diffusion of atmospheric oxygen and electron transfer

Such steps in the reaction have been supported by experimental evidence that has shown that oxidation is enhanced with a higher CaO and $\text{Ca}(\text{OH})_2$ content. This proved that the oxidation reactions are driven by the affinity of Cr^{3+} for oxygen centres. It has also been proven that the atmospheric oxygen is the electron acceptor since no appreciable oxidation was observed under nitrogen.

This understanding of the mechanism has been used to propose some preventative measures, which may be implemented prior to waste disposal. These have also been discussed in Chapter five.

Firstly, a reduction in the CaO content of the slag is recommended, as it was experimentally shown that higher CaO and $\text{Ca}(\text{OH})_2$ contents promote oxidation. Experimental evidence which shows that oxidation is enhanced when Cr_2O_3 and CaO are in intimate contact has also been presented in Chapter four (see Figure 4-5), so it has been proposed that intimate contact between these solid reactants must be avoided. If possible, Cr_2O_3 and CaO should not exist in the same mineralogical phase. In this regard, it has been recommended that the spinel content or rather the MgO content of the slags should be increased relative to the CaO content.

It has been proposed that the slags should be disposed of in the coarse particle form in order to minimise oxidation. Experimental evidence that showed that oxidation rates are enhanced with finer particle size distributions has been presented in Chapter four (see Figures 4-10 to 4-21). Other preventative measures such as introducing competing ligands for the Cr^{3+} centres or ions and competing cations for the oxygen centres on CaO and $\text{Ca}(\text{OH})_2$ have also been proposed. This follows on from a knowledge of the

literature where it was noted that in the presence of competing cations, the adsorption of Cr^{3+} onto surfaces that contain oxygen centres is reduced (see Chapter two). However, this is based on the aqueous chemistry of Cr(III), so an aqueous phase must be present when testing this preventative measure eg. the competing cations and ligands can be added in preferably an alkali solution in which Cr_2O_3 is soluble. This will ensure that Cr^{3+} ions are in solution for the aqueous chemistry of Cr^{3+} to come into effect.

7.1.3. The Oxidation of Cr_2O_3 in Ferrometallurgical Slags

Oxidation has been observed in all types of slags that have been studied where kinetic models have predicted maximum conversions of typically 1000 to 10000 μg per g Cr being attained (see Chapter four and Appendix A4). Chromium and calcium have been identified as elemental components of the slags (see Table 4-3 in Chapter four). The calcium contents of the slags are in excess of both the magnesium and the chromium contents. Furthermore, a mineralogical analysis of the slags by an external source (Nel and Mostert, 1999) has also revealed that most of the Cr_2O_3 exists in spinel phases where it is in intimate contact with MgO. However, a sizeable fraction of the oxide is found in silicate phases where it is in intimate contact with CaO. The studies on pure chemical systems have revealed that the oxidation of Cr_2O_3 in the presence of CaO and $\text{Ca}(\text{OH})_2$ occur under environmental conditions and the rates of these reactions increase with increasing quantities of these compounds and when Cr_2O_3 and CaO are in intimate contact.

It has therefore been concluded that the oxidation that has been observed in the slags is due mainly to the oxidation of Cr_2O_3 , which is in intimate contact with CaO in the silicate phases. The limited conversions that have been observed in the slags have been accounted for in terms of most of the Cr_2O_3 being locked away in spinel phases where it is in intimate contact with MgO and by the limited intimate contact of the solid phase reactants. However, it has also been acknowledged that the limited conversions and the decrease in the reaction rates could be due a rate-limiting step in the reaction such as the diffusion of atmospheric oxygen (see Chapters five and six for detailed discussions).

7.1.4. The Key Reactions Contributing to the Oxidation of Cr_2O_3 in Ferrometallurgical Slags

As outlined in Chapter three two reactions that result in the oxidation of Cr_2O_3 were investigated in this study. These were the oxidation of Cr_2O_3 in the presence of CaO and $\text{Ca}(\text{OH})_2$. The information supplied on the mineralogy of the slags has indicated that some Cr_2O_3 is in intimate contact with CaO. An elemental analysis has revealed that calcium and chromium are key elements in the slags and there is evidence from the literature (Korousic et.al., 2000) which indicates that elemental chromium is oxidised to Cr_2O_3 during slag formation, whilst CaO is added to the slags to improve slag viscosity.

Oxidation has also been experimentally observed in slag balls (see figures 4-10 to 4-18 in Chapter four). Since water was added to the supplied slag powders to prepare the balls

(see experimental procedure in Chapter three), it was concluded CaO was converted to Ca(OH)₂ so the oxidation that has been observed in the slag balls has been the oxidation of Cr₂O₃ in the presence of Ca(OH)₂. The slag powders that were exposed to ambient moisture also showed some uptake of atmospheric moisture (see Tables A62 to A64 in appendix A4). So, the possibility that atmospheric moisture converts CaO into Ca(OH)₂ thereby resulting in the oxidation of Cr₂O₃ in the presence of Ca(OH)₂ cannot be discounted.

Thus, it has been concluded that the key reactions contributing to the oxidation of Cr₂O₃ in the slags are the oxidation of Cr₂O₃ in the presence of CaO and Ca(OH)₂ respectively.

7.1.5 The Quantification of Reaction Rates

The conversion–time data obtained experimentally and presented in Chapter four has been used to quantify reaction rates and to identify kinetic models which best describe the oxidation reactions in the slags and in the pure chemical systems. This kinetic study was presented in Chapter six. Exponential models have been observed for the powder systems and pellet systems in the pure chemical studies. These models have predicted that the rates of oxidation become insignificant after the first year and the oxidation of Cr₂O₃ proceeds to a limited extent. The oxidation of Cr₂O₃ in Cr₂O₃–Ca(OH)₂ balls has been described by a linear rate law at ambient temperature (up to 334 days only – see Figure 4-9 in Chapter four) but a complex kinetic behaviour was noted at higher temperatures. It was also noted that although the oxidation in the presence of Ca(OH)₂ is temperature dependent, a classical Arrhenius kinetic model cannot describe such systems as the reaction is diffusion–controlled and the reaction rates vary with time.

Mainly exponential and parabolic models have been observed for the slag systems. The exponential models have been descriptive of the fine powder systems while the parabolic models have been descriptive of slag balls, which have remained intact and slags balls which did not completely disintegrate into powders but contained a fair amount of agglomerates. The observation of the parabolic model was attributed to the surface of the balls and the agglomerates presenting impervious layers for oxygen diffusion.

The exponential models have predicted that the reaction rates will decrease rapidly as time progresses resulting in the ultimate conversion being attained within the first year. The oxidation of Cr₂O₃ can therefore be viewed as being of limited extent, and to manifest itself essentially within a fairly short time span. However, the possibility that continuous leaching results in the removal of product layers thereby presenting an opportunity for continuous oxidation at slow reaction rates must not be overlooked.

7.2. Validation of Hypotheses

7.2.1. The Oxidation of Cr_2O_3 under Environmental Conditions

All the experimental results presented in Chapter four have showed quite clearly that the oxidation of Cr_2O_3 occurs under environmental conditions. This is true for both pure chemical systems where oxidation in the presence of CaO and $\text{Ca}(\text{OH})_2$ has been observed and for ferrometallurgical slags. Exponential models have predicted maximum conversions of typically 30-80 μg per g Cr for the pure chemicals and 1000 to 3000 μg per g Cr for slags. The hypothesis, which states that the oxidation of Cr_2O_3 can occur under environmental conditions in pure chemicals and slags, has thus been validated.

It was also noted that in both the pure chemicals and the slag systems, oxidation occurred faster in the powder or pellet than in the ball systems. This was attributed to limited oxygen access in the balls (see Chapters four and six for discussions).

7.2.2. The Reactions Leading to the Oxidation of Cr_2O_3 in Ferrometallurgical Slags

As discussed, in Sections 7.1.3 and 7.1.4, chromium and calcium have been identified as elemental constituents of the slags and information on the mineralogy of the slags showed that some Cr_2O_3 is in intimate contact with CaO in silicate phases. The oxidation of Cr_2O_3 has also been observed in slag balls, which were prepared by adding distilled water and some uptake of atmospheric moisture by the slag powders was noted. The oxidation of Cr_2O_3 in the presence of CaO and $\text{Ca}(\text{OH})_2$ was also observed in the pure chemical studies. Such observations have served as experimental evidence in support of the second hypothesis presented in Chapter three.

7.3. The Shortcomings of the Research

Although the objectives of the research have been fulfilled and the hypotheses have been validated, some shortcomings have been encountered in the research. Firstly, as stated earlier, the influence of pore moisture on the rates of oxidation is somewhat unresolved. This is due to the uncertainty as to whether the $\text{Cr}(\text{VI})$ which formed leached out and diffused onto the cotton wool that was used to maintain the pore moisture content of the Cr_2O_3 - $\text{Ca}(\text{OH})_2$ balls.

Secondly, the complex rate-time data that has been obtained for the Cr_2O_3 - $\text{Ca}(\text{OH})_2$ ball experiments, particularly for those at higher temperatures is not understood. Lastly, the parabolic model that was observed for the old mixed slag ball (with pore moisture evaporated) gave over-predictions for conversions, which was due to setting the y-intercept to zero.

The above phenomena could be investigated further. Recommendations for future work on these and other aspects of the research are therefore discussed in Section 7.4.

7.4. Recommendations for Future Work

7.4.1. The Influence of Pore Moisture

In order to verify that the reactions rates observed for the oxidation in $\text{Cr}_2\text{O}_3\text{-Ca(OH)}_2$ balls in which the pore moisture was maintained may have been misrepresented due to a loss of some the Cr(VI) that formed, experiments in which the $\text{Cr}_2\text{O}_3 - \text{Ca(OH)}_2$ balls are allowed to retain their excess pore moisture in another manner must be devised. For example, the balls can be moistened with distilled water on a regular basis. The oxidation rates observed in such experiments can then be compared to those observed for experiments in which the balls were maintained in close contact with moist cotton wool. Similar experiments should be devised for ferrometallurgical slags. This may thus help to resolve the issue of the influence of pore moisture on the oxidation rates.

7.4.2. Kinetic Models for $\text{Cr}_2\text{O}_3 - \text{Ca(OH)}_2$ Balls and Ferrometallurgical Slags

As discussed earlier, the complex rate-time data that have been obtained for the $\text{Cr}_2\text{O}_3 - \text{Ca(OH)}_2$ balls is not understood. The difficulties encountered in modelling such systems is possibly due to the complex three-dimensional geometry of the balls and perhaps an alternate and more rigorous approach to modelling such systems needs to be attempted.

7.4.3. Comparisons between the Relative Rates of Oxidation in Pure Chemicals and in Slags

As noted in Chapter four, the relative rates of oxidation in the pure chemicals and in the slag systems are not directly comparable because of the difference in $\text{Cr}_2\text{O}_3:\text{CaO}$ ratios. Thus, experiments on pure chemical systems in which the $\text{Cr}_2\text{O}_3:\text{CaO}$ ratios are similar to those in slags must be conducted for a more meaningful comparison between the relative rates of oxidation. An example of a suitable quantities of Cr_2O_3 and CaO which can be added to such systems include 2% Cr_2O_3 and 40% CaO (w/w).

7.5. Recommendations for Future Industrial Practices

7.5.1. Reduction in CaO content and Increase in MgO content

Since experimental evidence which showed that increasing CaO and $\text{Ca}(\text{OH})_2$ contents enhance the oxidation of Cr_2O_3 has been presented (see Chapter four), it was noted in Chapter five that the CaO content of the slags should be reduced prior to disposal. There is evidence from the literature, which suggests that Cr_2O_3 is not reactive when in contact with MgO (see Chapter two). Thus, it has been proposed that the MgO content of the slags should be increased prior to disposal.

Such preventative measures should however be tested in a laboratory prior to being implemented. The following experiments are therefore proposed in order to test such preventative measures:

- Experiments where balls and powder-mixes consisting of varying proportions of Cr_2O_3 , CaO and MgO are exposed to oxidising conditions at ambient temperature. This should ideally comprise systems where the MgO content is increased relative to the CaO content. Examples of the relative proportions or ratios of Cr_2O_3 , CaO and MgO include, 2% Cr_2O_3 , 4% CaO and 40% MgO. This is in accordance with the ratios in which these can be present in slag samples but might need some modifications depending on the actual slag samples being tested
- This should also be accompanied by parallel experiments on the slag samples where the CaO content has been reduced relative to the MgO content

It was also noted that intimate contact between Cr_2O_3 and CaO enhances oxidation. Thus, it was proposed in Chapter five that Cr_2O_3 and CaO should not exist in the same mineralogical phase. Experimental studies on slags where the mineralogy has been altered such that Cr_2O_3 and CaO are not found in the same mineralogical phase and where all of the Cr_2O_3 is found spinel phases should also be conducted. Parallel pure chemical experiments on Cr_2O_3 -MgO pellets may be conducted to test such a preventative measure.

7.5.2. Competing Cations for the Oxygen Centres of CaO and $\text{Ca}(\text{OH})_2$

As discussed earlier (see sections 5.5. and 7.1.) cations which may outcompete Cr^{3+} for the oxygen centres of CaO and $\text{Ca}(\text{OH})_2$ can be added to slags in an aqueous form. However, such competing cations are unknown. More research on cations which are likely to out compete Cr^{3+} for the oxygen centres of CaO and $\text{Ca}(\text{OH})_2$ needs to be initiated and tested in the laboratory, by firstly, identifying such cations and then adding these cations to Cr_2O_3 -CaO or $\text{Ca}(\text{OH})_2$ systems in an aqueous state (or rather in alkali solution) and examining the impact on oxidation.

7.5.3. Competing Ligands for Cr³⁺

In Chapter five, it was suggested that ligands which are likely to form complexes with Cr³⁺ should be introduced into a slag matrix to prevent Cr³⁺ from interacting with the oxygen centres of CaO or Ca(OH)₂. A good example of such a ligand is citrate, which is known to reduce the reactivity of Cr³⁺ upon complex formation. The reactivity of Cr³⁺ is reduced even when released from a citrate complex (see Chapter two).

To verify that citrate can reduce the reactivity of Cr³⁺ in slags, experiments in which citrate is added to ferrometallurgical slags in an aqueous form (preferably an alkaline solution) and also to pure Cr₂O₃-CaO or Ca(OH)₂ systems must be conducted and the impact on oxidation must be examined.

7.5.4. Oxidation in Other Cr(III) – Bearing Wastes

Sufficient experimental evidence has been gathered to prove that the oxidation of Cr(III) does indeed occur in ferrometallurgical slags. The possibility that this can apply to other types of Cr(III) bearing wastes cannot be discounted. Examples of other Cr(III) bearing wastes in which the oxidation of trivalent chromium can occur are neutralisation sludges from the metal-finishing industry which are known to contain Cr(OH)₃.

As discussed in Chapter two, reactions which lead to the oxidation of hydroxy-forms of Cr(III) are known to be thermodynamically feasible. This includes the oxidation of the solid hydroxide (Cr(OH)₃) which can undergo a direct oxidation by oxygen (see Chapter two for reactions). It is therefore of interest to investigate the possibility of such reactions occurring both in pure chemical systems and in actual neutralisation sludges. This should be conducted under moist conditions where Cr(OH)₃ is exposed to ambient moisture and it can thus be assessed whether the solid hydroxide undergoes conversion to the simple aqueous hydroxy forms which subsequently undergo oxidation upon exposure to atmospheric oxygen. Parallel experiments in which the hydroxide is stored in a desiccator must also be conducted in order to verify that the solid hydroxide can undergo a direct oxidation by oxygen.

Since lime (Ca(OH)₂) is also added to the sludges as solidifying agent (Jacobs, 1992), the possibility that this plays an important role in the oxidation by supplying oxygen centres for Cr(III) must also be investigated. Such studies should then be used to gain mechanistic insights for the oxidation reactions so that preventative measures can be proposed and to identify suitable kinetic models, which describe the oxidation reactions so that predictions for rates and conversions can be made.

REFERENCES

- Adams R.M. (1990), "Occupational Skin Diseases", 2nd. Ed. Philadelphia, W.B Saunders
- Baes, C.F. and Mesmer, R.E. (1976), "Chromium In: *The Hydrolysis of Cations*" pp.211-219, New York, John Wiley and Sons.
- Barnhart, J. (1997), "Chromium Chemistry and Implications for Environmental Fate and Toxicity", In: Proctor, D.M., Finley, B.L., Harris, M.A., Paustenbach, D.J. and Rabbe D. (Eds) *Chromium in Soil: Perspectives in Chemistry and Environmental Regulation*, Special Issue of Journal of Soil Contamination, pp.561-568 Volume 6, Number 6, New York, Boca Raton, Lewis Publishers
- Bartlett, R.J. (1991), "Chromium Cycling in Soils and Water: Links, Gaps and Methods," *Environmental Health Perspectives*, 92, pp.17-24
- Bartlett, R.J. and Kimble, J.M. (1976), "Behaviour of Chromium in Soils: I. Trivalent Forms", *J. Environ. Qual.*, 5, pp.379-382
- Baturay, O., Shirk, J.E. and Sigerson, A.L. (1991), "Method for Removing Chromium from Chromium Containing Waste Material", US Patent 5,007,960. Application No 421,136. (Apr.16, 1991)
- Bayer, G. and Wiedemann, H.G. (1977), "Formation and Decomposition of Calcium and Cadmium Chromate during Solid State Reactions between Cr₂O₃ and Carbonates and Hydroxides", *Proceedings, Fifth International Conference on Thermal Analysis*, H.H Chihara (Ed.), Heyden, Bellmawr, NJ, 1977, pp. 437-439
- Breeze, V. (1973), "Land reclamation and river pollution problems in the Croal Valley caused by waste from chromate manufacture", *J. Appl. Ecol.*, 10, pp.513-525
- Burke, T., Fagliano, J., Goldoft, M., Hazen, R.E., Iglewize, R. and McKee, T. (1991): "Chromite Ore Processing Residue in Hudson County, New Jersey", *Environmental Health Perspectives*, 92, pp. 131-137
- Calder, L.M., (1988), "Chromium Contamination in Ground Water, In: Nriagu J. (Ed.) *Chromium in the Human and Natural Environment*", pp.215-229, New York, John Wiley and Sons.
- Deltombe, E., De Zoubov, N. and Pourbaix, M. (1966), "Chromium In: Pourbaix, M. (Ed.) *Atlas of Electrochemical Equilibria*," pp.256-271, Oxford Pergamon Press.
- Dixon, F.W. (1929), "Perforation of the nasal septum in chromium workers," *J.Am. Med. Ass.*, 93, pp.837-838

- Eary, L.E. and Rai, D. (1988), "Kinetics of Chromium (III) Oxidation to Chromium (VI) by Reaction with Manganese Dioxide", *Environ. Sci. Technol.*, 22, pp.1187-1193
- Elderfield, H. (1970), "Chromium Speciation in Sea Water", *Earth Planet Sci. Lett.*, 9, pp. 10-16
- Fendorf, S.E. and Zasoski, R.J. (1992): "Cr(III) Oxidation By MnO₂. I) Characterisation", *Environ. Sci. Technol.*, 26 pp. 79-85
- Fendorf, S.E., Fendorf, M., Sparks, D.L. and Gronsky R. (1992), "Inhibitory Mechanisms of Cr(III) Oxidation by δ -MnO₂", *Journal of Colloid and Interface Science*, 155, No.1, pp.37-54
- Finholt, J.E. (1960), "Chemistry of Some Hydrolyzed Cr(III) Polymers," Report No. UCRL -8879, Lawrence Radiation Laboratory, Livermore, CA
- Franchini, J., Magnani, E. and Mutti, A. (1983), "Mortality Experienced Among Chrome-Plating Workers", *Scand. J. Work Environ. Health*, 9, pp. 247-252
- Gemmell, R.P. (1973), "Revegetation of Derelict Land Polluted by a Chromate Smelter Part I: Chemical Factors Causing Substrate Toxicity in Chromate Smelter Waste", *Environ. Pollut.*, 5, pp.181-197
- Hannay, N.B. (Ed.) (1976), "Treatise on Solid-State Chemistry", Volume 4: Reactivity of Solids, New York, London, Plenum Press
- Hartford, W.H. (1979), "Chromium Compounds In: Kirk and Othmer Encyclopaedia of Chemical Technology", 2nd ed., pp.82-120
- Hattori, M., Yaku, K. and Nakaya, K. (1978), "Treatment of Sludge Containing Calcium and Chromium by Heating with Silica," *Environ. Sci. Technol.*, 12, pp. 1431-1434
- Houding, G. (1970), "Cement Eczema and Chromium Allergy: Epidemiological Investigation", University of Bergen, Norway, Thesis
- Hunt, C. and Taube, H. (1951), "The Exchange of water between hydrated cations and solvent", *J. Phys. Chem.* 19, pp.201-203
- Jacobs, J.H., (1992). "Treatment and Stabilisation of Hexavalent Chromium -Containing Waste Material", *Environ. Prog.*, 11, pp.123-126
- James, B.R. and Bartlett, R.J. (1983a), "Behaviour of Chromium in Soils:V. Fate of Organically Complexed Cr(III) Added to Soil", *J. Environ. Qual.*, 12, pp.169-172

- James, B.R. and Bartlett, R.J. (1983b), "Behaviour of Chromium in Soils:VI.: Interactions Between Oxidation-Reduction and Organic Complexation", *J. Environ. Qual.*, 12, pp.173-176
- James, B.R. and Bartlett, R.J. (1983c), "Behaviour of Chromium in Soils:VII: Adsorption and Reduction of Hexavalent Forms", *J. Environ. Qual.*, 12, pp.177-181
- Johnson, C.A. and Xyla, A.G. (1991), "The oxidation of chromium (III) to chromium (VI) on the surface of manganite (γ -MnOOH)", *Geochim. Cosmochim. Acta*, 55, pp.2861-2866
- Kilau, H.W. and Shah, I.D. (1984), "Chromium Bearing Waste Slag: Evaluation of Leachability When Exposed to Simulated Acid Rain", *Hazardous Industrial Waste Management and Testing, Third Symposium, Philadelphia, ASTM STP, 851*. Jackson, L.P., Rohlik A.R. (Eds) pp.61-81
- Korallus, U., Undiche H. and Wusterfeld, E. (1974), "Trivalent Chromium Compounds: Results of Medical Investigations of working conditions", *Arbeitsmed. Sozialmed. Praventivemed.*, 9(30), pp.51-54
- Korousic, B., Triplat, J. and Rozman, A. (2000), "Evaluation of the Role of Slag Chemistry and Chemical Interactions for EAFS for Stainless Steel Production", *Sixth International Conference on Molten Slags, Fluxes and Salts-Topics/ Contents, Paper 112*, <http://www.print.kth.se/slagn/SLAGS/CONTENTS.htm> (14 February 2001)
- Language, P., Schmidt, F.O. and van Blerk, J., (1999), "Recycling of Ferrochrome Furnace Bagfiller Dust at Samancor Chrome-A Success Story", *Proceedings National Association for Clean Air (NACA) Annual Conference (7-8 October 1999)*, Cape Town, South Africa
- Laswick, J.A. and Plane, R.A. (1959), "Hydroxy Forms of Cr(III) in Aqueous Solution," *J. Am. Chem. Soc.*, 81, pp. 3564-3567
- Lee, H.I. and Goh, C.I. (1988), "Occupational dermatitis among chrome platers", *Contact Dermatitis*, 18, pp.89-93
- Mancuso, T.F. (1975), *International Conference on Heavy Metals in the Environment*, Toronto, Ontario, Canada, October 27-31
- Mancuso, T.F. and Hueper W.C. (1951), "Occupational cancer and other health hazards in a chromate plant: A Medical Appraisal. I. Lung Cancers in Chromate Workers". *Ind. Med. Surg.*, 20, pp.358-363
- Mayer, L.M. (1988), "Geochemistry of Chromium in the Oceans. In: Nriagu, J. (Ed) *Chromium in the Human and Natural Environment*", pp.81-103 New York: John Wiley and Sons.

McGrath, S.P. and Smith, S. (1991), "Chromium and Nickel In: Alloway, J. (Ed.) *Heavy Metals in Soils*", pp.125-150, Glasgow and London, Blackie

Mellor, J.W. (1931), "A Comprehensive Treatise in Inorganic and Theoretical Chemistry," Volume XI, Chapter LX, pp. 122-479, New York, London and Toronto, Longmans, Green and Co.

Milacic, R., Stupar, J., Kozuh, N. and Korosin, J. (1992), "Critical Evaluation of Three Analytical Techniques for the Determination of Cr(VI) in Soil Extracts," *Analyst*, 117, 125-130

Milacic, R. and Stupar, J. (1995), "Fractionation and Oxidation of Chromium in Tannery Waste – and Sewage Sludge- Amended Soils," *Environ. Sci. Technol.*, 29, pp.506-514

Nakayama, E. (1981), "Chemical Speciation of Chromium in Seawater. Part 2: Effects of Manganese Oxides and Reducible Organic Material on the Complex Formation of Chromium (III)", *Anal. Chim.*, 130, pp.289-294

Nakayama, E., Tokoro, H., Kuwamoto, T. and Fujinaga, T. (1981), "Dissolved State of Chromium in Seawater," *Nature*, 333, pp.134-139

Nell, J. and Mostert, J. (1999), "Mintek Report No: 4159801(28)", Mintek, Randburg

Nieboer E. and Jusys, A.A. (1988), "Biologic Chemistry of Chromium In: Nriagu (Ed.) *Chromium in the Human and Natural Environment*", pp. 21-79. New York, John Wiley and Sons.

Nriagu, J.O.(1988), "Production and Uses of Chromium In: Nriagu, J. (Ed.) *Chromium in the Human and Natural Environment*", pp.81-103, New York: John Wiley and Sons.

Nyholm, R.S. (1947), "The Aerial Oxidation of Trivalent In Aqueous Solution", *Journal of Science in the Chemical Industry*, 66, pp.449-451

Palmer, C.D. and Wittbrodt, P.R. (1991), "Processes Affecting the Remediation of Chromium Contaminated Sites", *Environmental Health Perspectives*, 92, pp.25-40

Peltonen, L. and Fraki, J. (1983), "Prevalence of dichromate sensitivity," *Contact Dermatitis*, 9, pp.190-194

Petersen, J. (1998), "Assessment and Modelling of Chromium Release in Minerals Processing Waste Deposits," PhD Thesis, University of Cape Town

Pretorius, E.B. and Nunnington, R.C. (2000), "Stainless Steel Fundamentals – From Furnace to Tundish," Sixth International Conference on Molten Slags, Fluxes and Salts-Topics/Contents, Paper 126, <http://www.print.kth.se/slags/SLAGS/CONTENTS.htm> (14 February 2001)

- Proctor, D.M., Shay, E.C. and Scott, P.K. (1997), "Health Based Soil Action Levels for Trivalent and Hexavalent Chromium: A Comparison with State and Federal Standards," In: Proctor, D.M., Finley, B.L., Harris, M.A., Paustenbach, D.J. and Rabbe, D. (Eds) *Chromium in Soil: Perspectives in Chemistry and Environmental Regulation*, Special Issue of Journal of Soil Contamination, pp.595-648 Volume 6, Number 6, New York, Boca Raton, Lewis Publishers
- Rai, D., Sass, B.M. and Moore, D.A. (1987), "Chromium(III) Hydrolysis Constants and Solubility of Chromium (III) Hydroxide", *Inorg. Chem.*, 26, pp.345-349
- Reartes, G.B., Morando, P.J. and Blesa, M.A. (1991), "Reactivity of Chromium Oxide in Aqueous Solutions. I. Oxidative Dissolution," *Chem. Mater.*, 3, pp.1101-1106
- Richard, F.C. and Bourg, A.C.M. (1991), "Aqueous Geochemistry of Chromium: A Review", *Water Reserves*, 25, pp.807-816
- Ross, D.S., Sjogren, R.E. and Bartlett, R.J. (1981), "Behaviour of Chromium in Soils: IV. Toxicity to Microorganisms". *J. Environ. Qual.* 10, pp.145-148
- Royle, H., (1975), "Toxicity of chromic acid in the chrome-plating industry (2)", *Environ. Res.*, 10, pp.111-116
- Saleh, F., Parkerton, T., Lewis, R., Huang, J. and Dickson, K.L. (1989), "Kinetics of Chromium Transformations in the Environment," *The Science of the Total Environment*, 86, pp. 25-41
- Sandell, E.B. (1950), "Chromium In: *Colorimetric Determination of Traces of Metals*", 2nd edn, pp.257-270, New York, Interscience Publishers
- Schmalzried, H. (1981), "Solid-State Reactions," 2nd ed., Weinheim, Deerfield Beach, Florida, Basel, Verlag Chemie
- Schroeder, D.C. and Lee, G.F. "Potential Transformations of Chromium in Natural Waters", *Water, Air and Soil Pollution*, 4, pp.355-365
- Segall, R.L., Smart, R. and Turner, P.S. (1986), "In: Surface and Planar-Surface Chemistry of Oxide Materials" Notwotny, J., Dufour, L.C., (Eds.), Elsevier Science Publishers B.V, Amsterdam, Chapter 13
- Sheehan, P.J., Meyer, D.M., Sauer, M.M and Paustenbach, D.J. (1991), "Assessment of the Human Health Risks Posed by Exposure to Chromium Contaminated Soil", *Journal of Toxicology and Environmental Health*, 12, pp. 161-201
- Smith, J.W. (1981), "Chemical Engineering Kinetics," New York, McGraw Hill

Stuenzi, H. and Marty, W. (1983), "Early Stages of the Hydrolysis of Cr(III) in Aqueous Solution. 1) Characterisation of a Tetrameric Species", *Inorg. Chem.*, 22, pp.2145-2150

Van der Weijden, C.H. and Reith, M. (1982), "Chromium (III) – Chromium (VI) Interconversions in Seawater," *Marine Chemistry*, 11, pp.565-572

Weng, C.H., Huang, C.P., Allen, A., Cheng, H.D. and Sanders, P.F. (1994), "Chromium leaching behaviour in soil derived from chromite ore processing waste", *The Science of the Total Environment*, 154, pp.71-86

Winston, J.R. and Walsh, L.N. (1951), "Chromate dermatitis in the railroad employees working with diesel locomotives", *J. Am. Med. Assoc.*, 147 (12), pp.1133-1134

Wood, J.R. and Black, V.K. (1916), "Amphoteric Metallic Hydroxides, Part III. Chromium Hydroxide", *Journal of Chemical Society*," 109, pp. 164

University of Cape Town

OVERVIEW OF APPENDICES

Appendix A: Raw Analytical Data, Conversion-Time Data and Moisture Contents

Appendix A1: Sample Calculation showing how the absorbance readings were converted into Cr(VI) concentrations (ppb)

Appendix A2: The Conversion of Absorbance Readings into Conversions for all Experimental Results shown

Appendix A3: Sample Calculation showing how the Cr(VI) Concentrations were used to calculate conversions ($\mu\text{g per g Cr}$)

Appendix A4: The Conversion-Time Data for and Moisture Contents for all the Results Presented

Appendix B: Malvern Particle Size Distribution Analysis Data

Appendix B1: Particle Size Distributions for Cr_2O_3 and CaO used for Ball experiments in 1999

Appendix B2: Particle Size Distributions for Cr_2O_3 and CaO used for powder and pellet experiments in 2000

Appendix B3: Particle Size Distributions for slag samples

Appendix C: The Analysis by UV-Visible Spectroscopy- Procedure, Limits of Detection and Reproducibility

Appendix D: Verification that Drying $\text{Cr}_2\text{O}_3\text{-Ca(OH)}_2$ Balls at 80°C does not Cause Additional Oxidation

Appendix E: Analysis of Pure Chemicals for Trace Contaminants that may contribute to Oxidation

Appendix F: Temperature Records fully tabulated results

Appendix G: Data for Kinetic Analysis

Appendix G1: The Kinetic Data for $\text{Cr}_2\text{O}_3\text{-CaO}$ Powders and Pellets fully tabulated results

Appendix G2: The Kinetic Data for $\text{Cr}_2\text{O}_3\text{-Ca(OH)}_2$ Balls fully tabulated results

Appendix G3: The Kinetic Data for Slag Balls (pore moisture evaporated) fully tabulated results and graphs not shown in Chapter Six

Appendix G4: The Kinetic Data for Slag Powders fully tabulated results and graphs not shown in Chapter Six

**APPENDIX A: RAW
ANALYTICAL DATA,
CONVERSION-TIME
DATA AND MOISTURE
CONTENTS**

University of Cambridge

**APPENDIX A1: SAMPLE
CALCULATION SHOWING
HOW THE ABSORBANCE
READINGS WERE
CONVERTED INTO Cr(VI)
CONCENTRATIONS**

University of Cambridge

SAMPLE CALCULATION FOR THE CONVERSION OF ABSORBANCE READINGS INTO CONCENTRATIONS

Example Chosen: Cr₂O₃-CaO (50% CaO) powders stored in a dessicator zero sample
The absorbance readings obtained for the standards analysed on the same day as this sample is tabulated below:-

Table A1: The Absorbance readings obtained for the standards analysed on the same day as the zero sample of the Cr₂O₃-CaO powders (50% CaO)

Standard Concentration (ppb)	Absorbance reading 1	Absorbance reading 2	Average Reading	In concentration	In average reading
100	0.0287	0.0289	0.0288	4.61	-3.55
200	0.0563	0.0564	0.0564	5.30	-2.88
500	0.1496	0.1499	0.1498	6.21	-1.90
1000	0.2832	0.2833	0.2833	6.91	-1.26
2000	0.5696	0.5666	0.5681	7.60	-0.57

A linear regression on the natural logarithms of the concentration and average absorbance readings gave an x-variable of 1.00 and an intercept of 8.16.

The average absorbance reading obtained for the sample was 0.0005.

So, the concentration of the sample in ppb

$$= (\exp(\text{intercept}) \times \text{average absorbance reading})^{\text{x-variable}}$$

$$= (3492.83 \times 0.0005)^1$$

$$= 1.55 \text{ ppb}$$

But the sample was diluted by a factor of 2 prior to the analysis, so the original concentration of the sample = $1.55 \times 2 = 3.10$ ppb

NB: The values obtained for the intercept and the x-variable, were fairly reproducible and are reported correct to two decimal places. All samples were diluted by a factor of two.

**APPENDIX A2: THE
CONVERSION OF
ABSORBANCE READINGS
INTO Cr(VI)
CONCENTRATIONS FOR ALL
EXPERIMENTAL RESULTS
SHOWN**

University of Cape Town

Table A1: The Conversion of Absorbance Readings to Cr(VI) Concentrations for Cr₂O₃-CaO Powders maintained in a dessicator

<i>Sample</i>	<i>Date Analysed</i>	<i>Average Absorbance Reading</i>	<i>Cr(VI) conc. (ppb)</i>
0 week	29-05-00	0.0005	3.10
1 week	18-06-00	0.0034	23.75
2 weeks	18-06-00	0.0075	52.36
4 weeks	2-07-00	0.0134	94.04
8 weeks	6-08-00	0.0165	115.35
12 weeks	17-09-00	0.0264	185.49

University of Cape Town

Table A2: The Conversion of Absorbance Readings to Cr(VI) Concentrations for Cr₂O₃-Ca(OH)₂ Balls (5% Ca(OH)₂ and with the pore moisture maintained)

<i>Sample</i>	<i>Date Analysed</i>	<i>Average Absorbance Reading</i>	<i>Cr(VI) conc.(ppb)</i>
0 weeks	23-6-99	0.0005	3.51
1 week	23-6-99	0.0008	5.85
2 weeks	30-6-99	0.0013	8.86
4 weeks	22-7-99	0.0015	10.29
8 weeks	23-8-99	0.0015	10.03
12 weeks	29-9-99	0.0026	18.48
16 weeks	7-11-99	0.0034	23.61
20 weeks	30-11-99	0.0037	25.90
28 weeks	18-02-00	0.0048	32.96
44 weeks	21-05-00	0.0047	32.77
56 weeks	13-08-00	0.0056	39.26

Repeat Experiments

0 weeks	23-6-99	0.0003	2.11
1 week	23-6-99	0.0007	5.15
2 weeks	30-6-99	0.0014	9.56
4 weeks	22-7-99	0.0016	10.64
8 weeks	23-8-99	0.0016	11.07
12 weeks	29-9-99	0.0026	17.41
16 weeks	7-11-99	0.0034	23.25
20 weeks	30-11-99	0.0037	25.90
28 weeks	18-02-00	0.0036	24.63
44 weeks	21-05-00	0.0047	33.12
56 weeks	13-08-00	0.0057	39.96

Table A3: The Conversion of the Absorbance readings into Cr(VI) Concentrations for Cr₂O₃-Ca(OH)₂ Balls (20% Ca(OH)₂ with pore moisture maintained)

<i>Sample</i>	<i>Date Analysed</i>	<i>Average Absorbance Reading</i>	<i>Cr(VI) conc. (ppb)</i>
0 weeks	23-6-99	0.0004	2.81
1 week	23-6-99	0.0008	5.62
2 weeks	30-6-99	0.0013	8.86
4 weeks	22-7-99	0.0016	10.98
8 weeks	23-8-99	0.0020	13.84
12 weeks	29-9-99	0.0036	25.57
16 weeks	7-11-99	0.0040	28.18
20 weeks	30-11-99	0.0058	41.08
28 weeks	18-02-00	0.0070	48.23
44 weeks	21-05-00	0.0064	44.70
56 weeks	13-08-00	0.0070	49.05
Repeat Experiments			
0 weeks	23-6-99	0.0007	5.15
1 week	30-6-99	0.0008	5.36
2 weeks	22-7-99	0.0014	9.26
4 weeks	22-7-99	0.0017	11.67
8 weeks	23-8-99	0.0018	12.11
12 weeks	29-9-99	0.0037	25.92
16 weeks	7-11-99	0.0042	29.23
20 weeks	30-11-99	0.0054	37.90
28 weeks	18-02-00	0.0058	39.90
44 weeks	21-05-00	0.0064	45.05
56 weeks	13-08-00	0.0065	45.32

Table A4: The Conversions of Absorbance Readings to Cr(VI) Concentrations for Cr₂O₃-Ca(OH)₂ Balls (50% Ca(OH)₂ with the excess pore moisture maintained)

<i>Sample</i>	<i>Date Analysed</i>	<i>Average Absorbance Reading</i>	<i>Cr(VI) conc. (ppb)</i>
0 weeks	23-6-99	0.0003	1.87
1 week	23-6-99	0.0010	7.25
2 weeks	30-6-99	0.0019	13.52
4 weeks	22-7-99	0.0028	19.25
8 weeks	23-8-99	0.0054	37.43
12 weeks	29-9-99	0.0070	49.30
16 weeks	7-11-99	0.0086	60.14
20 weeks	30-11-99	0.0096	67.49
28 weeks	18-02-00	0.0125	86.42
44 weeks	21-05-00	0.0130	90.95
56 weeks	13-08-99	0.0122	85.64
Repeat Experiments			
0 weeks	23-6-99	0.0004	2.81
1 week	30-6-99	0.0013	9.09
2 weeks	22-7-99	0.0023	15.81
4 weeks	22-7-99	0.0025	16.84
8 weeks	23-8-99	0.0053	36.73
12 weeks	29-9-99	0.0069	48.59
16 weeks	7-11-99	0.0086	60.49
20 weeks	30-11-99	0.0098	69.25
28 weeks	18-02-00	0.0123	85.03
44 weeks	21-05-00	0.0125	87.45
56 weeks	13-08-00	0.0124	86.57

Table A5: The Conversion of Absorbance Readings into Cr(VI) Concentrations for Cr₂O₃-Ca(OH)₂ Balls (20% Ca(OH)₂ with the excess pore moisture evaporated)

<i>Sample</i>	<i>Date Analysed</i>	<i>Average Absorbance Reading</i>	<i>Cr(VI) conc. (ppb)</i>
0 weeks	23-6-99	0.0001	0.94
1 week	23-6-99	0.0005	3.51
2 weeks	30-6-99	0.0011	7.46
4 weeks	22-7-99	0.0017	11.67
8 weeks	23-8-99	0.0066	45.76
12 weeks	29-9-99	0.0111	78.32
16 weeks	7-11-99	0.0153	107.14
20 weeks	30-11-99	0.0185	130.38
28 weeks	18-02-00	0.0286	198.58
44 weeks	21-05-00	0.0426	297.96
56 weeks	13-08-99	0.0344	240.60
Repeat Experiments			
0 weeks	23-6-99	0.0003	2.11
1 week	30-6-99	0.0009	6.30
2 weeks	22-7-99	0.0022	15.12
4 weeks	22-7-99	0.0016	10.64
8 weeks	23-8-99	0.0070	48.19
12 weeks	29-9-99	0.0116	81.86
16 weeks	7-11-99	0.0160	112.05
20 weeks	30-11-99	0.0187	131.43
28 weeks	18-02-00	0.0285	197.89
44 weeks	21-05-00	0.0307	214.97
56 weeks	13-08-00	0.0343	239.91

Table A6: The Conversion of Absorbance Readings into Cr(VI) Concentrations for Cr₂O₃-Ca(OH)₂ Balls (50% Ca(OH)₂ with the pore moisture evaporated)

<i>Sample</i>	<i>Date Analysed</i>	<i>Average Absorbance Reading</i>	<i>Cr(VI) conc. (ppb)</i>
0 weeks	19-01-00	0.0003	1.76
1 week	19-01-00	0.0017	11.95
2 weeks	19-01-00	0.0058	40.33
4 weeks	19-01-00	0.0089	62.39
10 weeks	18-02-00	0.0118	81.56
12 weeks	26-03-00	0.0158	110.54
16 weeks	18-04-00	0.0225	158.45
20 weeks	21-05-00	0.0377	263.80
28 weeks	5-07-00	0.0422	295.52

Repeat Experiments

0 weeks	18-02-00	0.0004	2.43
1 week	26-03-00	0.0011	7.73
2 weeks	26-03-00	0.0055	38.19
4 weeks	26-03-00	0.0087	60.92
8 weeks	26-03-00	0.0116	80.34
12 weeks	18-04-00	0.0148	102.78
16 weeks	21-05-00	0.0218	151.54
20 weeks	18-06-00	0.0370	257.94
28 weeks	6-08-00	0.0423	295.86

Table A7: The Conversion of Absorbance Readings into Cr(VI) Concentrations for Cr₂O₃-CaO Powders (20% CaO) exposed to ambient moisture

<i>Sample</i>	<i>Date Analysed</i>	<i>Average Absorbance Reading</i>	<i>Cr(VI) conc.(ppb)</i>
0 weeks	21-05-00	0.0002	1.42
1 week	29-05-00	0.0107	73.85
2 weeks	18-06-00	0.0118	82.00
4 weeks	18-06-00	0.0164	114.41
8 weeks	13-08-00	0.0216	151.06
12 weeks	17-09-00	0.0252	177.09

Table A8: The Conversion of Absorbance Readings into Cr(VI) Concentrations for Cr₂O₃-CaO Powders (50% CaO) exposed to ambient moisture

<i>Sample</i>	<i>Date Analysed</i>	<i>Average Absorbance Reading</i>	<i>Cr(VI) conc.(ppb)</i>
0 week	21-05-00	0.0001	0.71
1 week	18-06-00	0.0123	85.48
2 weeks	18-06-00	0.0423	294.85
4 weeks	18-06-00	0.0584	406.95
8 weeks	6-08-00	0.0682	477.35
12 weeks	17-09-00	0.0709	496.76

Table A9: The Conversion of Absorbance Readings into Cr(VI) Concentrations for Cr₂O₃-CaO Pellets (50% CaO) exposed to ambient moisture

<i>Sample</i>	<i>Date Analysed</i>	<i>Average Absorbance Reading</i>	<i>Cr(VI) conc.(ppb)</i>
0 week	2-07-00	0.0003	2.13
1 week	2-07-00	0.0417	291.14
2 weeks	2-07-00	0.0516	360.42
4 weeks	5-07-00	0.0768	536.85
8 weeks	6-08-00	0.0854	597.75
12 weeks	17-09-00	0.0880	616.19

Table A10: The Conversion of Absorbance Readings into Cr(VI) Concentrations for Cr₂O₃-Ca(OH)₂ Balls Under nitrogen (50% Ca(OH)₂ with the pore moisture evaporated)

<i>Sample</i>	<i>Date Analysed</i>	<i>Average Absorbance Reading</i>	<i>Cr(VI) conc. (ppb)</i>
0 weeks	2001/03/09	0.0001	0.70
1 week	2001/03/09	0.0002	1.05
2 weeks	2001/03/09	0.0002	1.05
4 weeks	2001/04/08	0.0002	1.12
7 weeks	2001/04/08	0.0002	1.12

Table A11: The Conversion of Absorbance Readings into Cr(VI) Concentrations for Experiments which served as control experiment for those under nitrogen (50% Ca(OH)₂ with the pore moisture evaporated)

<i>Sample</i>	<i>Date Analysed</i>	<i>Average Absorbance Reading</i>	<i>Cr(VI) conc. (ppb)</i>
2 weeks	2001/04/08	0.0003	1.85
4 weeks	2001/04/08	0.0065	46.05
7 weeks	2001/04/08	0.0077	54.86

University of Cape Town

Table A12: The Conversion of Absorbance Readings into Cr(VI) Concentrations for Cr₂O₃-Ca(OH)₂ Balls maintained at fifty degrees (20% Ca(OH)₂)

<i>Sample</i>	<i>Date Analysed</i>	<i>Average Absorbance Reading</i>	<i>Cr(VI) conc.(ppb)</i>
0 weeks	26-03-00	0.0005	3.16
1 week	26-03-00	0.0013	8.78
2 weeks	26-03-00	0.0024	16.84
4 weeks	26-03-00	0.0055	38.19
7 weeks	26-03-00	0.0136	94.82
10 weeks	18-04-00	0.0355	250.20
15 weeks	21-05-00	0.0564	394.11
19 weeks	5-07-00	0.0618	432.46
26 weeks	6-08-00	0.0665	465.22
Repeat Experiments			
0 weeks	26-03-00	0.0009	5.97
1 week	26-03-00	0.0012	8.43
2 weeks	26-03-00	0.0022	15.08
4 weeks	26-03-00	0.0054	37.49
7 weeks	26-03-00	0.0133	93.07
10 weeks	18-04-00	0.0352	247.74
15 weeks	21-05-00	0.0555	387.84
19 weeks	5-07-00	0.0616	431.07
26 weeks	6-08-00	0.0663	463.59

Table A13: The Conversion of Absorbance Readings into Cr(VI) Concentrations for Cr₂O₃-Ca(OH)₂ Balls maintained at eighty degrees (20% Ca(OH)₂)

<i>Sample</i>	<i>Date Analysed</i>	<i>Average Absorbance Reading</i>	<i>Cr(VI) conc. (ppb)</i>
0 weeks	23-6-99	0.0001	0.94
1 week	30-6-99	0.0016	10.96
2 weeks	22-7-99	0.0047	32.37
4 weeks	22-7-99	0.0088	60.72
8 weeks	23-8-99	0.0327	226.92
12 weeks	29-9-99	0.0658	464.91
16 weeks	7-11-99	0.0998	698.58
20 weeks	30-11-99	0.1219	851.96
28 weeks	18-02-00	0.1555	1080.08
44 weeks	18-06-00	0.1644	1144.52
56 weeks	13-08-00	0.1713	1193.80
Repeat Experiments			
0 weeks	30-6-99	0.0005	3.50
1 week	22-7-99	0.0019	12.70
2 weeks	22-7-99	0.0040	27.53
4 weeks	23-8-99	0.0086	59.65
8 weeks	23-8-99	0.0326	226.22
12 weeks	29-9-99	0.0651	459.97
16 weeks	7-11-99	0.0995	696.13
20 weeks	30-11-99	0.1214	848.83
28 weeks	18-02-00	0.1576	1095.02
44 weeks	18-06-00	0.1664	1158.43
56 weeks	13-08-00	0.1723	1200.52

Table A14 The Conversion of Absorbance Readings into Cr(VI) Concentrations for Old Mixed Slag Powder Exposed to Air (particle size class: 75-300um)

<i>Sample</i>	<i>Date Analysed</i>	<i>Average Absorbance Reading</i>	<i>Cr(VI) conc. (ppb)</i>
0 weeks	29-05-00	0.0842	585.50
1 week	18-06-00	0.1686	1173.73
2 weeks	18-06-00	0.2404	1673.03
4 weeks	2-07-00	0.2887	2004.17
8 weeks	6-08-00	0.2885	2019.98
12 weeks	24-09-00	0.2994	2067.53

Table .A15: The Conversion of Absorbance Readings into Cr(VI) Concentrations for Old Mixed Slag Powders exposed to air (particle size class:300-1000um)

<i>Sample</i>	<i>Date Analysed</i>	<i>Average Absorbance Reading</i>	<i>Cr(VI) conc. (ppb)</i>
0 weeks	18-06-00	0.0894	622.38
1 week	18-06-00	0.1626	1132.00
2 weeks	18-06-00	0.2445	1701.19
4 weeks	2-07-00	0.2502	1737.72
8 weeks	6-08-00	0.2804	1963.01
12 weeks	24-09-00	0.2887	1994.19

Table A16: The Conversion of Absorbance Readings into Cr(VI) Concentrations for New CLU Slag Powders (particle size class: <75um)

<i>Sample</i>	<i>Date Analysed</i>	<i>Average Absorbance Reading</i>	<i>Cr(VI) conc. (ppb)</i>
0 weeks	29-5-00	0.0405	281.11
1 week	18-06-00	0.0822	572.27
2 weeks	18-06-00	0.1684	1171.99
4 weeks	2-07-00	0.1817	1263.27
8 weeks	13-08-00	0.2016	1404.51
12 weeks	24-09-00	0.2419	1673.17

Table A17: The Conversion of Absorbance Readings into Cr(VI) Concentrations for New CLU Slag Powders (particle size class: 75-300um)

<i>Sample</i>	<i>Date Analysed</i>	<i>Average Absorbance Reading</i>	<i>Cr(VI) conc. (ppb)</i>
0 weeks	18-06-00	0.0382	265.94
1 week	18-06-00	0.0605	421.57
2 weeks	18-06-00	0.0918	639.08
4 weeks	2-07-00	0.1269	883.27
8 weeks	6-08-00	0.1587	1110.94
12 weeks	24-09-00	0.1695	1175.89

Table A18: The Conversion of the Absorbance Readings into Cr(VI) Concentrations for New CLU Slag Powders (Particle size class: 300-1000um)

<i>Sample</i>	<i>Date Analysed</i>	<i>Average Absorbance Reading</i>	<i>Cr(VI) conc. (ppb)</i>
0 week	18-06-00	0.0205	142.99
1 week	18-06-00	0.0453	315.74
2 weeks	18-06-00	0.0918	610.90
4 weeks	2-07-00	0.1624	1129.84
8 weeks	13-08-00	0.2664	1207.48
12 weeks	24-09-00	0.1887	1307.65

Table A19: The Conversion of Absorbance Readings into Cr(VI) Concentrations for New EAF Slag Powders (Particle size class: <75um)

<i>Sample</i>	<i>Date Analysed</i>	<i>Average Absorbance Reading</i>	<i>Cr(VI) conc. (ppb)</i>
0 week	2-07-00	0.0304	212.38
1 week	2-07-00	0.0625	436.26
2 weeks	2-07-00	0.1337	930.80
4 weeks	5-07-00	0.1564	1089.45
8 weeks	13-08-00	0.1574	1097.11
12 weeks	24-09-00	0.1588	1101.87

Table A20: The Conversion of Absorbance Readings into Cr(VI) Concentrations for New EAF Slag Powders (Particle size class: 75-300um)

<i>Sample</i>	<i>Date Analysed</i>	<i>Average Absorbance Reading</i>	<i>Cr(VI) conc. (ppb)</i>
0 week	2-07-00	0.0314	219.35
1 week	2-07-00	0.0615	428.96
2 week	2-07-00	0.1265	880.84
4 week	2-07-00	0.1328	924.55
8 weeks	13-08-00	0.1494	1041.23
12 weeks	24-09-00	0.1667	1156.27

Table A21: The Conversion of Absorbance Readings into Concentrations for New EAF Slag Powders (Particle size class: 300-1000um)

<i>Sample</i>	<i>Date Analysed</i>	<i>Average Absorbance Reading</i>	<i>Cr(VI) conc. (ppb)</i>
0 weeks	2-07-00	0.0256	178.90
1 week	2-07-00	0.0514	359.03
2 weeks	2-07-00	0.1046	728.83
4 weeks	2-07-00	0.1419	987.68
8 weeks	13-08-00	0.1604	1117.52
12 weeks	24-09-00	0.1826	1265.69

Table A22: The Conversion of Absorbance Readings into Cr(VI) Concentrations for Old Mixed Slag Balls with the pore moisture maintained (particle size class: <75um)

<i>Sample</i>	<i>Date Analysed</i>	<i>Average Absorbance Reading</i>	<i>Cr(VI) conc.(ppb)</i>
0 weeks	29-9-99	0.0304	214.73
1 week	29-9-99	0.0396	279.69
2 weeks	7-11-99	0.0486	340.32
4 weeks	7-11-99	0.0586	410.62
8 weeks	19-01-00	0.0830	579.67
12 weeks	18-02-00	0.1009	700.59
16 weeks	26-03-00	0.1117	778.91
20 weeks	18-04-00	0.1135	796.63
28 weeks	18-06-00	0.1343	935.14
44 weeks	13-08-00	0.1367	952.87

University of Cape Town

Table A23: The Conversion of Absorbance Readings into Cr(VI) Concentrations for Old Mixed Slag Balls with the pore moisture maintained (particle size class:75-300um)

<i>Sample</i>	<i>Date Analysed</i>	<i>Average Absorbance Reading</i>	<i>Cr(VI) conc.(ppb)</i>
0 weeks	29-9-99	0.0262	185.42
1 week	29-9-99	0.0592	418.00
2 weeks	7-11-99	0.0796	557.08
4 weeks	7-11-99	0.1082	756.90
8 weeks	19-01-00	0.1446	1008.97
12 weeks	18-02-00	0.1996	1386.62
16 weeks	26-03-00	0.2177	1517.30
20 weeks	18-04-00	0.2744	1921.04
28 weeks	18-06-00	0.2746	1910.47
44 weeks	13-08-00	0.2755	1917.99

Table A24: The Conversion of Absorbance Readings into Cr(VI) Concentrations for Old Mixed Slag Balls with the pore moisture maintained (particle size class:300-1000um)

<i>Sample</i>	<i>Date Analysed</i>	<i>Average Absorbance Reading</i>	<i>Cr(VI) conc.(ppb)</i>
0 weeks	29-9-99	0.0263	185.77
1 week	29-9-99	0.0537	379.20
2 weeks	7-11-99	0.0913	639.19
4 weeks	7-11-99	0.1093	764.59
8 weeks	19-01-00	0.1256	876.25
12 weeks	18-02-00	0.1566	1087.72
16 weeks	26-03-00	0.1922	1339.81
20 weeks	18-04-00	0.2008	1407.43
28 weeks	18-06-00	0.2056	1430.70
44 weeks	13-08-00	0.2877	2002.53

Table A25: The Conversion of Absorbance Readings into Cr(VI) Concentrations for Old Mixed Slag Balls with the pore moisture evaporated (particle size class: <75µm)

<i>Sample</i>	<i>Date Analysed</i>	<i>Average Absorbance Reading</i>	<i>Cr(VI) conc. (ppb)</i>
0 weeks	7-11-99	0.0304	213.29
1 week	7-11-99	0.0595	416.56
2 weeks	7-11-99	0.0813	568.96
4 weeks	30-11-99	0.1198	837.69
8 weeks	18-02-00	0.1383	960.87
12 weeks	26-03-00	0.1786	1245.14
16 weeks	18-04-00	0.1826	1280.25
20 weeks	21-05-00	0.1838	1279.20
28 weeks	18-06-00	0.1897	1320.13

Table A26: The Conversion of Absorbance Readings into Cr(VI) Concentrations for Old Mixed Slag Balls with the pore moisture evaporated (particle size class: 75-300µm)

<i>Sample</i>	<i>Date Analysed</i>	<i>Average Absorbance Reading</i>	<i>Cr(VI) conc. (ppb)</i>
0 weeks	7-11-99	0.0275	192.98
1 week	7-11-99	0.0794	556.03
2 weeks	7-11-99	0.0988	691.59
4 weeks	19-01-00	0.1542	1075.49
8 weeks	18-02-00	0.1775	1233.35
12 weeks	26-03-00	0.1858	1295.26
16 weeks	21-05-00	0.1931	1343.35
20 weeks	18-06-00	0.2137	1487.03
28 weeks	13-08-00	0.2295	1598.49

Table A27: The Conversion of Absorbance Readings into Cr(VI) Concentrations for Old Mixed Slag Balls with the pore moisture evaporated (particle size class:300-1000um)

<i>Sample</i>	<i>Date Analysed</i>	<i>Average Absorbance Reading</i>	<i>Cr(VI) conc. (ppb)</i>
0 weeks	7-11-99	0.0275	192.98
1 week	7-11-99	0.0855	598.66
2 weeks	19-01-00	0.1284	896.10
4 weeks	19-01-00	0.1784	1244.38
8 weeks	18-02-00	0.1960	1361.60
12 weeks	26-03-00	0.2037	1419.86
16 weeks	18-04-00	0.2126	1489.51
20 weeks	18-06-00	0.2345	1632.01
28 weeks	13-08-00	0.2457	1710.87

Table A28: The Conversion of Absorbance Readings into Cr(VI) Concentrations for New CLU Slag Balls with the pore maintained (particle size class:<75um)

<i>Sample</i>	<i>Date Analysed</i>	<i>Average Absorbance Reading</i>	<i>Cr(VI) conc. (ppb)</i>
0 weeks	29-9-99	0.0092	65.23
1 week	29-9-99	0.0118	83.27
2 week	7-11-99	0.0138	96.62
4 weeks	7-11-99	0.0170	119.41
8 weeks	30-11-99	0.0217	152.83
12 weeks	18-02-00	0.0249	172.53
16 weeks	26-03-00	0.0295	206.20
20 weeks	18-04-00	0.0314	221.04
28 weeks	2-07-00	0.0432	301.93
44 weeks	6-08-00	0.0436	304.95

Table A29: The Conversion of Absorbance Readings into Cr(VI) Concentrations for New CLU Slag Balls with the pore moisture maintained (particle size class:75-300um)

<i>Sample</i>	<i>Date Analysed</i>	<i>Average Absorbance Reading</i>	<i>Cr(VI) conc.(ppb)</i>
0 weeks	29-9-99	0.0098	69.12
1 week	29-9-99	0.0118	83.63
2 week	7-11-99	0.0130	91.36
4 weeks	7-11-99	0.0165	115.91
8 weeks	19-01-00	0.0216	151.19
12 weeks	18-02-00	0.0346	239.91
16 weeks	26-03-00	0.0396	276.68
20 weeks	18-04-00	0.0423	297.60
28 weeks	2-07-00	0.0558	389.30
44 weeks	6-08-00	0.0595	415.99

Table A30: The Conversion of Absorbance Readings into Concentrations for New CLU Slag Balls with the pore moisture maintained (particle size class:300-1000um)

<i>Sample</i>	<i>Date Analysed</i>	<i>Average Absorbance Reading</i>	<i>Cr(VI) conc.(ppb)</i>
0 weeks	30-11-99	0.0118	82.97
1 week	30-11-99	0.0128	90.35
2 week	19-01-00	0.0244	168.38
4 weeks	19-01-00	0.0346	238.43
8 weeks	18-02-00	0.0352	244.08
12 weeks	26-03-00	0.0400	279.12
16 weeks	18-04-00	0.0414	291.29
20 weeks	18-06-00	0.0454	316.09
28 weeks	6-08-00	0.0475	332.01

Table A31: The Conversion of Absorbance Readings into Concentrations for New CLU Slag Balls with the pore moisture evaporated (particle size class: <75um)

<i>Sample</i>	<i>Date Analysed</i>	<i>Average Absorbance Reading</i>	<i>Cr(VI) conc.(ppb)</i>
0 weeks	7-11-99	0.0094	66.10
1 week	7-11-99	0.0344	240.95
2 week	30-11-99	0.0376	263.85
4 weeks	30-11-99	0.0466	327.14
8 weeks	18-02-00	0.0533	370.17
12 weeks	26-03-00	0.0550	384.09
16 weeks	18-04-00	0.0607	427.07
20 weeks	2-07-00	0.0618	431.05
28 weeks	6-08-00	0.0935	438.16

Table A32: The Conversion of Absorbance Readings into Cr(VI) Concentrations for New CLU Slag Balls with pore moisture evaporated (particle size class: 75-300um)

<i>Sample</i>	<i>Date Analysed</i>	<i>Average Absorbance Reading</i>	<i>Cr(VI) conc.(ppb)</i>
0 weeks	7-11-99	0.0095	66.81
1 week	7-11-99	0.0379	265.45
2 week	30-11-99	0.0407	285.89
4 weeks	19-01-00	0.0565	394.50
8 weeks	18-02-00	0.0668	463.63
12 weeks	26-03-00	0.0696	485.89
16 weeks	18-04-00	0.0704	495.09
20 weeks	2-07-00	0.0716	499.55
28 weeks	6-08-00	0.0757	529.38

Table A33: The Conversion of Absorbance Readings into Cr(VI) Concentrations for New CLU Slags with the pore moisture evaporated (particle size class: 300-1000um)

<i>Sample</i>	<i>Date Analysed</i>	<i>Average Absorbance Reading</i>	<i>Cr(VI) conc. (ppb)</i>
0 weeks	30-11-99	0.0095	66.79
1 week	30-11-99	0.0304	213.45
2 week	19-01-00	0.0544	380.19
4 weeks	19-01-00	0.0688	480.65
8 weeks	18-02-00	0.0852	591.49
12 weeks	26-03-00	0.0893	623.19
16 weeks	18-04-00	0.0902	633.83
20 weeks	2-07-00	0.0914	636.80
28 weeks	6-08-00	0.0935	654.22

Table A34: The Conversion of Absorbance Readings into Cr(VI) Concentrations for New EAF Slag Balls with the pore moisture maintained (particle size class: <75um)

<i>Sample</i>	<i>Date Analysed</i>	<i>Average Absorbance Reading</i>	<i>Cr(VI) conc. (ppb)</i>
0 weeks	29-9-99	0.0105	74.43
1 week	7-11-99	0.0146	102.58
2 weeks	7-11-99	0.0166	116.61
4 weeks	7-11-99	0.0188	132.03
8 weeks	30-11-99	0.0194	136.35
12 weeks	18-02-00	0.0264	183.30
16 weeks	26-03-00	0.0313	218.41
20 weeks	18-04-00	0.0377	265.65
28 weeks	2-07-00	0.0395	275.81
44 weeks	6-08-00	0.0390	272.77

Table A35: The Conversion of Absorbance Readings into Cr(VI) Concentrations for New EAF Slag Balls with the pore moisture maintained (particle size class: 75-300um)

<i>Sample</i>	<i>Date Analysed</i>	<i>Average Absorbance Reading</i>	<i>Cr(VI) conc.(ppb)</i>
0 weeks	7-11-99	0.0088	61.89
1 week	7-11-99	0.0158	111.00
2 weeks	7-11-99	0.0175	122.92
4 weeks	7-11-99	0.0198	139.04
8 weeks	19-01-00	0.0330	230.47
12 weeks	18-02-00	0.0335	232.62
16 weeks	26-03-00	0.0354	247.37
20 weeks	18-04-00	0.0396	279.00
28 weeks	2-07-00	0.0533	372.25
44 weeks	6-08-00	0.0622	435.13

Table A36: The Conversion of Absorbance Readings into Cr(VI) Concentrations for New EAF Slag Balls with the pore moisture maintained (particle size class:300-1000um)

<i>Sample</i>	<i>Date Analysed</i>	<i>Average Absorbance Reading</i>	<i>Cr(VI) conc.(ppb)</i>
0 weeks	29-9-99	0.0108	76.55
1 week	29-9-99	0.0203	143.37
2 weeks	7-11-99	0.0224	156.91
4 weeks	7-11-99	0.0238	166.71
8 weeks	30-11-99	0.0168	118.45
12 weeks	18-02-00	0.0482	334.74
16 weeks	26-03-00	0.0498	347.83
20 weeks	18-04-00	0.0514	361.48
28 weeks	2-07-00	0.0516	360.07
44 weeks	6-08-00	0.0546	381.70

Table A37: The Conversion of Absorbance Readings into Cr(VI) Concentrations for New EAF Slag Balls with the pore moisture evaporated (particle size class:<75um)

<i>Sample</i>	<i>Date Analysed</i>	<i>Average Absorbance Reading</i>	<i>Cr(VI) conc.(ppb)</i>
0 weeks	7-11-99	0.0107	74.88
1 week	19-01-00	0.0213	148.74
2 weeks	19-01-00	0.0337	235.36
4 weeks	19-01-00	0.0508	354.72
8 weeks	18-02-00	0.0713	494.90
17 weeks	26-03-00	0.0758	529.10
20 weeks	18-04-00	0.0790	555.01
26 weeks	18-06-00	0.0769	535.73
34 weeks	6-08-00	0.0791	553.65

Table A 38: The Conversion of Absorbance Readings into Concentrations for New EAF Slag Balls with the pore moisture evaporated (particle size class:75-300um)

<i>Sample</i>	<i>Date Analysed</i>	<i>Average Absorbance Reading</i>	<i>Cr(VI) conc.(ppb)</i>
0 weeks	7-11-00	0.0104	72.77
1 week	19-01-00	0.0166	115.89
2 weeks	19-01-00	0.0216	150.84
4 weeks	19-01-00	0.0395	275.86
8 weeks	18-02-00	0.0740	513.66
17 weeks	26-03-00	0.0746	520.39
20 weeks	18-04-00	0.0755	530.83
26 weeks	18-06-00	0.0776	540.60
34 weeks	6-08-00	0.0748	523.08

Table A39: The Conversion of Absorbance Readings into Cr(VI) Concentrations for New EAF Slag Balls with the pore moisture evaporated (particle size class: 300-1000um)

<i>Sample</i>	<i>Date Analysed</i>	<i>Average Absorbance Reading</i>	<i>Cr(VI) conc. (ppb)</i>
0 weeks	7-11-99	0.0109	76.28
1 week	19-01-00	0.0298	208.12
2 weeks	19-01-00	0.0399	278.65
4 weeks	19-01-00	0.0618	431.47
8 weeks	18-02-00	0.0741	514.35
12 weeks	26-03-00	0.0755	526.67
16 weeks	18-04-00	0.0779	547.30
20 weeks	18-06-00	0.0788	548.95
28 weeks	6-08-00	0.0785	548.98

University of Cape Town

**APPENDIX A3: SAMPLE
CALCULATION SHOWING
HOW THE Cr(VI)
CONCENTRATIONS (ppb)
WERE USED TO CALCULATE
CONVERSIONS ($\mu\text{g per g Cr}$)**

University of Cape Town

SAMPLE CALCULATION FOR THE CALCULATION OF CONVERSIONS FROM CONCENTRATIONS

Example chosen: Cr₂O₃-CaO Powders (50% CaO) in a dessicator 1 week sample

Concentration of Cr(VI) in the sample = 23.75 ppb = 23.75 µg per litre

Therefore the mass of Cr(VI) that leached out in 1litre of NaOH = 23.75 µg

Mass of the sample weighed out initially =25.21g

Since the ratio of Cr₂O₃ to CaO is 1:1, the mass of Cr₂O₃ in the sample = 0.5 x 25.21
= 12.61g

Mass of Cr in Cr₂O₃ = (2 x 52) ÷ (152) = 0.68

Mass of Cr in the sample = 0.68 x 12.61g = 8.62 g

So, the conversion of Cr(III) to Cr(VI) = 23.75 ÷ 8.62 = 2.76µg per g Cr

For the slags, taking Old Mixed Slag Powder 75-300µm (0weeks) as an example :

Cr(VI) conc. (ppb) = 585.50µg per litre

The mass of Cr(VI) that leached out in 1l NaOH = 585.50µg

%Cr in the sample determined prior to leaching = 0.85

Mass of sample analysed = 25.01

Mass of Cr in the sample = 0.85 % of 25.01 = 0.21g

Conversion of Cr(III) to Cr(VI) = 585.5 ÷ 0.21 = 2754µg per g Cr

Notes:

1. In all cases, the number of days have been calculated from the date on which the experiment was set up to the date that the sample was taken.
2. For all of the ball samples mass of Cr was calculated relative to the mass analysed.
3. For the pure chemical powder and pellet samples mass of Cr was calculated relative to mass initially weighed out (excluding moisture uptake).
4. For slag powders mass of Cr was calculated relative to mass analysed as % Cr of the sample was determined after the uptake of moisture.

**APPENDIX A4: THE FULLY
TABULATED CONVERSION-
TIME DATA AND MOISTURE
CONTENTS FOR ALL THE
RESULTS SHOWN**

University of Cape Town

THE AMOUNT OF WATER ADDED TO $\text{Cr}_2\text{O}_3\text{-Ca(OH)}_2$ BALLS-SAMPLE CALCULATION

Example: $\text{Cr}_2\text{O}_3\text{-Ca(OH)}_2$ Balls with the pore moisture evaporated

Mass of water added (g): 185.23

Moles of water added = $185.23 \div 18 = 10.29$

Mass of CaO added in a 250g batch (g) = 125

Moles of CaO added = $125 \div 56 = 2.23$

Therefore enough water was added to convert CaO to Ca(OH)_2

University of Cape Town

Table A40: The conversion-time data for Cr₂O₃.CaO powder mixes containing 50% CaO and maintained in a dessicator

Sample	Mass initially weighed out (g)	Mass analysed (g)	Date of Analysis	Conc. Cr(VI) (ppb)	Mass of Cr(VI) in 1l NaOH (ug)	Mass of Cr ₂ O ₃ (g)	Mass of Cr(g)	Conversion (ug per g Cr)	Days	Sampling Dates
0 week	21.17	21.17	29-05-00	3.10	3.10	10.59	7.24	0.43	0	25-05-00
1 week	25.21	25.21	18-06-00	23.75	23.75	12.61	8.62	2.75	7	1-06-00
2 weeks	25.33	25.33	18-06-00	52.36	52.36	12.67	8.67	6.04	14	8-06-00
4 weeks	25.57	25.57	2-07-00	94.04	94.04	12.79	8.75	10.75	28	22-06-00
8 weeks	25.88	25.88	6-08-00	115.35	115.35	12.94	8.85	13.03	56	20-07-00
12 weeks	26.34	26.34	17-09-00	185.49	185.49	13.17	9.01	20.59	91	24-08-00

Date on which experiment was set up: 25-May-00

Table A41: The conversion-time data for Cr₂O₃ -CaO powders containing 20% CaO and exposed to ambient moisture

Sample	Mass initially weighed out (g)	Date of Analysis	Conc. Cr(VI) (ppb)	Mass of Cr(VI) in 1l NaOH (ug)	Mass of Cr ₂ O ₃ (g)	Mass of Cr (g)	Conversion (ug per g Cr)	Days	Sampling Dates
0 weeks	21.15	21-05-00	1.42	1.42	16.92	11.58	0.12	0	14-05-00
1 week	25.03	29-05-00	73.85	73.85	20.02	13.70	5.39	7	21-05-00
2 weeks	25.02	18-06-00	82.00	82.00	20.02	13.70	5.99	14	28-05-00
4 weeks	25.08	18-06-00	114.41	114.41	20.06	13.73	8.33	27	10-06-00
8 weeks	25.03	13-08-00	151.06	151.06	20.02	13.70	11.03	56	9-07-00
12 weeks	25.04	17-09-00	177.09	177.09	20.03	13.71	12.92	96	18-08-00

Date on which experiment was set up: 14-May-00

Table A42: The conversion-time data for Cr₂O₃-CaO powders containing 50% CaO and exposed to ambient moisture

Sample	Mass initially weighed out (g)	Date of Analysis	Cr(VI) conc. (ppb)	Mass of Cr(VI) in 1l NaOH (ug)	Mass of Cr ₂ O ₃ (g)	Mass of Cr (g)	Conversion (ug per g Cr)	Days	Sampling Dates
0 week	22.52	21-05-00	0.71	0.71	11.26	7.70	0.09	0	14-05-00
1 week	25.01	18-06-00	85.48	85.48	12.51	8.56	9.99	7	21-05-00
2 weeks	25.02	18-06-00	294.85	294.85	12.51	8.56	34.45	14	28-05-00
4 weeks	25.03	18-06-00	406.95	406.95	12.52	8.56	47.52	27	10-06-00
8 weeks	25.09	6-08-00	477.35	477.35	12.55	8.58	55.61	56	9-07-00
12 weeks	25.07	17-09-00	496.76	496.76	12.54	8.58	57.92	96	18-08-00

Date on which experiment was set up:14-May-00

Table A43: The conversion-time data for Cr₂O₃-CaO pellets containing 50% CaO and exposed to ambient moisture

Sample	Mass initially weighed out (g)	Date of Analysis	Cr(VI) conc. (ppb)	Mass of Cr(VI) in 1l NaOH (ug)	Mass of Cr ₂ O ₃ (g)	Mass of Cr (g)	Conversion (ug per g Cr)	Days	Sampling Dates
0 week	20.05	2-07-00	2.13	2.13	10.03	6.86	0.31	0	08-Jun-00
1 week	20.06	2-07-00	291.14	291.14	10.03	6.86	42.42	7	15-Jun-00
2 weeks	20.08	2-07-00	360.42	360.42	10.04	6.87	52.47	14	22-Jun-00
4 weeks	20.03	5-07-00	536.85	536.85	10.02	6.85	78.35	26	04-Jul-00
8 weeks	20.01	6-08-00	597.75	597.75	10.01	6.85	87.32	57	04-Aug-00
12 weeks	20.09	17-09-00	616.19	616.19	10.05	6.87	89.66	92	08-Sep-00

Date on which experiment was set up:8-Jun-00

Table A44: The Moisture Contents of Cr₂O₃-CaO powders containing 20% CaO and exposed to ambient moisture

<i>Sample</i>	<i>Mass initially weighed out (g)</i>	<i>Mass Analysed (g)</i>	<i>Moisture Content (g)</i>	<i>% Moisture Dry Mass Basis</i>	<i>Moles of atmospheric moisture</i>	<i>Mass of CaO in original sample (g)</i>	<i>Moles of CaO</i>
0 weeks	21.15	21.15	0	0.00	0.00	4.23	0.08
1 week	25.03	26.32	1.29	5.15	0.07	5.01	0.09
2 weeks	25.02	27.10	2.08	8.31	0.12	5.00	0.09
4 weeks	25.08	26.77	1.69	6.74	0.09	5.02	0.09
8 weeks	25.03	27.46	2.43	9.71	0.14	5.01	0.09
12 weeks	25.04	27.15	2.11	8.43	0.12	5.01	0.09

Table A45: The Moisture Contents of Cr₂O₃-CaO powders 50% CaO and exposed to ambient moisture

<i>Sample</i>	<i>Mass initially weighed out (g)</i>	<i>Mass Analysed (g)</i>	<i>Moisture Content (g)</i>	<i>% Moisture Dry Mass Basis</i>	<i>Moles of atmospheric moisture</i>	<i>Mass of CaO in original sample (g)</i>	<i>Moles of CaO</i>
0 week	22.52	22.52	0	0.00	0.00	11.26	0.20
1 week	25.01	28.06	3.05	12.20	0.17	12.51	0.22
2 weeks	25.02	28.77	3.75	14.99	0.21	12.51	0.22
4 weeks	25.03	28.76	3.73	14.90	0.21	12.52	0.22
8 weeks	25.09	30.5	5.41	21.56	0.30	12.55	0.22
12 weeks	25.07	30.35	5.28	21.06	0.29	12.54	0.22

Table A46: The Moisture Contents of Cr₂O₃-CaO pellets containing 50% CaO and exposed to ambient moisture

<i>Sample</i>	<i>Mass initially weighed out (g)</i>	<i>Mass Analysed (g)</i>	<i>Moisture Content (g)</i>	<i>% Moisture Dry Mass Basis</i>	<i>Moles of atmospheric moisture</i>	<i>Mass of CaO in the original sample (g)</i>	<i>Moles of CaO</i>
0 week	20.05	20.05	0	0.00	0.00	10.03	0.18
1 week	20.06	25.69	5.63	21.92	0.31	10.03	0.18
2 weeks	20.08	25.45	5.37	21.10	0.30	10.04	0.18
4 weeks	20.03	25.68	5.65	22.00	0.31	10.02	0.18
8 weeks	20.01	27.66	7.65	27.66	0.43	10.01	0.18
12 weeks	20.09	23.00	2.91	12.65	0.16	10.05	0.18

Table A47: The conversion-time data for Cr₂O₃-Ca(OH)₂ Balls containing 5% Ca(OH)₂ with the pore moisture maintained

Sample	Mass analysed (g)	Date of analysis	Conc. Cr(VI) (ppb)	Mass of Cr(VI) in 1l NaOH (ug)	Mass of Cr ₂ O ₃ (g)	Mass of Cr(g)	Conversion (ug per g Cr)	days	Sampling Date
0 weeks	15.87	23-6-99	3.51	3.51	15.08	10.32	0.34	0	10/06/99
1 week	24.43	23-6-99	5.85	5.85	23.21	15.88	0.37	8	18/06/99
2 weeks	23.35	30-6-99	8.86	8.86	22.18	15.18	0.58	15	25/06/99
4 weeks	22.07	22-7-99	10.29	10.29	20.97	14.35	0.72	29	9/07/99
8 weeks	22.78	23-8-99	10.03	10.03	21.64	14.81	0.68	64	13/08/99
12 weeks	23.28	29-9-99	18.48	18.48	22.12	15.13	1.22	92	10/09/99
16 weeks	21.42	7-11-99	23.61	23.61	20.35	13.92	1.70	120	8/10/99
20 weeks	20.68	30-11-99	25.90	25.90	19.65	13.44	1.93	154	11/11/99
28 weeks	23.62	18-02-00	32.96	32.96	22.44	15.35	2.15	225	21/01/00
44 weeks	20.04	21-05-00	32.77	32.77	19.04	13.03	2.52	337	12/05/00
56 weeks	23.68	13-08-00	39.26	39.26	22.50	15.39	2.55	421	4/08/00
Mass of water added to prepare balls (g): 72.95									
Date on which experiments were set up : 10 June 1999									
Repeat Experiments									
0 weeks	13.92	23-6-99	2.11	2.11	13.22	9.05	0.23	0	17/6/99
1 week	24.43	23-6-99	5.15	5.15	23.21	15.88	0.32	6	23/6/99
2 weeks	23.39	30-6-99	9.56	9.56	22.22	15.20	0.63	13	30/6/99
4 weeks	19.1	22-7-99	10.64	10.64	18.15	12.42	0.86	29	16/7/99
8 weeks	23.99	23-8-99	11.07	11.07	22.79	15.59	0.71	64	20/8/99
12 weeks	23.49	29-9-99	17.41	17.41	22.32	15.27	1.14	92	17/9/99
16 weeks	23.97	7-11-99	23.25	23.25	22.77	15.58	1.49	120	15/10/99
20 weeks	23.49	30-11-99	25.90	25.90	22.32	15.27	1.70	155	19/11/99
28 weeks	22.7	18-02-00	24.63	24.63	21.57	14.76	1.67	225	28/1/00
44 weeks	20.57	21-05-00	33.12	33.12	19.54	13.37	2.48	337	19/5/00
56 weeks	24.39	13-08-00	39.96	39.96	23.17	15.85	2.52	421	11/8/00
Date on which experiments were set up : 17 June 1999									
Mass of water added (g): 64.71									

Table A48: The Conversion -Time Data for Cr₂O₃-Ca(OH)₂ Balls containing 20% Ca(OH)₂ with the pore moisture maintained

Sample	Mass Analysed (g)	Date of Analysis	Cr(VI) conc. ppb	Mass of Cr(VI) in 1l NaOH (ug)	Mass of Cr ₂ O ₃ (g)	Mass of Cr(g)	Conversion (ug per g Cr)	days	Sampling Date
0 weeks	31.32	23-6-99	2.81	2.81	25.06	17.14	0.16	0	10/06/99
1 week	21.13	23-6-99	5.62	5.62	16.90	11.57	0.49	8	18/06/99
2 weeks	22.1	30-6-99	8.86	8.86	17.68	12.10	0.73	15	25/06/99
4 weeks	21.95	22-7-99	10.98	10.98	17.56	12.01	0.91	29	9/07/99
8 weeks	21.59	23-8-99	13.84	13.84	17.27	11.82	1.17	64	13/08/99
12 weeks	22.92	29-9-99	25.57	25.57	18.34	12.55	2.04	92	10/09/99
16 weeks	21.95	7-11-99	28.18	28.18	17.56	12.01	2.35	120	8/10/99
20 weeks	20.76	30-11-99	41.08	41.08	16.61	11.36	3.61	155	11/11/99
28 weeks	22.67	18-02-00	48.23	48.23	18.14	12.41	3.89	225	21/01/00
44 weeks	20.41	21-05-00	44.70	44.70	16.33	11.17	4.00	337	12/05/00
56 weeks	22.63	13-08-00	49.05	49.05	18.10	12.39	3.96	421	4/08/00

Mass of water added to prepare balls (g):106.36

Date on which experiment was set up:10 June 1999

Repeat Experiments

0 weeks	31.96	23-6-99	5.15	5.15	25.57	17.49	0.29	0	17/6/99
1 week	23.87	30-6-99	5.36	5.36	19.10	13.07	0.41	6	23/6/99
2 weeks	21.14	22-7-99	9.26	9.26	16.91	11.57	0.80	13	30/6/99
4 weeks	21.75	22-7-99	11.67	11.67	17.40	11.91	0.98	29	16/7/99
8 weeks	19.14	23-8-99	12.11	12.11	15.31	10.48	1.16	64	20/8/99
12 weeks	20.68	29-9-99	25.92	25.92	16.54	11.32	2.29	92	17/9/99
16 weeks	22.1	7-11-99	29.23	29.23	17.68	12.10	2.42	120	15/10/99
20 weeks	20.61	30-11-99	37.90	37.90	16.49	11.28	3.36	155	19/11/99
28 weeks	20.14	18-02-00	39.90	39.90	16.11	11.02	3.62	225	28/1/00
44 weeks	22.69	21-05-00	45.05	45.05	18.15	12.42	3.63	337	19/5/00
56 weeks	21.6	13-08-00	45.32	45.32	17.28	11.82	3.83	421	11/8/00

Mass of water added to prepare balls (g):107.4

Date on which experiment was set up:17-Jun-99

Table A49: The Conversion-Time Data for Cr₂O₃-Ca(OH)₂ Balls containing 50% Ca(OH)₂ with the pore moisture was maintained

Sample	Mass analysed (g)	Date of analysis	Conc. Cr(VI) (ppb)	Mass of Cr(VI) in 1l NaOH (ug)	Mass of Cr ₂ O ₃ (g)	Mass of Cr(g)	Conversion (ug per g Cr)	days	Sampling Date
0 weeks	15.82	23-6-99	1.87	1.87	7.91	5.41	0.35	0	14-Jun-99
1 week	24.43	23-6-99	7.25	7.25	12.22	8.36	0.87	8	22-Jun-99
2 weeks	27.97	30-6-99	13.52	13.52	13.99	9.57	1.41	15	29-Jun-99
4 weeks	23.48	22-7-99	19.25	19.25	11.74	8.03	2.40	28	12-Jul-99
8 weeks	27.17	23-8-99	37.43	37.43	13.59	9.30	4.03	60	13-Aug-99
12 weeks	26.3	29-9-99	49.30	49.30	13.15	9.00	5.48	92	14-Sep-99
16 weeks	25.92	7-11-99	60.14	60.14	12.96	8.87	6.78	120	12-Oct-99
20 weeks	26.46	30-11-99	67.49	67.49	13.23	9.05	7.46	155	16-Nov-99
28 weeks	26.78	18-02-00	86.42	86.42	13.39	9.16	9.43	225	25-Jan-00
44 weeks	27.11	21-05-00	90.95	90.95	13.56	9.27	9.81	337	"16-May-00"
56 weeks	25.92	13-08-99	85.64	85.64	12.96	8.87	9.66	421	"8-Aug-00"

Mass of water added to prepare balls (g): 165.22

Date on which experiment was set up: 14-Jun-99

Repeat Experiments

0 weeks	14.47	23-6-99	2.81	2.81	7.24	4.95	0.57	0	17/6/99
1 week	28.09	30-6-99	9.09	9.09	14.05	9.61	0.95	6	23/6/99
2 weeks	27.41	22-7-99	15.81	15.81	13.71	9.38	1.69	13	30/6/99
4 weeks	25.69	22-7-99	16.84	16.84	12.85	8.79	1.92	29	16/7/99
8 weeks	26.04	23-8-99	36.73	36.73	13.02	8.91	4.12	64	20/8/99
12 weeks	29.8	29-9-99	48.59	48.59	14.90	10.19	4.77	92	17/9/99
16 weeks	24.2	7-11-99	60.49	60.49	12.10	8.28	7.31	120	15/10/99
20 weeks	25.19	30-11-99	69.25	69.25	12.60	8.62	8.04	155	19/11/99
28 weeks	26.71	18-02-00	85.03	85.03	13.36	9.14	9.31	225	28/1/00
44 weeks	25.34	21-05-00	87.45	87.45	12.67	8.67	10.09	337	19/5/00
56 weeks	24.42	13-08-00	86.57	86.57	12.21	8.35	10.36	421	11/8/00

Date on which experiment was set up : 17-Jun-99

Mass of water added to prepare balls (g): 178.58

Table A50: The Conversion-Time Data for Cr₂O₃-Ca(OH)₂ Balls containing 20% Ca(OH)₂ and where the excess pore moisture was allowed to evaporate

Sample	Mass analysed (g)	Date of analysis	Conc. Cr(VI) (ppb)	Mass of Cr(VI) in 1l NaOH (ug)	Mass of Cr ₂ O ₃ (g)	Mass of Cr(g)	Conversion (ug per g Cr)	days	Sampling Date
0 weeks	18.01	23-6-99	0.94	0.94	14.41	9.86	0.09	0	14-Jun-99
1 week	26.38	23-6-99	3.51	3.51	21.10	14.44	0.24	8	22-Jun-99
2 weeks	25.86	30-6-99	7.46	7.46	20.69	14.15	0.53	15	29-Jun-99
4 weeks	27.13	22-7-99	11.67	11.67	21.70	14.85	0.79	28	12-Jul-99
8 weeks	27.2	23-8-99	45.76	45.76	21.76	14.89	3.07	60	13-Aug-99
12 weeks	28.08	29-9-99	78.32	78.32	22.46	15.37	5.10	92	14-Sep-99
16 weeks	23.22	7-11-99	107.14	107.14	18.58	12.71	8.43	120	12-Oct-99
20 weeks	27.7	30-11-99	130.38	130.38	22.16	15.16	8.60	155	16-Nov-99
28 weeks	28.61	18-02-00	198.58	198.58	22.89	15.66	12.68	225	25-Jan-00
44 weeks	28.24	21-05-00	297.96	297.96	22.59	15.46	19.28	337	16th-May-00
56 weeks	28.58	13-08-99	240.60	240.60	22.86	15.64	15.38	421	8th-Aug-00

Date on which experiment was set up: 14 June 1999

Mass of water added to prepare balls (g): 101.1

Repeat Experiments

0 weeks	26.38	23-6-99	2.11	2.11	21.10	14.44	0.15	0	21-Jun-99
1 week	25.08	30-6-99	6.30	6.30	20.06	13.73	0.46	8	29-Jun-99
2 weeks	24.91	22-7-99	15.12	15.12	19.93	13.63	1.11	15	06-Jul-99
4 weeks	21.29	22-7-99	10.64	10.64	17.03	11.65	0.91	29	20-Jul-99
8 weeks	23.02	23-8-99	48.19	48.19	18.42	12.60	3.82	60	20-Aug-99
12 weeks	26.88	29-9-99	81.86	81.86	21.50	14.71	5.56	92	21-Sep-99
16 weeks	26.71	7-11-99	112.05	112.05	21.37	14.62	7.66	120	19-Oct-99
20 weeks	27.9	30-11-99	131.43	131.43	22.32	15.27	8.61	155	23-Nov-99
28 weeks	27.62	18-02-00	197.89	197.89	22.10	15.12	13.09	225	01-Feb-00
44 weeks	27.62	21-05-00	214.97	214.97	22.10	15.12	14.22	330	16-May-00
56 weeks	28.49	13-08-00	239.91	239.91	22.79	15.59	15.38	416	10-Aug-00

Mass of water added to prepare balls (g):

102

Date on which experiment was set up:

21-Jun-99

Table A51: The Conversion-Time Data for Cr₂O₃-Ca(OH)₂ Balls containing 50% Ca(OH)₂ and where the excess pore moisture evaporated

Sample	Mass analysed (g)	Date of analysis	Conc. Cr(VI) (ppb)	Mass of Cr(VI) in 1l NaOH (ug)	Mass of Cr ₂ O ₃ (g)	Mass of Cr(g)	Conversion (ug per g Cr)	days	Sampling Date
0 weeks	27.75	19-01-00	1.76	1.76	13.88	9.49	0.19	0	9-11-99
1 week	27.56	19-01-00	11.95	11.95	13.78	9.43	1.27	8	17-11-99
2 weeks	24.21	19-01-00	40.33	40.33	12.11	8.28	4.87	15	24-11-99
4 weeks	29.8	19-01-00	62.39	62.39	14.90	10.19	6.12	24	3-12-99
10 weeks	29.03	18-02-00	81.56	81.56	14.52	9.93	8.21	73	21-01-00
12 weeks	26.82	26-03-00	110.54	110.54	13.41	9.18	12.05	91	8-02-00
16 weeks	27.51	18-04-00	158.45	158.45	13.76	9.41	16.84	119	7-03-00
20 weeks	25.31	21-05-00	263.80	263.80	12.66	8.66	30.47	147	4-04-00
28 weeks	26.7	5-07-00	295.52	295.52	13.35	9.13	32.35	210	6-06-00

Mass of water added (g): 185.23
 Date on which experiment was set up: 09-Nov-00

Repeat Experiments

0 weeks	19.96	18-02-00	2.43	2.43	9.98	6.83	0.36	0	23-Jan-00
1 week	24.98	26-03-00	7.73	7.73	12.49	8.55	0.90	8	31-Jan-00
2 weeks	22.01	26-03-00	38.19	38.19	11.01	7.53	5.07	15	07-Feb-00
4 weeks	21.58	26-03-00	60.92	60.92	10.79	7.38	8.25	29	21-Feb-00
8 weeks	23.45	26-03-00	80.34	80.34	11.73	8.02	10.01	57	20-Mar-00
12 weeks	22.72	18-04-00	102.78	102.78	11.36	7.77	13.22	85	17-Apr-00
16 weeks	22.1	21-05-00	151.54	151.54	11.05	7.56	20.04	118	20-May-00
20 weeks	21.19	18-06-00	257.94	257.94	10.60	7.25	35.58	146	17-Jun-00
28 weeks	20.12	6-08-00	295.86	295.86	10.06	6.88	42.98	195	06-Aug-00

Mass of water added (g): 189.39
 Date on which experiment was set up: 23-Jan-00

Table A52: The Conversion-Time Data for Cr₂O₃-Ca(OH)₂ (50% Ca(OH)₂) maintained under nitrogen and with the excess pore moisture evaporated

Sample	Mass analysed (g)	Date of analysis	Conc. Cr(VI) (ppb)	Mass of Cr(VI) in 1l NaOH (ug)	Mass of Cr ₂ O ₃ (g)	Mass of Cr(g)	Conversion (ug per g Cr)	days	Sampling Date
0 weeks	25.49	"9-Mar-2001"	0.70	0.70	12.75	8.72	0.08	0	"2001/02/13"
1 week	24.93	"9-Mar-2001"	1.05	1.05	12.47	8.53	0.12	7	"2001/02/20"
2 weeks	25.71	"9-Mar-2001"	1.05	1.05	12.86	8.80	0.12	14	"2001/02/27"
4 weeks	25.18	"8-Apr-2001"	1.12	1.12	12.59	8.61	0.13	29	"2001/03/14"
7 weeks	24.97	"8-Apr-2001"	1.12	1.12	12.49	8.54	0.13	49	"2001/04/03"

Mass of water added to prepare balls (g):191.68

Date on which experiment was set up :13 February 2001

Table A53: The Conversion-time Data for Cr₂O₃-Ca(OH)₂ Balls (50% Ca(OH)₂) exposed to air (Controls for Nitrogen Experiments)

Sample	Mass analysed (g)	Date of analysis	Conc. Cr(VI) (ppb)	Mass of Cr(VI) in 1l NaOH (ug)	Mass of Cr ₂ O ₃ (g)	Mass of Cr(g)	Conversion (ug per g Cr)	days	Sampling Date
2 weeks	25.60	8-Apr-01	1.85	1.85	12.80	8.76	0.21	14	27-Feb-01
4 weeks	25.39	8-Apr-01	46.05	46.05	12.70	8.69	5.30	29	14-Mar-01
7 weeks	25.21	8-Apr-01	54.86	54.86	12.61	8.62	6.36	49	03-Apr-01

Mass of water added (g):191.68

Date on which experiment was set up :13 February 2001

Table A54: The Conversion-time Data for Cr₂O₃-Ca(OH)₂ Balls (20% Ca(OH)₂) maintained 50°C (pore moisture evaporated)

Sample	Mass analysed (g)	Date of analysis	Conc. Cr(VI) (ppb)	Mass of Cr(VI) in 1l NaOH (ug)	Mass of Cr ₂ O ₃ (g)	Mass of Cr(g)	Conversion (ug per g Cr)	days	Sampling Date
0 weeks	21.71	26-03-00	3.16	3.16	17.37	11.88	0.27	0	06-Feb-00
1 week	22.65	26-03-00	8.78	8.78	18.12	12.40	0.71	8	14-Feb-00
2 weeks	21.82	26-03-00	16.84	16.84	17.46	11.94	1.41	15	21-Feb-00
4 weeks	24.32	26-03-00	38.19	38.19	19.46	13.31	2.87	29	06-Mar-00
7 weeks	23.62	26-03-00	94.82	94.82	18.90	12.93	7.33	48	25-Mar-00
10 weeks	22.49	18-04-00	250.20	250.20	17.99	12.31	20.32	71	17-Apr-00
15 weeks	22.32	21-05-00	394.11	394.11	17.86	12.22	32.26	104	20-May-00
19 weeks	23.62	5-07-00	432.46	432.46	18.90	12.93	33.45	132	17-Jun-00
26 weeks	24.89	6-08-00	465.22	465.22	19.91	13.62	34.15	180	04-Aug-00

Mass of water added (g):90.51

Date on which experiment was set up:6-Feb-00

0 weeks	22.23	26-03-00	5.97	5.97	17.78	12.17	0.49	0	08-Feb-00
1 week	27.56	26-03-00	8.43	8.43	22.05	15.09	0.56	8	16-Feb-00
2 weeks	24.73	26-03-00	15.08	15.08	19.78	13.54	1.11	15	23-Feb-00
4 weeks	32.00	26-03-00	37.49	37.49	25.60	17.52	2.14	29	08-Mar-00
7 weeks	28.76	26-03-00	93.07	93.07	23.01	15.74	5.91	46	25-Mar-00
10 weeks	25.62	18-04-00	247.74	247.74	20.50	14.02	17.67	69	17-Apr-00
15 weeks	26.42	21-05-00	387.84	387.84	21.14	14.46	26.82	102	May-00
19 weeks	27.45	5-07-00	431.07	431.07	21.96	15.03	28.69	130	17-Jun-00
26 weeks	23.32	6-08-00	463.59	463.59	18.66	12.76	36.32	178	04-Aug-00

Mass of water added (g):111.86

Date on which experiment was set up:8-Feb-00

Table A55: The Conversion-Time Data for $\text{Cr}_2\text{O}_3\text{-Ca(OH)}_2$ (20% Ca(OH)_2) maintained at eighty degrees (pore moisture evaporated)

Sample	Mass analysed (g)	Date of analysis	Conc. Cr(VI) (ppb)	Mass of Cr(VI) in 1l NaOH (ug)	Mass of Cr ₂ O ₃ (g)	Mass of Cr(g)	Conversion (ug per g Cr)	days	Sampling Date
0 weeks	21.1	23-6-99	0.94	0.94	16.88	11.55	0.08	0	21-Jun-99
1 week	23.37	30-6-99	10.96	10.96	18.70	12.79	0.86	8	29-Jun-99
2 weeks	24.03	22-7-99	32.37	32.37	19.22	13.15	2.46	15	06-Jul-99
4 weeks	20.94	22-7-99	60.72	60.72	16.75	11.46	5.30	29	20-Jul-99
8 weeks	25.68	23-8-99	226.92	226.92	20.54	14.06	16.14	60	20-Aug-99
12 weeks	26.54	29-9-99	464.91	464.91	21.23	14.53	32.00	92	21-Sep-99
16 weeks	23.36	7-11-99	698.58	698.58	18.69	12.79	54.63	120	19-Oct-99
20 weeks	28.96	30-11-99	851.96	851.96	23.17	15.85	53.75	155	23-Nov-99
28 weeks	22.48	18-02-00	1080.08	1080.08	17.98	12.30	87.78	225	01-Feb-00
44 weeks	19.76	18-06-00	1144.52	1144.52	15.81	10.82	105.82	330	16-May-00
56 weeks	20.28	13-08-00	1193.80	1193.80	16.22	11.10	107.54	416	10-Aug-00

Mass of water added (g):85.41

Date on which experiment was set up:21June 1999

0 weeks	26.4	30-6-99	3.50	3.50	21.12	14.45	0.24	0	24-Jun-99
1 week	23.37	22-7-99	12.70	12.70	18.70	12.79	0.99	7	01-Jul-99
2 weeks	22.52	22-7-99	27.53	27.53	18.02	12.33	2.23	14	08-Jul-99
4 weeks	20.94	23-8-99	59.65	59.65	16.75	11.46	5.20	27	21-Jul-99
8 weeks	21.28	23-8-99	226.22	226.22	17.02	11.65	19.42	57	20-Aug-99
12 weeks	29.9	29-9-99	456.96	456.96	23.92	16.37	27.92	90	22-Sep-99
16 weeks	25.66	7-11-99	696.13	696.13	20.53	14.05	49.56	118	20-Oct-99
20 weeks	24.91	30-11-99	848.83	848.83	19.93	13.63	62.25	153	24-Nov-99
28 weeks	23.9	18-02-00	1095.02	1095.02	19.12	13.08	83.70	225	04-Feb-00
44 weeks	22.51	18-06-00	1158.43	1158.43	18.01	12.32	94.02	329	18-May-00
56 weeks	21.69	13-08-00	1200.52	1200.52	17.35	11.87	101.12	413	10-Aug-00

Mass of water added (g):87.8

Date on which experiment was set up:24-Jun-99

Table A56: The Moisture Contents of Cr₂O₃-Ca(OH)₂ Balls (5% Ca(OH)₂ with excess pore moisture maintained)

<i>Sample</i>	<i>wet mass</i> (g)	<i>dry mass</i> (g)	<i>Moisture Content (g)</i>	<i>% Moisture</i> <i>dry mass basis</i>
0 weeks	20.1	16.06	4.04	25.16
1 week	30.03	25.08	4.95	19.74
2 weeks	28.86	23.44	5.42	23.12
4 weeks	26.55	22.13	4.42	19.97
8 weeks	25.69	22.89	2.8	12.23
12 weeks	25.52	23.33	2.19	9.39
16 weeks	23.59	21.47	2.12	9.87
20 weeks	21.74	20.72	1.02	4.92
28 weeks	27.71	23.63	4.08	17.27
44 weeks	25.1	20.08	5.02	25.00
56 weeks	29.89	24.03	5.86	24.39

Repeat Experiments

0 weeks	16.75	14.44	2.31	16.00
1 week	30.03	25.08	4.95	19.74
2 weeks	28.88	23.55	5.33	22.63
4 weeks	23.57	19.19	4.38	22.82
8 weeks	27.52	24.02	3.5	14.57
12 weeks	25.82	23.55	2.27	9.64
16 weeks	24.53	24.02	0.51	2.12
20 weeks	25.63	23.58	2.05	8.69
28 weeks	28.81	22.74	6.07	26.69
44 weeks	25.62	20.6	5.02	24.37
56 weeks	29.41	24.45	4.96	20.29

Table A57: The Moisture Contents of Cr₂O₃-Ca(OH)₂ Balls (20% Ca(OH)₂ with excess pore moisture maintained)

<i>Sample</i>	<i>wet mass</i>	<i>dry mass</i>	<i>Moisture Content (g)</i>	<i>% Moisture</i>
	<i>(g)</i>	<i>(g)</i>		<i>dry mass basis</i>
0 weeks	35.18	31.77	3.41	10.73
1 week	28.8	21.67	7.13	32.90
2 weeks	29.38	22.18	7.2	32.46
4 weeks	28.78	21.98	6.8	30.94
8 weeks	27.97	24.4	3.57	14.63
12 weeks	26.73	22.95	3.78	16.47
16 weeks	23.27	21.97	1.3	5.92
20 weeks	22.83	20.81	2.02	9.71
28 weeks	28.67	22.71	5.96	26.24
44 weeks	25.49	20.47	5.02	24.52
56 weeks	27.92	22.83	5.09	22.30

Repeat Experiments

0 weeks	38.93	33	5.93	17.97
1 week	32.05	23.9	8.15	34.10
2 weeks	28.23	21.14	7.09	33.54
4 weeks	29.01	21.79	7.22	33.13
8 weeks	23.5	19.18	4.32	22.52
12 weeks	24.41	20.6	3.81	18.50
16 weeks	26.3	22.13	4.17	18.84
20 weeks	25.09	20.67	4.42	21.38
28 weeks	23.59	20.16	3.43	17.01
44 weeks	30.12	22.74	7.38	32.45
56 weeks	28.89	21.67	7.22	33.32

Table A 58: The Moisture Contents of Cr₂O₃-Ca(OH)₂ Balls (50% Ca(OH)₂ with pore moisture maintained)

Sample	wet mass (g)	dry mass (g)	Moisture Content (g)	% Moisture dry mass basis
0 weeks	20.31	16.59	3.72	22.42
1 week	30.03	25.08	4.95	19.74
2 weeks	41.21	28.11	13.1	46.60
4 weeks	33.56	23.64	9.92	41.96
8 weeks	37.85	27.36	10.49	38.34
12 weeks	35.03	26.48	8.55	32.29
16 weeks	34.69	25.95	8.74	33.68
20 weeks	30.48	26.63	3.85	14.46
28 weeks	36.96	26.93	10.03	37.24
44 weeks	31.91	27.2	4.71	17.32
56 weeks	34.39	26.21	8.18	31.21

Repeat Experiments

0 weeks	20.65	18.92	1.73	9.14
1 week	42.07	28.22	13.85	49.08
2 weeks	40.98	27.47	13.51	49.18
4 weeks	36.79	25.75	11.04	42.87
8 weeks	37.97	26.14	11.83	45.26
12 weeks	35.98	30.5	5.48	17.97
16 weeks	31.75	24.24	7.51	30.98
20 weeks	28.77	25.28	3.49	13.81
28 weeks	37.45	26.83	10.62	39.58
44 weeks	32.19	25.61	6.58	25.69
56 weeks	33.37	24.48	8.89	36.32

Table A59: The Conversion Time Data for Old Mixed Slag Powders Exposed to Air

Sample	Mass Analysed (g)	%Cr prior to leaching	Date of Analysis	Conc. Cr(VI) (ppb)	Mass of Cr(VI) in 1l NoOH	Mass Cr (g)	Conversion (ug per g Cr)	Days	Sampling Date
75-300um									
0 weeks	25.01	0.85	29-05-00	585.50	585.50	0.21	2754	0	25-May-00
1 week	26.33	0.91	18-06-00	1173.73	1173.73	0.24	4899	8	02-Jun-00
2 weeks	27.43	0.96	18-06-00	1673.03	1673.03	0.26	6353	15	09-Jun-00
4 weeks	27.49	0.97	2-07-00	2004.17	2004.17	0.27	7516	29	23-Jun-00
8 weeks	27.99	0.99	6-08-00	2019.98	2019.98	0.28	7290	57	21-Jul-00
12 weeks	28.55	0.8	24-09-00	2067.53	2067.53	0.23	9052	92	25-Aug-00
Date on which experiment was set up: 25 May 2000									
300-1000um									
0 weeks	25.08	2.65	18-06-00	622.38	622.38	0.66	936	0	25-May-00
1 week	25.25	2.62	18-06-00	1132.00	1132.00	0.66	1711	8	02-Jun-00
2 weeks	26.36	2.69	18-06-00	1701.19	1701.19	0.71	2399	15	09-Jun-00
4 weeks	27.42	2.68	2-07-00	1737.72	1737.72	0.73	2365	29	23-Jun-00
8 weeks	26.81	2.74	6-08-00	1963.01	1963.01	0.73	2672	57	21-Jul-00
12 weeks	27.29	2.77	24-09-00	1994.19	1994.19	0.76	2638	92	25-Aug-00
Date on which experiment was set up: 25 May 2000									

Table A60: The Conversion-Time Data for New CLU Powders Exposed to Air

Sample	Mass analysed (g)	%Cr prior to leaching	Date of Analysis	Conc. Cr(VI) (ppb)	Mass of Cr(VI) in 1l NaOH (ug)	Mass Cr (g)	Conversion (ug per g Cr)	Days	Sampling Date
<75um									
0 weeks	25.01	0.85	29-5-00	281.11	281.11	0.21	1322	0	25-May-00
1 week	25.12	0.75	18-06-00	572.27	572.27	0.19	3038	7	01-Jun-00
2 weeks	25.45	0.91	18-06-00	1171.99	1171.99	0.23	5061	14	08-Jun-00
4 weeks	25.23	0.92	2-07-00	1263.27	1263.27	0.23	5442	28	22-Jun-00
8 weeks	25.39	0.93	13-08-00	1404.51	1404.51	0.24	5948	56	20-Jul-00
12 weeks	26.42	0.99	24-09-00	1673.17	1673.17	0.26	6397	91	24-Aug-00
75-300um									
0 weeks	24.95	1.51	18-06-00	265.94	265.94	0.38	706	0	25-May-00
1 week	25.06	1.54	18-06-00	421.57	421.57	0.39	1092	7	01-Jun-00
2 weeks	27.85	1.52	18-06-00	639.08	639.08	0.42	1510	14	08-Jun-00
4 weeks	28.05	1.51	2-07-00	883.27	883.27	0.42	2085	28	22-Jun-00
8 weeks	25.16	1.55	6-08-00	1110.94	1110.94	0.39	2849	56	20-Jul-00
12 weeks	26.79	1.49	24-09-00	1175.89	1175.89	0.40	2946	91	24-Aug-00
300-1000um									
0 week	25.06	2.57	18-06-00	142.99	142.99	0.64	222	0	25-May-00
1 week	25.39	2.59	18-06-00	315.74	315.74	0.66	480	7	01-Jun-00
2 weeks	25.85	2.61	18-06-00	610.90	610.90	0.67	905	14	08-Jun-00
4 weeks	27.92	2.56	2-07-00	1129.84	1129.84	0.71	1581	28	22-Jun-00
8 weeks	25.2	2.57	13-08-00	1207.48	1207.48	0.65	1864	56	20-Jul-00
12 weeks	27.29	2.52	24-09-00	1307.65	1307.65	0.69	1901	91	24-Aug-00
Date on which experiments were set up: 25 May 2000									

Table A61: The Conversion-Time Data for New EAF Slag Powders Exposed to Air

Sample	Mass analysed (g)	%Cr prior to leaching	Date of Analysis	Conc. Cr(VI) (ppb)	Mass of Cr(VI) in 1l NaOH (ug)	Mass Cr (g)	Conversion (ug per g Cr)	Days	Sampling Date
<75um									
0 week	25.09	0.75	2-07-00	212.38	212.38	0.19	1129	0	09-Jun-00
1 week	25.14	0.72	2-07-00	436.26	436.26	0.18	2410	7	16-Jun-00
2 weeks	25.52	0.79	2-07-00	930.80	930.80	0.20	4617	14	23-Jun-00
4 weeks	27.89	0.75	5-07-00	1089.45	1089.45	0.21	5208	25	04-Jul-00
8 weeks	26.49	0.71	13-08-00	1097.11	1097.11	0.19	5833	59	07-Aug-00
12 weeks	28.59	0.8	24-09-00	1101.87	1101.87	0.23	4818	91	08-Sep-00
75-300um									
0 week	25.09	1.03	2-07-00	219.35	219.35	0.26	849	0	09-Jun-00
1 week	25.59	0.99	2-07-00	428.96	428.96	0.25	1693	7	16-Jun-00
2 week	28.74	1.09	2-07-00	880.84	880.84	0.31	2812	14	23-Jun-00
4 week	28.49	1.03	2-07-00	924.55	924.55	0.29	3151	25	04-Jul-00
8 weeks	25.32	1.02	13-08-00	1041.23	1041.23	0.26	4032	59	07-Aug-00
12 weeks	29.49	0.98	24-09-00	1156.27	1156.27	0.29	4001	91	08-Sep-00
300-1000um									
0 weeks	25.06	2.23	2-07-00	178.90	178.90	0.56	320	0	09-Jun-00
1 week	25.14	2.34	2-07-00	359.03	359.03	0.59	610	7	16-Jun-00
2 weeks	27.47	2.25	2-07-00	728.83	728.83	0.62	1179	14	23-Jun-00
4 weeks	28.89	2.21	2-07-00	987.68	987.68	0.64	1547	25	04-Jul-00
8 weeks	25.61	2.49	13-08-00	1117.52	1117.52	0.64	1752	59	07-Aug-00
12 weeks	29.89	2.22	24-09-00	1265.69	1265.69	0.66	1907	91	08-Sep-00
Dates on which experiments were set up: 9 June 2000									

Table A62: The Moisture Content of Old Mixed Slag Powders Exposed to Ambient Moisture

<i>Sample</i>	<i>Initial Mass (g)</i>	<i>Mass analysed (g)</i>	<i>Moisture content (g)</i>	<i>% Moisture (Dry Mass Basis)</i>
75-300um				
0 weeks	25.01	25.01	0	0.00
1 week	25.03	26.33	1.3	5.19
2 weeks	25.04	27.43	2.39	9.54
4 weeks	25.05	27.49	2.44	9.74
8 weeks	25.04	27.99	2.95	11.78
12 weeks	25.09	28.55	3.46	13.79
300-1000um				
0 weeks	25.08	25.08	0	0.00
1 week	25.01	25.25	0.24	0.96
2 weeks	25	26.36	1.36	5.44
4 weeks	25.06	27.42	2.36	9.42
8 weeks	25.05	26.81	1.76	7.03
12 weeks	25.07	27.29	2.22	8.86

Table A63 The Moisture Content of New CLU Slag Powders Exposed to Ambient Moisture

<i>Sample</i>	<i>Initial Mass (g)</i>	<i>Mass analysed (g)</i>	<i>Moisture content (g)</i>	<i>% Moisture (Dry Mass Basis)</i>
75um				
0 weeks	25.01	25.01	0	0.00
1 week	25.09	25.12	0.03	0.12
2 weeks	25.08	25.45	0.37	1.48
4 weeks	25.04	25.23	0.19	0.76
8 weeks	25.01	25.39	0.38	1.52
12 weeks	25.03	26.42	1.39	5.55
75-300 um				
0 weeks	24.95	24.95	0	0.00
1 week	24.93	25.06	0.13	0.52
2 weeks	25.01	27.85	2.84	11.36
4 weeks	25.07	28.05	2.98	11.89
8 weeks	25.06	25.16	0.1	0.40
12 weeks	25.09	26.79	1.7	6.78
300-1000um				
0 week	25.06	25.06	0	0.00
1 week	25.04	25.39	0.35	1.40
2 weeks	25.03	25.85	0.82	3.28
4 weeks	25.02	27.92	2.9	11.59
8 weeks	25.01	25.2	0.19	0.76
12 weeks	25.06	27.29	2.23	8.90

Table A64: The Moisture Contents for New EAF Slag Powders Exposed to Ambient Moisture

<i>Sample</i>	<i>Initial Mass (g)</i>	<i>Mass analysed (g)</i>	<i>Moisture content (g)</i>	<i>% Moisture (Dry Mass Basis)</i>
<75um				
0 week	25.09	25.09	0	0.00
1 week	25.03	25.14	0.11	0.44
2 weeks	25.08	25.52	0.44	1.72
4 weeks	25.01	27.89	2.88	10.33
8 weeks	25.06	26.49	1.43	5.40
12 weeks	25.04	28.59	3.55	12.42
75-300um				
0 week	25.09	25.09	0	0.00
1 week	24.97	25.59	0.62	2.48
2 week	25.01	28.74	3.73	14.91
4 week	25.07	28.49	3.42	13.64
8 weeks	25.02	25.32	0.3	1.20
12 weeks	25.09	29.49	4.4	17.54
300-1000um				
0 weeks	25.06	25.06	0	0.00
1 week	25.03	25.14	0.11	0.44
2 weeks	25.09	27.47	2.38	9.49
4 weeks	25.02	28.89	3.87	15.47
8 weeks	25.04	25.61	0.57	2.28
12 weeks	25.01	29.89	4.88	19.51

Table A65: The Conversion-Time Data for Old Mixed Slag Balls with the excess pore moisture maintained (particle size class: <75um)

Sample	Mass analysed (g)	%Cr prior to leaching	Date of Analysis	Conc. Cr(VI) (ppb)	Mass of Cr(VI) in 1l NaOH (ug)	Mass Cr (g)	Conversion (ug per g Cr)	Days	Sampling Date
0 weeks	25.83	0.79	29-9-99	214.73	214.73	0.20	1052	0	15-Sep-99
1 week	22.26	0.77	29-9-99	279.69	279.69	0.17	1632	7	22-Sep-99
2 weeks	21.69	0.78	7-11-99	340.32	340.32	0.17	2012	15	30-Sep-99
4 weeks	20.73	0.74	7-11-99	410.62	410.62	0.15	2677	27	12-Oct-99
8 weeks	25.62	0.73	19-01-00	579.67	579.67	0.19	3099	62	16-Nov-99
12 weeks	20.67	0.71	18-02-00	700.59	700.59	0.15	4774	79	03-Dec-99
16 weeks	20.41	0.74	26-03-00	778.91	778.91	0.15	5157	124	17-Jan-00
20 weeks	20.14	0.75	18-04-00	796.63	796.63	0.15	5274	159	21-Feb-00
28 weeks	24.35	0.77	18-06-00	935.14	935.14	0.19	4988	215	17-Apr-00
44 weeks	23.78	0.76	13-08-00	952.87	952.87	0.18	5272	332	12-Aug-00

mass of water added to prepare balls (g):93.51
Date on which experiment was set up:15-Sep-99

Table A66: The Conversion-Time Data for Old Mixed Slag Balls with the excess pore moisture maintained (particle size class:75-300um)

Sample	Mass analysed (g)	%Cr prior to leaching	Date of Analysis	Conc. Cr(VI) (ppb)	Mass of Cr(VI) in 1l NaOH (ug)	Mass Cr (g)	Conversion (ug per g Cr)	Days	Sampling Date
0 weeks	22.45	0.85	29-9-99	185.42	185.42	0.19	972	0	15-Sep-99
1 week	25.37	0.87	29-9-99	418.00	418.00	0.22	1894	7	22-Sep-99
2 weeks	23.62	0.86	7-11-99	557.08	557.08	0.20	2742	15	30-Sep-99
4 weeks	16.72	0.88	7-11-99	756.90	756.90	0.15	5144	27	12-Oct-99
8 weeks	21.21	0.82	19-01-00	1008.97	1008.97	0.17	5801	62	16-Nov-99
12 weeks	24.16	0.89	18-02-00	1386.62	1386.62	0.22	6449	79	03-Dec-99
16 weeks	20.65	0.83	26-03-00	1517.30	1517.30	0.17	8853	124	17-Jan-00
20 weeks	21.12	0.84	18-04-00	1921.04	1921.04	0.18	10828	159	21-Feb-00
28 weeks	25.89	0.81	18-06-00	1910.47	1910.47	0.21	9110	215	17-Apr-00
44 weeks	20.53	0.8	13-08-00	1917.99	1917.99	0.16	11678	332	12-Aug-00

Mass of water added : (g):51.12
Date on which experiment was set up: 15 September 1999

Table A67: The Conversion-Time Data for Old Mixed Slag Balls with the pore moisture maintained (particle size class: 300-1000um)

Sample	Mass analysed (g)	%Cr prior to leaching	Date of Analysis	Conc. Cr(VI) (ppb)	Mass of Cr(VI) in 1l NaOH (ug)	Mass Cr (g)	Conversion (ug per g Cr)	Days	Sampling Date
0 weeks	35.04	2.45	29-9-99	185.77	185.77	0.86	216	0	15-Sep-99
1 week	23.94	2.49	29-9-99	379.20	379.20	0.60	636	7	22-Sep-99
2 weeks	17.6	2.5	7-11-99	639.19	639.19	0.44	1453	15	30-Sep-99
4 weeks	20.83	2.41	7-11-99	764.59	764.59	0.50	1523	27	12-Oct-99
8 weeks	26.63	2.42	19-01-00	876.25	876.25	0.64	1360	62	16-Nov-99
12 weeks	20.18	2.45	18-02-00	1087.72	1087.72	0.49	2200	79	03-Dec-99
16 weeks	23.4	2.43	26-03-00	1339.81	1339.81	0.57	2356	124	17-Jan-00
20 weeks	23.19	2.4	18-04-00	1407.43	1407.43	0.56	2529	159	21-Feb-00
28 weeks	18.58	2.49	18-06-00	1430.70	1430.70	0.46	3092	215	17-Apr-00
44 weeks	26.1	2.41	13-08-00	2002.53	2002.53	0.63	3184	332	12-Aug-00
Mass of water added to prepare balls (g):37.43 Date on which experiment was set up: 15 September 1999									

Table A68: The Conversion-Time Data for Old Mixed Slag Balls with the pore moisture evaporated (particle size class:<75um)

Sample	Mass analysed (g)	%Cr prior to leaching	Date of Analysis	Conc. Cr(VI) (ppb)	Mass of Cr(VI) in 1l NaOH (ug)	Mass Cr (g)	Conversion (ug per g Cr)	Days	Sampling Date
0 weeks	28.92	0.81	7-11-99	213.29	213.29	0.23	911	0	25-Sep-99
1 week	27.87	0.75	7-11-99	416.56	416.56	0.21	1993	7	02-Oct-99
2 weeks	21.63	0.8	7-11-99	568.96	568.96	0.17	3288	14	09-Oct-99
4 weeks	25.71	0.77	30-11-99	837.69	837.69	0.20	4231	28	23-Oct-99
8 weeks	21.39	0.75	18-02-00	960.87	960.87	0.16	5990	63	27-Nov-99
12 weeks	26.42	0.72	26-03-00	1245.14	1245.14	0.19	6546	103	06-Jan-00
16 weeks	27.52	0.71	18-04-00	1280.25	1280.25	0.20	6552	121	24-Jan-00
20 weeks	24.9	0.7	21-05-00	1279.20	1279.20	0.17	7339	156	28-Feb-00
28 weeks	24.32	0.75	18-06-00	1320.13	1320.13	0.18	7238	215	27-Apr-00
Mass of water added to prepare balls (g): 87.94 Date on which experiment was set up:25-Sep-99									

Table A69: The Conversion-Time Data for Old Mixed Slag Balls with the pore moisture evaporated (particle size class:75-300um)

Sample	Mass analysed (g)	%Cr prior to leaching	Date of Analysis	Conc. Cr(VI) (ppb)	Mass of Cr(VI) in 1l NaOH (ug)	Mass Cr (g)	Conversion (ug per g Cr)	Days	Sampling Date
0 weeks	38.71	0.8	7-11-99	192.98	192.98	0.31	623	0	25-Sep-99
1 week	21.18	0.84	7-11-99	556.03	556.03	0.18	3125	7	02-Oct-99
2 weeks	20.08	0.87	7-11-99	691.59	691.59	0.17	3959	14	09-Oct-99
4 weeks	26.59	0.83	19-01-00	1075.49	1075.49	0.22	4873	28	23-Oct-99
8 weeks	21.21	0.81	18-02-00	1233.35	1233.35	0.17	7179	63	27-Nov-99
12 weeks	24.34	0.84	26-03-00	1295.26	1295.26	0.20	6335	103	06-Jan-00
16 weeks	23.69	0.83	21-05-00	1343.35	1343.35	0.20	6832	121	24-Jan-00
20 weeks	22.39	0.85	18-06-00	1487.03	1487.03	0.19	7814	156	28-Feb-00
28 weeks	23.42	0.88	13-08-00	1598.49	1598.49	0.21	7756	215	27-Apr-00
Mass of water added to prepare balls (g):49.46 Date on which experiment was set up:25-Sep-99									

Table A70: The Conversion-Time Data for Old Mixed Slag Balls with the excess pore moisture evaporated (particle size class:300-1000um)

<i>Sample</i>	<i>Mass analysed (g)</i>	<i>%Cr prior to leaching</i>	<i>Date of Analysis</i>	<i>Conc. Cr(VI) (ppb)</i>	<i>Mass of Cr(VI) in 1l NaOH (ug)</i>	<i>Mass Cr (g)</i>	<i>Conversion (ug per g Cr)</i>	<i>Days</i>	<i>Sampling Date</i>
0 weeks	30.41	2.41	7-11-99	192.98	192.98	0.73	263	0	25-Sep-99
1 week	21.31	2.4	7-11-99	598.66	598.66	0.51	1171	7	02-Oct-99
2 weeks	26.42	2.45	19-01-00	896.10	896.10	0.65	1384	14	09-Oct-99
4 weeks	29.35	2.47	19-01-00	1244.38	1244.38	0.72	1717	28	23-Oct-99
8 weeks	20.04	2.42	18-02-00	1361.60	1361.60	0.48	2808	63	27-Nov-99
12 weeks	23.42	2.51	26-03-00	1419.86	1419.86	0.59	2415	103	06-Jan-00
16 weeks	24.52	2.53	18-04-00	1489.51	1489.51	0.62	2401	121	24-Jan-00
20 weeks	23.2	2.49	18-06-00	1632.01	1632.01	0.58	2825	156	28-Feb-00
28 weeks	22.4	2.42	13-08-00	1710.87	1710.87	0.54	3156	215	27-Apr-00
Mass of water added to prepare balls (g):35.98 Date on which experiment was set up : 25 September 1999									

Table A71: The Conversion -Time Data for New CLU Slag Balls with the excess pore moisture maintained (particle size class:<75um)

Sample	Mass analysed (g)	%Cr prior to leaching	Date of Analysis	Conc. Cr(VI) (ppb)	Mass of Cr(VI) in 1l NaOH (ug)	Mass Cr (g)	Conversion (ug per g Cr)	Days	Sampling Date
0 weeks	23.45	0.71	29-9-99	65.23	65.23	0.17	392	0	17-Sep-99
1 week	25.12	0.72	29-9-99	83.27	83.27	0.18	460	8	25-Sep-99
2 week	23.68	0.69	7-11-99	96.62	96.62	0.16	591	15	02-Oct-99
4 weeks	21.35	0.65	7-11-99	119.41	119.41	0.14	860	29	16-Oct-99
8 weeks	19.8	0.68	30-11-99	152.83	152.83	0.13	1135	64	20-Nov-99
12 weeks	21.32	0.67	18-02-00	172.53	172.53	0.14	1208	111	06-Jan-00
16 weeks	20.41	0.61	26-03-00	206.20	206.20	0.12	1656	122	17-Jan-00
20 weeks	21.4	0.65	18-04-00	221.04	221.04	0.14	1589	157	21-Feb-00
28 weeks	26.08	0.63	2-07-00	301.93	301.93	0.16	1838	213	17-Apr-00
44 weeks	20.82	0.61	6-08-00	304.95	304.95	0.13	2401	323	05-Aug-00
Mass of water to prepare balls added (g):92.77									
Date on which experiment was set up: 17-Sep-99									

Table A72: The Conversion-Time Data for New CLU Slag Balls with the pore moisture maintained (particle size class:75-300um)

<i>Sample</i>	<i>Mass analysed (g)</i>	<i>%Cr prior to leaching</i>	<i>Date of Analysis</i>	<i>Conc. Cr(VI) (ppb)</i>	<i>Mass of Cr(VI) in 1l NaOH (ug)</i>	<i>Mass Cr (g)</i>	<i>Conversion (ug per g Cr)</i>	<i>Days</i>	<i>Sampling Date</i>
0 weeks	17.29	1.35	29-9-99	69.12	69.12	0.23	296	0	17-Sep-99
1 week	19.83	1.32	29-9-99	83.63	83.63	0.26	319	8	25-Sep-99
2 week	21.34	1.33	7-11-99	91.36	91.36	0.28	322	15	02-Oct-99
4 weeks	23.67	1.36	7-11-99	115.91	115.91	0.32	360	29	16-Oct-99
8 weeks	20.42	1.39	19-01-00	151.19	151.19	0.28	533	64	20-Nov-99
12 weeks	22.95	1.39	18-02-00	239.91	239.91	0.32	752	111	06-Jan-00
16 weeks	21.18	1.45	26-03-00	276.68	276.68	0.31	901	122	17-Jan-00
20 weeks	22.19	1.42	18-04-00	297.60	297.60	0.32	944	157	21-Feb-00
28 weeks	16.58	1.45	2-07-00	389.30	389.30	0.24	1619	213	17-Apr-00
44 weeks	22.4	1.41	6-08-00	415.99	415.99	0.32	1317	323	05-Aug-00

Date on which experiment was set up: 17 September 1999

Mass of water added to prepare balls (g):70.27

Table A73: The Conversion -Time Data for New CLU Slag Balls with the pore moisture maintained (particle size class: 300-1000um)

Sample	Mass analysed (g)	%Cr prior to leaching	Date of Analysis	Conc. Cr(VI) (ppb)	Mass of Cr(VI) in 1l NaOH (ug)	Mass Cr (g)	Conversion (ug per g Cr)	Days	Sampling Date
0 weeks	24.63	2.23	30-11-99	82.97	82.97	0.55	151	0	06-Nov-99
1 week	20.87	2.39	30-11-99	90.35	90.35	0.50	181	8	14-Nov-99
2 week	25.82	2.25	19-01-00	168.38	168.38	0.58	290	15	21-Nov-99
4 weeks	24.6	2.21	19-01-00	238.43	238.43	0.54	439	27	03-Dec-99
8 weeks	22.59	2.22	18-02-00	244.08	244.08	0.50	487	61	06-Jan-00
12 weeks	20.64	2.29	26-03-00	279.12	279.12	0.47	591	96	10-Feb-00
16 weeks	19.95	2.31	18-04-00	291.29	291.29	0.46	632	124	09-Mar-00
20 weeks	21.2	2.4	18-06-00	316.09	316.09	0.51	621	152	06-Apr-00
28 weeks	22	2.23	6-08-00	332.01	332.01	0.49	677	213	06-Jun-00
Mass of water added to prepare balls (g):40.57									
Date on which experiment was set up:6-Nov-99									

Table A74: The Conversion-time Data for New CLU Slag Balls with the pore moisture evaporated (particle size class: <75um)

Sample	Mass analysed (g)	%Cr prior to leaching	Date of Analysis	Conc. Cr(VI) (ppb)	Mass of Cr(VI) in 1l NaOH (ug)	Mass Cr (g)	Conversion (ug per g Cr)	Days	Sampling Date
0 weeks	25.02	0.74	7-11-99	66.10	66.10	0.19	357	0	17-Sep-99
1 week	21.17	0.76	7-11-99	240.95	240.95	0.16	1498	8	25-Sep-99
2 week	22.34	0.69	30-11-99	263.85	263.85	0.15	1712	15	02-Oct-99
4 weeks	27.65	0.65	30-11-99	327.14	327.14	0.18	1820	29	16-Oct-99
8 weeks	20.62	0.71	18-02-00	370.17	370.17	0.15	2528	64	20-Nov-99
12 weeks	21.42	0.73	26-03-00	384.09	384.09	0.16	2456	111	06-Jan-00
16 weeks	20.07	0.64	18-04-00	427.07	427.07	0.13	3325	122	17-Jan-00
20 weeks	22.29	0.67	2-07-00	431.05	431.05	0.15	2886	157	21-Feb-00
28 weeks	21.31	0.63	6-08-00	438.16	438.16	0.13	3264	213	17-Apr-00

Mass of water added to prepare balls (g):95.54
Date on which experiment was set up: 27 September 1999

Table A75: The Conversion-Time Data for New CLU Slag Balls with the excess pore moisture evaporated (particle size class: 75-300um)

Sample	Mass analysed (g)	%Cr prior to leaching	Date of Analysis	Conc. Cr(VI) (ppb)	Mass of Cr(VI) in 1l NaOH (ug)	Mass Cr (g)	Conversion (ug per g Cr)	Days	Sampling Date	
0 weeks	25.02	1.39	7-11-99	66.81	66.81	0.35	192	0	17-Sep-99	
1 week	23.32	1.35	7-11-99	265.45	265.45	0.31	843	8	25-Sep-99	
2 week	24.62	1.32	30-11-99	285.89	285.89	0.32	880	15	02-Oct-99	
4 weeks	25.71	1.42	19-01-00	394.50	394.50	0.37	1081	29	16-Oct-99	
8 weeks	22.42	1.44	18-02-00	463.63	463.63	0.32	1436	64	20-Nov-99	
12 weeks	23.4	1.45	26-03-00	485.89	485.89	0.34	1432	111	06-Jan-00	
16 weeks	21.11	1.42	18-04-00	495.09	495.09	0.30	1652	122	17-Jan-00	
20 weeks	20.75	1.43	2-07-00	499.55	499.55	0.30	1684	157	21-Feb-00	
28 weeks	21.62	1.45	6-08-00	529.38	529.38	0.31	1689	213	17-Apr-00	
Mass of water added to prepare balls (g):69										
Date on which experiment was set up: 27 September 1999										

Table A76: The Conversion-Time Data for New CLU Slag Balls with the pore moisture evaporated (particle size class:300-1000um)

Sample	Mass analysed (g)	%Cr prior to leaching	Date of Analysis	Conc. Cr(VI) (ppb)	Mass of Cr(VI) in 1l NaOH (ug)	Mass Cr (g)	Conversion (ug per g Cr)	Days	Sampling Date
0 weeks	19.09	2.35	30-11-99	66.79	66.79	0.45	148.88	0	08-Nov-99
1 week	21.39	2.37	30-11-99	213.45	213.45	0.51	421.05	8	16-Nov-99
2 week	20.45	2.24	19-01-00	380.19	380.19	0.46	829.97	15	23-Nov-99
4 weeks	23.41	2.26	19-01-00	480.65	480.65	0.53	908.48	25	03-Dec-99
8 weeks	23.67	2.23	18-02-00	591.49	591.49	0.53	1120.58	59	06-Jan-00
12 weeks	24.5	2.21	26-03-00	623.19	623.19	0.54	1150.97	95	11-Feb-00
16 weeks	22.02	2.25	18-04-00	633.83	633.83	0.50	1279.30	123	10-Mar-00
20 weeks	23.61	2.26	2-07-00	636.80	636.80	0.53	1193.44	151	07-Apr-00
28 weeks	22.11	2.29	6-08-00	654.22	654.22	0.51	1292.11	214	09-Jun-00

Mass of water added to prepare balls (g):37.8
 Date on which experiment was set up: 8 November1999

Table A77: The Conversion-Time Data for New EAF Slag Balls with pore moisture maintained (particle size class: <75um)

Sample	Mass analysed (g)	%Cr prior to leaching	Date of Analysis	Conc. Cr(VI) (ppb)	Mass of Cr(VI) in 1l NaOH (ug)	Mass Cr (g)	Conversion (ug per g Cr)	Days	Sampling Date
0 weeks	14.49	0.7	29-9-99	74.43	74.43	0.10	734	0	19-Sep-99
1 week	23.86	0.62	7-11-99	102.58	102.58	0.15	693	8	27-Sep-99
2 weeks	27.52	0.64	7-11-99	116.61	116.61	0.18	662	13	02-Oct-99
4 weeks	24.32	0.67	7-11-99	132.03	132.03	0.16	810	27	16-Oct-99
8 weeks	23.31	0.61	30-11-99	136.35	136.35	0.14	959	57	15-Nov-99
12 weeks	22.26	0.63	18-02-00	183.30	183.30	0.14	1307	75	03-Dec-99
16 weeks	21.92	0.65	26-03-00	218.41	218.41	0.14	1533	120	17-Jan-00
20 weeks	22.31	0.61	18-04-00	265.65	265.65	0.14	1952	150	16-Feb-00
28 weeks	22.27	0.64	2-07-00	275.81	275.81	0.14	1935	209	15-Apr-00
44 weeks	26.8	0.66	6-08-00	272.77	272.77	0.18	1542	321	05-Aug-00

mass of water added to prepare balls (g):73.97
 Date on which experiment was set up: 19 September 1999

Table A78: The Conversion-time Data for New EAF Slag Balls with the pore moisture maintained (particle size class:75-300um)

Sample	Mass analysed (g)	%Cr prior to leaching	Date of Analysis	Conc. Cr(VI) (ppb)	Mass of Cr(VI) in 1l NaOH (ug)	Mass Cr (g)	Conversion (ug per g Cr)	Days	Sampling Date
0 weeks	13.22	0.89	7-11-99	61.89	61.89	0.12	526	0	19-Sep-99
1 week	27.44	0.8	7-11-99	111.00	111.00	0.22	506	8	27-Sep-99
2 weeks	32.25	0.85	7-11-99	122.92	122.92	0.27	448	13	02-Oct-99
4 weeks	28.52	0.86	7-11-99	139.04	139.04	0.25	567	27	16-Oct-99
8 weeks	29.67	0.82	19-01-00	230.47	230.47	0.24	947	57	15-Nov-99
12 weeks	23.44	0.81	18-02-00	232.62	232.62	0.19	1225	75	03-Dec-99
16 weeks	22.1	0.86	26-03-00	247.37	247.37	0.19	1302	120	17-Jan-00
20 weeks	20.4	0.82	18-04-00	279.00	279.00	0.17	1668	150	16-Feb-00
28 weeks	19.87	0.83	2-07-00	372.25	372.25	0.16	2257	209	15-Apr-00
44 weeks	24.64	0.87	6-08-00	435.13	435.13	0.21	2030	321	05-Aug-00
Mass of water added to prepare balls (g):98.89									
Date on which experiment was set up: 19 September 1999									

Table A79: The Conversion-Time Data for New EAF Slag Balls with the pore moisture maintained (particle size class: 300-1000um)

Sample	Mass analysed (g)	%Cr prior to leaching	Date of Analysis	Conc. Cr(VI) (ppb)	Mass of Cr(VI) in 1l NaOH (ug)	Mass Cr (g)	Conversion (ug per g Cr)	Days	Sampling Date
0 weeks	25.46	1.92	29-9-99	76.55	76.55	0.49	157	0	19-Sep-99
1 week	15.74	1.95	29-9-99	143.37	143.37	0.31	467	8	27-Sep-99
2 weeks	15.47	1.89	7-11-99	156.91	156.91	0.29	537	13	02-Oct-99
4 weeks	21.52	1.94	7-11-99	166.71	166.71	0.42	399	27	16-Oct-99
8 weeks	23.84	1.97	30-11-99	118.45	118.45	0.47	252	57	15-Nov-99
12 weeks	21.19	1.92	18-02-00	334.74	334.74	0.41	823	75	03-Dec-99
16 weeks	20.1	1.96	26-03-00	347.83	347.83	0.39	883	120	17-Jan-00
20 weeks	21.42	1.99	18-04-00	361.48	361.48	0.43	848	150	16-Feb-00
28 weeks	17.93	1.99	2-07-00	360.07	360.07	0.36	1009	209	15-Apr-00
44 weeks	20.5	2.01	6-08-00	381.70	381.70	0.41	926	321	05-Aug-00
Mass of water added (g):36.14									
Date on which experiment was set up: 19 September 1999									

Table A80: The Conversion -Time Data for New EAF Slag Balls with the pore moisture evaporated (particle size class: <75um)

Sample	Mass analysed (g)	%Cr prior to leaching	Date of Analysis	Conc. Cr(VI) (ppb)	Mass of Cr(VI) in 1l NaOH (ug)	Mass Cr (g)	Conversion (ug per g Cr)	Days	Sampling Date
0 weeks	16.54	0.66	7-11-99	74.88	74.88	0.11	686	0	29-Sep-99
1 week	18.62	0.62	19-01-00	148.74	148.74	0.12	1288	4	03-Oct-99
2 weeks	25.4	0.69	19-01-00	235.36	235.36	0.18	1343	11	10-Oct-99
4 weeks	25.04	0.71	19-01-00	354.72	354.72	0.18	1995	25	24-Oct-99
8 weeks	26.53	0.65	18-02-00	494.90	494.90	0.17	2870	55	23-Nov-99
17 weeks	25.62	0.68	26-03-00	529.10	529.10	0.17	3037	119	26-Jan-00
20 weeks	24.59	0.65	18-04-00	555.01	555.01	0.16	3472	152	28-Feb-00
26 weeks	23.48	0.61	18-06-00	535.73	535.73	0.14	3740	182	29-Mar-00
34 weeks	24.6	0.63	6-08-00	553.65	553.65	0.15	3572	241	27-May-00

Mass of water added to prepare balls (g):79.88

Date on which experiment was set up: 29 September 1999

Table A81: The Conversion-time Data for New EAF Slag Balls with pore moisture evaporated (particle size class: 75-300um)

Sample	Mass analysed (g)	%Cr prior to leaching	Date of Analysis	Conc. Cr(VI) (ppb)	Mass of Cr(VI) in 1l NaOH (ug)	Mass Cr (g)	Conversion (ug per g Cr)	Days	Sampling Date
0 weeks	22.09	0.84	7-11-00	72.77	72.77	0.19	392	0	29-Sep-99
1 week	23.94	0.88	19-01-00	115.89	115.89	0.21	550	4	03-Oct-99
2 weeks	21.64	0.85	19-01-00	150.84	150.84	0.18	820	11	10-Oct-99
4 weeks	24.39	0.83	19-01-00	275.86	275.86	0.20	1363	25	24-Oct-99
8 weeks	23.21	0.82	18-02-00	513.66	513.66	0.19	2699	55	23-Nov-99
17 weeks	22.41	0.87	26-03-00	520.39	520.39	0.19	2669	119	26-Jan-00
20 weeks	23.54	0.84	18-04-00	530.83	530.83	0.20	2685	152	28-Feb-00
26 weeks	21.1	0.86	18-06-00	540.60	540.60	0.18	2979	182	29-Mar-00
34 weeks	23.18	0.82	6-08-00	523.08	523.08	0.19	2752	241	27-May-00

Mass of water added (g):100.12

Date on which experiment was set up: 29 September 1999

Table A82: The Conversion-Time Data for New EAF Slag Ball with pore moisture evaporated (particle size class: 300-1000um)

Sample	Mass analysed (g)	%Cr prior to leaching	Date of Analysis	Conc. Cr(VI) (ppb)	Mass of Cr(VI) in 1l NaOH (ug)	Mass Cr (g)	Conversion (ug per g Cr)	Days	Sampling Date
0 weeks	23.61	1.93	7-11-99	76.28	76.28	0.46	167	0	29-Sep-99
1 week	26.57	1.9	19-01-00	208.12	208.12	0.50	412	4	03-Oct-99
2 weeks	23.42	1.91	19-01-00	278.65	278.65	0.45	623	11	10-Oct-99
4 weeks	20.32	1.99	19-01-00	431.47	431.47	0.40	1067	25	24-Oct-99
8 weeks	20.47	1.93	18-02-00	514.35	514.35	0.40	1302	55	23-Nov-99
12 weeks	21.63	2.02	26-03-00	526.67	526.67	0.44	1205	119	26-Jan-00
16 weeks	20.31	1.99	18-04-00	547.30	547.30	0.40	1354	152	28-Feb-00
20 weeks	24.87	1.94	18-06-00	548.95	548.95	0.48	1138	182	29-Mar-00
28 weeks	25.6	2.03	6-08-00	548.98	548.98	0.52	1056	241	27-May-00

Mass of water added to prepare balls (g):39.47
 Date on which experiment was set up:29 September 1999

Table A 83: The Moisture Content of Old Mixed Slag Balls where the Pore Moisture was Maintained (particle size class: <75um)

<i>Sample</i>	<i>wet mass</i> (g)	<i>dry mass</i> (g)	<i>Moisture content (g)</i>	<i>% Moisture- dry mass basis</i>
0 weeks	36.27	25.85	10.42	40.31
1 week	30.81	22.39	8.42	37.61
2 weeks	29.07	21.74	7.33	33.72
4 weeks	26.28	20.86	5.42	25.98
8 weeks	25.89	25.67	0.22	0.86
12 weeks	27.06	20.71	6.35	30.66
16 weeks	25.49	20.44	5.05	24.71
20 weeks	26.74	20.2	6.54	32.38
28 weeks	29.74	24.39	5.35	21.94
44 weeks	29.47	23.89	5.58	23.36

Table A84: The Moisture Content of Old Mixed Slag Balls where the Pore Moisture was Maintained (particle size class: 75-1000um)

<i>Sample</i>	<i>wet mass</i> (g)	<i>dry mass</i> (g)	<i>Moisture content (g)</i>	<i>% Moisture- dry mass basis</i>
0 weeks	24.93	22.47	2.46	10.95
1 week	31.11	25.54	5.57	21.81
2 weeks	33.13	23.64	9.49	40.14
4 weeks	21.52	16.78	4.74	28.25
8 weeks	23.45	21.39	2.06	9.63
12 weeks	28.69	24.19	4.5	18.60
16 weeks	26.59	20.74	5.85	28.21
20 weeks	27.59	21.19	6.4	30.20
28 weeks	30.43	26.01	4.42	16.99
44 weeks	30.51	20.92	9.59	45.84

Table A85: The Moisture Content of Old Mixed Slag Balls with the pore moisture maintained (particle size class: 300-1000um)

<i>Sample</i>	<i>wet mass</i> (g)	<i>dry mass</i> (g)	<i>Moisture content (g)</i>	<i>% Moisture- dry mass basis</i>
0 weeks	41.26	35.12	6.14	17.48
1 week	29.21	24.02	5.19	21.61
2 weeks	20.45	17.65	2.8	15.86
4 weeks	27.52	20.85	6.67	31.99
8 weeks	29.95	26.67	3.28	12.30
12 weeks	25.98	20.31	5.67	27.92
16 weeks	34.45	23.45	11	46.91
20 weeks	29.75	23.34	6.41	27.46
28 weeks	25.45	18.61	6.84	36.75
44 weeks	31.49	27.55	3.94	14.30

Table A86: The Moisture Content of New CLU Slag with the pore moisture maintained (particle size class: <75um)

<i>Sample</i>	<i>wet mass</i> (g)	<i>dry mass</i> (g)	<i>Moisture content (g)</i>	<i>% Moisture- dry mass basis</i>
0 weeks	31.86	23.58	8.28	35.11
1 week	34.21	25.24	8.97	35.54
2 week	32.21	23.74	8.47	35.68
4 weeks	29.38	21.37	8.01	37.48
8 weeks	25.49	19.87	5.62	28.28
12 weeks	25.68	21.38	4.3	20.11
16 weeks	27.47	20.49	6.98	34.07
20 weeks	28.89	21.49	7.4	34.43
28 weeks	34.95	26.14	8.81	33.70
44 weeks	29.59	21.13	8.46	40.04

Table A87: The Moisture Content of New CLU Slag Balls where the pore moisture was maintained (particle size class: 75-300um)

<i>Sample</i>	<i>wet mass</i> (g)	<i>dry mass</i> (g)	<i>Moisture content (g)</i>	<i>% Moisture- dry mass basis</i>
0 weeks	22.08	17.31	4.77	27.56
1 week	25.07	19.93	5.14	25.79
2 week	25.88	21.45	4.43	20.65
4 weeks	26.87	23.68	3.19	13.47
8 weeks	27.83	20.49	7.34	35.82
12 weeks	29.37	22.98	6.39	27.81
16 weeks	26.89	21.17	5.72	27.02
20 weeks	27.59	22.28	5.31	23.83
28 weeks	22.15	16.61	5.54	33.35
44 weeks	26.01	22.42	3.59	16.01

Table A88: The Moisture Content of New CLU Slag Balls where the pore moisture was maintained (particle size 300-1000um)

<i>Sample</i>	<i>wet mass</i> (g)	<i>dry mass</i> (g)	<i>Moisture content (g)</i>	<i>% Moisture- dry mass basis</i>
0 weeks	28.41	24.77	3.64	14.70
1 week	24.98	20.91	4.07	19.46
2 week	29.97	25.89	4.08	15.76
4 weeks	30.41	24.66	5.75	23.32
8 weeks	25.99	22.72	3.27	14.39
12 weeks	25.49	20.92	4.57	21.85
16 weeks	26.78	19.97	6.81	34.10
20 weeks	24.59	21.21	3.38	15.94
28 weeks	31.19	22.06	9.13	41.39

Table A89: The Moisture Contents of New EAF Slag Balls where the pore moisture (particle size class: <75um)

<i>Sample</i>	<i>wet mass</i> (g)	<i>dry mass</i> (g)	<i>Moisture content (g)</i>	<i>% Moisture- dry mass basis</i>
0 weeks	18.83	14.55	4.28	29.42
1 week	31.28	24.12	7.16	29.68
2 weeks	30.94	27.67	3.27	11.82
4 weeks	29.83	24.45	5.38	22.00
8 weeks	30.47	23.39	7.08	30.27
12 weeks	29.5	22.28	7.22	32.41
16 weeks	27.78	21.96	5.82	26.50
20 weeks	29.39	22.35	7.04	31.50
28 weeks	30.35	22.42	7.93	35.37
44 weeks	36.98	26.89	10.09	37.52

Table A90: The Moisture Contents of New EAF Slag Balls where the pore moisture was maintained (particle size class: 75-300um)

<i>Sample</i>	<i>wet mass</i> (g)	<i>dry mass</i> (g)	<i>Moisture content (g)</i>	<i>% Moisture- dry mass basis</i>
0 weeks	16.01	13.28	2.73	20.56
1 week	33.13	27.68	5.45	19.69
2 weeks	37.69	32.32	5.37	16.62
4 weeks	35.15	28.67	6.48	22.60
8 weeks	36.49	31.28	5.21	16.66
12 weeks	29.46	23.46	6	25.58
16 weeks	25.43	22.19	3.24	14.60
20 weeks	27.98	20.41	7.57	37.09
28 weeks	25.89	19.93	5.96	29.90
44 weeks	29.94	24.7	5.24	21.21

Table A91: The Moisture Contents of the New EAF Slag Balls where the pore moisture was maintained (particle size class:300-1000um)

<i>Sample</i>	<i>wet mass</i> (g)	<i>dry mass</i> (g)	<i>Moisture content (g)</i>	<i>% Moisture- dry mass basis</i>
0 weeks	28.92	25.5	3.42	13.41
1 week	17.72	15.87	1.85	11.66
2 weeks	17.51	15.49	2.02	13.04
4 weeks	22.12	21.53	0.59	2.74
8 weeks	27.47	23.92	3.55	14.84
12 weeks	27.06	21.27	5.79	27.22
16 weeks	27.65	20.09	7.56	37.63
20 weeks	28.49	21.41	7.08	33.07
28 weeks	23.67	17.99	5.68	31.57
44 weeks	29.81	20.77	9.04	43.52

University of Cape Town

**APPENDIX B:
MALVERN PARTICLE
SIZE DISTRIBUTION
DATA**

University of Cape Town

**APPENDIX B1: PARTICLE
SIZE DISTRIBUTIONS FOR
 Cr_2O_3 AND CaO USED FOR
BALL EXPERIMENTS IN 1999**

University of Cape Town

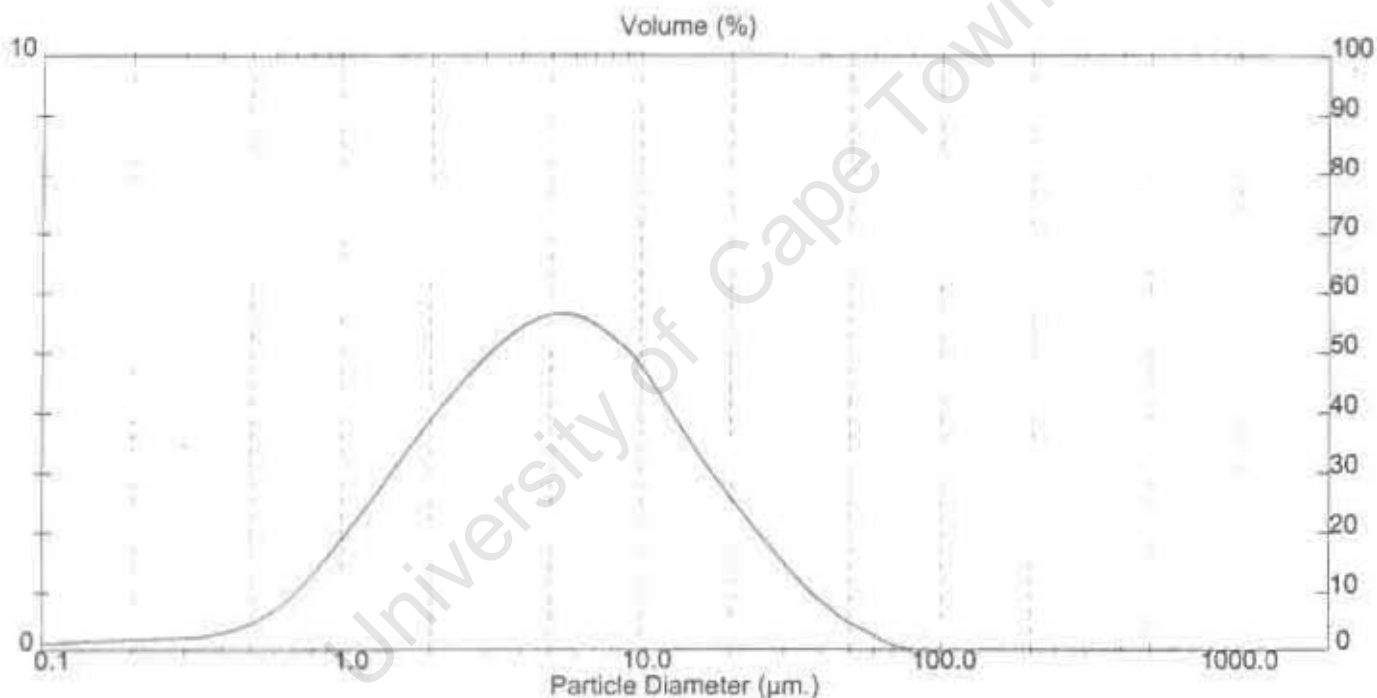
Result: Analysis Table

ID: Kriveshini Cr2O3 Run No: 2 Measured: 3/11/1999 14:22
 File: HELEN Rec No: 337 Analysed: 3/11/1999 14:22
 Path: C:\SIZERS\DATA\HELEN Source: Analyzed

Range: 300RF mm Beam: 2.40 mm Sampler: None Cts: 25.1 %
 Presentation: 3THD Analysis: Polydisperse Residual: 0.479 %
 Modifications: None

Conc. = 0.0088 %Vol Density = 1.000 g/cm³ S.S.A. = 2.5785 m²/g
 Distribution: Volume D[4, 3] = 8.14 µm D[3, 2] = 2.33 µm
 D(v, 0.1) = 1.22 µm D(v, 0.5) = 5.03 µm D(v, 0.9) = 19.05 µm
 Span = 3.547E+00 Uniformity = 1.125E+00

Size (µm)	Volume In %	Size (µm)	Volume In %	Size (µm)	Volume In %	Size (µm)	Volume In %
0.05	0.02	0.58	0.74	6.63	5.44	76.32	0.00
0.06	0.05	0.67	1.05	7.72	5.19	88.91	0.00
0.07	0.07	0.78	1.42	9.00	4.88	103.58	0.00
0.08	0.09	0.91	1.82	10.46	4.39	120.67	0.00
0.09	0.11	1.06	2.25	12.21	3.87	140.58	0.00
0.11	0.13	1.24	2.69	14.22	3.38	163.77	0.00
0.13	0.14	1.44	3.15	16.57	2.91	190.80	0.00
0.15	0.16	1.68	3.60	19.31	2.47	222.28	0.00
0.17	0.17	1.95	4.03	22.49	2.05	258.95	0.00
0.20	0.19	2.28	4.42	26.20	1.65	301.68	0.00
0.23	0.20	2.65	4.79	30.53	1.27	351.48	0.00
0.27	0.21	3.09	5.11	35.58	0.93	409.45	0.00
0.31	0.23	3.60	5.37	41.43	0.64	477.01	0.00
0.36	0.29	4.19	5.56	48.27	0.42	555.71	0.00
0.42	0.38	4.88	5.64	56.23	0.25	647.41	0.00
0.49	0.53	5.69	5.60	65.51	0.08	754.23	0.00
0.58		6.63		76.32		878.67	0.00



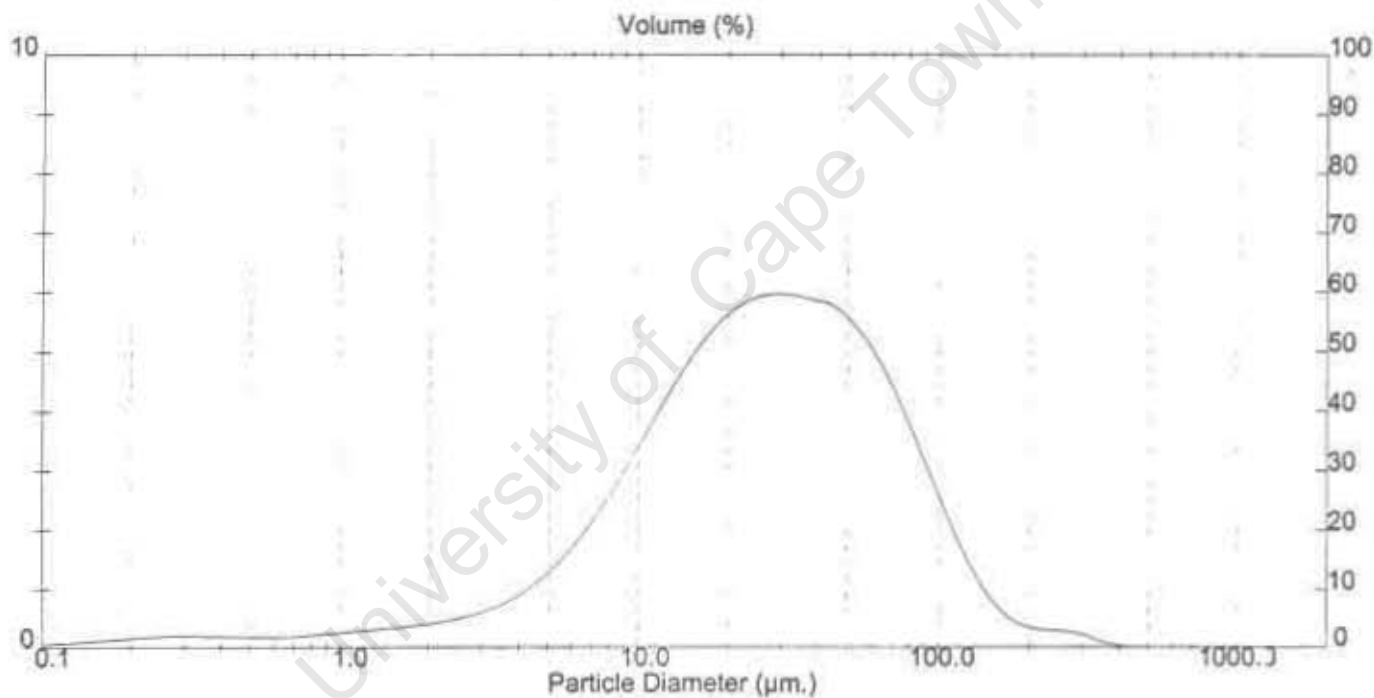
Result: Analysis Table

ID: Khivshini CaO (2)	Run No: 7	Measured: 3/11/1999 14:54
File: HELEN	Rec. No: 341	Analysed: 3/11/1999 14:55
Path: C:\SIZERS\DATA\HELEN		Source: Analysed

Range: 300RF mm	Beam: 2.40 mm	Sampler: None	Obs: 7.4 %
Presentation: 3CHD	Analysis: Polydisperse		Residual: 0.506 %
Modifications: None			

Conc. = 0.0096 %Vol	Density = 2.500 g/cm ³	S.S.A. = 0.3762 m ² /g
Distribution: Volume	D[4, 3] = 36.30 um	D[3, 2] = 6.38 um
D(v, 0.1) = 6.01 um	D(v, 0.5) = 26.51 um	D(v, 0.9) = 82.90 um
Span = 2.901E+00	Uniformity = 9.522E-01	

Size (um)	Volume In %	Size (um)	Volume In %	Size (um)	Volume In %	Size (um)	Volume In %
0.05	0.00	0.58	0.18	5.63	2.19	76.32	3.64
0.06	0.01	0.67	0.19	7.72	2.71	86.91	2.61
0.07	0.02	0.78	0.22	9.00	3.28	103.58	2.00
0.08	0.03	0.91	0.25	10.48	3.86	120.67	1.30
0.09	0.05	1.06	0.28	12.21	4.44	140.58	0.78
0.11	0.07	1.24	0.31	14.22	4.95	163.77	0.46
0.13	0.09	1.44	0.34	16.57	5.38	190.60	0.33
0.15	0.11	1.68	0.38	19.31	5.69	222.26	0.29
0.17	0.14	1.95	0.42	22.49	5.88	258.95	0.26
0.20	0.17	2.28	0.48	26.20	5.95	301.68	0.18
0.23	0.19	2.65	0.57	30.53	5.93	351.46	0.05
0.27	0.20	3.09	0.69	35.56	5.86	409.45	0.00
0.31	0.19	3.60	0.85	41.43	5.76	477.01	0.00
0.36	0.18	4.19	1.08	48.27	5.47	555.71	0.00
0.42	0.18	4.88	1.38	56.23	5.02	647.41	0.00
0.49	0.18	5.69	1.75	65.51	4.40	754.23	0.00
0.58	0.18	6.63	1.75	76.32	4.40	878.67	0.00



**APPENDIX B2: PARTICLE
SIZE DISTRIBUTIONS FOR
Cr₂O₃ AND CaO USED FOR
POWDER AND PELLET
EXPERIMENTS IN 2000**

University of Cape Town

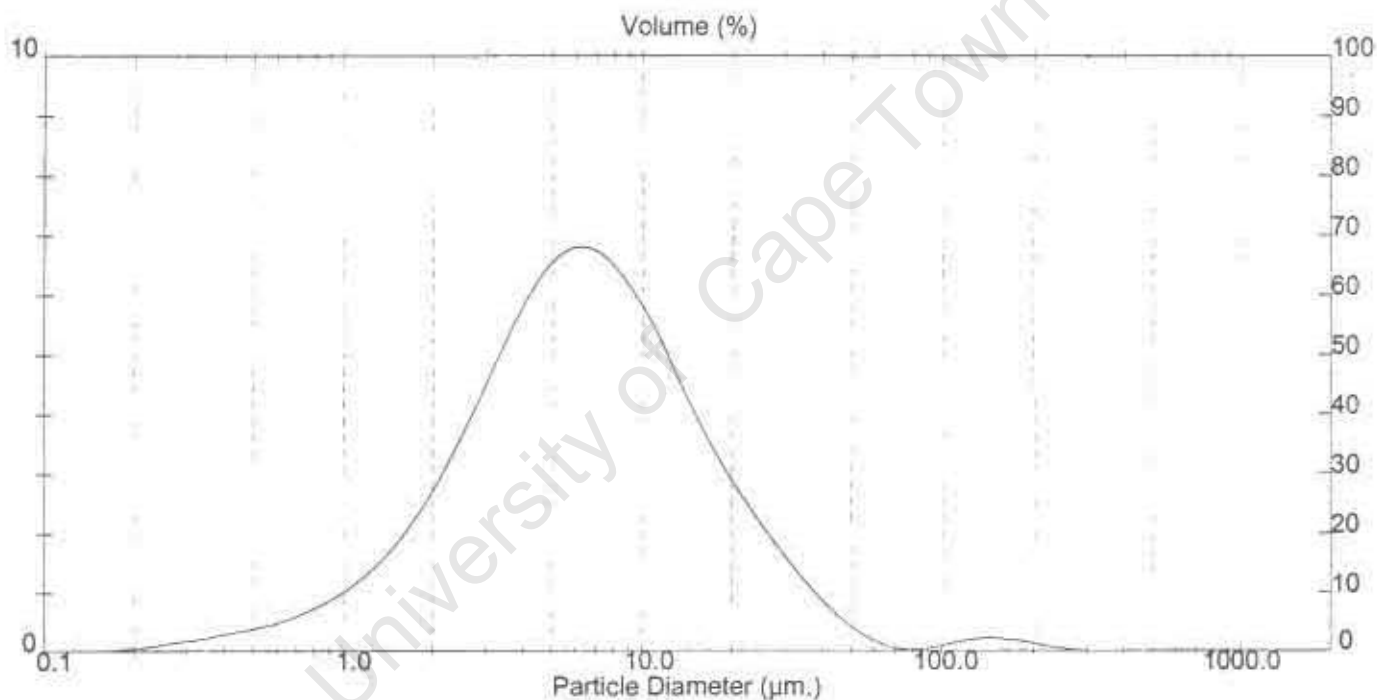
Result: Analysis Table

ID: Chromium oxide -Krev Run No: 2 Measured: 13/9/2000 14:29
 File: HELEN Rec. No: 579 Analysed: 13/9/2000 14:29
 Path: C:\SIZERS\DATA\HELEN Source: Analysed

Range: 300RF mm Beam: 2.40 mm Sampler: None Obs: 21.4 %
 Presentation: 3THD Analysis: Polydisperse Residual: 0.464 %
 Modifications: None

Conc. = 0.0097 %Vol Density = 7.000 g/cm³ S.S.A. = 0.2373 m²/g
 Distribution: Volume D[4, 3] = 10.51 µm O[3, 2] = 3.61 µm
 D[v, 0.1] = 1.78 µm D[v, 0.5] = 6.25 µm O[v, 0.9] = 20.73 µm
 Span = 3.031E+00 Uniformity = 1.143E+00

Size (µm)	Volume In %	Size (µm)	Volume In %	Size (µm)	Volume In %	Size (µm)	Volume In %
0.05	0.00	0.58	0.50	6.63	6.69	76.32	0.03
0.06	0.00	0.67	0.63	7.72	6.38	86.91	0.07
0.07	0.00	0.78	0.78	9.00	5.90	103.58	0.15
0.08	0.00	0.91	0.98	10.48	5.33	120.87	0.21
0.09	0.00	1.06	1.22	12.21	4.59	140.58	0.22
0.11	0.00	1.24	1.52	14.22	3.90	163.77	0.18
0.13	0.00	1.44	1.90	16.57	3.28	190.80	0.12
0.15	0.01	1.68	2.36	19.31	2.73	222.28	0.06
0.17	0.03	1.95	2.92	22.49	2.24	258.95	0.02
0.20	0.06	2.28	3.56	26.20	1.78	301.68	0.00
0.23	0.11	2.65	4.27	30.53	1.35	351.46	0.00
0.27	0.17	3.09	4.99	35.56	0.95	409.45	0.00
0.31	0.21	3.60	5.68	41.43	0.63	477.01	0.00
0.36	0.28	4.19	6.25	48.27	0.35	555.71	0.00
0.42	0.34	4.88	6.63	56.23	0.16	647.41	0.00
0.49	0.41	5.69	6.78	65.51	0.05	754.23	0.00
0.58		6.63		76.32		876.67	



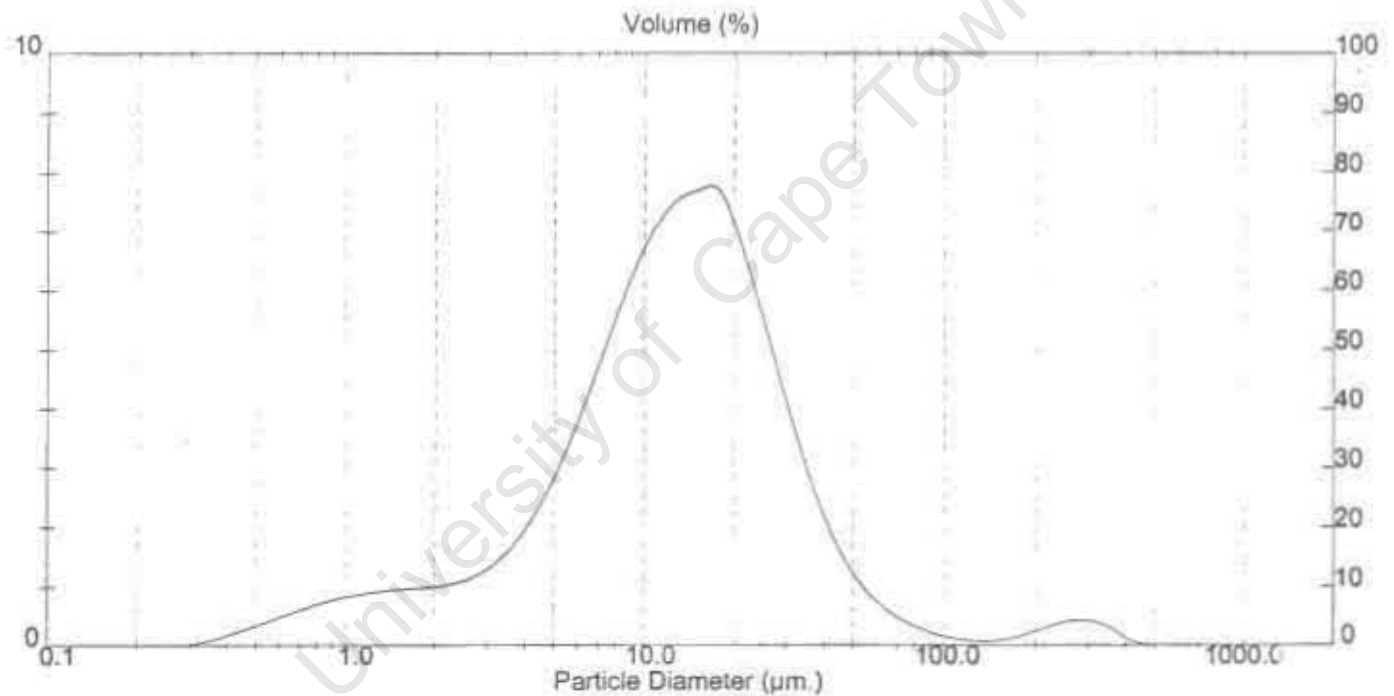
Result: Analysis Table

ID: Calcium oxide -Krev Run No: 7 Measured: 13/9/2000 14:44
 File: HELEN Rec. No: 584 Analysed: 13/9/2000 14:44
 Path: C:\SIZERS\DATA\HELEN Source: Analysed

Range: 300RF mm Beam: 2.40 mm Sampler: None Obs: 11.8 %
 Presentation: 3RHD Analysis: Polydisperse Residual: 0.709 %
 Modifications: None

Conc. = 0.0083 %Vol Density = 2.000 g/cm³ S.S.A. = 0.5126 m²/g
 Distribution: Volume D[4, 3] = 20.73 um D[3, 2] = 5.85 um
 D(v, 0.1) = 2.86 um D(v, 0.5) = 12.84 um D(v, 0.9) = 33.73 um
 Span = 2.404E+00 Uniformity = 1.089E+00

Size (um)	Volume In %	Size (um)	Volume In %	Size (um)	Volume In %	Size (um)	Volume In %
0.05	0.00	0.58	0.51	6.53	4.80	76.32	0.30
0.06	0.00	0.67	0.63	7.72	5.72	88.91	0.18
0.07	0.00	0.78	0.73	9.00	6.54	103.58	0.10
0.08	0.00	0.91	0.82	10.48	7.18	120.67	0.07
0.09	0.00	1.06	0.88	12.21	7.56	140.58	0.08
0.11	0.00	1.24	0.93	14.22	7.70	163.77	0.15
0.13	0.00	1.44	0.96	16.57	7.86	190.80	0.26
0.15	0.00	1.68	0.98	19.31	8.88	222.28	0.26
0.17	0.00	1.95	1.01	22.49	9.76	258.95	0.37
0.20	0.00	2.28	1.09	26.20	10.58	301.68	0.43
0.23	0.00	2.65	1.23	30.53	11.40	351.46	0.38
0.27	0.00	3.09	1.48	35.56	12.41	409.45	0.21
0.31	0.00	3.60	1.85	41.43	13.65	477.01	0.04
0.36	0.16	4.19	2.38	48.27	15.10	555.71	0.00
0.42	0.27	4.88	3.07	56.23	16.73	647.41	0.00
0.49	0.38	5.69	3.89	65.51	18.58	754.23	0.00
0.58		6.63		76.32	20.67	878.87	0.00



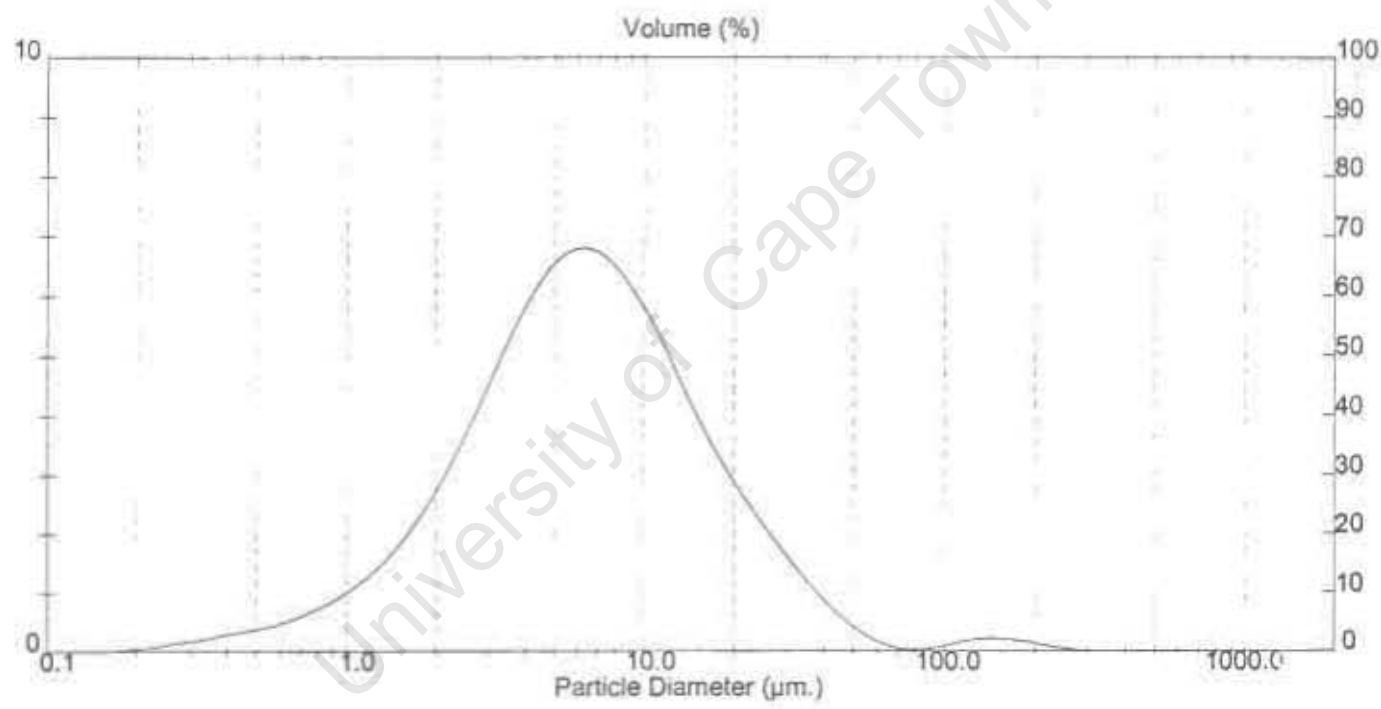
Result: Analysis Table

ID: Chromium oxide -Krev Run No: 2 Measured: 13/9/2000 14:29
 File: HELEN Rec. No: 579 Analysed: 13/9/2000 14:29
 Path: C:\SIZERS\DATA\HELEN Source: Analysed

Range: 300RF mm Beam: 2.40 mm Sampler: None Obs: 21.4 %
 Presentation: 3THD Analysis: Polydisperse Residual: 0.464 %
 Modifications: None

Conc. = 0.0097 %Vol Density = 7.000 g/cm³ S.S.A = 0.2373 m²/g
 Distribution: Volume D[4,3] = 10.51 μ m D[3,2] = 3.81 μ m
 D(v, 0.1) = 1.78 μ m D(v, 0.5) = 6.25 μ m D(v, 0.9) = 20.73 μ m
 Span = 3.031E+00 Uniformity = 1.143E+00

Size (μ m)	Volume In %	Size (μ m)	Volume In %	Size (μ m)	Volume In %	Size (μ m)	Volume In %
0.05	0.00	0.58	0.50	6.63	5.69	76.32	0.03
0.06	0.00	0.67	0.63	7.72	6.38	86.91	0.07
0.07	0.00	0.76	0.78	9.00	5.90	103.56	0.15
0.08	0.00	0.91	0.98	10.48	5.33	120.67	0.21
0.09	0.00	1.06	1.22	12.21	4.59	140.58	0.22
0.11	0.00	1.24	1.52	14.22	3.90	163.77	0.18
0.13	0.00	1.44	1.90	16.57	3.28	190.80	0.12
0.15	0.01	1.68	2.36	19.31	2.73	222.28	0.06
0.17	0.03	1.95	2.92	22.49	2.24	258.95	0.02
0.20	0.06	2.28	3.56	26.20	1.78	301.66	0.00
0.23	0.11	2.65	4.27	30.53	1.35	351.46	0.00
0.27	0.17	3.09	4.99	35.56	0.96	409.45	0.00
0.31	0.21	3.60	5.68	41.43	0.63	477.01	0.00
0.36	0.28	4.19	6.25	48.27	0.35	555.71	0.00
0.42	0.34	4.88	6.63	56.23	0.16	647.41	0.00
0.49	0.41	5.69	6.78	65.51	0.05	754.23	0.00
0.58		6.63		76.32		878.67	



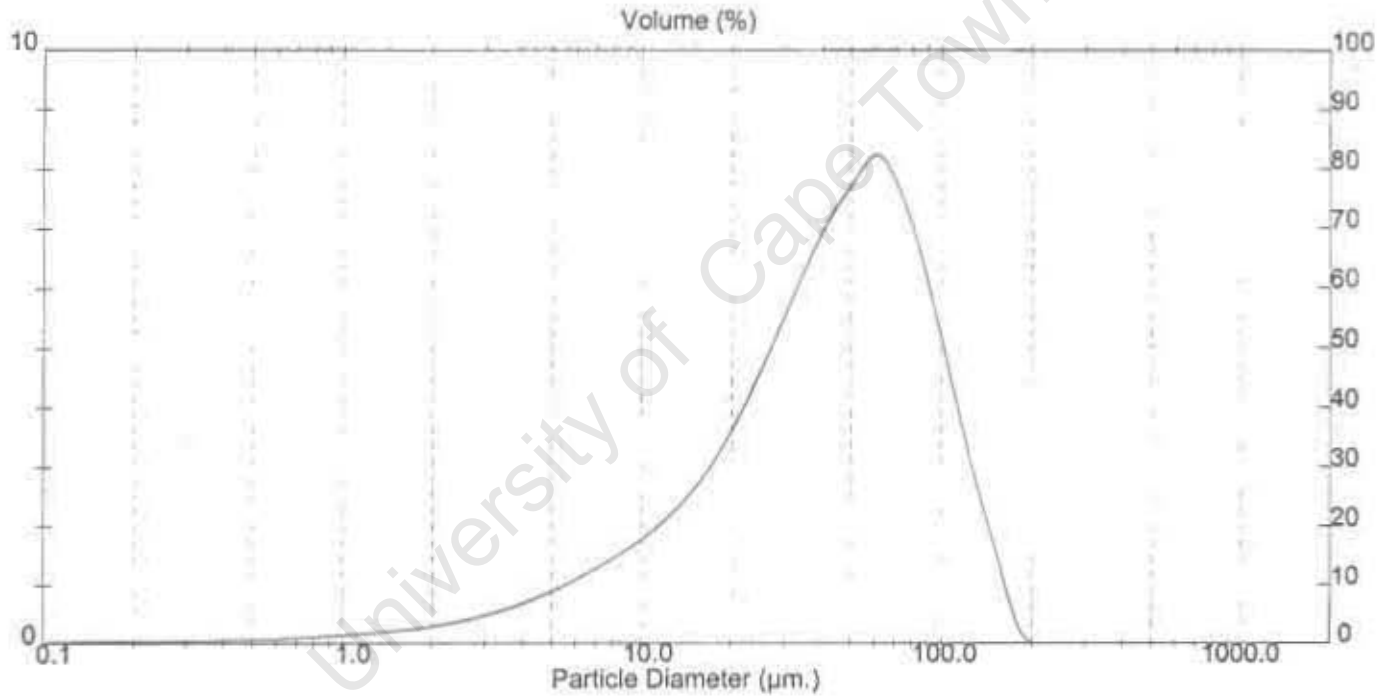
Result: Analysis Table

ID: Calcium oxide -Krev	Run No: 5	Measured: 13/9/2000 14:38
File: HELEN	Rec No: 582	Analysed: 13/9/2000 14:38
Path: C:\SIZERS\DATA\HELEN		Source: Analysed

Range: 300RF mm	Beam: 2.40 mm	Sampler: None	Cbs: 4.5 %
Presentation: 3RHD	Analysis: Polydisperse		Residual: 0.489 %
Modifications: None			

Conc. = 0.0088 %Vol	Density = 2.000 g/cm ³	S.S.A. = 0.2543 m ² /g
Distribution: Volume	D[4, 3] = 50.09 um	D[3, 2] = 11.80 um
D(v, 0.1) = 9.18 um	D(v, 0.5) = 43.61 um	D(v, 0.9) = 100.05 um
Span = 2.084E+00	Uniformity = 6.428E-01	

Size (um)	Volume In %	Size (um)	Volume In %	Size (um)	Volume In %	Size (um)	Volume In %
0.05	0.00	0.58	0.08	6.83	1.29	76.32	8.83
0.06	0.01	0.67	0.10	7.72	1.49	88.91	5.56
0.07	0.02	0.78	0.12	8.00	1.71	103.58	4.13
0.08	0.02	0.91	0.14	10.48	1.97	120.67	2.74
0.09	0.03	1.06	0.16	12.21	2.28	140.58	1.58
0.11	0.03	1.24	0.18	14.22	2.87	163.77	0.41
0.13	0.04	1.44	0.22	16.57	3.15	190.80	0.00
0.15	0.04	1.68	0.26	19.31	3.74	222.28	0.00
0.17	0.04	1.95	0.31	22.48	4.43	258.95	0.00
0.20	0.04	2.28	0.37	26.20	5.19	301.68	0.00
0.23	0.04	2.65	0.44	30.53	5.97	351.48	0.00
0.27	0.05	3.09	0.54	35.56	6.70	409.45	0.00
0.31	0.05	3.60	0.65	41.43	7.34	477.01	0.00
0.36	0.05	4.19	0.79	48.27	7.83	555.71	0.00
0.42	0.06	4.88	0.94	56.23	8.22	647.41	0.00
0.49	0.06	5.69	1.10	65.51	7.77	754.23	0.00
0.58	0.07	6.63		76.32		878.67	0.00



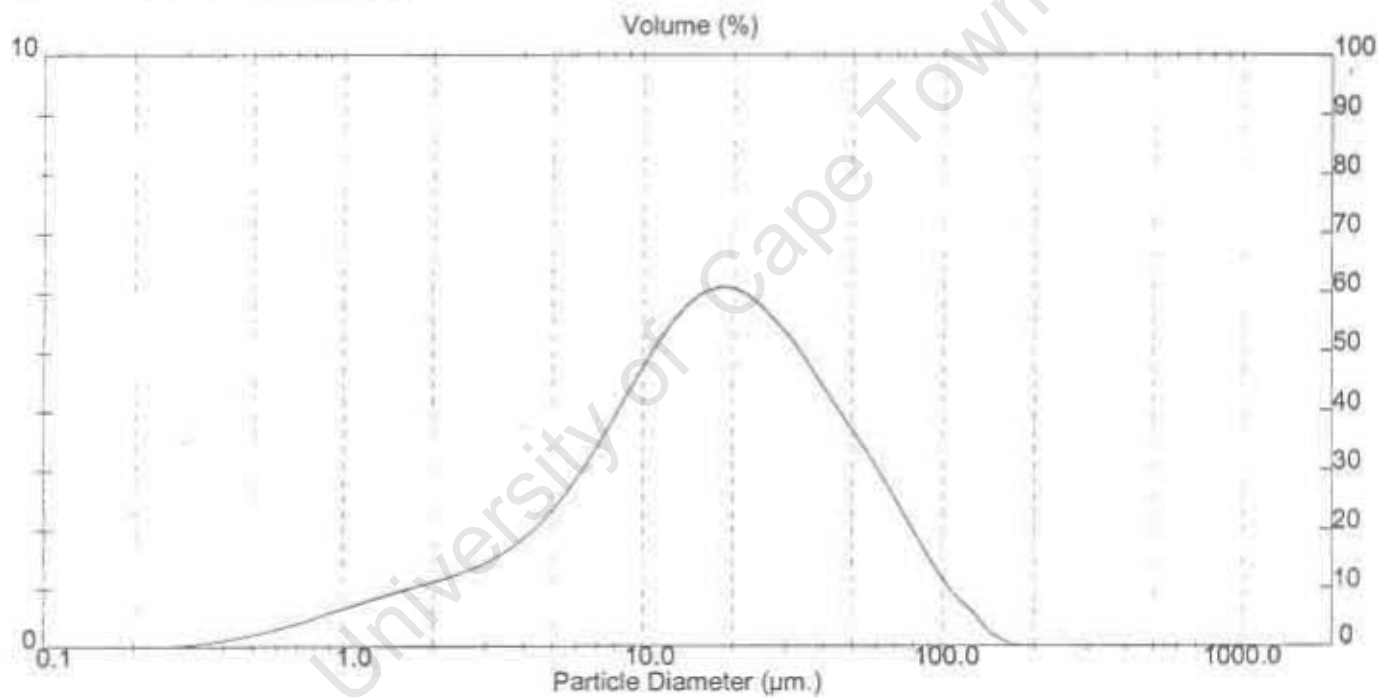
Result: Analysis Table

ID: Calcium oxide -Krev Run No: 6 Measured: 13/9/2000 14:40
 File: HELEN Rec. No: 583 Analysed: 13/9/2000 14:40
 Path: C:\SIZERS\DATA\HELEN Source: Analysed

Range: 300RF mm Beam: 2.40 mm Sampler: None Obs: 6.1 %
 Presentation: 3PHD Analysis: Polydisperse Residual: 0.777 %
 Modifications: None

Conc: = 0.0050 %Vol Density = 2.000 g/cm³ S.S.A = 0.4323 m²/g
 Distribution: Volume D[4, 3] = 24.36 um D[3, 2] = 18.94 um
 D(v, 0.1) = 3.12 um D(v, 0.5) = 16.78 um D(v, 0.9) = 56.38 um
 Span = 3.174E+00 Uniformity = 9.716E-01

Size (um)	Volume In %	Size (um)	Volume In %	Size (um)	Volume In %	Size (um)	Volume In %
0.05	0.00	0.58	0.33	6.83	3.45	76.32	1.85
0.06	0.00	0.67	0.42	7.72	4.03	88.91	1.29
0.07	0.00	0.76	0.42	9.00	4.62	103.58	0.82
0.08	0.00	0.91	0.54	10.48	5.16	120.67	0.49
0.09	0.00	1.08	0.63	12.21	5.61	140.58	0.15
0.11	0.00	1.24	0.75	14.22	5.93	163.77	0.00
0.13	0.00	1.44	0.85	16.57	6.06	190.80	0.00
0.15	0.00	1.68	0.95	19.31	6.01	222.28	0.00
0.17	0.00	1.95	1.05	22.49	5.79	258.95	0.00
0.20	0.00	2.28	1.14	26.20	5.45	301.68	0.00
0.23	0.00	2.65	1.25	30.53	5.04	351.46	0.00
0.27	0.00	3.09	1.38	35.56	4.52	409.45	0.00
0.31	0.02	3.60	1.56	41.43	4.03	477.01	0.00
0.36	0.06	4.19	1.79	48.27	3.53	555.71	0.00
0.42	0.10	4.88	2.09	56.23	3.01	647.41	0.00
0.49	0.17	5.69	2.46	65.51	2.44	754.23	0.00
0.58	0.24	6.63	2.92	76.32	2.44	878.67	0.00



**APPENDIX B3: PARTICLE
SIZE DISTRIBUTIONS FOR
ALL SLAG SAMPLES**

University of Cape Town

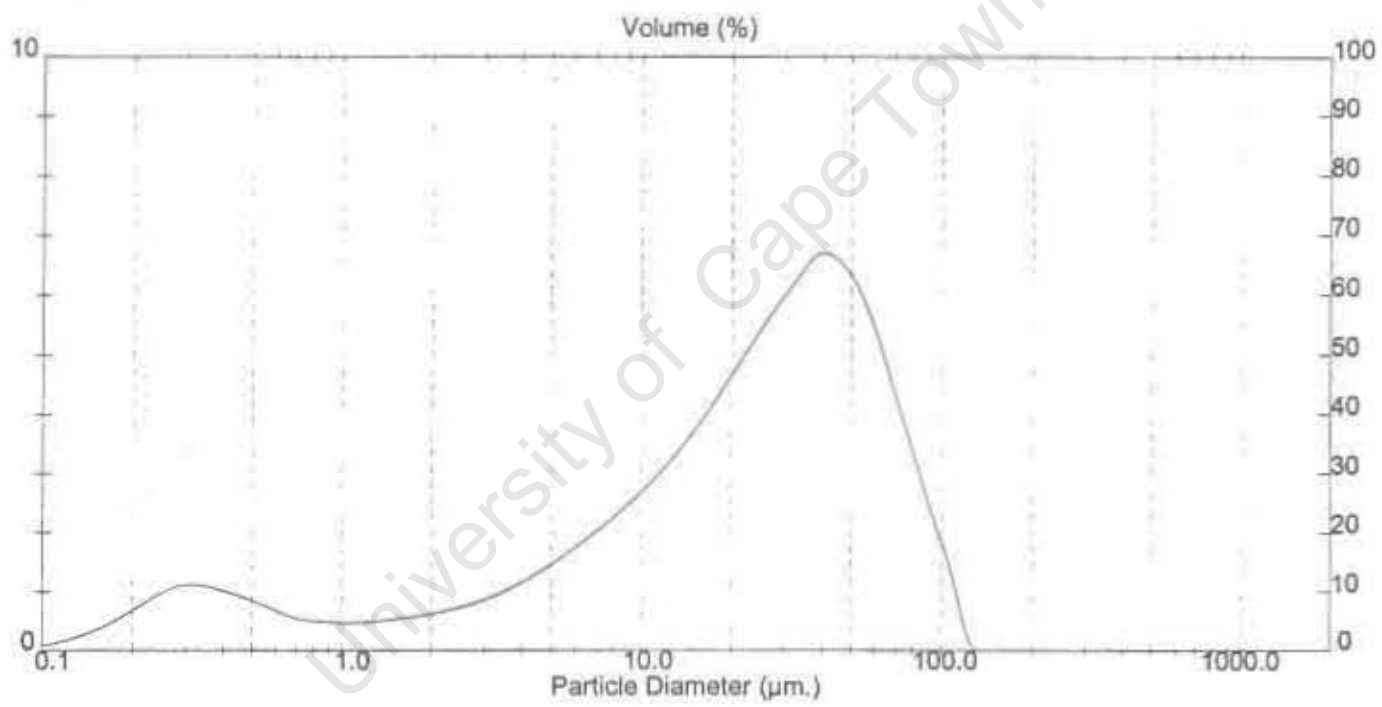
Result: Analysis Table

ID: Old mixed <75u Run No: 31 Measured: 26/1/2000 15:11
 File: HELEN Rec. No: 436 Analysed: 26/1/2000 15:11
 Path: C:\SIZERS\DATA\HELEN Source: Analyzed

Range: 300RE mm Beam: 2.40 mm Sampler: None Obs: 22.5 %
 Presentation: 30HD Analysis: Polydisperse Residual: 0.573 %
 Modifications: None

Conc. = 0.0209 %Vol Density = 3.000 g/cm³ S.S.A. = 0.8301 m²/g
 Distribution: Volume D[4, 3] = 29.80 um D[3, 2] = 2.41 um
 D(v, 0.1) = 0.94 um D(v, 0.5) = 24.26 um D(v, 0.9) = 66.53 um
 Span = 2.704E+00 Uniformity = 8.339E-01

Size (um)	Volume In %	Size (um)	Volume In %	Size (um)	Volume In %	Size (um)	Volume In %
0.05	0.00	0.58	0.65	5.63	2.03	76.32	3.16
0.06	0.01	0.67	0.53	7.72	2.31	88.91	2.06
0.07	0.02	0.78	0.49	9.00	2.61	103.58	0.99
0.08	0.05	0.91	0.47	10.46	2.95	120.67	0.00
0.09	0.09	1.06	0.47	12.21	3.34	140.58	0.00
0.11	0.15	1.24	0.50	14.22	3.78	163.77	0.00
0.13	0.25	1.44	0.54	16.57	4.27	190.80	0.00
0.15	0.39	1.68	0.58	19.31	4.79	222.26	0.00
0.17	0.57	1.95	0.65	22.49	5.31	258.95	0.00
0.20	0.78	2.26	0.73	26.20	5.80	301.66	0.00
0.23	0.97	2.65	0.83	30.53	6.25	351.46	0.00
0.27	1.10	3.09	0.95	35.56	6.66	409.45	0.00
0.31	1.11	3.60	1.11	41.43	6.99	477.01	0.00
0.36	1.03	4.19	1.31	48.27	7.15	555.71	0.00
0.42	0.92	4.88	1.53	56.23	7.15	647.41	0.00
0.49	0.80	5.69	1.77	65.51	6.86	754.23	0.00
0.58	0.80	6.63	1.77	76.32	4.25	878.67	0.00



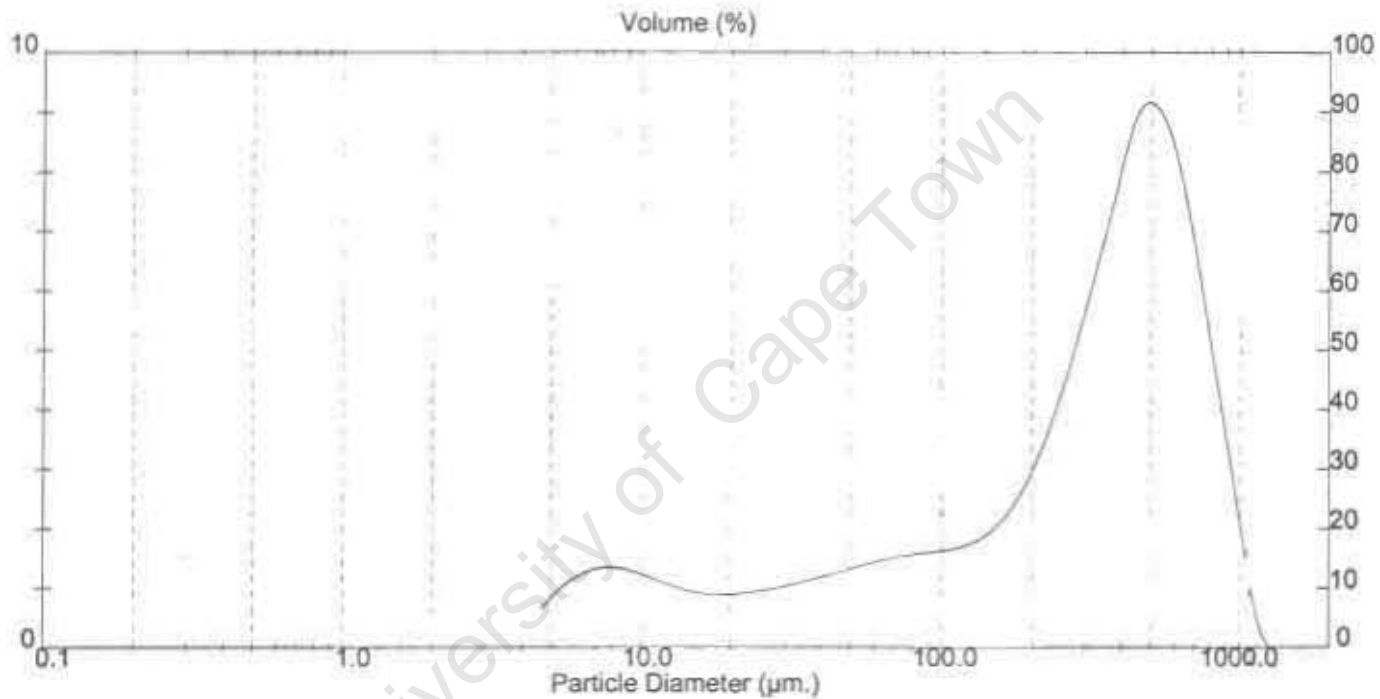
Result: Analysis Table

ID: Old mixed 300-1000u Run No: 34 Measured: 26/1/2000 15:43
 File: HELEN Rec. No: 438 Analysed: 26/1/2000 18:43
 Path: C:\SIZERS\DATA\HELEN Source: Analysed

Range: 1000 µm Beam: 2.40 mm Sampler: None Obs: 19.2 %
 Presentation: 30HD Analysis: Polydisperse Residual: 1.137 %
 Modifications: None

Conc: = 0.1567 %Vol Density = 3.000 g/cm³ S.S.A = 0.0361 m²/g
 Distribution: Volume D[4,3] = 359.04 µm D[3,2] = 55.44 µm
 D(v, 0.1) = 17.30 µm D(v, 0.5) = 345.85 µm D(v, 0.9) = 727.06 µm
 Span = 2.052E+00 Uniformity = 8.445E-01

Size (µm)	Volume In %	Size (µm)	Volume In %	Size (µm)	Volume In %	Size (µm)	Volume In %
4.19	0.83	22.49	0.94	120.67	1.78	647.41	6.84
4.86	0.95	26.20	1.00	140.56	2.02	754.23	4.84
5.69	1.19	30.53	1.07	163.77	2.44	878.67	2.84
6.63	1.32	35.56	1.16	190.80	3.08	1023.66	0.84
7.72	1.34	41.43	1.25	222.29	3.96	1192.56	0.00
9.00	1.28	48.27	1.35	258.95	5.04	1389.33	0.00
10.46	1.13	56.23	1.44	301.58	6.28	1618.57	0.00
12.21	1.01	65.51	1.52	351.46	7.58	1885.84	0.00
14.22	0.92	76.32	1.57	409.45	8.85	2196.77	0.00
16.57	0.89	88.91	1.61	477.01	9.09	2559.23	0.00
19.31	0.90	103.58	1.67	555.71	8.39	2961.51	0.00
22.49	0.90	120.67	1.67	647.41	8.39	3473.45	0.00



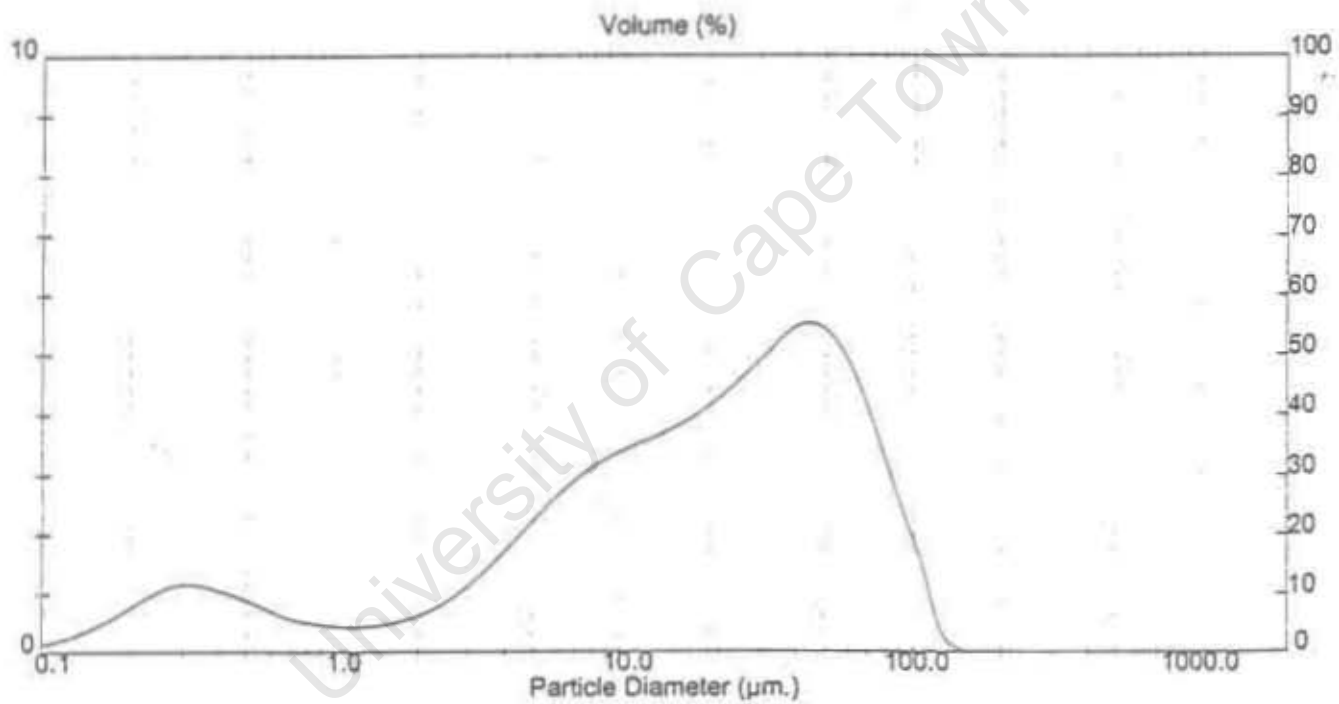
Result: Analysis Table

ID: New EAF <75 Run No: 25 Measured: 28/1/2000 14:48
 File: HELEN Rec. No: 570 Analysed: 28/1/2000 14:48
 Path: C:\SIZERS\DATA\HELEN Source: Analysed

Range: 300RF mm Beam: 2.40 mm Sampler: None Obs: 15.3 %
 Presentation: 3CHD Analysis: Polydisperse Residual: 0.656 %
 Modifications: None

Conc. = 0.0125 %Vol Density = 3.000 g/cm³ S.S.A. = 0.9344 m²/g
 Distribution: Volume D[4, 3] = 27.51 μm D[3, 2] = 2.14 μm
 D[v, 0.1] = 0.73 μm D[v, 0.5] = 18.44 μm D[v, 0.9] = 68.85 μm
 Span = 3.406E+00 Uniformity = 1.055E+00

Size (μm)	Volume In %	Size (μm)	Volume In %	Size (μm)	Volume In %	Size (μm)	Volume In %
0.05	0.01	0.56	0.68	6.83	2.94	78.32	3.09
0.06	0.02	0.67	0.55	7.72	3.18	86.91	2.13
0.07	0.04	0.78	0.49	9.00	3.34	103.58	1.16
0.08	0.07	0.91	0.44	10.48	3.49	120.87	0.19
0.09	0.13	1.06	0.42	12.21	3.62	140.58	0.00
0.11	0.21	1.24	0.44	14.22	3.77	163.77	0.00
0.13	0.32	1.44	0.46	16.57	3.95	190.80	0.00
0.15	0.47	1.68	0.55	19.31	4.18	222.28	0.00
0.17	0.68	1.95	0.67	22.49	4.48	258.95	0.00
0.20	0.86	2.28	0.83	26.20	4.78	301.68	0.00
0.23	1.04	2.65	1.05	30.53	5.08	351.48	0.00
0.27	1.15	3.09	1.33	35.56	5.40	409.45	0.00
0.31	1.15	3.60	1.54	41.43	5.50	477.01	0.00
0.36	1.07	4.19	1.99	48.27	5.33	555.71	0.00
0.42	0.98	4.86	2.33	56.23	4.84	647.41	0.00
0.49	0.83	5.68	2.66	65.51	4.06	754.23	0.00
0.56		6.63		76.32		878.67	0.00



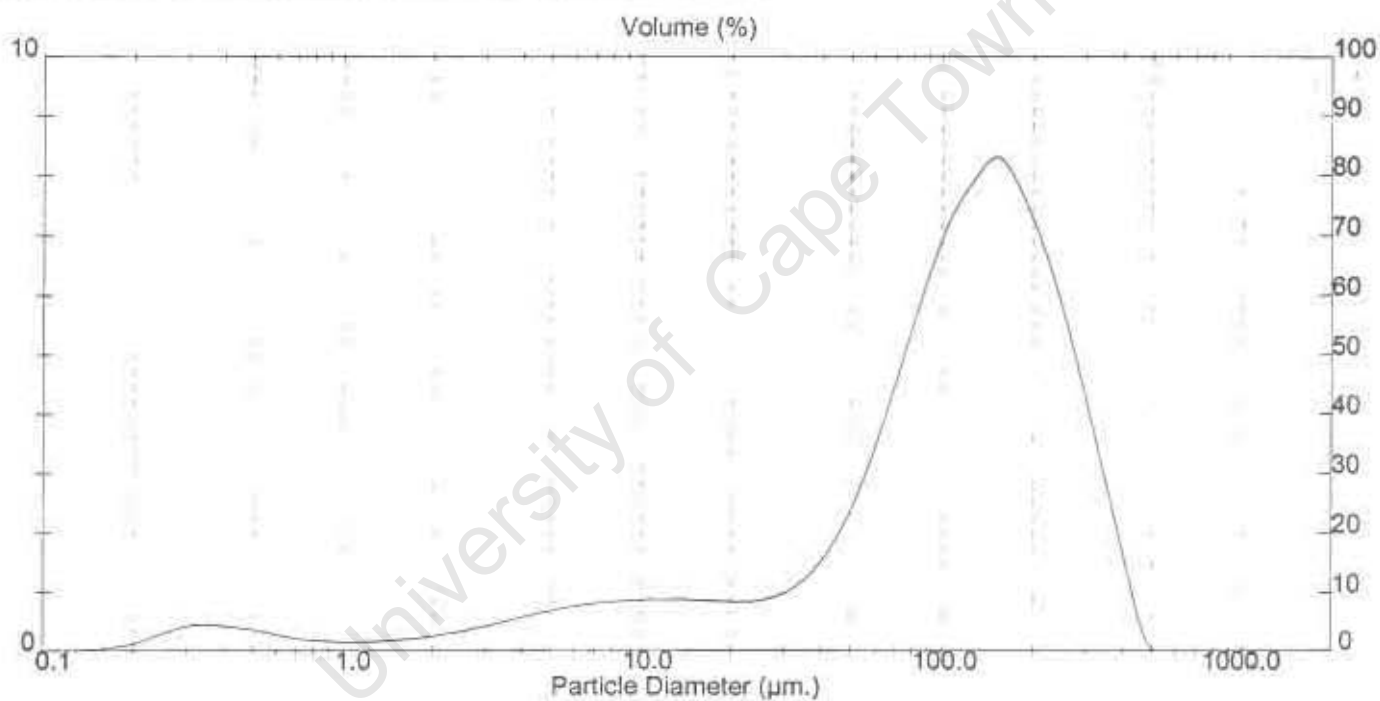
Result: Analysis Table

ID: New EAF 75-300	Run No: 23	Measured: 26/1/2000 14:32
File: HELEN	Rec. No: 431	Analysed: 26/1/2000 14:32
Path: C:\SIZERS\DATA\HELEN		Source: Analysed

Range: 300RF mm	Beam: 2.40 mm	Sampler: None	Obs: 18.6 %
Presentation: 3OHD	Analysis: Polydisperse		Residual: 0.330 %
Modifications: None			

Conc. = 0.0455 %Vol	Density = 3.000 g/cm ³	S.S.A. = 0.2397 m ² /g
Distribution: Volume	D[4, 3] = 131.68 µm	D[3, 2] = 8.34 µm
D(v, 0.1) = 9.30 µm	D(v, 0.5) = 117.21 µm	D(v, 0.9) = 288.01 µm
Span = 2.207E+00	Uniformity = 8.524E-01	

Size (µm)	Volume In %	Size (µm)	Volume In %	Size (µm)	Volume In %	Size (µm)	Volume In %
0.05	0.00	0.58	0.26	5.83	0.81	76.32	5.84
0.06	0.00	0.67	0.20	7.72	0.84	88.91	6.68
0.07	0.00	0.78	0.17	9.00	0.86	103.58	7.45
0.08	0.00	0.91	0.15	10.48	0.87	120.67	7.98
0.09	0.00	1.06	0.15	12.21	0.87	140.58	8.29
0.11	0.01	1.24	0.16	14.22	0.86	163.77	7.88
0.13	0.01	1.44	0.19	16.57	0.85	190.80	7.11
0.15	0.04	1.68	0.22	19.31	0.84	222.28	6.12
0.17	0.08	1.95	0.27	22.49	0.85	258.95	4.88
0.20	0.18	2.28	0.32	26.20	0.92	301.68	3.50
0.23	0.28	2.65	0.39	30.53	1.10	351.48	2.11
0.27	0.40	3.09	0.47	35.56	1.41	409.45	0.72
0.31	0.44	3.60	0.55	41.43	1.69	477.01	0.00
0.36	0.42	4.18	0.63	48.27	2.57	555.71	0.00
0.42	0.38	4.88	0.71	56.23	3.47	647.41	0.00
0.49	0.33	5.69	0.77	65.51	4.53	754.23	0.00
0.58	0.33	6.63	0.77	76.32	4.53	876.67	0.00



Result: Analysis Table

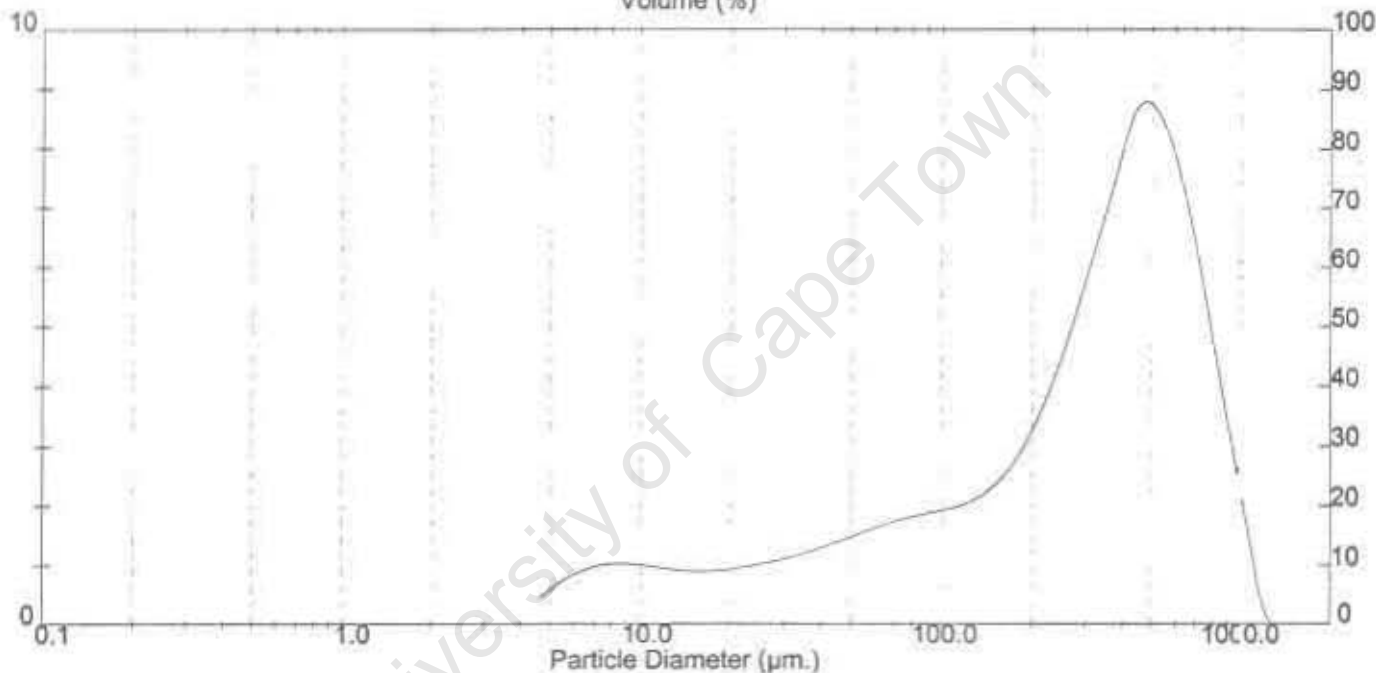
ID: New EAF 300-1000 Run No: 32 Measured: 26/1/2000 15:37
 File: HELEN Rec No: 437 : Analysed: 26/1/2000 15:37
 Path: C:\SIZERS\DATA\HELEN Source: Analyzed

Range: 1000 mm Beam: 2.40 mm Sampler: None Obs: 18.9 %
 Presentation: 3DHD Analysis: Polydisperse Residual: 0.735 %
 Modifications: None

Conc. = 0.1795 %Vol Density = 3.000 g/cm³ S.S.A. = 0.0311 m²/g
 Distribution: Volume D[4, 3] = 354.98 um D[3, 2] = 84.32 um
 D(v, 0.1) = 24.09 um D(v, 0.5) = 333.11 um D(v, 0.9) = 729.84 um
 Span = 2.107E+00 Uniformity = 8.814E-01

Size (um)	Volume In %	Size (um)	Volume In %	Size (um)	Volume In %	Size (um)	Volume In %
4.19	0.42	22.49	1.00	120.67	2.11	647.41	8.43
4.86	0.68	26.20	1.07	140.58	2.36	754.23	4.64
5.69	0.86	30.53	1.15	163.77	2.77	878.67	2.85
6.63	0.98	35.56	1.26	190.60	3.39	1023.66	1.06
7.72	1.02	41.43	1.26	222.28	4.21	1192.56	0.00
9.00	1.01	48.27	1.37	258.95	5.22	1369.33	0.00
10.48	0.96	56.23	1.50	301.68	6.35	1618.57	0.00
12.21	0.91	65.51	1.62	351.46	7.52	1885.64	0.00
14.22	0.91	76.32	1.73	409.45	8.61	2196.77	0.00
16.57	0.90	88.91	1.82	477.01	8.66	2559.23	0.00
19.31	0.94	103.56	1.89	555.71	7.86	2961.51	0.00
22.49	0.94	120.67	1.97	647.41	7.86	3473.45	0.00

Volume (%)



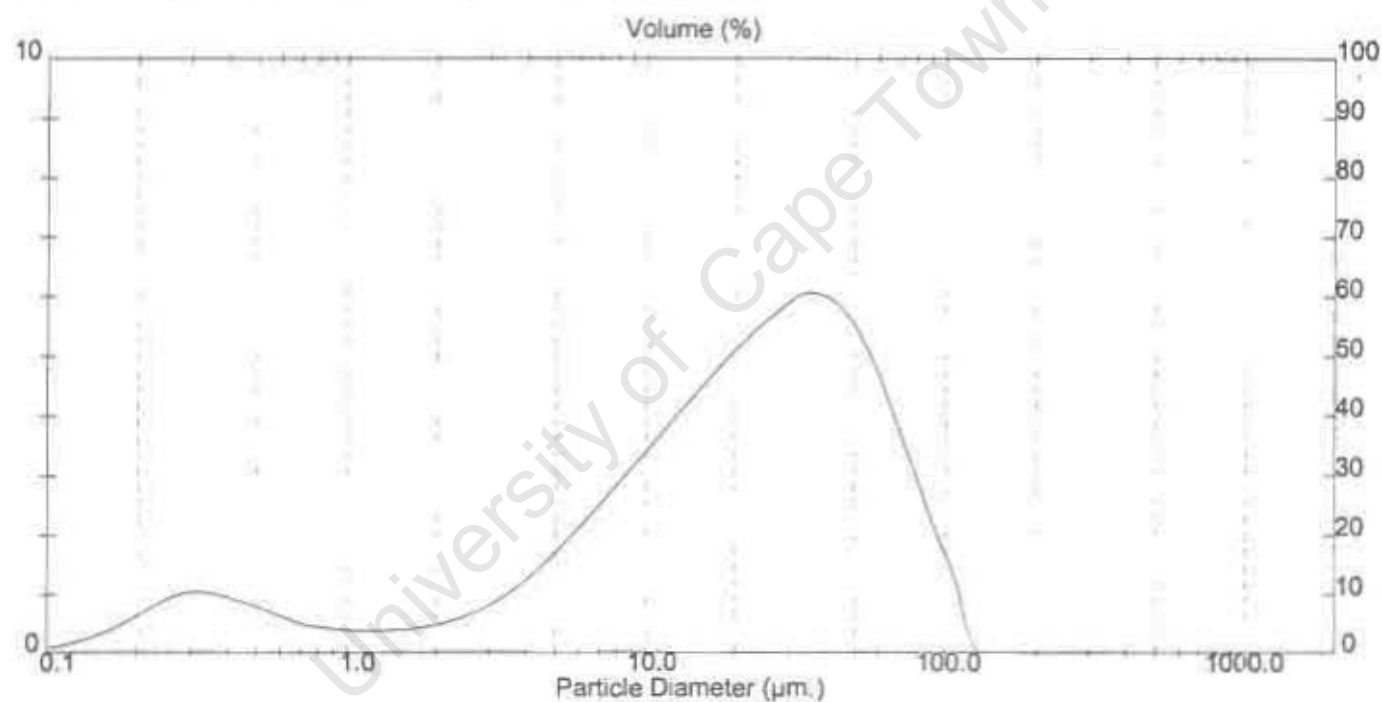
Result: Analysis Table

ID: New CLU <75 Run No: 20 Measured: 25/1/2000 14:25
 File: HELEN Rec. No: 430 Analysed: 26/1/2000 14:25
 Path: C:\SIZERS\DATA\HELEN Source: Analysed

Range: 300RF mm Beam: 2.40 mm Sampler: None Obs.: 20.3 %
 Presentation: 3OHD Analysis: Polydisperse Residual: 0.587 %
 Modifications: None

Conc. = 0.0195 %Vol Density = 3.000 g/cm³ S.S.A. = 0.7782 m²/g
 Distribution: Volume D[4,3] = 28.06 um D[3,2] = 2.58 um
 D[v, 0.1] = 1.29 um D[v, 0.5] = 21.48 um D[v, 0.9] = 83.99 um
 Span = 2.919E+00 Uniformity = 8.900E-01

Size (um)	Volume In %	Size (um)	Volume In %	Size (um)	Volume In %	Size (um)	Volume In %
0.05	0.00	0.58	0.59	6.83	2.55	78.32	2.79
0.06	0.01	0.67	0.46	7.72	2.93	88.91	1.88
0.07	0.02	0.78	0.43	9.00	3.31	103.58	0.97
0.08	0.04	0.91	0.39	10.48	3.69	120.67	0.00
0.09	0.08	1.06	0.37	12.21	4.08	140.58	0.00
0.11	0.14	1.24	0.36	14.22	4.46	163.77	0.00
0.13	0.23	1.44	0.40	16.57	4.83	190.80	0.00
0.15	0.36	1.68	0.43	19.31	5.18	222.28	0.00
0.17	0.53	1.95	0.50	22.49	5.48	258.95	0.00
0.20	0.72	2.28	0.60	26.20	5.77	301.68	0.00
0.23	0.91	2.65	0.75	30.53	6.02	351.46	0.00
0.27	1.02	3.09	0.94	35.56	6.22	409.45	0.00
0.31	1.03	3.60	1.19	41.43	6.38	477.01	0.00
0.36	0.96	4.19	1.48	48.27	6.51	555.71	0.00
0.42	0.85	4.88	1.82	56.23	6.59	647.41	0.00
0.49	0.74	5.69	2.18	65.51	6.62	754.23	0.00
0.58	0.74	6.63	2.55	76.32	6.62	878.67	0.00



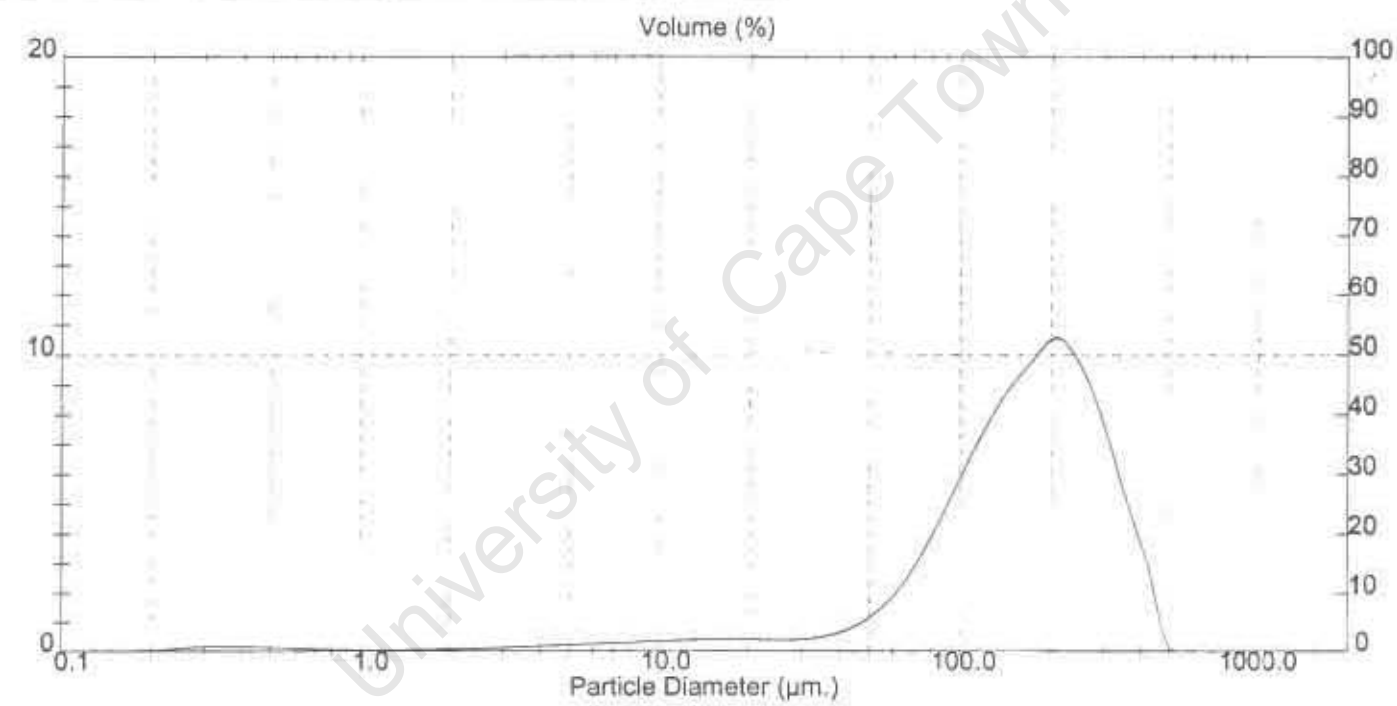
Result: Analysis Table

ID: New CLU 75-300	Run No: 18	Measured: 26/1/2000 14:17
File: HELEN	Rec. No: 429	Analysed: 26/1/2000 14:17
Path: C:\SIZERS\DATA\HELEN		Source: Analysed

Range: 300RF mm	Beam: 2.40 mm	Sampler: None	Obs: 14.7 %
Presentation: 3CHD	Analysis: Polydisperse		Residual: 0.376 %
Modifications: None			

Conc. = 0.0844 %Vol	Density = 3.000 g/cm ³	S.S.A = 0.0926 m ² /g
Distribution: Volume	D(4, 3) = 180.20 μ m	D[3, 2] = 21.61 μ m
D(v, 0.1) = 58.46 μ m	D(v, 0.5) = 169.07 μ m	D(v, 0.9) = 321.63 μ m
Span = 1.557E+00	Uniformity = 4.628E-01	

Size (μ m)	Volume In %	Size (μ m)	Volume In %	Size (μ m)	Volume In %	Size (μ m)	Volume In %
0.05	0.00	0.58	0.10	6.83	0.28	76.32	4.08
0.06	0.00	0.67	0.07	7.72	0.31	88.91	5.46
0.07	0.00	0.78	0.07	9.00	0.34	103.58	6.85
0.08	0.00	0.91	0.06	10.48	0.36	120.67	8.11
0.09	0.00	1.06	0.05	12.21	0.39	140.58	9.10
0.11	0.00	1.24	0.05	14.22	0.40	163.77	9.88
0.13	0.00	1.44	0.06	16.57	0.40	190.80	10.54
0.15	0.01	1.68	0.07	19.31	0.39	222.28	9.98
0.17	0.03	1.95	0.07	22.49	0.38	258.95	8.59
0.20	0.05	2.28	0.10	26.20	0.39	301.68	6.54
0.23	0.10	2.65	0.12	30.53	0.45	351.46	4.34
0.27	0.14	3.09	0.15	35.56	0.59	409.45	2.14
0.31	0.16	3.60	0.17	41.43	0.85	477.01	0.00
0.36	0.16	4.19	0.20	48.27	1.26	555.71	0.00
0.42	0.14	4.88	0.23	56.23	1.95	647.41	0.00
0.49	0.12	5.69	0.25	65.51	2.89	754.23	0.00
0.58		6.63		76.32		878.67	0.00



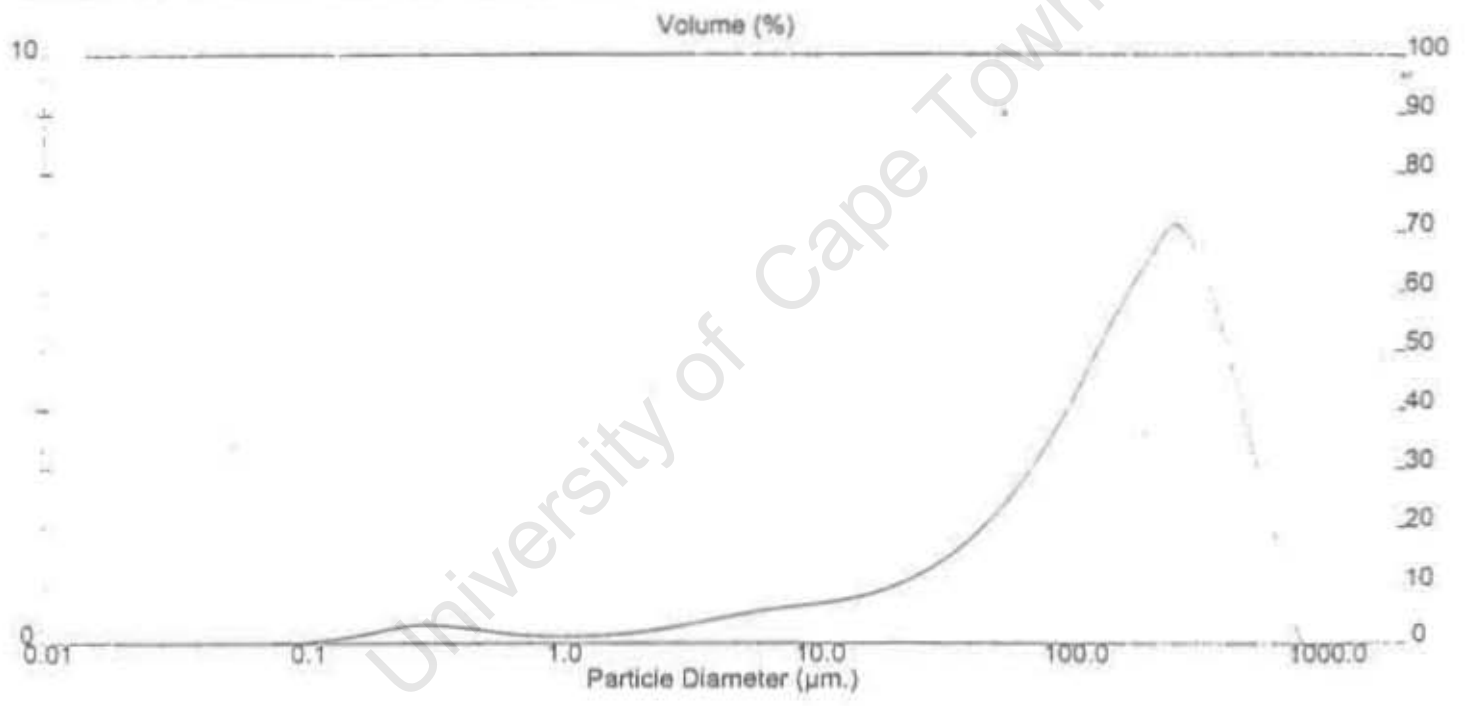
Result: Analysis Table

ID: New-CLU300-1000UL Run No: 38 Measured: 25/1/2000 14:19
 File: HELEN Rec. No: 552 Analysed: 25/1/2000 14:20
 Path: C:\SIZER\DATA\HELEN Source: Analysed

Range: 300RF mm Beam: 2.40 mm Sampler: None Obs: 14.5 %
 Presentation: 3CHD Analytic: Polydisperse Residual: 0.385 %
 Modifier: t: None

Conc. = 0.0418 %Vol Density = 3.000 g/cm³ S.S.A. = 0.2481 m²/g
 Distribution: Volume D[4, 3] = 191.57 μ m D[3, 2] = 8.06 μ m
 D[v, 0.1] = 14.66 μ m D[v, 0.5] = 158.51 μ m D[v, 0.9] = 414.78 μ m
 Span = 2.506E+00 Uniformity = 7.732E-01

Size (μ m)	Volume In %	Size (μ m)	Volume In %	Size (μ m)	Volume In %	Size (μ m)	Volume In %
0.05	0.00	0.56	0.19	5.53	0.59	78.32	3.48
0.06	0.00	0.67	0.15	7.72	0.63	86.91	4.01
0.07	0.01	0.78	0.14	9.00	0.67	103.56	4.58
0.08	0.01	0.91	0.13	10.46	0.71	120.87	5.16
0.09	0.03	1.06	0.12	12.21	0.76	140.56	5.72
0.11	0.05	1.24	0.13	14.22	0.82	163.77	6.23
0.13	0.07	1.44	0.14	16.57	0.90	190.60	6.68
0.15	0.11	1.66	0.16	19.31	1.00	222.28	7.09
0.17	0.17	1.95	0.19	22.49	1.13	256.95	8.90
0.20	0.22	2.28	0.23	26.20	1.29	301.68	8.30
0.23	0.28	2.65	0.28	30.53	1.46	351.46	5.37
0.27	0.32	3.09	0.33	35.56	1.70	409.45	4.26
0.31	0.32	3.60	0.39	41.43	1.97	477.01	3.15
0.36	0.30	4.19	0.45	48.27	2.27	555.71	2.05
0.42	0.27	4.86	0.50	56.23	2.63	647.41	0.94
0.49	0.23	5.69	0.55	65.51	3.03	754.23	0.00
0.58	0.23	6.63	0.55	76.32	3.03	878.67	0.00



**APPENDIX C: THE
ANALYSIS BY UV-
VISIBLE
SPECTROSCOPY,
PROCEDURE, LIMITS
OF DETECTION AND
REPRODUCIBILITY**

University of Cape Town

A Description of the Method of Cr(VI) Analysis by UV-Visible Spectroscopy

Preparation of Standard Solutions

As in the case of other instrumental methods, analysis by UV-Visible Spectroscopy requires the preparation of standard solutions to construct a calibration curve that is used as a basis for the calculation of the sample concentrations from absorbance readings. A 1000ppm potassium dichromate ($K_2Cr_2O_7$) solution was used as the main standard Cr(VI) solution. This solution was prepared by dissolving 2.829g of potassium dichromate (which had been pre-dried in an oven at $103^{\circ}C$ overnight) in distilled water. Once all the dichromate had dissolved, the solution was transferred to a 1l volumetric flask and made up to mark with distilled water. The Cr(VI) standard was then stored in a brown bottle and stored in a refrigerator. As long as this solution is always kept in a refrigerator it retains its quality for extended periods of time. This solution was diluted to prepare a 10ppm stock solution and a series of Cr(VI) standards in the concentration range 100-1000 ppb. The reason for selecting this concentration range was that this is the medium concentration range, which can be detected by the instrument used for the analysis and is fairly easy to work with. The stock solution and the range of standards was prepared as follows:-

10 ppm stock solution: 9.9ml of distilled water was added to 0.1ml of 1000ppm standard solution in a sample vial

100 ppb standard solution: 9.9ml of distilled water was added to 0.1ml of the 10ppm stock solution in a sample vial. 5ml of this solution was transferred to a separate sample vial for analysis

200 ppb standard solution: 4.9ml distilled water was added to 0.1ml of the 10ppm stock solution in a sample vial

500 ppb standard solution: 4.75ml distilled water was added to 0.25ml of the 10ppm stock solution in a sample vial

1000 ppb standard solution: 4.5ml distilled water was added to 0.5ml of the 10ppm stock solution in a sample vial

2000 ppb standard solution: 4ml distilled water was added to 1ml of the 10ppm stock solution in a sample vial.

Note: Only 5ml of each standard solution was used for analysis. The 10ppm stock solution and all standard solutions were prepared on the day of analysis (ie. 1-2 hours prior to analysis)

i) Preparation of the Diphenylcarbazide solution

A diphenylcarbazide solution was used as the colorimetric reagent for this analysis. This is because diphenylcarbazide forms a complex with Cr(VI) species particularly chromate ions in acidic solutions and at low concentrations. The complex formation results in a purple colour which has an intensity that can be easily measured on a UV-Visible spectrophotometer at 543nm.

The diphenylcarbazide solution was prepared by dissolved 0.2g of diphenylcarbazide in 50 ml ethanol in a Erlenmayer flask on a magnetic stirrer. The solution was covered with a watchglass to avoid contamination. Once all the diphenylcarbazide had dissolved in the ethanol, the solution was transferred to 500ml volumetric flask where 250ml of 0.5M H₂SO₄ (prepared by dissolving 50g of concentrated sulphuric in 1l of water) was added to it. The solution was then made up to the mark using distilled water and stored in a refrigerator.

ii) Sample Pre-treatment

As discussed earlier, all solid samples were leached in 1M NaOH and the filtrates were collected and analysed for their Cr(VI) content. However, the complex formation with diphenylcarbazide only occurs in acidic solutions. Thus, to ensure that any Cr(VI) species (chromate ions) form a complex with diphenylcarbazide so that these species could be easily detected on the UV, the samples were acidified prior to analysis. In order to achieve a reasonably acidic solution, 2.5ml of 0.5M H₂SO₄ was added to 2.5ml of each sample in a sample vial.

iii) The Instrumental Analysis

The standard solutions were analysed first in the order of increasing concentration. Three standard solutions or samples were analysed at a time. The diphenylcarbazide solution was diluted in a ratio of 2:1 and 7.5ml of the diluted diphenylcarbazide solution was added to each standard or sample. These solutions were left to stand for 5 minutes to allow the colour to develop while the Cr(VI) in the forms complexes with the diphenylcarbazide. The wavelength of the instrument was set to 543nm and its signal averaging time was set to one second.

A blank solution in which 7.5ml of diphenylcarbazide was added to 5ml distilled water was also prepared. Some of this was poured into a cuvette and placed into the back cuvette holder of the instrument to act as a reference sample. The rest of the blank solution was poured into a cuvette and placed into the front cuvette holder to set the instrument to zero. The cuvette containing the blank solution was rinsed in distilled water and the first sample or standard was poured into the cuvette to record the first stable absorbance reading for the sample or standard solution. This procedure was repeated until a stable absorbance reading for each sample was obtained. Each sample or standard solution was analysed either twice or thrice using different cuvettes to check the accuracy of the absorbance readings. Each time that a different cuvette was used, the instrument was set to zero using the blank solution. All unstable or unreliable absorbance readings were ignored and the analysis for the sample in question was repeated.

The Limits of Detection

The procedure outlined above has indicated that a calibration range of 100ppb-2000ppb was selected. The lower analytical limit is therefore 100ppb. For a standard ball of 25g which contains 50% Cr₂O₃ this translates into a conversion of 11.69 µg per g Cr. Thus any conversions below this value and particularly those of the pure chemical experiments must be treated with care. This must also be noted when assessing the reproducibility of the results.

The Reproducibility of the Analytical Data

i) The Reproducibility of the Sample Readings

The reproducibility of the results was ascertained by conducting repeat analyses for each sample on different days. Typically, the analyses were conducted in triplicate but in cases where unreliable analytical data was obtained further repeat analyses were conducted. For the purpose of discussion a selected portion of these results are shown in Table C1.

University of Cape Town

TableC1: A Statistical Analysis of the Analytical Data Obtained for the Experiment
 Series: Cr₂O₃-Ca(OH)₂ Balls with the pore moisture maintained and Containing 50 %
 Ca(OH)₂

SAMPLE	ABSORBANCE READING			MEAN	STANDARD DEVIATION	% DIFFERENCE BETWEEN ANALYSIS AND REPEATS
	1	2	3			
0 WEEK	0.0003	0.0003	0.0003	0.0003	3.33×10^{-5}	66.67
0 WEEK REPEAT	0.0004	0.0008	0.0003	0.0005	2.33×10^{-4}	
1 WEEK	0.0010	0.0011	0.0010	0.0011	5.77×10^{-5}	20.83
1 WEEK REPEAT	0.0013	0.0013	0.0013	0.0013	1.92×10^{-5}	
2 WEEKS	0.0019	0.0020	0.0019	0.0019	1.92×10^{-5}	16.57
2 WEEKS REPEAT	0.0023	0.0023	0.0022	0.0023	5.77×10^{-5}	
4 WEEKS	0.0028	0.0028	0.0029	0.0028	5.77×10^{-5}	13.53
4 WEEKS REPEAT	0.0025	0.0024	0.0025	0.0025	5.00×10^{-5}	
8 WEEKS	0.0054	0.0054	0.0050	0.0052	2.47×10^{-4}	1.27
8 WEEKS REPEAT	0.0053	0.0052	0.0054	0.0053	1.00×10^{-4}	
12 WEEKS	0.0070	0.0067	0.0072	0.0069	2.52×10^{-4}	3.37
12 WEEKS REPEAT	0.0069	0.0066	0.0066	0.0067	1.44×10^{-4}	
16 WEEKS	0.0086	0.0085	0.0089	0.0087	2.18×10^{-4}	3.28
16 WEEKS REPEAT	0.0086	0.0083	0.0083	0.0084	2.02×10^{-4}	
20 WEEKS	0.0096	0.0096	0.0096	0.0096	1.65×10^{-10}	1.05
20 WEEKS REPEAT	0.0098	0.0094	0.0098	0.0097	2.60×10^{-4}	
28 WEEKS	0.0125	0.0124	0.0125	0.0124	2.89×10^{-5}	0.94
28 WEEKS REPEAT	0.0123	0.0126	0.0121	0.0123	2.57×10^{-4}	
44 WEEKS	0.0130	0.0125	0.0125	0.0127	2.60×10^{-4}	1.45
44 WEEKS REPEAT	0.0125	0.0126	0.0124	0.0125	7.64×10^{-5}	
56 WEEKS	0.0121	0.0125	0.0126	0.0124	2.46×10^{-4}	0.81
56 WEEKS REPEAT	0.0121	0.0128	0.0125	0.0125	3.67×10^{-4}	

The statistical analysis shows that a high level of reproducibility has been obtained for the analyses conducted and the standard deviations are very low. As noted earlier, the initial absorbance readings are much lower than that of the lower analytical limit (100ppb standard) so there is a high percentage difference between readings for the original and the repeat experiments initially. However, as the lower analytical limit is approached the percentage difference between the readings of the original and the repeat experiments becomes smaller. In this instance, the readings are more accurate and reliable.

ii) The Reproducibility of the Standard Readings

The absorbance readings obtained for the standards solutions are shown in Table C2. This shows a comparison of the average absorbance readings obtained for the standards over approximately a one –year period.

Table C2: The Reproducibility of the Absorbance Readings for the Standards

Standard Concentration (ppb)	Average Absorbance Reading on 23 August 1999	Average Absorbance Reading on 13 August 2000	Mean	Standard Deviation	% RSD
100	0.0288	0.0284	0.0286	2.83×10^{-4}	9.89×10^{-1}
200	0.0562	0.0564	0.0563	2.00×10^{-4}	3.56×10^{-1}
500	0.1498	0.1497	0.1497	5.89×10^{-5}	3.94×10^{-2}
1000	0.2856	0.2878	0.2867	1.61×10^{-3}	5.63×10^{-1}
2000	0.5646	0.5631	0.5639	1.06×10^{-3}	1.88×10^{-1}

The statistical analysis in Table C2 shows that the level of reproducibility for the absorbance readings of the standards is good. This is supported by the low standard deviations and the fact that all relative standard deviations are below 1%. The corresponding x-variables and intercepts obtained on the respective days were 8.16 and 1.00 and 8.15 and 1.00 on the respective days. This also indicated a high level of reproducibility.

**APPENDIX D:
VERIFICATION THAT
DRYING THE Cr_2O_3 -
 $\text{Ca}(\text{OH})_2$ BALLS AT 80°C
DID NOT CAUSE ANY
ADDITIONAL
OXIDATION**

Table D : A comparison of the Conversions in $\text{Cr}_2\text{O}_3\text{-Ca(OH)}_2$ Balls which oven dried and dried under nitrogen respectively

<i>Experimental Series</i>	<i>Sample</i>	<i>Method of Drying</i>	<i>Conversion (ug per g Cr)</i>
Cr ₂ O ₃ -Ca(OH) ₂ Balls with 50% Ca(OH) ₂	1 week	Oven dried at 80°C	1.03
		Dried under nitrogen	1.02
Old Mixed Slag Ball <75um	1 week	Oven dried at 80°C	1738.46
		Dried under nitrogen	1712.24

Note: These tests were conducted only on balls where the pore moisture maintained.

University of Cape Town

**APPENDIX E:
ANALYSIS OF THE
PURE CHEMICALS FOR
TRACE
CONTAMINANTS THAT
MAY CONTRIBUTE TO
OXIDATION**

University of Groningen

Table E: The background concentrations of elements likely to cause oxidation the reagents used for experimental work

<i>Reagent</i>	<i>Mn (ppm)</i>	<i>Mn (%)</i>	<i>Ag (ppm)</i>	<i>Ag (%)</i>	<i>Ca (ppm)</i>	<i>Ca (%)</i>	<i>Cr(VI) (ppb)</i>
CaO	0.29	0.027	0.05	0.005	ND	ND	ND
Cr2O3	0.13	0.01	0.04	0.003	0.95	0.08	ND
NaOH	ND	ND	ND	ND	ND	ND	4.61

Notes:

1. ND implies not determined
2. All elements besides Cr(VI) were determined by Atomic Absorption Spectroscopy (AAS). The solid samples were subjected to a used ore digestion method prior to analysis.
3. Cr(VI) was determined by UV-Visible Spectroscopy using the analytical protocol outlined in Appendix C. The NaOH was analysed in solution form and was acidified for the reason outlined in Appendix C,
4. Overall it can be concluded that since the elements are not present in the significant quantities these are not likely to have had any impact on the oxidation patterns observed.
5. The Cr(VI) concentration detected in the NaOH must be viewed with care as this concentration is below the calibration range.

**APPENDIX F:
TEMPERATURE
RECORDS**

University of Cape Town

Table F1: Temperature Records for June 1999

<i>Date</i>	<i>Temperature Readings (degrees celcius)</i>			
	<i>Morning</i>	<i>Noon</i>	<i>Afternoon</i>	<i>Average Temperature (degrees celcius)</i>
10-Jun	20.5	20	20	20.2
11-Jun	21	21	22	21.3
14-Jun	20	20	21	20.3
15-Jun	20	21	21	20.7
17-Jun	20	21	22	21.0
18-Jun	20.5	20	20	20.2
21-Jun	20	21	21	20.7
22-Jun	21	21	21	21.0
23-Jun	21	21.5	22	21.5
24-Jun	21	20	22	21.0
25-Jun	20	21	21	20.7
28-Jun	17	17.5	19	17.8
29-Jun	20	21	21	20.7
30-Jun	21	20	20	20.3

University of Cape Town

Table F2: The Temperature Records for July 1999

<i>Date</i>	<i>Temperature Readings (degrees celcius)</i>			
	<i>Morning</i>	<i>Noon</i>	<i>Afternoon</i>	<i>Average Temperature (degrees celcius)</i>
1-Jul	21	22	22	21.7
2-Jul	20	20	21	20.3
5-Jul	23	23	23	23.0
6-Jul	20	21	21	20.7
7-Jul	21	22	22	21.7
8-Jul	20	20	21	20.3
9-Jul	20	21	21	20.7
12-Jul	20	20	20	20.0
13-Jul	20	20	21	20.3
14-Jul	20	21	21	20.7
15-Jul	20	20	20	20.0
16-Jul	20	21	22	21.0
17-Jul	20	20.5	20.5	20.3
18-Jul	20	21.5	22	21.2
19-Jul	19	21	20	20.0
20-Jul	21	21	21	21.0
21-Jul	20	21	21	20.7
22-Jul	21	21	21	21.0
23-Jul	20	20.5	20.5	20.3
26-Jul	20	20	20	20.0
27-Jul	20	20	21	20.3
28-Jul	20	20	20	20.0
29-Jul	20	21	21	20.7
30-Jul	21	20	20	20.3

Table F3: Temperature Records For August 1999

Date	Temperature Readings (degrees celcius)			
	Morning	Noon	Afternoon	Average Temperature (degrees celcius)
2-Aug	20	21	21	20.7
3-Aug	20	20	20	20.0
4-Aug	20	21	21	20.7
5-Aug	20	20	20	20.0
6-Aug	20	22	22	21.3
10-Aug	20	20	21	20.3
11-Aug	21	22	22	21.7
12-Aug	20	20	20	20.0
13-Aug	20	20	21	20.3
16-Aug	20	20	20	20.0
17-Aug	21	21	21.5	21.2
18-Aug	21	22	22	21.7
19-Aug	20	20	20	20.0
20-Aug	20	20	20	20.0
23-Aug	21	22	22	21.7
24-Aug	20	21	21	20.7
25-Aug	20	20.5	21	20.5
26-Aug	20	20	21	20.3
27-Aug	20	20	20	20.0
30-Aug	21	22	22	21.7
31-Aug	19	22	22	21.0

University of Cape Town

Table F4: Temperature records for September 1999

Date	Temperature Readings (degrees celcius)			
	Morning	Noon	Afternoon	Average Temperature (degrees celcius)
1-Sep	20	22	23	21.7
2-Sep	20	21	21	20.7
3-Sep	20	20	20	20.0
6-Sep	19	22.5	23	21.5
7-Sep	20	20.5	20	20.2
8-Sep	18	21	21	20.0
9-Sep	19	22	22	21.0
10-Sep	20	20.5	20	20.2
13-Sep	20	21	22	21.0
14-Sep	20	20	20	20.0
15-Sep	18	21	21	20.0
16-Sep	19	20	21	20.0
17-Sep	18	22	22.5	20.8
20-Sep	19	20.5	21	20.2
21-Sep	18	23	23	21.3
22-Sep	19	20	22	20.3
23-Sep	17	22	22	20.3
24-Sep	20	20	21	20.3
27-Sep	19	22	23	21.3
28-Sep	18	22	22	20.7
29-Sep	17	24	24	21.7
30-Sep	20	25	25	23.3

Table F5: Temperature records for October 1999

<i>Date</i>	<i>Temperature Readings (degrees celcius)</i>			
	<i>Morning</i>	<i>Noon</i>	<i>Afternoon</i>	<i>Average Temperature (degrees celcius)</i>
01-Oct	19	24	25	22.7
04-Oct	18	25	26	23.0
05-Oct	18	23	24	21.7
06-Oct	19	22	22	21.0
07-Oct	17	23	24	21.3
08-Oct	19	24	24	22.3
11-Oct	19	25	27	23.7
12-Oct	19	26	26	23.7
13-Oct	17	24	24	21.7
14-Oct	19	24	25	22.7
15-Oct	18	25	25	22.7
18-Oct	18	25	27	23.3
19-Oct	19	26	26	23.7
20-Oct	20	20	20	20.0
21-Oct	18	24	25	22.3
22-Oct	17	23	21	20.3
25-Oct	19	26	27	24.0
26-Oct	18	27	27	24.0
27-Oct	19	25	26	23.3
28-Oct	20	24	25	23.0
29-Oct	20	26	26	24.0
31-Oct	21	25	27	24.3

University of Cape Town

Table F6: Temperature Records for November

<i>Date</i>	<i>Temperature Readings (degrees celcius)</i>			
	<i>Morning</i>	<i>Noon</i>	<i>Afternoon</i>	<i>Average Temperature (degrees celcius)</i>
01-Nov	20	25	25	23.3
02-Nov	19	24	26	23.0
03-Nov	21	27	27	25.0
04-Nov	18	24	24	22.0
05-Nov	20	21	23	21.3
07-Nov	21	24	25	23.3
08-Nov	20	22	22	21.3
09-Nov	19	25	26	23.3
10-Nov	20	27	28	25.0
11-Nov	19	24	25	22.7
12-Nov	21	25	25	23.7
14-Nov	19	26	27	24.0
15-Nov	18	21	21	20.0
16-Nov	20	24	24	22.7
17-Nov	19	22	23	21.3
18-Nov	20	23	23	22.0
19-Nov	20	25	25	23.3
21-Nov	20	26	26	24.0
22-Nov	21	24	25	23.3
23-Nov	20	23	23	22.0
24-Nov	19	24	25	22.7
25-Nov	18	25.5	26	23.2
26-Nov	21	25	25	23.7
28-Nov	20	23	24	22.3
29-Nov	21	23	23	22.3
30-Nov	20	26	27	24.3

Table F7: Temperature Records for December 1999

<i>Date</i>	<i>Temperature Readings (degrees celcius)</i>			
	<i>Morning</i>	<i>Noon</i>	<i>Afternoon</i>	<i>Average Temperature (degrees celcius)</i>
01-Dec	20	25	25	23.3
02-Dec	21	26	26	24.3
03-Dec	22	26	27	25.0

University of Cape Town

Table F8: Temperature Records for January 2000

<i>Date</i>	<i>Temperature Readings (degrees ceicius)</i>			
	<i>Moming</i>	<i>Noon</i>	<i>Afternoon</i>	<i>Average Temperature (degrees celcius)</i>
17-Jan	23	28	29	26.7
18-Jan	24	29	29	27.3
19-Jan	26	30	30	28.7
20-Jan	20	27	27	24.7
21-Jan	23	27.5	29	26.5
23-Jan	24	28	28	26.7
24-Jan	20	25	26	23.7
25-Jan	24	29	29	27.3
26-Jan	23	25	25	24.3
27-Jan	25	28	28	27.0
28-Jan	20	27	27	24.7
30-Jan	18	22	22	20.7
31-Jan	20	24	24	22.7

University of Cape Town

Table F9: Temperature Records for February 2000

Date	Temperature Readings (degrees celcius)			
	Morning	Noon	Afternoon	Average Temperature (degrees celcius)
01-Feb	20	24	25	23.0
02-Feb	21	27	27	25.0
03-Feb	20	28	28.5	25.5
04-Feb	20	24	24	22.7
06-Feb	21	26	26.5	24.5
07-Feb	19	21	21	20.3
08-Feb	17	22	22	20.3
09-Feb	19	24	24	22.3
10-Feb	18	21	21	20.0
11-Feb	20	26	26	24.0
13-Feb	20	24	24	22.7
14-Feb	21	25	25	23.7
15-Feb	20	24	24	22.7
16-Feb	19	23	23	21.7
17-Feb	18	24	25	22.3
18-Feb	19	21	21	20.3
20-Feb	20	25	26	23.7
21-Feb	24	28	28	26.7
22-Feb	19	24	24	22.3
23-Feb	19	20	21	20.0
24-Feb	19	21	21	20.3
26-Feb	20	21	23	21.3
28-Feb	20	21	21	20.7
29-Feb	19	21	22	20.7

Table F10: Temperature Records for March 2000

<i>Date</i>	<i>Temperature Readings (degrees celcius)</i>			
	<i>Morning</i>	<i>Noon</i>	<i>Afternoon</i>	<i>Average Temperature (degrees celcius)</i>
01-Mar	20	23	23	22.0
02-Mar	20	22	24	22.0
03-Mar	19	21	21	20.3
04-Mar	20	25	26	23.7
06-Mar	19	22	22	21.0
07-Mar	18	21	21	20.0
08-Mar	20	24	24	22.7
09-Mar	20	20	20	20.0
10-Mar	18	22	22	20.7
11-Mar	19	23	24	22.0
12-Mar	20	20	20	20.0
13-Mar	19	21	21	20.3
14-Mar	20	24	24	22.7
15-Mar	19	22	23	21.3
16-Mar	20	20	20	20.0
17-Mar	19	20	22	20.3
18-Mar	20	24	24	22.7
19-Mar	20	25	26	23.7
20-Mar	19	22	22	21.0
21-Mar	20	22	22	21.3
22-Mar	20	24	24	22.7
23-Mar	19	22	23	21.3
24-Mar	18	24	24	22.0
25-Mar	20	21	21	20.7
26-Mar	20	24	24	22.7
27-Mar	21	23	23	22.3
28-Mar	20	24	24	22.7
29-Mar	20	21	21	20.7
30-Mar	20	23	24	22.3
31-Mar	19	21	22	20.7

Table A11: Temperature Records for April 2000

Date	Temperature Readings (degrees celcius)			
	Morning	Noon	Afternoon	Average Temperature (degrees celcius)
01-Apr	19	22	22	21.0
02-Apr	20	21	21	20.7
03-Apr	20	24	24	22.7
04-Apr	19	21	22	20.7
05-Apr	18	22	22	20.7
06-Apr	20	23	23	22.0
07-Apr	18	21	21	20.0
08-Apr	19	24	24	22.3
09-Apr	20	24	24	22.7
10-Apr	19	23	23	21.7
11-Apr	20	23	23	22.0
12-Apr	19	20	21	20.0
13-Apr	20	22	22	21.3
14-Apr	19	22	23	21.3
15-Apr	20	20	20	20.0
16-Apr	20	20	21	20.3
17-Apr	19	21	22	20.7
18-Apr	20	24	24	22.7
19-Apr	20	23	25	22.7
20-Apr	21	26	27	24.7
21-Apr	20	20	20	20.0
22-Apr	19	21	21	20.3
27-Apr	19	21	22	20.7
29-Apr	19	22	23	21.3
30-Apr	20	20	20	20.0

Table F12: Temperature Records for May 2000

Date	Temperature Readings (degrees celcius)			
	Morning	Noon	Afternoon	Average Temperature (degrees celcius)
01-May	20	20	20	20.0
02-May	20	20	21	20.3
03-May	17	22	22	20.3
04-May	19	23	24	22.0
05-May	18	21	22	20.3
06-May	19	21	22	20.7
07-May	20	20	21	20.3
08-May	19	22	22	21.0
09-May	18	20	22	20.0
10-May	19	21	21	20.3
11-May	19	23	23	21.7
12-May	20	20	20	20.0
13-May	18	22	24	21.3
14-May	19	23	23	21.7
15-May	19	21	21	20.3
16-May	19	22	23	21.3
17-May	19	24	24	22.3
18-May	19	22	22	21.0
19-May	18	21	21	20.0
20-May	17	22	22	20.3
21-May	20	20	21	20.3
22-May	19	22	23	21.3
23-May	17	22	23	20.7
24-May	19	23	23	21.7
25-May	20	20	21	20.3
26-May	20	20	20	20.0
29-May	17	22	22	20.3
30-May	18	21	23	20.7
31-May	18	24	24	22.0

Table F13: Temperature Records for June 2000

Date	Temperature Readings (degrees celcius)			
	Morning	Noon	Afternoon	Average Temperature (degrees celcius)
01-Jun	20	20	21	20.3
02-Jun	19	22	23	21.3
03-Jun	18	22	22	20.7
04-Jun	19	20	23	20.7
05-Jun	18	24	24	22.0
06-Jun	19	21	21	20.3
07-Jun	19	20	22	20.3
08-Jun	18	23	23	21.3
09-Jun	20	20	21	20.3
10-Jun	19	22	22	21.0
11-Jun	18	23	23	21.3
12-Jun	18	21	23	20.7
13-Jun	20	20	20	20.0
14-Jun	18	21	21	20.0
15-Jun	19	20	22	20.3
16-Jun	19	21	21	20.3
17-Jun	20	20	20	20.0
18-Jun	18	20	24	20.7
19-Jun	20	22	22	21.3
20-Jun	19	21	21	20.3
21-Jun	20	20	20	20.0
22-Jun	18	21	21	20.0
23-Jun	19	22	22	21.0
24-Jun	19	20	21	20.0
25-Jun	20	21	23	21.3
26-Jun	19	21	21	20.3
27-Jun	19	20	22	20.3
28-Jun	20	21	22	21.0
29-Jun	19	20	23	20.7
30-Jun	19	20	21	20.0

Table F14: Temperature Records for July 2000

<i>Date</i>	<i>Temperature Readings (degrees celcius)</i>			
	<i>Morning</i>	<i>Noon</i>	<i>Afternoon</i>	<i>Average Temperature (degrees celcius)</i>
01-Jul	19	21	21	20.3
02-Jul	19	22	23	21.3
03-Jul	18	21	21	20.0
04-Jul	19	20	21	20.0
05-Jul	18	20	22	20.0
06-Jul	19	22	22	21.0
07-Jul	19	20	21	20.0
08-Jul	20	20	20	20.0
09-Jul	18	21	21	20.0
10-Jul	18	22	22	20.7
11-Jul	18	21	22	20.3
12-Jul	20	20	20	20.0
13-Jul	20	20	21	20.3
14-Jul	19	21	21	20.3
15-Jul	19	20	21	20.0
16-Jul	19	22	22	21.0
17-Jul	20	20	21	20.3
18-Jul	20	20	20	20.0
19-Jul	19	21	21	20.3
20-Jul	19	20	22	20.3
21-Jul	18	21	22	20.3
22-Jul	20	20	20	20.0
23-Jul	19	21	21	20.3
24-Jul	20	20	20	20.0
25-Jul	19	23	23	21.7
26-Jul	20	21	21	20.7
27-Jul	18	21	21	20.0
28-Jul	19	21	22	20.7
29-Jul	20	20	20	20.0
30-Jul	20	20.5	20	20.2
31-Jul	19	21	21	20.3

Table F15: Temperature Records for August 2000

Date	Temperature Readings (degrees celcius)			
	Morning	Noon	Afternoon	Average Temperature (degrees celcius)
01-Aug	20	21	21	20.7
02-Aug	19	20	21	20.0
03-Aug	19	21	23	21.0
04-Aug	20	22	22	21.3
05-Aug	19	21	21	20.3
06-Aug	20	21	21	20.7
07-Aug	19	22	22	21.0
08-Aug	18	21	21	20.0
09-Aug	20	20	20	20.0
10-Aug	20	20	21	20.3
12-Aug	19	21	21	20.3
13-Aug	18	21	22	20.3
14-Aug	19	20	21	20.0
15-Aug	19	20	21	20.0
16-Aug	19	20	21	20.0
17-Aug	20	21	21	20.7
18-Aug	19	21	21	20.3
19-Aug	18	21	21	20.0
20-Aug	19	20	21	20.0
21-Aug	18	21	21	20.0
22-Aug	19	20	21	20.0
23-Aug	19	22	22	21.0
24-Aug	19	20	21	20.0
25-Aug	18	21	21	20.0
26-Aug	19	20	21	20.0
27-Aug	20	21	21	20.7
28-Aug	20	22	22	21.3
29-Aug	19	21	21	20.3
30-Aug	20	20	20	20.0
31-Aug	19	21	21	20.3

Table F16: Temperature Records for September 2000

<i>Date</i>	<i>Temperature Readings (degrees celcius)</i>			
	<i>Morning</i>	<i>Noon</i>	<i>Afternoon</i>	<i>Average Temperature (degrees celcius)</i>
01-Sep	19	22	22	21.0
02-Sep	18	21	21	20.0
03-Sep	19	20	21	20.0
04-Sep	20	20	21	20.3
05-Sep	20	20	20	20.0
06-Sep	18	21	22	20.3
07-Sep	20	20	20	20.0
08-Sep	20	21	21	20.7
09-Sep	20	22	22	21.3
10-Sep	19	21	21	20.3
11-Sep	19	22	22	21.0
12-Sep	20	22	23	21.7
13-Sep	19	23	23	21.7
14-Sep	20	21	21	20.7
15-Sep	20	23	23	22.0
16-Sep	20	21	21	20.7
17-Sep	20	22	22	21.3
18-Sep	20	21	21	20.7
19-Sep	20	21	21	20.7
20-Sep	19	22	22	21.0
21-Sep	20	21	21	20.7
22-Sep	20	21	21	20.7
23-Sep	19	23	23	21.7
24-Sep	19	21	21	20.3
25-Sep	20	22	22	21.3
26-Sep	20	23	23	22.0
27-Sep	20	22	22	21.3
28-Sep	20	24	24	22.7
29-Sep	20	23	25	22.7
30-Sep	20	24	25	23.0

APPENDIX G: DATA FOR KINETIC ANALYSES

University of Cape Town

SAMPLE CALCULATIONS FOR KINETIC ANALYSIS

i) Calculation of Reaction Rates from Conversions

Example : Old Mixed Slag Powder (300-1000 μ m)

The conversions at time = 0 days and time = 8 days were 936.44 and 1711.13 μ g per g Cr respectively.

So, the reaction rate = slope of the conversion = $(1711.13 - 936.44) \div (8 - 0)$
= 96.84 μ g per g Cr per day

ii) Calculation of Average Times

Using the above example, the average time can be calculated as: $(8 - 0) \div 2 = 4$ days

**APPENDIX G1: THE KINETIC
DATA FOR $\text{Cr}_2\text{O}_3\text{-CaO}$
POWDERS AND PELLETS**

University of Cape Town

Table G1: Data for the Kinetic Analysis on Cr₂O₃-CaO Powders (50% CaO) maintained in a dessicator (excluding the datapoint at 56 days)

<i>Sample</i>	<i>Conversion</i> <i>(ug per g Cr)</i>	<i>Corrected Conversion</i> <i>(ug per g Cr)</i>	<i>Time in Days</i>	<i>Reaction Rates</i> <i>(ug per g Cr per day)</i>	<i>Average Time in Days</i>
0 week	0.43	0	0		
1 week	2.75	2.33	7	0.33	4
2 weeks	6.04	5.61	14	0.47	11
4 weeks	10.75	10.32	28	0.34	21
12 weeks	20.59	20.16	91	0.16	60

Table G2: The Results from the Long-term Model Predictions for Cr₂O₃-CaO Powders Maintained in a dessicator

<i>Time in Months</i>	<i>Time in Days</i>	<i>Average time</i> <i>in Days</i>	<i>Predicted Reaction Rates</i> <i>(ug per g Cr per day)</i>	<i>Predicted Conversions</i> <i>(ug per g Cr)</i>
3	91			
6	180	136	4.54E-02	23.86
9	270	225	1.00E-02	25.96
12	360	315	2.19E-03	26.42
15	450	405	4.78E-04	26.52
18	540	495	1.04E-04	26.54
21	630	585	2.28E-05	26.55
24	720	675	4.99E-06	26.55

Table G3: Data for the Kinetic Analysis on the Cr₂O₃-CaO Powders (50% CaO) exposed to ambient moisture

Sample	Conversion (ug per g Cr)	Corrected Conversion (ug per g Cr)	Time in Days	Reaction Rate (ug per g Cr)	Average Time (Days)
0 week	0.09	0.00	0		
1 week	9.99	9.90	7	1.41	4
2 weeks	34.45	34.35	14	3.49	11
4 weeks	47.52	47.43	27	1.01	21
8 weeks	55.61	55.52	56	0.28	42
12 weeks	57.92	57.83	96	0.06	76

Table G4: The Results from the Long -Term Model Predictions for Cr₂O₃-CaO Powders (50% CaO) exposed to ambient moisture

Time in Months	Time in Days	Average time in Days	Predicted Reaction Rates (ug per g Cr per day)	Predicted Conversions (ug per g Cr)
3	96			
6	180	138	2.19E-03	56.46
9	270	225	2.34E-05	56.50
12	360	315	2.13E-07	56.50
15	450	405	1.94E-09	56.50
18	540	495	1.77E-11	56.50
21	630	585	1.61E-13	56.50
24	720	675	1.47E-15	56.50

Table G5: Data for the Kinetic Analysis on Cr₂O₃-CaO Pellets (50% CaO) exposed to ambient moisture

<i>Sample</i>	<i>Conversion</i> <i>(ug per g Cr)</i>	<i>Corrected Conversion</i> <i>(ug per g Cr)</i>	<i>Time in Days</i>	<i>Reaction Rate</i> <i>(ug per g Cr per day)</i>	<i>Average Time (Days)</i>
0 week	0.31	0.00	0		
1 week	42.42	42.11	7	6.02	4
2 weeks	52.47	52.16	14	1.43	11
4 weeks	78.35	78.03	26	2.16	20
8 weeks	87.32	87.01	57	0.29	42
12 weeks	89.66	89.34	92	0.07	75

Table G6: The Results from the Long -Term Model Predictions for Cr₂O₃-CaO Pellets (50% CaO) exposed to ambient moisture

<i>Time in Months</i>	<i>Time in Days</i>	<i>Average time</i> <i>in Days</i>	<i>Predicted Reaction Rates</i> <i>(ug per g Cr per day)</i>	<i>Predicted Conversions</i> <i>(ug per g Cr)</i>
3	92			
6	180	136	1.44E-03	81.90
9	270	225	7.03E-06	81.92
12	360	315	3.23E-08	81.92
15	450	405	1.49E-10	81.92
18	540	495	6.83E-13	81.92
21	630	585	3.14E-15	81.92
24	720	675	1.44E-17	81.92

**APPENDIX G2: THE KINETIC
DATA FOR $\text{Cr}_2\text{O}_3\text{-Ca(OH)}_2$
BALLS**

University of Cape Town

Table G7: The Kinetic Data for Cr₂O₃-Ca(OH)₂ Balls maintained at ambient temperature

<i>Sample</i>	<i>Conversion</i> <i>(ug per g Cr)</i>	<i>Corrected Conversion</i> <i>(ug per g Cr)</i>	<i>Time in</i> <i>Days</i>	<i>Reaction Rate</i> <i>(ug per g Cr per day)</i>	<i>Average Time (Days)</i>
0 weeks	0.12	0.00	0		
1 week	0.35	0.23	8	0.029	4
2 weeks	0.82	0.70	15	0.067	12
4 weeks	0.85	0.73	29	0.002	22
8 weeks	3.45	3.33	60	0.083	44
12 weeks	5.33	5.21	92	0.059	76
16 weeks	8.05	7.93	120	0.097	106
20 weeks	8.60	8.48	155	0.016	138
28 weeks	12.88	12.76	225	0.061	190
44 weeks	16.75	16.63	334	0.036	279
56 weeks	15.38	15.26	419	-0.016 point ignored	

University of Cape Town

Table G8: The Kinetic Data for the Cr₂O₃-Ca(OH)₂ Balls maintained at fifty degrees

<i>Sample</i>	<i>Conversion</i> <i>(ug per g Cr)</i>	<i>Corrected Conversion</i> <i>(ug per g Cr)</i>	<i>Time in</i> <i>Days</i>	<i>Reaction Rate</i> <i>(ug per g Cr per day)</i>	<i>Average Time</i> <i>in Days</i>
0 weeks	0.38	0.00	0		
1 week	0.63	0.25	8	0.032	4
2 weeks	1.26	0.88	15	0.090	12
4 weeks	2.50	2.13	29	0.089	22
7 weeks	6.62	6.24	47	0.229	38
10 weeks	18.99	18.62	70	0.538	59
15 weeks	29.54	29.16	103	0.320	87
19 weeks	31.07	30.69	131	0.055	117
26 weeks	35.23	34.85	179	0.087	155

University of Cape Town

Table G9: The Kinetic Data for Cr₂O₃-Ca(OH)₂ Balls maintained at eighty degrees

<i>Sample</i>	<i>Conversion</i> <i>(ug per g Cr)</i>	<i>Corrected Conversion</i> <i>(ug per g Cr)</i>	<i>Time in</i> <i>Days</i>	<i>Reaction Rate</i> <i>(ug per g Cr per day)</i>	<i>Average Time</i> <i>in Days</i>
0 weeks	0.16	0.00	0		
1 week	0.92	0.76	8	0.10	4
2 weeks	2.54	2.38	15	0.23	11
4 weeks	5.25	5.09	28	0.20	21
8 weeks	17.78	17.62	59	0.41	43
12 weeks	29.96	29.80	91	0.37	75
16 weeks	52.10	51.94	119	0.79	105
20 weeks	58.00	57.84	154	0.17	137
28 weeks	85.74	85.58	225	0.39	190
44 weeks	99.92	99.76	330	0.14	277
56 weeks	104.33	104.17	415	0.05	372

University of Cape Town

APPENDIX G3: THE KINETIC DATA FOR SLAG BALLS

University of Cape Town

Table G10: The Kinetic Data for Old Mixed Slag Balls with pore moisture evaporated (particle size class:<75um)

<i>SAMPLE</i>	<i>Conversion</i> <i>(ug per g Cr)</i>	<i>Time in</i> <i>Days</i>	<i>Reaction Rate</i> <i>(ug per g Cr per day)</i>	<i>Average Time</i> <i>in Days</i>
0 weeks	910.52	0		
1 week	1992.87	7	154.62	4
2 weeks	3288.03	14	185.02	11
4 weeks	4231.46	28	67.39	21
8 weeks	5989.55	63	50.23	46
12 weeks	6545.65	103	13.90	83
16 weeks	6552.19	121	0.36	112
20 weeks	7339.05	156	22.48	139
28 weeks	7237.55	215	-1.72 point ignored	

University of Cape Town

Figure G1: The Rate versus Average Time for Old Mixed Slag Balls with the pore moisture evaporated (particle size class: <75um)

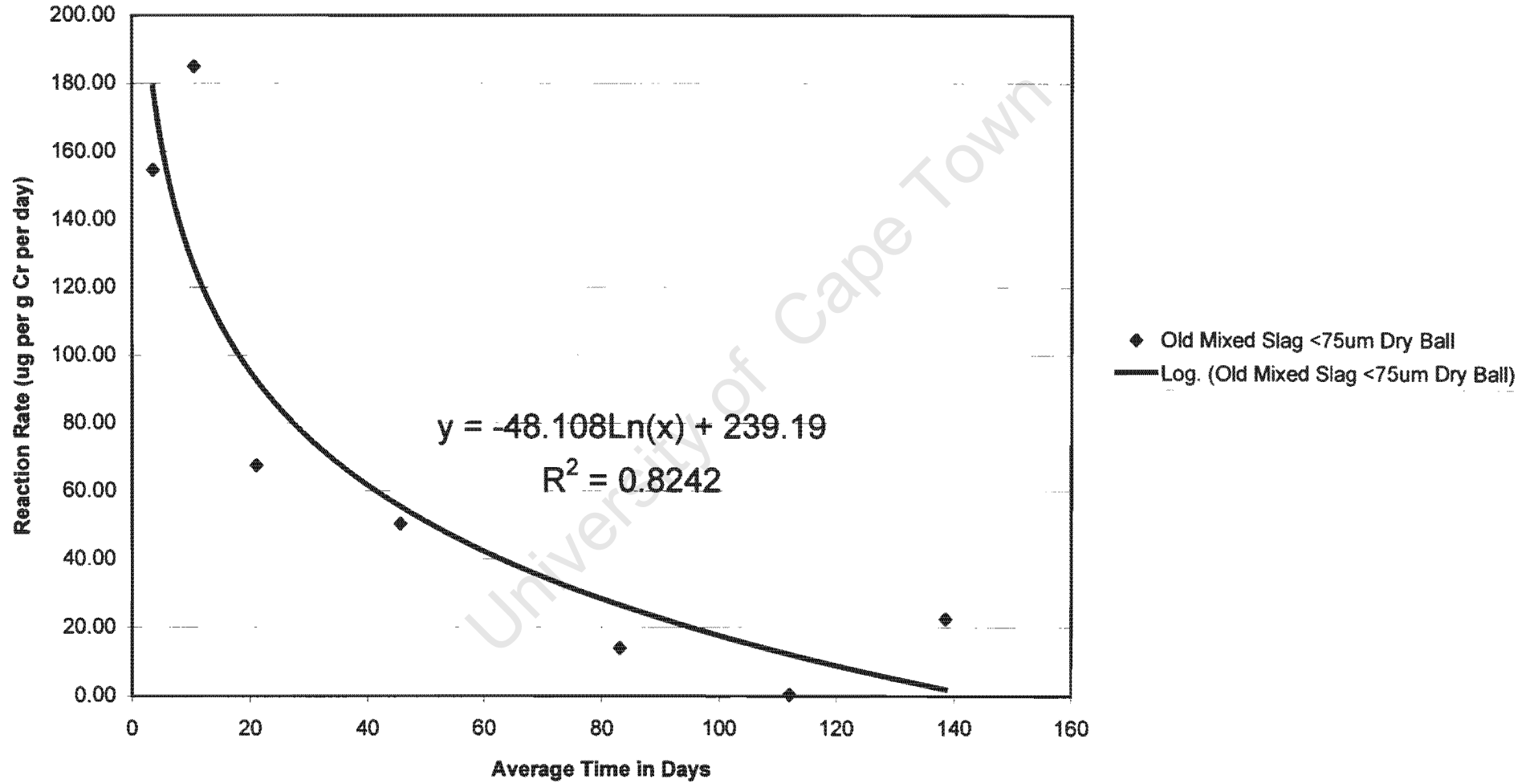


Table G11: The First Kinetic Analysis on Old Mixed Slag Balls (particle size class:75-300um)

SAMPLE	Conversion	Time in	Reaction Rates	First Recalculation of Reaction Rates		
	(ug per g Cr)	Days	(ug per g Cr per day)	Conversion	Time in	Reaction Rate
				(ug per g Cr)	Days	(ug per g Cr per day)
0 weeks	623.16	0				
1 week	3125.31	7	357.45			
2 weeks	3958.82	14	119.07	623.16	0	
4 weeks	4873.15	28	65.31	3125.31	7	357.45
8 weeks	7178.93	63	65.88	3958.82	14	119.07
12 weeks	6335.16	103	-21.09 point ignored	4873.15	28	65.31
16 weeks	6831.97	121	27.60	7178.93	63	65.88
20 weeks	7813.52	156	28.04	6831.97	121	-5.98 point ignored
28 weeks	7756.05	215	-0.97 point ignored	7813.52	156	28.04

Table G12: The Recalculated Reaction Rates for Old Mixed Slag Balls (particle size class: 75-300um)

SAMPLE	Conversion	Time	Reaction Rate	Inverse of the Square Root	
	(ug per g Cr)	in Days	(ug per g Cr per day)	Average Time (Days)	of the average time
0 weeks	623.16	0			
1 week	3125.31	7	357.45	4	0.53
2 weeks	3958.82	14	119.07	11	0.31
4 weeks	4873.15	28	65.31	21	0.22
8 weeks	7178.93	63	65.88	46	0.15
20 weeks	7813.52	156	6.82	110	0.10

Figure G2: The Rate versus Time Graph for Old Mixed Slag Balls (particle size class:75-300um)

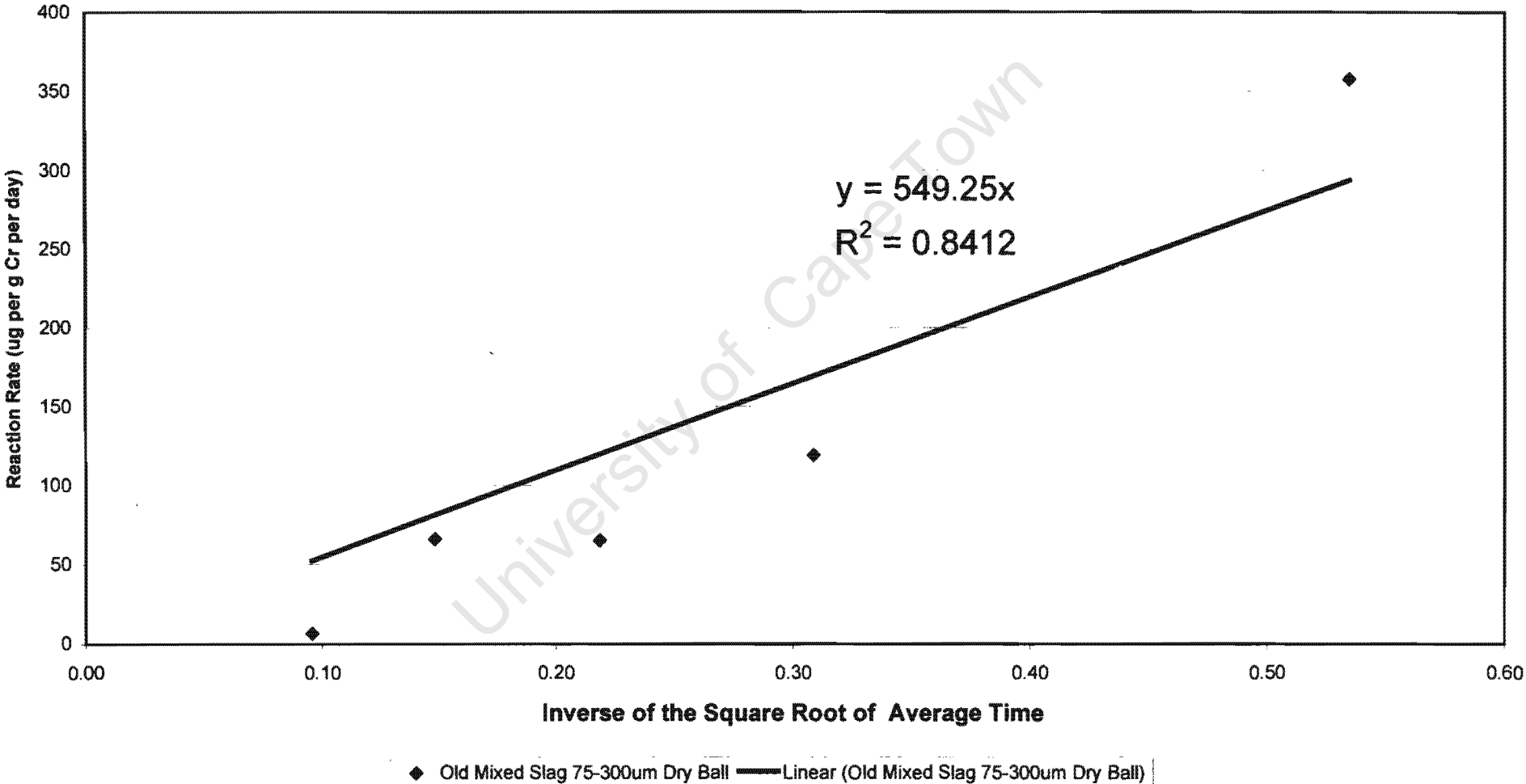


Table G13: The Kinetic Analysis for Old Mixed Slag Balls (particle size class: 300-1000um)

<i>Sample</i>	<i>Conversion</i> <i>(ug per g Cr)</i>	<i>Average Time</i> <i>in Days</i>	<i>Reaction Rate</i> <i>(ug per g Cr per day)</i>
0 weeks	263.32	0	
1 week	1170.54	7	129.60
2 weeks	1384.39	14	30.55
4 weeks	1716.52	28	23.72
8 weeks	2807.61	63	31.17
12 weeks	2415.38	103	-9.81 point ignored
16 weeks	2401.06	121	-0.80 point ignored
20 weeks	2825.11	156	12.12
28 weeks	3156.12	215	5.61

Table G14: The Recalculated Reaction Rates for Old Mixed Slag Balls (Particle Size Class: 300-1000um)

<i>Sample</i>	<i>Conversion</i> <i>(ug per g Cr)</i>	<i>Time in</i> <i>Days</i>	<i>Reaction Rate</i> <i>(ug per g Cr per day)</i>	<i>Average Time</i> <i>in Days</i>	<i>Inverse of the Square Root</i> <i>of Time</i>
0 weeks	263	0			
1 week	1171	7	129.60	4	0.53
2 weeks	1384	14	30.55	11	0.31
4 weeks	1717	28	23.72	21	0.22
8 weeks	2808	63	31.17	46	0.15
20 weeks	2825	156	0.19	110	0.10
28 weeks	3156	215	5.61	186	0.07

Table G15: The Long-Term Model Predictions for Oxidation in the Old Mixed Slag Balls (particle size class: 300-1000µm)

<i>Time in Months</i>	<i>Time in Days</i>	<i>Average time Days</i>	<i>Square root of time</i>	<i>Predicted Reaction Rates (ug per g Cr per day)</i>	<i>Predicted Conversions (ug per g Cr)</i>	<i>Adjusted Predicted Conversions (ug per g Cr)</i>
7	215					
9	270	243	16	12.79	6205	6468
12	360	315	18	11.22	7072	7335
15	450	405	20	9.90	8018	8281
18	540	495	22	8.95	8865	9128
21	630	585	24	8.24	9637	9900
24	720	675	26	7.67	10352	10615

University of Cape Town

Table G16: The Kinetic Data for New CLU Slag Balls (Particle Size Class: <75um)

Sample	Conversion (ug per g Cr)	Time in Days	Reaction Rate (ug per g Cr per day)
0 weeks	357.03	0	
1 week	1497.56	8	142.57
2 week	1711.69	15	30.59
4 weeks	1820.25	29	7.75
8 weeks	2528.48	64	20.24
12 weeks	2456.37	111	-1.53 point ignored
16 weeks	3324.87	122	78.95
20 weeks	2886.28	157	-12.53 point ignored
28 weeks	3263.67	213	6.74

Table G17: The Recalculated Reaction Rates for New CLU Slag Balls (Particle Size Class: <75um)

Samples	Conversion ug per g Cr	Time in Days	Reaction Rate (ug per g Cr per day)	Average Time (Days)	Inverse of the Square Root of Time
0 weeks	357.03	0			
1 week	1497.56	8	142.57	4	0.50
2 week	1711.69	15	30.59	12	0.29
4 weeks	1820.25	29	7.75	22	0.21
8 weeks	2528.48	64	20.24	47	0.15
16 weeks	3324.87	122	13.73	93	0.10
28 weeks	3263.67	213	-0.67	168	0.08 point ignored

Figure G3: The Relationship between Reaction Rate and Time for New CLU Slag Balls (particle size class: <75um)

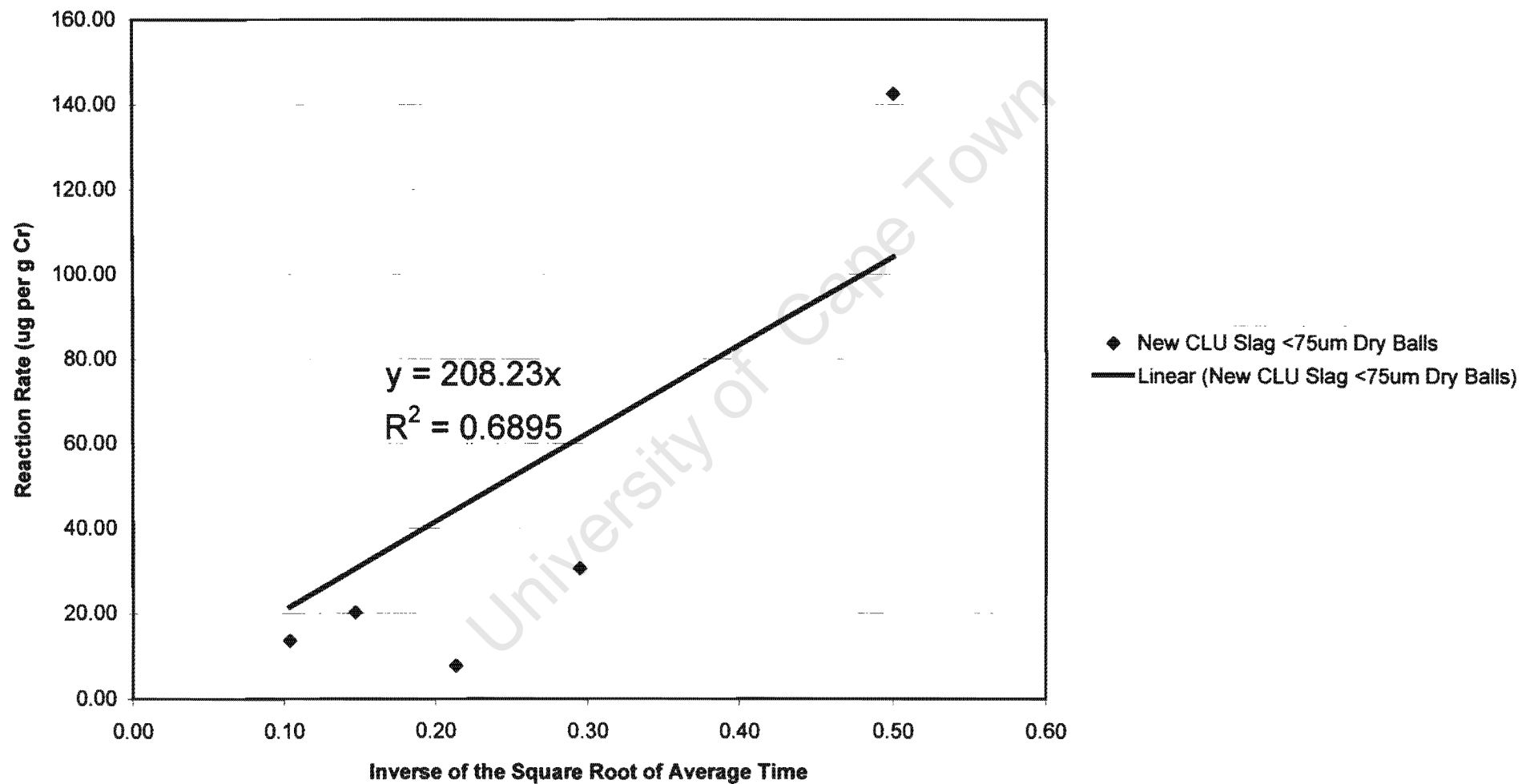


Table G18: The Kinetic Data for New CLU Slag Balls (particle size class: 75-300um)

<i>Sample</i>	<i>Conversion</i> (ug per g Cr)	<i>Time in</i> <i>Days</i>	<i>Reaction Rate</i> (ug per g Cr per day)
0 weeks	192.09	0	
1 week	843.17	8	81.38
2 week	879.70	15	5.22
4 weeks	1080.57	29	14.35
8 weeks	1436.05	64	10.16
12 weeks	1432.03	111	-0.09 Point ignored
16 weeks	1651.60	122	19.96
20 weeks	1683.54	157	0.91
28 weeks	1688.68	213	0.09

Table G19: The Recalculated Reaction Rates for New CLU Slag Balls (particle size class: 75-300um)

<i>Sample</i>	<i>Conversion</i> (ug per g Cr)	<i>Time in</i> <i>Days</i>	<i>Reaction Rate</i> (ug per g Cr per day)	<i>Average Time</i> <i>in Days</i>
0 weeks	192.09	0		
1 week	843.17	8	81.38	4
2 week	879.70	15	5.22	12
4 weeks	1080.57	29	14.35	22
8 weeks	1436.05	64	10.16	47
16 weeks	1651.60	122	3.72	93
20 weeks	1683.54	157	0.91	140
28 weeks	1688.68	213	0.09	185

Figure G4: The Relationship between Reaction Rate and Time for New CLU Slag Balls (particle size class:75-300um)

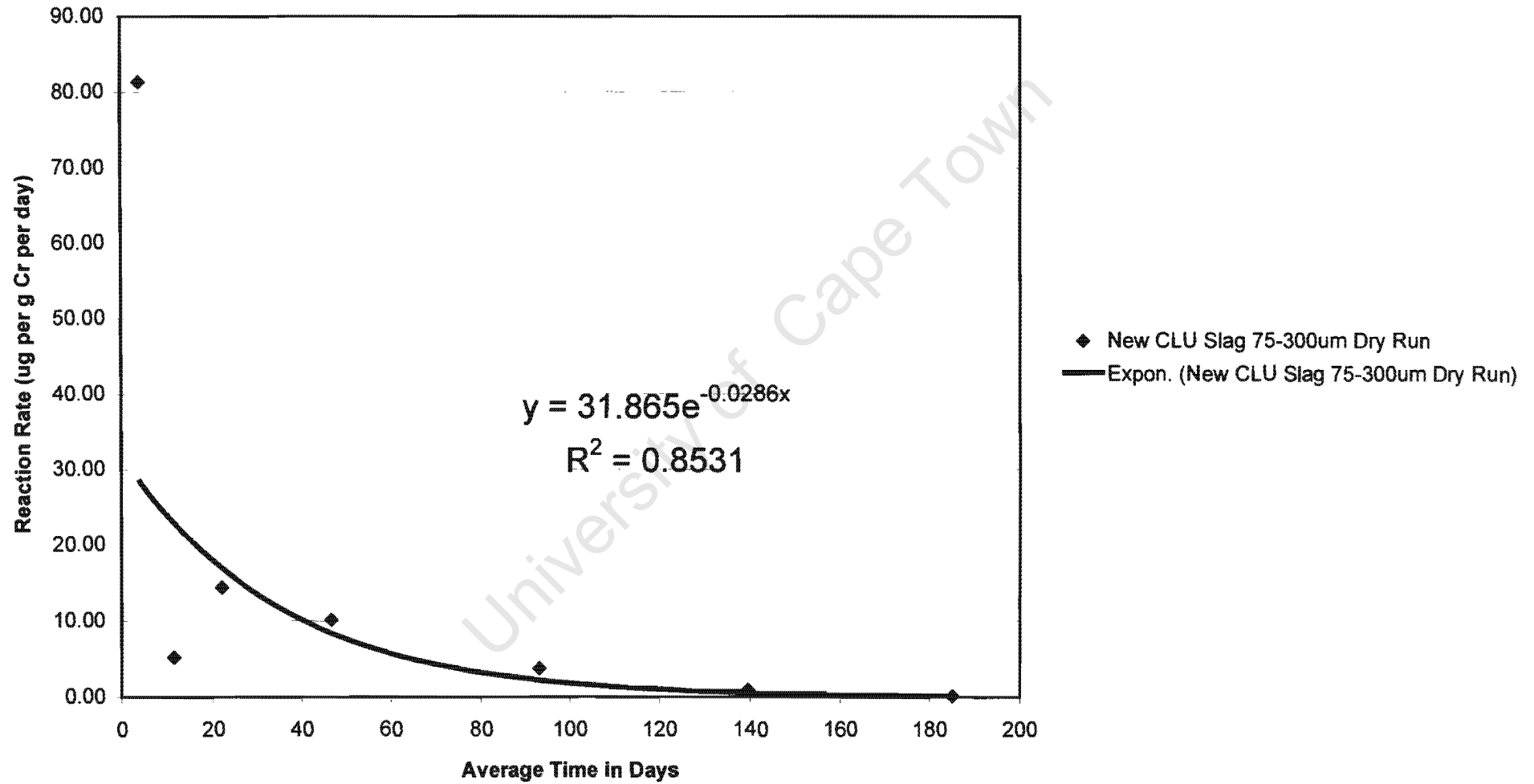


Table G20: The Kinetic Data for the New CLU Slag Balls (particle size class: 300-1000um)

<i>Sample</i>	<i>Conversion</i> <i>(ug per g Cr)</i>	<i>Time in</i> <i>Days</i>	<i>Reaction Rate</i> <i>(ug per g Cr per day)</i>
0 weeks	148.88	0	
1 week	421.05	8	34.02
2 week	829.97	15	58.42
4 weeks	908.48	25	7.85
8 weeks	1120.58	59	6.24
12 weeks	1150.97	95	0.84
16 weeks	1279.30	123	4.58
20 weeks	1193.44	151	-3.07 point ignored
28 weeks	1292.11	214	1.57

Table G21: The Recalculated Reaction Rates for New CLU Slag Balls (particle size class: 300-1000um)

<i>Sample</i>	<i>Conversion</i> <i>(ug per g Cr)</i>	<i>Time in Days</i>	<i>Reaction Rate</i> <i>(ug per g Cr per day)</i>	<i>Average Time</i> <i>in Days</i>
0 weeks	149	0		
1 week	421	8	34.02	4
2 week	830	15	58.42	12
4 weeks	908	25	7.85	20
8 weeks	1121	59	6.24	42
12 weeks	1151	95	0.84	77
16 weeks	1279	123	4.58	109
28 weeks	1292	214	0.14	169

Table G22: The Long-Term Model Predictions for the Oxidation Reactions in the New CLU Slag Balls (particle size class:300-1000um)

<i>Time in months</i>	<i>Time in Days</i>	<i>Average Time in Days</i>	<i>Predicted Conversions (ug per g Cr)</i>	<i>Adjusted Conversions (ug per g Cr)</i>	<i>Predicted Reaction Rates (ug per g Cr per day)</i>
7	214				
9	270	242	1021	1170	1.86E-02
12	360	315	1022	1171	1.98E-03
15	450	405	1022	1171	1.25E-04
18	540	495	1022	1171	7.88E-06
21	630	585	1022	1171	4.97E-07
24	720	675	1022	1171	3.14E-08

University of Cape Town

Table G23: The Kinetic Data for New EAF Slag Balls with the pore moisture evaporated (particle size class: <75um)

<i>Sample</i>	<i>Conversion (ug per g Cr)</i>	<i>Time in Days</i>	<i>Reaction Rate (ug per g Cr)</i>	<i>Average Time in Days</i>	<i>Inverse of the Square Root of Time</i>
0 weeks	685.90	0			
1 week	1288.44	4	150.63	2	0.71
2 weeks	1342.92	11	7.78	8	0.37
4 weeks	1995.26	25	46.60	18	0.24
8 weeks	2869.88	55	29.15	40	0.16
12 weeks	3037.06	119	2.61	87	0.11
16 weeks	3472.41	152	13.19	136	0.09
20 weeks	3740.40	182	8.93	167	0.08
28 weeks	3572.39	241	-2.85	212	0.07 point ignored

University of Cape Town

Fig. G5: The Relationship between Reaction Rate and Time for New EAF Slag Balls (particle size class: <75um)

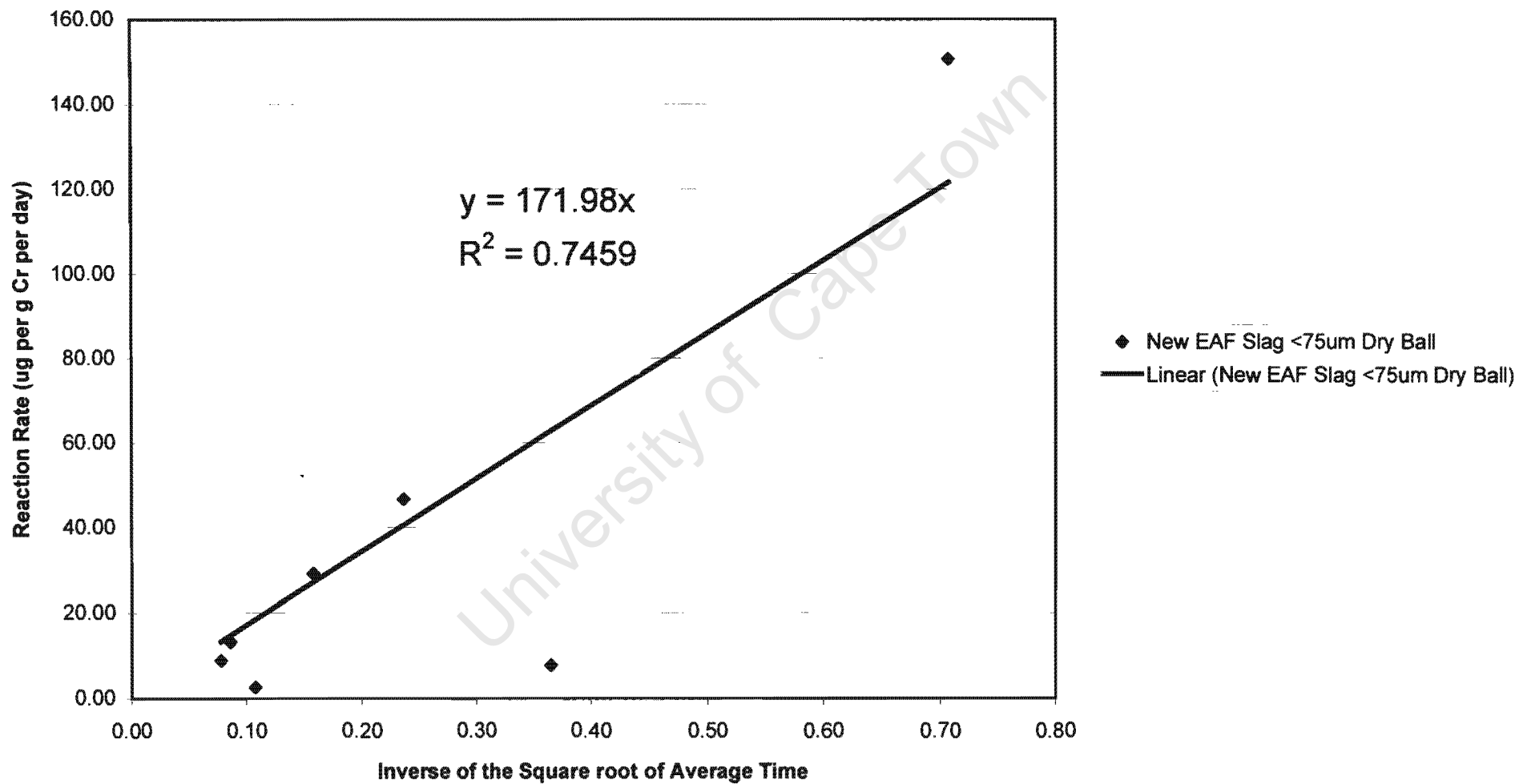


Table G24: The Kinetic Data for New EAF Slag Balls (particle size class: 75-300um)

<i>Sample</i>	<i>Conversion</i>	<i>Time in</i>	<i>Reaction Rate</i>
	<i>(ug per g Cr)</i>	<i>Days</i>	<i>(ug per g Cr per day)</i>
0 weeks	392.18	0	
1 week	550.11	4	39.48
2 weeks	820.05	11	38.56
4 weeks	1362.68	25	38.76
8 weeks	2698.89	55	44.54
12 weeks	2669.13	119	-0.46 point ignored
16 weeks	2684.56	152	0.47
20 weeks	2979.18	182	9.82
28 weeks	2751.97	241	-3.85 point ignored

Table G25: The First R ecalculation of Reaction Rates for New EAF Slag Balls (particle size class:75-300um)

<i>Sample</i>	<i>Conversion</i>	<i>Time in</i>	<i>Reaction Rate</i>
	<i>(ug per g Cr)</i>	<i>Days</i>	<i>(ug per g Cr per day)</i>
0 weeks	392.18	0	
1 week	550.11	4	39.48
2 weeks	820.05	11	38.56
4 weeks	1362.68	25	38.76
8 weeks	2698.89	55	44.54
16 weeks	2684.56	152	-0.15 point ignored
20 weeks	2979.18	182	9.82

Table G26: The Final Recalculation of Reaction Rates and Kinetic Data for New EAF Slag Balls (particle size class: 75-300um)

<i>Sample</i>	<i>Conversion</i> <i>(ug per g Cr)</i>	<i>Time in</i> <i>Days</i>	<i>Reaction Rate</i> <i>(ug per g Cr per day)</i>	<i>Average Time</i> <i>(Days)</i>
0 weeks	392.18	0		
1 week	550.11	4	39.48	2
2 weeks	820.05	11	38.56	8
4 weeks	1362.68	25	38.76	18
8 weeks	2698.89	55	44.54	40
20 weeks	2979.18	182	2.21	119

University of Cape Town

Figure G6: The Relationship between Reaction Rate and Time for New EAF Slag Balls (particle size class: 75-300um)

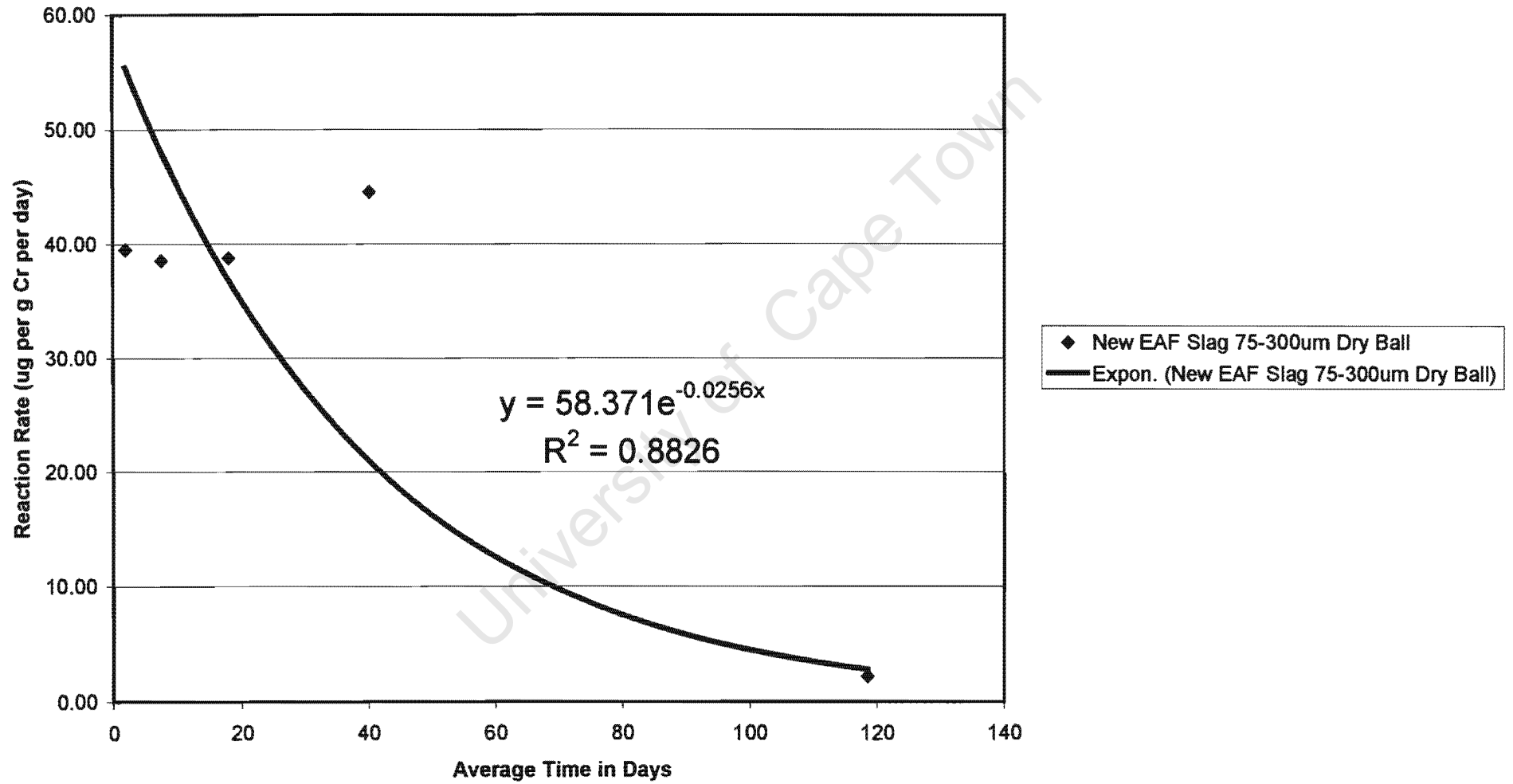


Table G27: The Kinetic Data for New EAF Slag Balls (particle size class: 300-1000um)

<i>Sample</i>	<i>Conversion</i> <i>(ug per g Cr)</i>	<i>Time in</i> <i>Days</i>	<i>Reaction Rate</i> <i>(ug per g Cr per day)</i>
0 weeks	167.40	0	
1 week	412.27	4	61.22
2 weeks	622.93	11	30.09
4 weeks	1067.03	25	31.72
8 weeks	1301.92	55	7.83
12 weeks	1205.39	119	-1.51 point ignored
16 weeks	1354.15	152	4.51
20 weeks	1137.78	182	-7.21 point ignored
28 weeks	1056.39	241	-1.38 point ignored

Table G28: The Recalculation of Reaction Rates for New EAF Slag Balls (particle size class: 300-1000um)

<i>Sample</i>	<i>Conversion</i> <i>(ug per g Cr)</i>	<i>Time in</i> <i>Days</i>	<i>Reaction Rate</i> <i>(ug per g Cr per day)</i>	<i>Average Time</i> <i>in Days</i>
0 weeks	167.40	0		
1 week	412.27	4	61.22	2
2 weeks	622.93	11	30.09	8
4 weeks	1067.03	25	31.72	18
8 weeks	1301.92	55	7.83	40
16 weeks	1354.15	152	0.54	104

Table G29: The Long-Term Model Predictions for the Oxidation Reactions in the New EAF Slag Balls (particle size class: 300-1000um)

<i>Time in months</i>	<i>Time in Days</i>	<i>Average Time in Days</i>	<i>Predicted Reaction Rates (ug per g Cr per day)</i>	<i>Predicted Conversions (ug per g Cr)</i>	<i>Adjusted Conversions (ug per g Cr)</i>
5	152				
6	180	166	3.06E-02	1245	1412
9	270	225	2.11E-03	1245	1412
12	360	315	3.58E-05	1245	1412
15	450	405	6.08E-07	1245	1412
18	540	495	1.03E-08	1245	1412
21	630	585	1.75E-10	1245	1412
24	720	675	2.96E-12	1245	1412

University of Cape Town

APPENDIX G4: THE KINETIC DATA FOR SLAG POWDERS

University of Cape Town

Table G30: The Kinetic Data for Old Mixed Slag Powders exposed to air (particle size class:75-300um)

<i>Sample</i>	<i>Conversion</i> <i>(ug per g Cr)</i>	<i>Time in</i> <i>Days</i>	<i>Reaction Rate</i> <i>(ug per g Cr per day)</i>
0 weeks	2754.20	0	
1 week	4898.64	8	268.05
2 weeks	6353.42	15	207.83
4 weeks	7516.04	29	83.04
8 weeks	7289.68	57	-8.08 point ignored
12 weeks	9052.23	92	50.36

Table G31: The Recalculation of Reaction Rates for the Old Mixed Slag Powders exposed to air (particle size class:75-300um)

<i>Sample</i>	<i>Conversion</i> <i>(ug per g Cr)</i>	<i>Time in</i> <i>Days</i>	<i>Reaction Rate</i> <i>(ug per g Cr per day)</i>	<i>Average Time</i> <i>(Days)</i>
0 weeks	2754	0		
1 week	4899	8	268.05	4
2 weeks	6353	15	207.83	12
4 weeks	7516	29	83.04	22
12 weeks	9052	92	24.38	61

Figure G7: The Relationship between Reaction Rate and Average Time for Old Mixed Slag Powders Exposed to Air (particle size class: 75-300um)

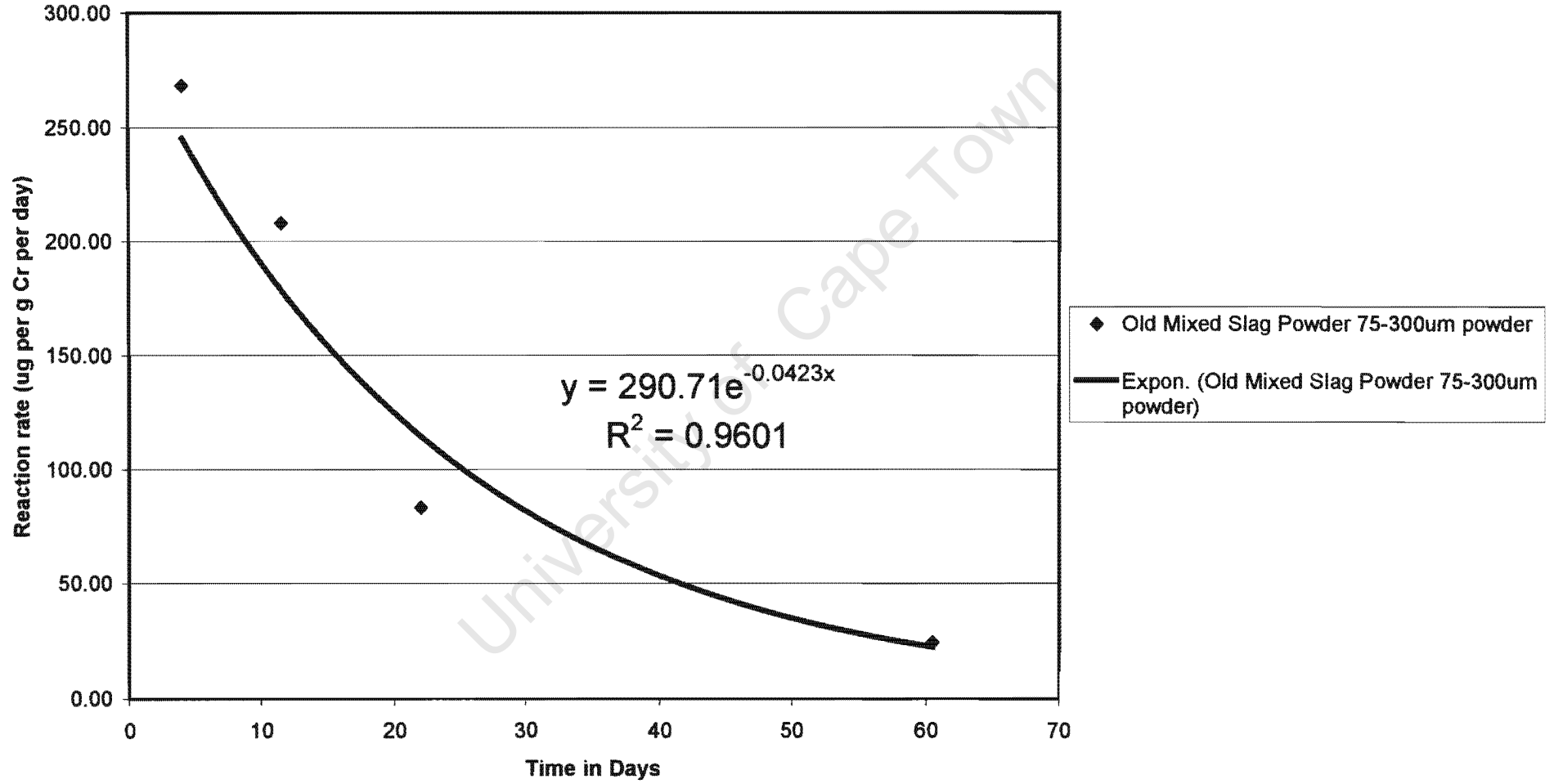


Table G32: The Kinetic Data for Old Mixed Slag Powders exposed to air (particle size class: 300-1000um)

<i>Sample</i>	<i>Conversion</i> <i>(ug per g Cr)</i>	<i>Time in</i> <i>Days</i>	<i>Reaction Rate</i> <i>(ug per g Cr per day)</i>
0 weeks	936	0	
1 week	1711	8	96.84
2 weeks	2399	15	98.29
4 weeks	2365	29	-2.46 point ignored
8 weeks	2672	57	10.98
12 weeks	2638	92	-0.98 point ignored

Table G33: The Recalculated Reaction Rates for Old Mixed Slag Powders Exposed to Air (particle size class: 300-1000um)

<i>Sample</i>	<i>Conversion</i> <i>(ug per g Cr)</i>	<i>Time in</i> <i>Days</i>	<i>Reaction Rate</i> <i>(ug per g Cr per day)</i>	<i>Average time</i> <i>(Days)</i>
0 weeks	936	0		0
1 week	1711	8	96.84	4
2 weeks	2399	15	98.29	12
8 weeks	2672	57	6.50	36

Table G34: The Long -Term Model Predictions for the Oxidation Reactions in the Old Mixed Slag Powders (particle size class:300-1000um)

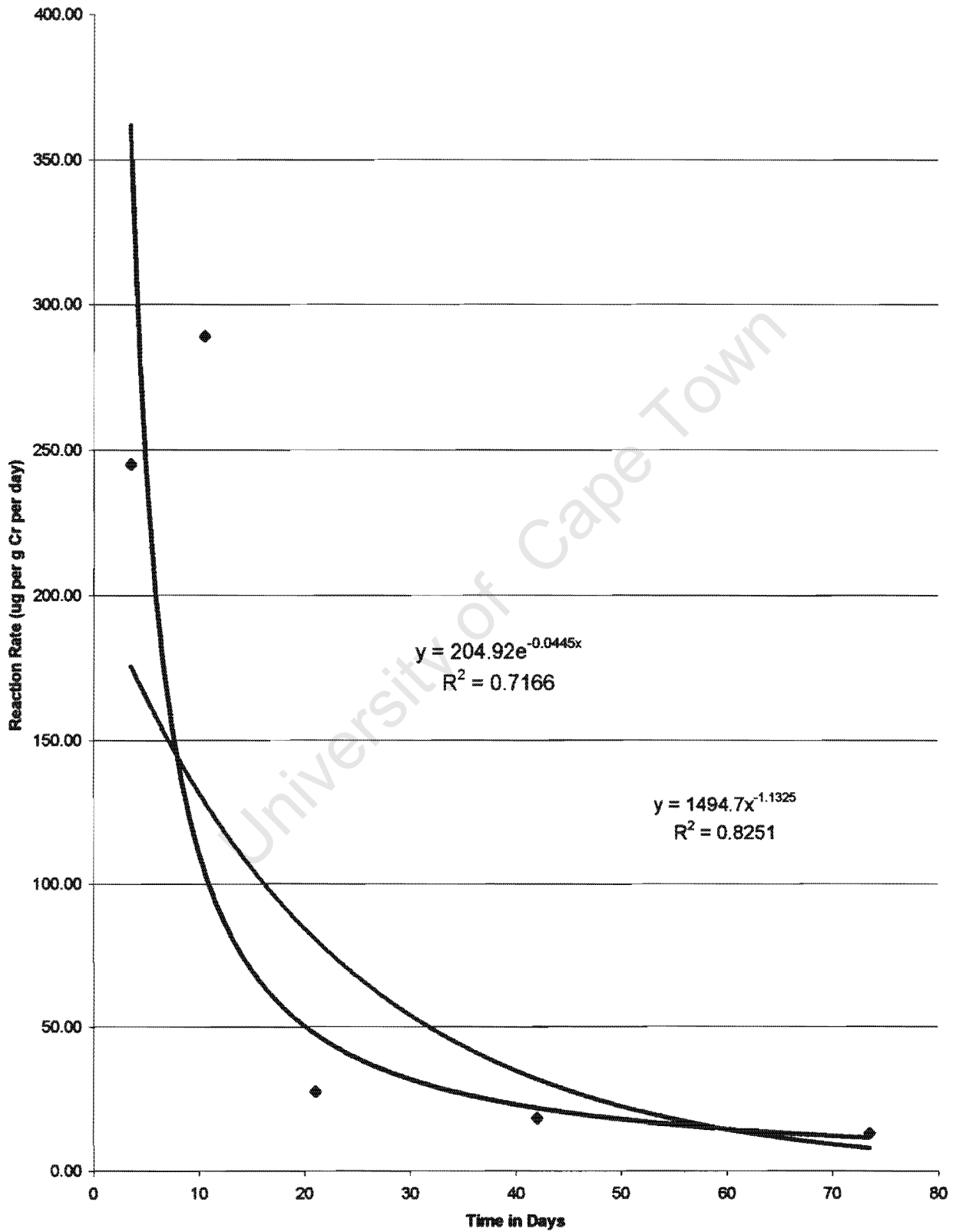
<i>Time in Months</i>	<i>Time in Days</i>	<i>Average Time in Days</i>	<i>Predicted Reaction Rates (ug per g Cr per day)</i>	<i>Predicted Conversions (ug per g Cr)</i>	<i>Adjusted Conversions (ug per g Cr)</i>
2	57				
3	90	74	2.35E-01	2069	3005
6	180	135	8.71E-04	2071	3007
9	270	225	2.42E-07	2071	3007
12	360	315	6.70E-11	2071	3007
15	450	405	1.86E-14	2071	3007
18	540	495	5.16E-18	2071	3007
21	630	585	1.43E-21	2071	3007
24	720	675	3.97E-25	2071	3007

Table G35: The Kinetic Data for New CLU Slag Powders exposed to air (particle size class: <75um)

<i>Sample</i>	<i>Conversion</i> <i>(ug per g Cr)</i>	<i>Time in</i> <i>Days</i>	<i>Reaction Rate</i> <i>(ug per g Cr per day)</i>	<i>Average Time</i> <i>in Days</i>
0 weeks	1322.35	0		
1 week	3037.53	7	245.03	4
2 weeks	5060.51	14	289.00	11
4 weeks	5442.42	28	27.28	21
8 weeks	5948.13	56	18.06	42
12 weeks	6396.94	91	12.82	74

University of Cape Town

Figure G8: A comparison of the Power and exponential models for New CLU Slag Powders (particle size class:<75um)



◆ New CLU Slag <75um powder — Power (New CLU Slag <75um powder) — Expon. (New CLU Slag <75um powder)

Table G36: The Kinetic Data for New CLU Slag Powders (particle size class: 75-300um)

<i>Sample</i>	<i>Conversion</i> <i>(ug per g Cr)</i>	<i>Time in</i> <i>Days</i>	<i>Reaction Rate</i> <i>(ug per g Cr per day)</i>	<i>Average Time</i> <i>(Days)</i>
0 weeks	705.90	0		
1 week	1092.37	7	55.21	4
2 weeks	1509.69	14	59.62	11
4 weeks	2085.37	28	41.12	21
8 weeks	2848.72	56	27.26	42
12 weeks	2945.82	91	2.77	74

University of Cape Town

Figure G9: A Comparison of the linear and exponential models for New CLU Slag Powders (particle size class:75-300um)

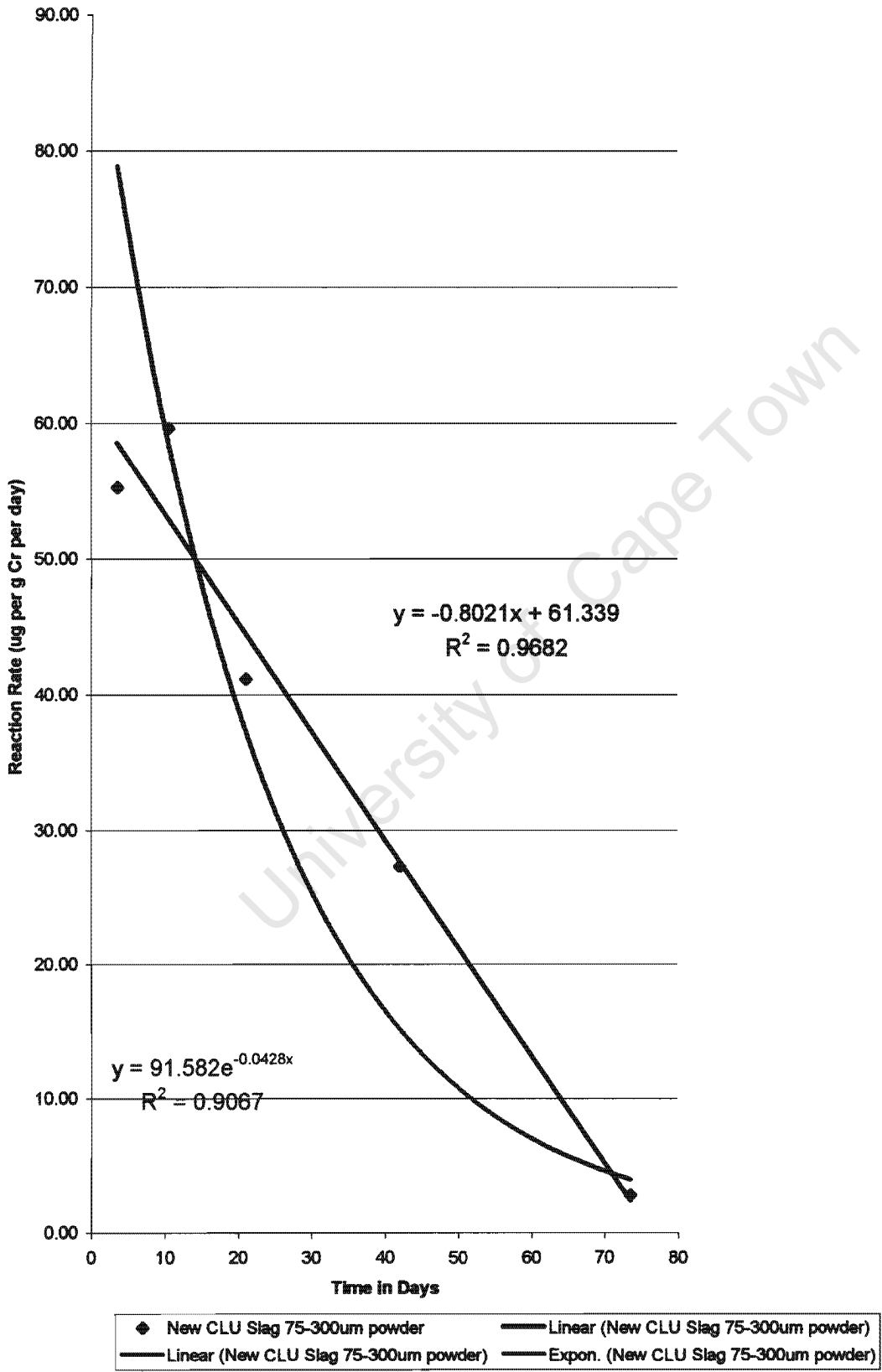


Table G37: The Kinetic Data for New CLU Slag Powders exposed to air (particle size class:300-1000um)

<i>Sample</i>	<i>Conversion</i> (ug per g Cr)	<i>Time in</i> <i>Days</i>	<i>Reaction Rate</i> (ug per g Cr per day)	<i>Average time</i> (Days)
0 week	222	0		
1 week	480	7	36.87	4
2 weeks	905	14	60.76	11
4 weeks	1581	28	48.23	21
8 weeks	1864	56	10.13	42
12 weeks	1901	91	1.06	74

Table G38: The Long-term Model Predictions for the Oxidation Reactions in the New CLU Slag Powders (particle size class: 300-1000um)

<i>Time in</i> <i>Months</i>	<i>Time in days</i>	<i>Average Time</i> <i>in Days</i>	<i>Predicted Reaction Rate</i> (ug per g Cr per day)	<i>Predicted Conversions</i> (ug per g Cr)	<i>Adjusted Conversions</i> (ug per g Cr)
3	91				
6	180	136	4.10E-02	1587	1809
9	270	225	2.54E-04	1588	1810
12	360	315	1.53E-06	1588	1810
15	450	405	9.22E-09	1588	1810
18	540	495	5.55E-11	1588	1810
21	630	585	3.35E-13	1588	1810
24	720	675	2.02E-15	1588	1810

Table G39: The Kinetic Data for New EAF Slag Powders (particle size class:<75um)

<i>Sample</i>	<i>Conversion</i> <i>(ug per g Cr)</i>	<i>Time in</i> <i>Days</i>	<i>Reaction Rate</i> <i>(ug per g Cr per day)</i>	<i>Average Time</i> <i>(Days)</i>
0 week	1129	0		
1 week	2410	7	183.08	4
2 weeks	4617	14	315.24	11
4 weeks	5208	25	53.77	20
8 weeks	5833	59	18.38	42
12 weeks	4818	91	-31.74	75 point ignored

University of Cape Town

Figure G10: The Relationship Between Reaction Rate and Time in New EAF slag Powders (particle size class:<75um)

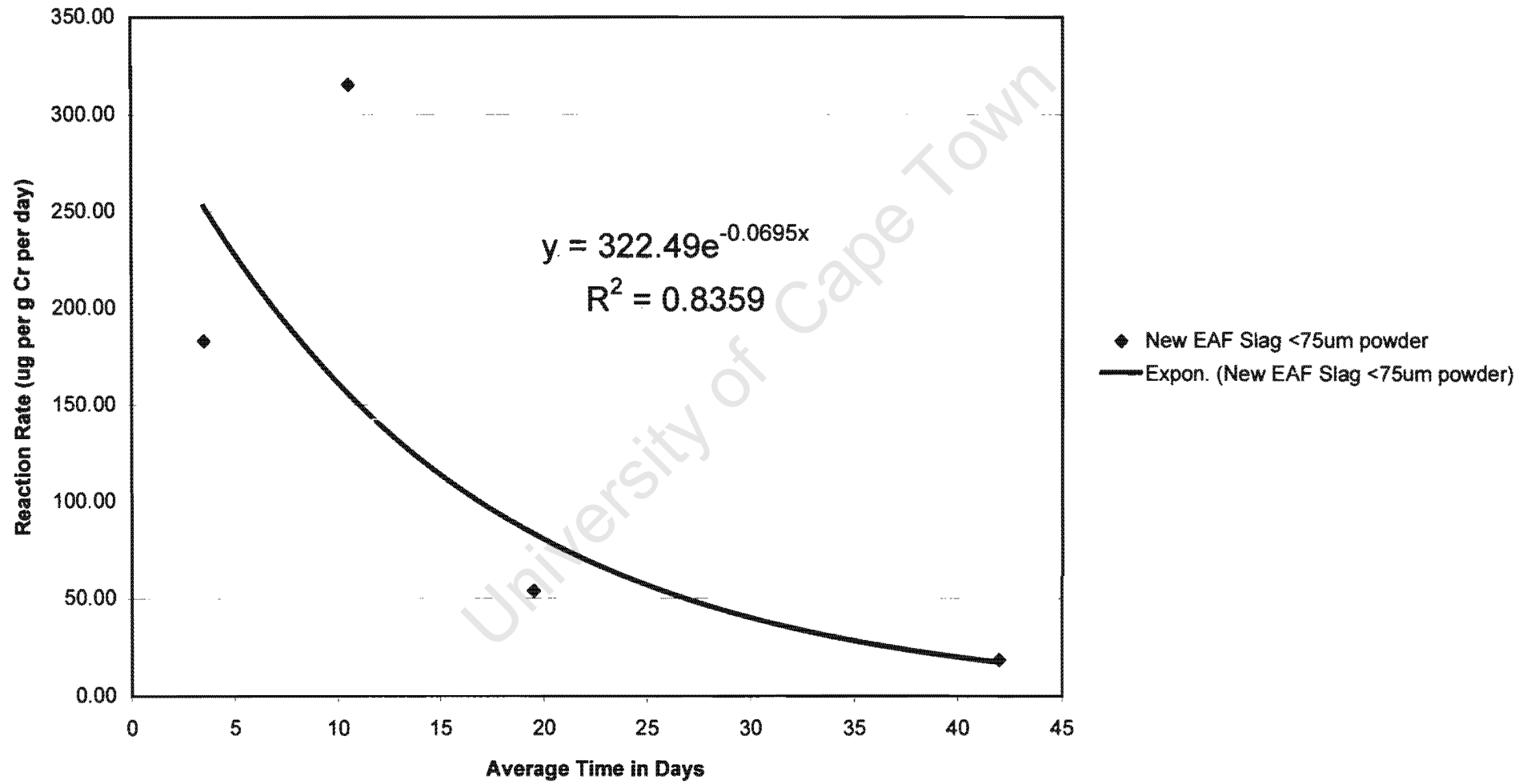


Table G40: The Kinetic Data for New EAF Slag Powders (particle size class: 75-300um)

<i>Sample</i>	<i>Conversion</i> <i>(ug per g Cr)</i>	<i>Reaction Rate</i> <i>(ug per g Cr per day)</i>	<i>Time in</i> <i>Days</i>	<i>Average Time</i> <i>(Days)</i>
0 week	848.80		0	
1 week	1693.21	120.63	7	4
2 week	2811.80	159.80	14	11
4 week	3150.66	30.81	25	20
8 weeks	4031.64	25.91	59	42
12 weeks	4000.90	-0.96	91	75 point ignored

University of Cape Town

Figure G11: The Relationship between Reaction Rate and Time in New EAF Slag Powders (particle size: 75-300um)

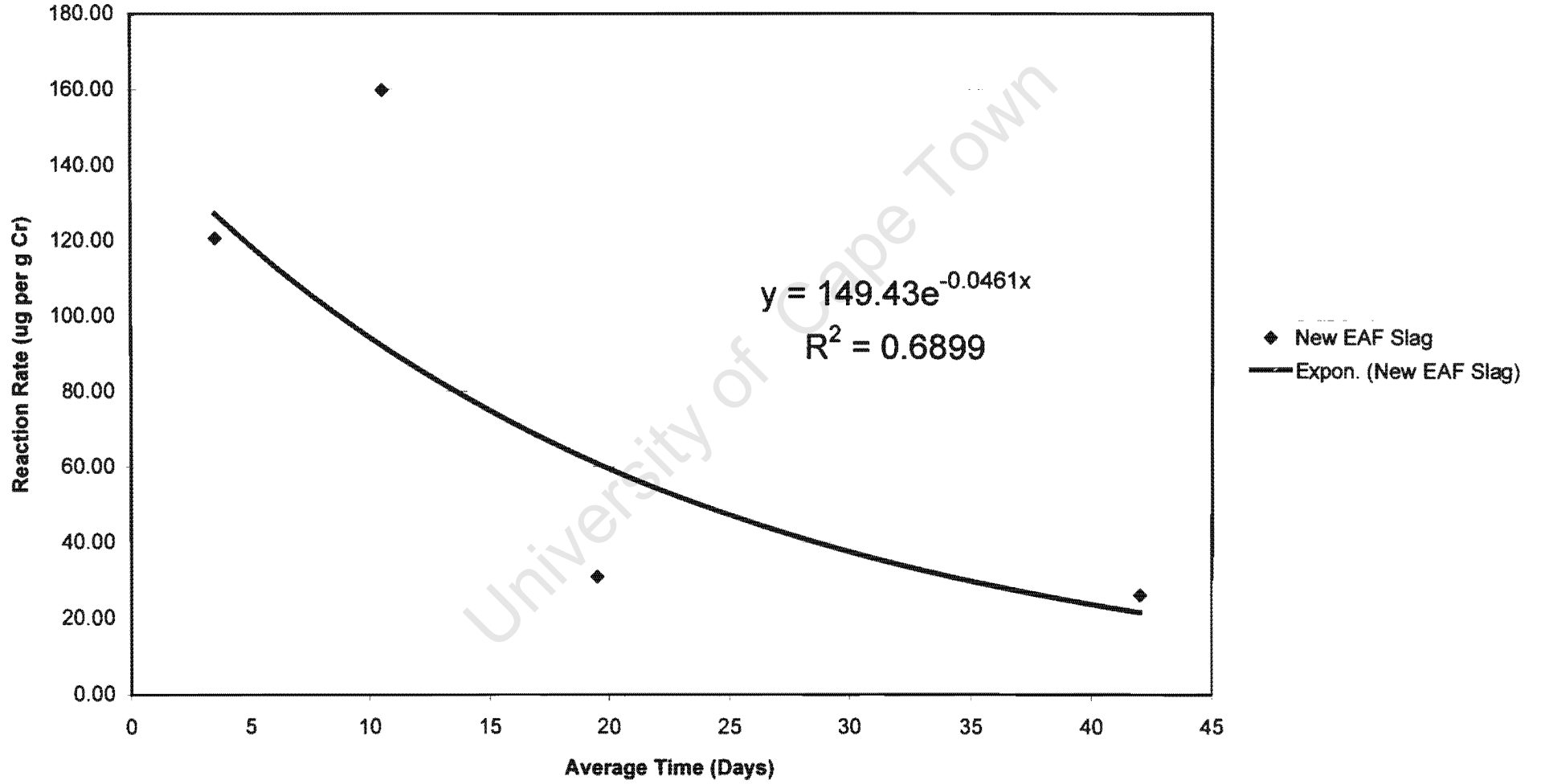


Table G41: The Kinetic Data for New EAF Slag Powders exposed to air (particle size class: 300-1000um)

<i>Sample</i>	<i>Conversion</i> <i>(ug per g Cr)</i>	<i>Time in</i> <i>Days</i>	<i>Reaction Rate</i> <i>(ug per g Cr per day)</i>	<i>Average Time</i> <i>in Days</i>
0 weeks	320.13	0		
1 week	610.30	7	41.45	4
2 weeks	1179.19	14	81.27	11
4 weeks	1546.95	25	33.43	20
8 weeks	1752.45	59	6.04	42
12 weeks	1907.43	91	4.84	75

Table G42: The Long-Term Model Predictions for the oxidation reactions in New EAF Slag Powders (particle size class: 300-1000um)

<i>Time</i> <i>in Months</i>	<i>Time in Days</i>	<i>Average Time</i> <i>in Days</i>	<i>Predicted Reaction Rates</i> <i>(ug per g Cr per day)</i>	<i>Predicted Conversion</i> <i>(ug per g Cr)</i>	<i>Adjusted Conversion</i> <i>(ug per g Cr)</i>
3	91				
6	180	136	3.41E-01	1660	1980
9	270	225	1.07E-02	1668	1988
12	360	315	3.28E-04	1668	1988
15	450	405	1.01E-05	1669	1989
18	540	495	3.09E-07	1669	1989
21	630	585	9.50E-09	1669	1989
24	720	675	2.92E-10	1669	1989